UNIVERSITÀ DEGLI STUDI DI PADOVA

Dipartimento di Biologia

Centro di Ricerca Interdipartimentale per le Biotecnologie Innovative
- CRIBI -

SCUOLA DI DOTTORATO DI RICERCA IN BIOSCIENZE E BIOTECNOLOGIE
INDIRIZZO DI BIOTECNOLOGIE
XXVI CICLO

α -SYNUCLEIN OLIGOMERS INDUCED BY DOCOSAHEXAENOIC ACID
A STUDY OF ACTIVITY AND MOLECULAR CHARACTERIZATION

Direttore della scuola: Ch.mo Prof. Giuseppe ZANOTTI

Coordinatore di Indirizzo: Ch.ma Prof.ssa Fiorella LO SCHIAVO

Supervisore: Prof.ssa Patrizia POLVERINO DE LAURETO

Dottoranda: Chiara FECCHIO

A. A. 2013/2014

THESIS CONTENTS

List of figures

Abbreviations

aS	α-Synuclein
A30P	aS variant, Ala30→Pro30
A53T	aS variant, Ala53→Thr53
E46K	aS variant, Glu46→Lys46
G51D	aS variant, Gly51→Asp51
H50Q	aS variant, His50→Gln50

AFM	Atomic force microscopy
CD	Circular dichroism
DHA	Docosahexaenoic acid
DLS	Dynamic light scattering
DLB	Dementia with Lewy bodies
FA	Fatty acids
FPLC	Fast protein liquid chromatography
IEX	Ions exchange chromatography
LBs	Lewy bodies
LUV	Large unilamellar vesicles
MS	Mass spectrometry
MW	Molecular weight
SDS	Sodium dodecyl sulphate
PD	Parkinson's disease
PI	Propidium Iodide
PLM	Planar lipid membrane
PUFA	Polyunsatured fatty acids
RP-HPLC	Reverse phase high pressure liquid chromatography
SUV	Small unilamellar vesicles
TEM	Transmission electron microscopy
ThT	Thioflavin T
Tris	tris(hydroxymethyl)aminomethane
UV	ultraviolet

Ala	A	Alanine	Gly	G	Glycine	Pro	P	Proline
Arg	R	Arginine	His	H	Histidine	Ser	S	Serine
Asn	N	Asparagine	Ile	I	Isoleucine	Thr	T	Threonine
Asp	D	Aspartic acid	Leu	L	Leucine	Trp	W	Tryptophan
Cys	C	Cysteine	Lys	K	Lysine	Tyr	Y	Tyrosine
Glu	E	Glutamic acid	Met	M	Methionine	Val	V	Valine
Gln	Q	Glutamine	Phe	F	Phenylalanine			

RIASSUNTO

Il morbo di Parkinson (PD) è la principale malattia neurodegenerativa riguardante la funzionalità motoria. L'1% della popolazione sopra i 65 anni è affetto da questa malattia. I sintomi principali sono bradichinesia, tremore a riposo, instabilità posturale, rigidità muscolare e, talvolta, problemi cognitivi e della personalità. Le principali caratteristiche neuropatologiche del PD sono la morte dei neuroni dopaminergici a livello della *substantia nigra pars compacta* e la formazione di corpi d'inclusione citoplasmatici composti da aggregati proteici fibrillari di tipo amiloide, *Lewy bodies* (LBs), il cui costituente principale è α-sinucleina (aS) (Spillantini et al., 1998). aS è proteina di 140 amminoacidi, *natively unfolded,* la cui funzione, nonostante il suo ruolo chiave nel PD, non è ancora completamente chiarita. È espressa in livelli alti nel sistema nervoso centrale ed è abbondante nei terminali presinaptici neuronali. Strutturalmente è caratterizzata dalla presenza di sette ripetizioni imperfette di sequenza aminoacidica (KTKEGV) nella regione N-terminale, da una regione idrofobica centrale (NAC, non-amyloid component) e da una coda C-terminale con numerosi residui acidi. La sovraespressione di aS e mutazioni nel suo gene sono associati a forme precoci della sindrome di Parkinson. Il meccanismo con cui un cambiamento nella struttura e nell'espressione della proteina possa portare allo sviluppo della malattia non è ancora stato chiarito, ma è sempre più accreditata l'ipotesi che siano le forme oligomeriche e non gli aggregati finali fibrillari ad essere responsabili della malattia.

Il progetto di questa Tesi riguarda la caratterizzazione di oligomeri tossici di α-sinucleina (aS) ottenuti in presenza di acido docosaesaenoico (DHA) e lo studio della loro interazione con membrane lipidiche, allo scopo di comprendere il meccanismo con cui esercitano la loro tossicità. Il DHA è uno dei principali acido grassi cerebrali, strettamente correlato al PD e ad aS. L'esposizione di colture cellulari dopaminergiche a PUFAs porta all'accumulo di oligomeri solubili di aS, responsabili della citotossicità associata alla neurodegenerazione (Assayag et al., 2007). Esistono poi evidenze dell'implicazione di aS nella regolazione del metabolismo degli acidi grassi (Golovko et al., 2007). Inoltre è stato osservato che, nei pazienti affetti da PD, la presenza di DHA è maggiore nelle aree cerebrali contenenti inclusioni di aS. Studi *in vivo,* infine, hanno dimostrato che il DHA induce la formazione di oligomeri di aS (Sharon et al., 2003). In precedenti studi condotti

nel laboratorio dove è stata svolta questa Tesi è stato analizzato il processo di aggregazione di aS in presenza di DHA, utilizzando due diversi rapporti molari proteina/acido grasso) (De Franceschi et al., 2009) e gli aggregati proteici ottenuti in queste condizioni sono stati caratterizzati da un punto di vista morfologico e strutturale (De Franceschi et al., 2011). È stato osservato che la presenza di DHA in rapporto molare 50:1 rispetto alla proteina, porta alla formazione di oligomeri stabili, *off-pathway* nel processo di fibrillazione, che presentano una significativa attività tossica sulle cellule rispetto al monomero di aS.

Nella prima parte di questa ricerca è stata condotta una caratterizzazione di queste specie oligomeriche che sono sufficientemente stabili nel tempo da consentire l'uso di diverse tecniche biofisiche. In particolare gli oligomeri sono stati analizzati mediante microscopia elettronica a trasmissione (TEM) e a forza atomica (AFM), per studiare le dimensioni e la morfologia. Il tipo di struttura secondaria è stata valutata mediante dicroismo circolare che ha dimostrato un'altra peculiarità di questi oligomeri, ovvero la presenza di struttura parzialmente in α-elica, diversamente dalla maggior parte degli oligomeri descritti in letteratura. È stata analizzata anche la capacità degli oligomeri di interagire con le membrane, utilizzando liposomi di diversa dimensione e diversa composizione e colture cellulari. L'interazione tra gli oligomeri e i liposomi, studiata mediante CD e saggi di *leakage*, causa il rilascio di piccole molecole interne alle vescicole, dimostrando così un loro effetto destabilizzante sulle membrane. L'attività degli oligomeri è stata anche testata su cellule in coltura che mostrano un'alterata permeabilità in loro presenza. Per determinare quale sia il meccanismo di destabilizzazione degli oligomeri, sono stati eseguiti vari saggi. Si è dimostrato tramite *dynamic light scattering* (DLS) e TEM che le vescicole, in seguito al legame con gli oligomeri, non vengono distrutte. Inoltre mediante studi di aggregazione e analisi su *planar lipid membrane* portano a ipotizzare un meccanismo di tossicità dovuto alla formazione di un'apertura transiente o un aumento di flip-flop a livello delle membrane. I risultati di questa parte di tesi sono oggetto di una pubblicazione (Fecchio *et al.,* 2013).

Un altro aspetto che è stato approfondito in questo lavoro di Tesi è lo studio degli oligomeri da un punto di vista chimico, allo scopo di caratterizzare le modifiche chimiche presenti sulla sequenza della proteina in seguito all'esposizione al DHA. Sono state evidenziate diverse modifiche mediante spettrometria di massa tra cui carbonilazioni e

presenza di addotti. Quest'ultimo tipo di modifica in particolare avviene a livello dell'istidina in posizione 50. Per approfondire il ruolo di questo aminoacido nell'interazione con gli acidi grassi è stato studiato il mutante H50Q di aS. Questa proteina modificata è tra l'altro responsabile di forme familiari del PD.

Infine è stata studiata anche l'interazione di altre varianti patologiche di aS associate a PD, A30P, E46K e A53T con DHA. In particolare, è stata analizzata la loro struttura e la loro tendenza ad aggregare in presenza di DHA, nonché la loro capacità di formare oligomeri, in confronto ai risultati ottenuti con aS.

In conclusione questo studio ha permesso di fornire maggiori informazioni sulla struttura e di studiare l'attività di specie oligomeriche che sono potenzialmente molto rilevanti per la patogenesi del PD. La struttura e l'attività di questi oligomeri potrà essere confrontata con quelle di oligomeri prodotti in diverse condizioni sperimentali o di oligomeri prodotti da altre proteine amiloidogeniche. Questa conoscenza è fondamentale per sviluppare agenti terapeutici che prevengano o debellino queste malattie debilitanti ed in continuo aumento.

SUMMARY

Parkinson disease (PD) is the main neurodegenerative disease that involves motor symptoms. About 1% of population above 65 years is affected by PD. Main symptoms are bradikinesia, resting tremor, postural instability, muscle rigidity, and sometimes, cognitive problems and personality. Neuropathological features of PD are neuronal death in the *substantia nigra pars compacta* and formation of cytoplasmatic inclusion, named Lewy bodies, constituted by fibrillar form of α-synuclein (aS). aS is a 140 amino acid protein, whose structure and function is yet not well defined. As a consequence of specific genetic mutations or environmental factors, it undergoes aggregation and forms amyloid fibrils. It is highly expressed in neuronal pre-synaptic nerve terminals. Its sequence is characterized by an amphipathic lysine-rich amino terminus, which governs binding to lipids and interactions with membranes and contains seven imperfect repetition of the sequence KTKEGV; by a hydrophobic central region (NAC, non-amyloid component), responsible for protein aggregation and β-sheet formation and a highly acidic C-terminal, rich in Pro and acidic residues. Overexpression of aS and mutations in its gene are associated with a premature development of PD. Mechanism that make aS a toxic protein has not yet been well clarified, but it seems clear that oligomeric forms, and not the final fibrillar forms, are the main responsible for the pathogenesis of PD.

The project of this thesis focuses on the characterization of oligomers of aS that form in the presence of docosahexaenoic acid (DHA), and their interaction with membrane, to understand the mechanism of toxicity. DHA is one of the most abundant fatty acids in neuronal membrane and it has been correlated to PD. It has been demonstrated that dopaminergic cell cultures exposed to PUFAs accumulate soluble cytotoxic aS oligomers (Assayag et al., 2007). Indeed, aS seems to be involved in fatty acids metabolism (Golovko et al., 2007). Moreover, it was reported that, in PD patients, DHA concentration is enhanced in those area affected by aS inclusions. *In vivo* studies demonstrated that a DHA enriched diet enhances formation of aS oligomers (Sharon et al., 2003). In previous studies in this laboratory, it was analyzed the aggregation process of aS in the presence of DHA using different protein to DHA molar ratios (De Franceschi et al., 2009; 2011). Oligomers obtained in these conditions were characterized from a morphological point of view (De Franceschi et al., 2011). The presence of DHA (50:1

lipid:protein molar ratio) leads to the formation of stable oligomers, off-pathway in the aggregation process of aS, that have significant toxic activity on cells, suggesting that they are potentially relevant in the pathogenesis of PD (De Franceschi et al., 2011).

In the first part of this thesis a characterization of oligomers have been conducted using several biophysical methods, since these oligomers are sufficiently stable to allow the use of these techniques. In particular, transmission electron (TEM) and atomic force (AFM) microscopy were used to study oligomers morphology and dimension. The secondary structure was evaluated by circular dichroism (CD). This spectroscopic analysis reveals that oligomers have a partial α-helix structure, in contrast with the majority of oligomeric species described in literature. It was analyzed also the ability of oligomers to interact with membrane, using liposomes of different size and composition and cell cultures. Interaction of oligomers with membrane, analyzed by CD measurements and leakage assays, causes the leakage of small molecule, demonstrating their ability to destabilize membranes. Oligomers activity was tested also on dopaminergic cell culture that showed an altered permeabilization after treatment. To determine the mechanism by which oligomers cause membrane permeabilization, different tests were performed. Initially, dynamic light scattering (DLS) and TEM allow to exclude a detergent-like effect. Moreover, aggregation studies and planar lipid membrane (PLM) measurements lead to hypothesize a toxicity mechanism that depends on the formation of a transient aperture or on the enhancement of flip-flop. This part of the thesis is object of a publication (Fecchio et al., 2013).

Another aspect faced in this thesis is the study of chemical modification occurring on oligomers after exposition to DHA. Different chemical modification were evidenced by mass spectrometry: carbonylation and the formation of adduct with DHA at the level of His50. To deepen the role of this residue in the interaction with FA, it was used an aS variant, H50Q, that has recently been linked to familiar form of PD.

Finally, also the interaction with DHA of other pathological variants of aS (A30P, E46K, A53T) was studied. In particular their secondary structure and oligomerization in the presence of DHA were analyzed, in comparison with results obtained with aS.

In conclusion, this study supplied further information about structure and activity of oligomeric species that are potentially relevant in PD pathogenesis. These data can be compared to oligomers produced in different conditions or formed by different

amyloidogenic proteins: this knowledge would be fundamental to the development of therapeutic agent that would prevent or defeat these kind of debilitative diseases.

1. INTRODUCTION

1.1 Parkinson disease

Parkinson's disease (PD), after Alzheimer's disease, is the second most-prevalent neurodegenerative disorder, affecting about 1 of peolpe over 60 (Van Den Eeden *et al.,* 2003). It was first described in 1817 by James Parkinson: it is an irreversible, progressive disease that impairs movement causing tremors, bradykinesia, muscular rigidity and postural instability, but the disease can be also associated to poorly treatable nonmotor symptoms, such as depression, personality changes, dementia, sleep disturbances, speech impairments (Lim and Lang, 2010). Aging is the only known definitive risk factor for both idiopathic and sporadic PD (Tolleson and Fang, 2013): indeed, incidence increases markedly with age. Young-onset Parkinson's disease, defined as occurrence before age 40, accounts for just 5% of newly diagnosed cases (Irvine *et al.,* 2008). Moreover, upon reaching the 65-69 age range, 0.6% of the population is affected, increasing to 2.6 % of those aged 85-89 (De Rijk *et al.,* 2000). The majority of cases of PD are believed to be idiopathic and sporadic, except for 5-10% of cases for which there is a genetic component, showing both recessive and dominant modes of inheritance. An other train of thought support that environmental or genetic cause for PD are a false dichotomy: many, if not all, cases of PD contain contribution of both, albeit in varying degrees (Singleton *et al.,* 2013).

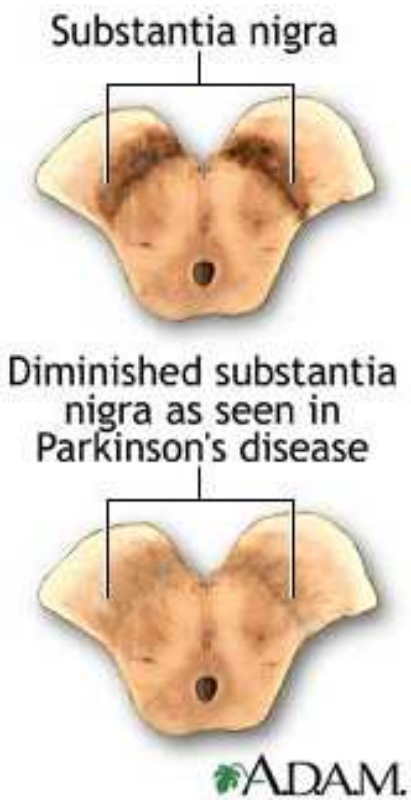

Fig. 1.1. *substantia nigra*: it is evident the loss of pigmented neurons in PD patients.

PD is caused by degeneration of dopaminergic (DA) neurons that leads to depigmentation of the *substantia nigra pars compacta* (SNpc) (Fig. 1.1). Pathologically, PD is highlighted by the presence of eosinophillic, intraneuronal proteinaceous inclusions known as Lewy bodies (LBs) and dystrophic Lewy neurites in the surviving neurons (Fig. 1.2 B, C). These intraneural inclusions were described in 1912 by Friederick H. Lewy, after investigation of histological features of sixty PD patients' brain (Lewy, 1912). LBs represent the cardinal

hallmark of PD pathology, and have been considered to be a marker for neuronal degeneration, because neuronal loss is found in the predilection sites for LBs (Wakabayashi, 2007; Lees, 2009). However, it is not clear if the formation of LBs is a primary mechanism or a consequence (Tolleson and Fang, 2013). Because patients suffering from other neurological disorders can display parkinsonian features, a definitive diagnosis of Parkinson's disease can be confirmed only by *post mortem* histopathological examination of the *substantia nigra* for the loss of pigmented neurons and presence of LBs in remaining neurons. Identification of LBs has been facilitated by immunostaining for particular proteins; initially for ubiquitin and more recently for aS, now regarded as the major protein constituent (Shults, 2006). Such staining reveals filaments that, when purified and examined by immuno-electron microscopy, can be seen to contain aS (Spillantini *et al.,* 1998). The recombinant protein forms similar filaments (Fig. 1.2 A) when it is allowed to aggregate *in vitro* (Crowther *et al.,* 1998).

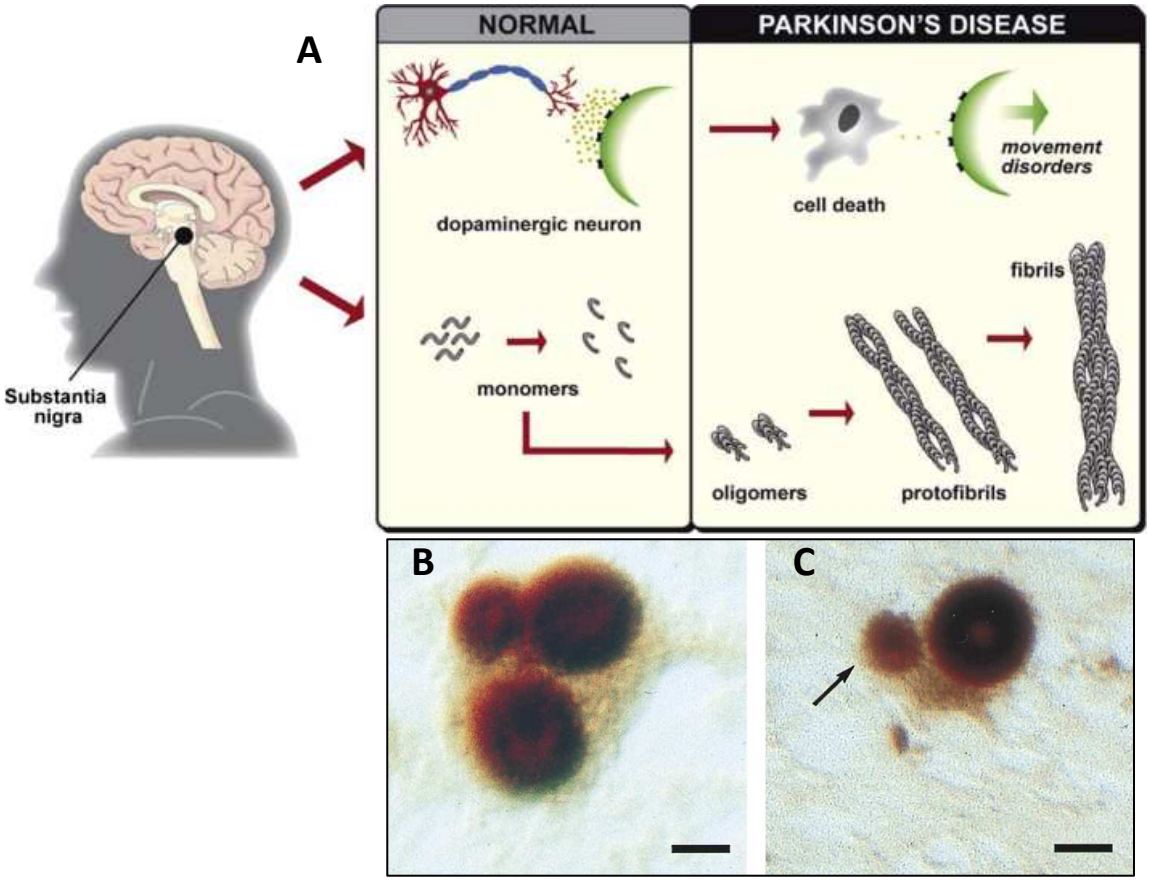

Fig. 1.2. Schematic representation of neuronal loss in substantia nigra due to aS fibril formation, in brain of patience of PD. (reprinted from Ruipérez *et al.,* 2010). Draw of LBs by Dr. Lewy (reprinted from Lewy 1923). **(B)** and **(C)** Nerve cell with three and two LBs that are double-stained for aS and ubiquitin. The halo of each LB is strongly immunoreactive for ubiquitin, whereas both the core and the halo of each Lewy body are immunoreactive for α-synuclein (Bar = 10 µm) (reprinted from Spillantini et al. 1998).

The motor complications caused by PD appear only after a significant loss of of dopamine cells: approximately 50% in the SNpc and 80% in the striatum (Ozansoy and Basak, 2012). The role of dopamine (DA) as neurotransmitter was defined in the late 1950s by the Swedish scientist Arvid Carlsson, who deserved for this reason the Nobel Prize in 2000. His studies were rapidly converted into clinical investigations and resulted within a few years in the first clinical treatment of PD, a therapy that is still in wide use today (Andersen, 2009). DA neurons operate in a pathway that controls voluntary movement. This involves signals being relayed from the cerebral cortex through the basal ganglia back to the cortex and then on to muscles. Neurons from the *substantia nigra pars compacta* project axons that release dopamine in synapses on interneurons in the striatum. As the dopamine containing neurons die, failure to complete this circuit results in inability to coordinate movement (Fig. 1.3). Neuromelanin, the black pigment that gives its name to the *substantia nigra (SN)*, is a byproduct from the metabolic pathway for dopamine synthesis. When the symptoms of PD first become apparent, more than 70% of the dopamine containing neurons have already been lost, releasing their neuromelanin and hence turning the tissue less black

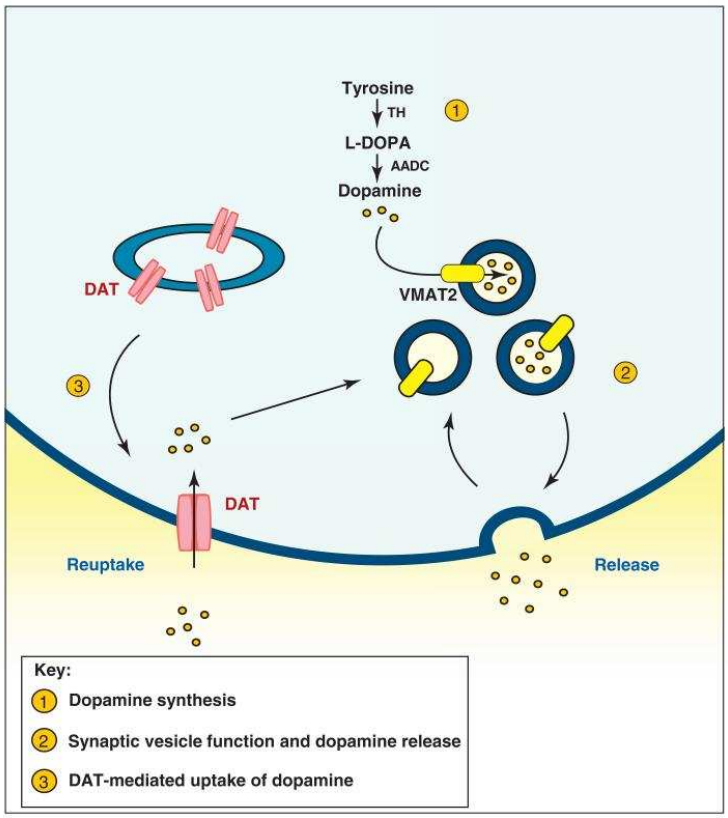

Fig. 1.3. DA is synthesized in the cytoplasm by the action of tyrosine hydroxylase (TH) and amino acid decarboxylase (AADC). **1-** *As* has been shown to regulate the activity of these enzymes. **2-** Once synthesized, DA is immediately sequestered into vesicles by the vesicular monoamine transporter 2 (VMAT2). Several lines of evidence suggest that α-synuclein is involved in regulating synaptic vesicle function and dopamine release into the synaptic cleft. **3-** Dopaminergic signaling at the synapse is terminated by the reuptake of dopamine via the dopamine transporter (DAT), with co-transport of two Na^+ and one Cl^- ions. Studies in cell culture systems have shown that α-synuclein is necessary for the trafficking of DAT to the cell surface (Reprinted from Venda *et al.,* 2010).

(Fig. 1.1). It is now apparent, however, that many regions of the brain are affected in Parkinson's disease, and indeed in the early stages it may affect only a lower region of the brain stem called the *medulla oblongata*, spreading gradually upward through the basal ganglia into the cortical areas (Irvine *et al.,* 2008; Braak *et al.,* 2003). Symptoms of PD could be reversed temporarily by restoring striatal dopaminergic neurotransmission with pharmacologic interventions (LeWitt, 2008; Hornykiewicz, 2002), using DA agonists, compounds that directly stimulate postsynaptic receptors. The administration of dopamine itself is ineffective because dopamine cannot cross the blood–brain barrier (Nutt *et al.,* 1984). Levodopa (3, 4-dihydroxy-L-phenylalanine), a naturally occurring amino acid, is an intermediate in the pathway of dopamine synthesis (Fig. 3). After oral ingestion, levodopa is actively transported from the upper small intestine into the circulation by a mechanism specific for large, neutral L-amino acids. Because of ongoing metabolism and the distribution of levodopa throughout the body, only a small fraction of the drug reaches the brain after active transport across the blood–brain barrier. Once there, dopamine is rapidly formed from levodopa by aromatic L-amino acid decarboxylase (AAAD). Moreover, the coadministration of other drugs can improve the efficacy of levodopa. In conclusion, current medications only provide symptomatic relief and fail to halt the death of DA neurons. A major hurdle in development of neuroprotective therapies are due to limited understanding of disease processes leading to death of DA neurons (Thomas & Beal, 2007).

1.1.1 Pathogenesis

Although the majority of PD cases are idiopathic, about 10% of cases report with a family history, and a growing number of mutations have been associated with familial and sporadic forms of the disease (Lesage and Brice, 2009; Westerlund *et al.,* 2010). The primary pathological change in Parkinson's disease is the destruction of dopamine containing cells in the zona compacta of substantia nigra (Jenner, 1989), so one important question to study Parkinson's disease is why dopaminergic neurons are particularly vulnerable. One hypothesis is that the metabolic pathways for dopamine synthesis might be at the root of the problem (Jenner, 1989). There is evidence that dopamine metabolites can increase levels of reactive oxygen species that damage cells, especially mitochondria; for example, neuromelanin binds heavy metals that can lead to free radical

production (Turnbull*et al.,* 2001). The unique susceptibility of dopaminergic neurons to some toxins, such as 1-methyl-4-phenyl-1, 2, 3, 6-tetrahydropyridine (MPTP) or Rotenone, leads to another hypothesis that postulated exposure to environmental toxins as the cause. For example, MPTP is taken up by the dopamine transporter, and this fact explains the localization of pathological effects (Langston *et al.,* 1983; Ramsay *et al.,* 1986; Dauer *et al.,* 2003). However, while there are some cases where a single environmental or monogenetic factor may lead to PD (MPTP poisoning or triplication of aS, respectively) (Farrer *et al.,* 2004, Przedborski *et al.,* 2001 and Singleton *et al.,* 2003), it is more likely that a subtle yet complex interplay exists between genetic and environmental factors in the etiology of disease. For example, the autosomal dominant G2019S mutation in leucine-rich repeat kinase 2 (LRRK2) is the most common known cause of familial and sporadic patients with PD, yet its penetrance is age-dependent, and some individuals may never be afflicted (Goldwurm *et al.,* 2007 and Kachergus *et al.,* 2005). The manifestation of such a predominant mutation as a late onset disorder, where it is still not fully penetrant, suggests that genetic defects may serve to predispose individuals to certain environmental challenges (Jason *et al.,* 2011).

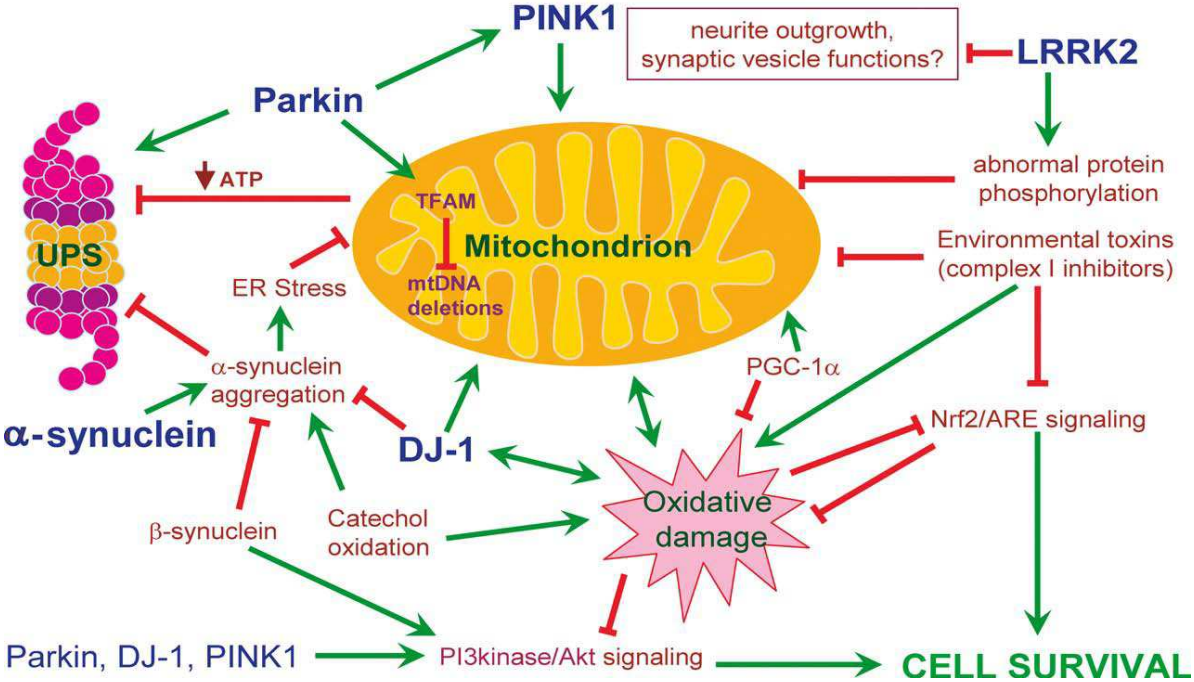

Fig. 1.4. Common pathways in PD pathogenesis that involve aS, with promoting (green arrows) or inhibitory (red lines) effects (reprinted from Thomas & Beal, 2007).

In Fig. 1.4 is reported a schematic representation of several different pathways that are important in modulating pathogenic events. aS undergoes aggregation either due to pathogenic mutations or catechol oxidation which in turn compromise UPS function,

induce endoplasmic reticulum stress and cause mitochondrial dysfunction. Mitochondrial dysfunction and oxidative damage lead to deficits in ATP which may compromise US function promoting abnormal protein aggregation. β-Synuclein is known to prevent aS aggregation through activation of Akt signaling. Parkin, an ubiquitin E3 ligase, promotesproteasomal degradation, increases mitochondrial biogenesis by activating mitochondrial transcription factor A (TFAM) and block PINK1-induced mitochondrial dysfunction, while pathogenic mutations, oxidative and nitrosative damage, severely compromise its protective function. DJ-1 protects against oxidative stress, functions as a chaperone to block aS aggregation and protects against mitochondrial dysfunction. PINK1 seems to protect against mitochondrial dysfunction which is compromised due to pathogenic mutations, although the precise function of PINK1 in mitochondria still needs to be determined. L-RRK2 seems to play a role in synaptic vesicle functions, neurite outgrowth. Pathogenic mutations in LRRK2 cause abnormal protein phosphorylation which induce mitochondria-dependent cell death. In addition, a pathogenic role of PI3kinase-Akt (phosphatidylinositol 3-kinase/Akt) and Nrf2/ARE signaling is implicated in PD pathogenesis. Familial PD-linked genes namely parkin, DJ-1 and PINK1 activate PI3 kinase-Akt signaling, while activation of Nrf2/ARE pathway prevents against oxidative damage and mitochondrial dysfunction promoting cell survival (Thomas and Beal, 2007).

Genetic factors in PD

Ninety per cent of PD cases are sporadic. The remaining minority fraction of PD patients carries genetic form of the disease: both autosomic dominant or autosomic recessive gene mutations have been found. A distinction has to be done between two terminologies. Parkinsonism defines the syndromic features of PD patients movement disorders. It is consistent with the loss of dopaminergic neurons in SNpc and consequent nigral degeneration. The second term is synucleinopathy that identifies all the pathologies linked to aS accumulation in LB. This definition includes PD, dementia with Lewy bodies and multiple system atrophy. All PD patients shows parkinsonism, but not all present aS accumulation. Generally, these latter cases are directly correlated with autosomic recessive PD. While autosomic dominant PD is linked to point mutant of aS A53T (Polymeropoulos *et al.,* 1997), A30P (Kruger *et al.,* 1998) E46K (Zarranz *et al.,* 2004), and recently with H50Q (Proukakis *et al.,* 2013) and G51D (Kiely *et al.,* 2013) some recessive

genes are associated with mitochondria and oxidative-stress related survival pathways, other with ubiquitin proteasomal system (Table 1.1).

Table 1.1. Summary of genetic locus and candidate genes for PD (Lai *et al.,* 2012):

Locus	Chromosome	Gene	Inheritance
PARK ¼	4q21.3	SNCA	Autosomal dominant
PARK 2	6q25.2-27	Parkin	Autosomal recessive
PARK 3	2p13	Unknown	Autosomal dominant
PARK 5	4p14	UCHL-1	Autosomal dominant
PARK 6	1p35-p36	PINK1	Autosomal recessive
PARK 7	1p36	DJ1	Autosomal recessive
PARK 8	12q12-q13.1	LRRK2	Autosomal dominant
PARK 9	1p36	ATP13A2	Autosomal recessive
PARK 10	1p32	Unknown	Susceptibility locus
PARK 11	2q36-37	GIGYF2	Autosomal dominant
PARK 12	Xq21-25	Unknown	X-linked
PARK 13	2p13.1	HTRA2/Omi	Autosomal dominant
PARK 14	22q13.1	PLA2G6	Autosomal recessive
PARK 15	22q11.2-qter	FBXO7	Autosomal recessive
PARK 16	1q32	Unknown	Susceptibility locus
PARK 17	4p16	GAK	Susceptibility locus
PARK 18	6p21.3	HLA-DRA	Susceptibility locus

Till now, linkage studies have identified seventeen loci, named PARK, correlated with PD or related disorders (Parkinsonism syndromes and LBD) (table 1.1, from Lai *et al.,* 2012). The loci include six autosomal dominant genes, the main are aS (SNCA) and leucine-rich repeat kinase 2 (LRRK2), and six autosomal recessive genes, parkin, PTEN-induced putative kinase 1 (PINK1), DJ-1, lysosome ATPase type (ATP13A2), PLA2G6, and FBXO7. The ubiquitin carboxyl-terminal esterase L1 gene, (UCHL1, previously known as *PARK5*), has only been found in one small family, and its importance in familial PD is still uncertain. Identification of other Mendelian forms of PD still remains a main challenge in PD research. PARK1 and PARK4 were initially assigned to different regions on chromosome 4, but later ascribed to the same locus. Moreover, other genes, coming from different loci, have been linked to PD and Parkinsonism, such as GBA (glucocerebroside), MAPT (microtubule associated protein tau), spatacsin, ataxin 3 and actasin 2 (Hardy, 2010). Unsurprisingly, the application of new techniques such as next

generation sequencing (NGS), genome-wide association studies (GWAS) and meta-analyses have allowed for the discovery of new genes and genetic risk factors for Parkinson disease and also other movement disorders, such as dystonia, essential tremor and restless legs syndrome (RLS) (Kumar *et al.,* 2012). As an example, two independent studies utilized exome sequencing in a Swiss and an Austrian kindred to identify the same p.D620N (c.1858G>A) mutation in the *vacuolar protein sorting 5 homolog (VPS35)* gene as the cause of autosomal dominant Parkinson disease in these families (Vilarino-Guell *et al.,* 2011; Zimprich *et al.,* 2011).

PARK1: aS gene

The discovery that aS is the main component of LBs is subsequent to the recognition of a mutation linked to PD in the *SNCA* gene (Polymeropoulos *et al.,* 1997). Autosomal dominant early-onset PD has been linked to several point mutations (A30P, A53T, E46K, H50Q and G51D) in the gene encoding aS (Polymeropoulos *et al.,* 1997; Kruger *et al.,* 1998; Zarranz *et al.,* 2004; Proukakis *et al.,* 2013; Kiely *et al.,* 2013. All mutations are reported in Fig. 1.5.

1 10 20 30 40 50 60
MDVFMKGLSK AKEGVVAAAE KTKQGVAEAA GKTKEGVLYV GSKTKEGVVH GVATVAEKTK
70 80 90 100 110 120
EQVTNVGGAV VTGVTAVAQK TVEGAGSIAA ATGFVKKDQL GKNEEGAPQE GILEDMPVDP
130 140
DNEAYEMPSE EGYQDYEPEA

Fig. 1.5. Sequence of aS. The point mutations linked to autosomal dominant early-onset PD are colored.

A53T was the first mutation to be identified: it causes earlier onset of the disease (about 7-10 years earlier), and much lower prevalence of tremor compared with patients with sporadic PD (Papapetropuolus *et al.,* 2001). PD patients with A30P and E46K mutation display as well earlier onset of the disease. Moreover, also duplications and triplications of PARK1 locus cause autosomal dominant, early onset PD (Singleton *et al.,* 2003; Chartier-Harlin *et al.,* 2004). The age of onset and severity of the disease phenotype seems to correlate with SNCA copy number, suggesting a gene-dosage effect (Cookson, 2005). PD patients who carry duplications, which generate three copies of the gene, tend to have PD which develops slowly from the 40s. Locus triplications, which produce four

copies of the SNCA gene, are responsible of earlier onset disease (mid 20-mid 30) (Farrer *et al.,* 2004; Wood-Kaczmar et al. 2006).

AS variants differ for the kinetics of fibrillation: the rate is increased for the A53T and the E46K substitutions (Conway *et al.,* 1998; Greenbaum *et al.,* 2005), while it is decreased in the case of A30P (Conway *et al.,* 2000). Moreover, both the A53T and the A30P mutations promote accumulation of prefibrillar oligomeric species (Conway *et al.,* 2000), while the E46K protein reduces the formation of such aggregates (Fredenburg *et al.,* 2007). Deep structural studies on the point-mutated aS variants have been performed for the first mutants discovered, while poor data are available for the latest, i.e. H50Q and G51D. NMR analyses have shown, for A30P, A53T and E46K, that these mutations have no global effects on the structural properties of the protein or on the dynamic behaviour of the aS backbone (Bussell & Eliezer, 2001, Fredenburg *et al.,* 2007). Nevertheless, the secondary structure propensity for the free disordered state of the wt protein is different the three PD-linked variants. Specifically, the analysis of the Cα secondary shifts revealed that the A30P mutation decrease the helical propensity found in the N-terminal region of wt aS. The A53T mutation induces a more subtle and local preference for extended β-sheet like conformations around the site of mutation (Bussell & Eliezer, 2001). The study on E46K indicated that this mutation results in only very minor conformational changes in the free state of aS (Fredenburg *et al.,* 2007). Bertoncini et al. (2005b) analyzed the perturbation induced by A30P and A53T mutantion in aS conformers ensemble. The two variants show increased backbone flexibility and the absence of the long-range interactions that were previously observed in the wt protein. In these mutants the number of conformation available are larger and possibly there is a reduced shielding of hydrophobic NAC. The possibility to an easier overcome of the energetic barrier for self-association is reported as apossible cause for the increased propensity of these variants to aggregate. Of interest, aS mutations have effect on the interactio of aS with lipids and membranes: the A53T mutation seems to have little effect on membrane binding (Perrin *et al.,* 2000; Bussell & Eliezer, 2004). Instead, the A30P mutation decreases the extent of lipid interactions *in vitro* and *in vivo* (Perrin *et al.,* 2000; Jo *et al.,* 2002; Jensen *et al.,* 1998), beacouse of the presence of a pro residue that act as a helical breaker. Specifically, a N-terminal helix is interrupted at level of A27 to A37, leading to the formation of two antiparallel helix (Ulmer and Bax, 2005). In contrast, E46K mutation increases the ability

of the protein to bind to negatively charged liposomes (Choi *et al.,* 2004), since Lys residue shift the net charge of the first 100 residues from +4 to +6 (Bodner *et al.,* 2010). Several different study have been conducted to study the consequence of aS variants expression. Theei presence in cells seems to promote mitochondrial defects and cell death and enhance susceptibility to oxidative stress. On the other hand, mice deficient in aS are resistant to toxicity induced by MPTP and other mitochondrial toxins (Klivenyi *et al.,* 2006).

Post translational modification on aS

There are >300 different protein posttranslational modifications (PTMs), which include such diverse processes as proteolysis, phosphorylation, lipidation, S-nitrosylation, nitration, oxidation, glycosylation, methylation, adenosine diphosphate (ADP)-ribosylation, acylation (acetylation, isoprenylation, myristoylation), ubiquitination, sumoylation, sulfation, farnesylation, dityrosine crosslinking, methionine oxidation, crosslinking by transglutaminase, truncation, and N-terminal acetylation and many others (Aebersold *et al.,* 2001). PTMs change the size, charge, structure and conformation of proteins. As a result, characteristics of proteins, such as enzyme activity, binding affinity, and protein hydrophobicity, are altered. PTMs cannot only directly change the proteins' function but also indirectly affect function by leading to cell compartmentalization, sequestration, degradation, elimination, and protein–protein interactions. Individual proteins can undergo multiple and different PTMs (Aebersold *et al.,* 2001). Protein aggregation is a highly cooperative process, and even a small subpopulation of modified aS could have a substantial impact on kinetics and product distribution. It has been pointed out that only few post-translational modification have been described for aS. This includes phosphorilation, methionine oxidation, dityrosine crosslinking, crosslinking by transglutaminase, truncation, and N-terminal acetylation (Beyer, 2006). The known sites of main PTMs in α-synuclein and their known effects on its conversion into disease-related forms are discussed below.

- Phosphorylation

In human α-synuclein *in vivo*, serine 129 was established as a major phosphorylation site, with a second phosphorylation site located at serine 87. The major phosphorylation site was found to be located within a consensus recognition sequence of casein kinase 1 (CK-1). In vitro experiments and two-dimensional phosphopeptide mapping provided further evidence that serine 129 was phosphorylated by CK-1 and CK-2, both highly conserved sites (Okochi *et al.,* 2000). About 90% of α-synuclein in LBs is phosphorylated at Ser-129 (Fujiwara *et al.,* 2002).

The effect of phosphorylation at Ser-129 on aggregation of α-synuclein has been studied by expressing the S129A, to abolish phosphorylation at this site. Expression of S129A alpha-synuclein instead of wild-type alpha-synuclein decreased the parkin-mediated ubiquitination of synphilin-1 and the formation of ubiquitinated inclusions. Moreover, treatment of SH-SY5Y cells with H_2O_2 increased alpha-synuclein phosphorylation and enhanced the formation of inclusions, whereas treatment with the casein kinase 2 inhibitor 5,6-dichloro-1-beta-d-ribofuranosylbenzimidazole had the opposite affect. (Smith *et al.,* 2005). This data shows that Ser-129 phosphorylation promotes aggregation of α-synuclein. Phosphorylation at Ser-87, on the other hand, expands the structure of α-synuclein, increases its conformational flexibility, and blocks its aggregation *in vitro.* Furthermore, phosphorylation at S87, but not S129, results in significant reduction of alpha-syn binding to membranes. *(*Paleologou *et al.,* 2010)

- Oxidative modifications

The primary targets for oxidative modifications in α-synuclein are its methionine and tyrosine residues. The α-synuclein primary sequence contains four tyrosine residues: Tyr-39, Tyr-125, Tyr-133, and Tyr-136. These tyrosine residues are conserved in all α-synuclein orthologs and in β-synuclein paralogs, suggesting that these residues might play important functional roles (Dev *et al.,* 2003). Studies have shown that exposure to oxidative and nitrative species stabilizes alpha-synuclein filaments in vitro, and this stabilization may be due to dityrosine cross-linking. (Norris *et al.,* 2003). However, in a cellular model of PD, only a significant increase in nitration of Tyr-39 was detected while nitration levels of other tyrosine residues were unchanged (Danielson *et al.,* 2009). The difference could be due to a higher accessibility of Tyr-39 to a nitrating agent.

Methionine residues are also susceptible to oxidation to sulfoxide and ultimately sulfone (Fig. 1.6). All four methionines in α-synuclein (Met-1, Met-5, Met-116, and Met-127) located outside the repeat-containing region are highly susceptible to oxidation to methionine sulfoxide MetO. Their oxidation inhibits fibrillation of this protein in vitro and MetO protein also inhibits fibrillation of unmodified alpha-synuclein. Moreover, the degree of inhibition of fibrillation by MetO alpha-synuclein is proportional to the number of oxidized methionines (Hokenson *et al.,* 2004).

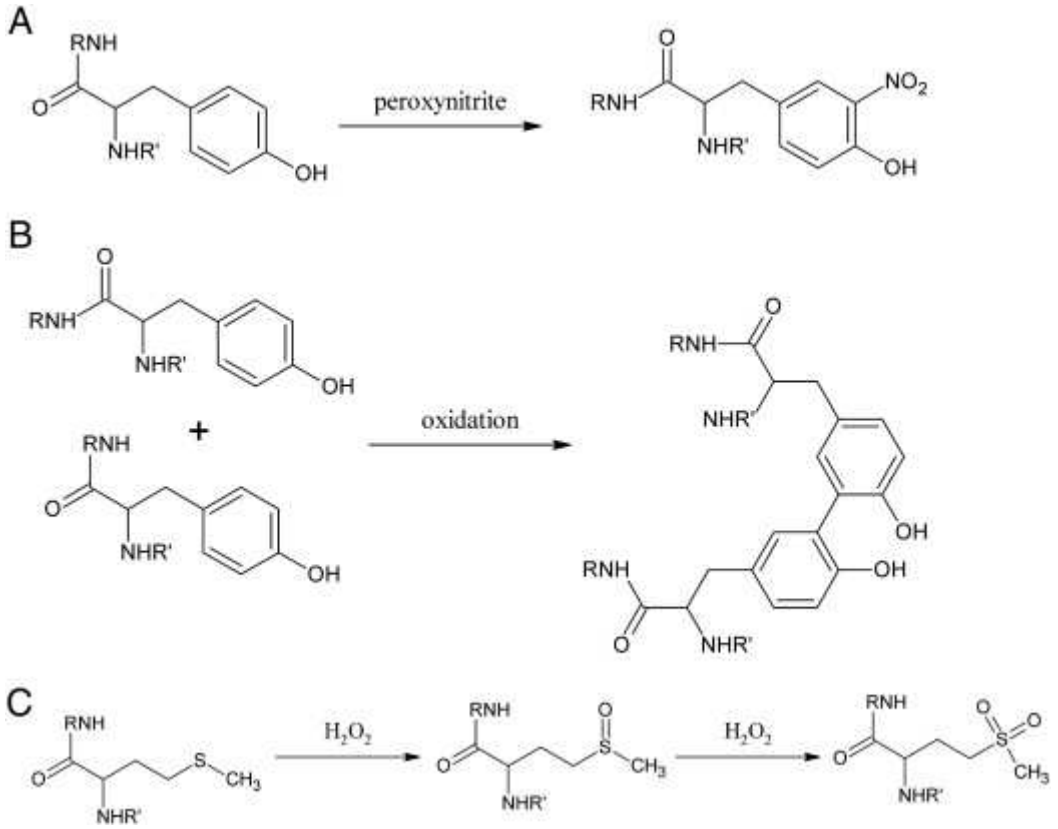

Fig. 1.6. Methionine and tyrosine oxidation scheme. A — Tyr nitration, B — Tyr dimerization, and C — Met oxidation.

Since PD pathology is associated with dopaminergic neurons, the interaction between aS and dopamine has been extensively investigated. Dopamine is known to bind to α-synuclein non-covalently, inhibiting its fibrillation and stabilizing the oligomers (Herrera *et al.,* 2008). However, dopamine is highly susceptible to oxidation, and its oxidation products can inhibit aS fibril formation, because DAQ might stabilize aS protofibrils. These adducts drive aggregation of α-synuclein into aS/DAQ adducts that retain an unfolded conformation. Only a small fraction of aS molecules interacts with DAQ in a covalent way (Bisaglia *et al.,* 2010).

Overall, oxidative modification can significantly alter the aggregation pathway of α-synuclein, usually toward oligomer formation. The structure and toxicity of these oligomers depend on the nature of modification and other experimental variables (Breydo *et al.,* 2012).

- *Ubiquitination*

Ubiquitin is a small protein that can be enzymatically attached to lysine residues of various cellular proteins. Ubiquitination is used to target proteins for proteolytic degradation. Although α-synuclein contains 15 lysine residues, Lys21, Lys23, Lys32, and Lys34 are the major ubiquitination sites in vitro. Notably, filamentous alpha-synuclein is less ubiquitinated than the soluble form and the major ubiquitination sites are localized to Lys6, Lys10, and Lys12 at the amino-terminal region of filamentous alpha-synuclein in vivo (Nonaka *et al.,* 2005). Since ubiquitination is not required for the degradation of the α-synuclein monomer, it appears that α-synuclein ubiquitination occurs after its aggregation (Sampathu *et al.,* 2003). The effect of monoubiquitination of aS on its aggregation depends on the site of modification. However, monoubiquitination of aS by SIAH ligase at multiple lysine residues promotes its aggregation in vitro and in vivo, which is toxic to cells. Mass spectrometry analysis demonstrates that SIAH monoubiquitylates aS at lysines 12, 21, and 23, which were previously shown to be ubiquitylated in Lewy bodies. SIAH ubiquitylates lysines 10, 34, 43, and 96 as well (Rott *et al.,* 2008).

- *Modification by lipid-derived aldehydes*

Highly reactive aldehydes (for example, 4-hydroxy-2-nonenal and malondialdehyde) are produced by lipid peroxidation (H. Esterbauer, R.J. Schaur, H. Zollner, Chemistry and biochemistry of 4-hydroxynonenal, malonaldehyde and related aldehydes, Free Radic. Biol. Med.11 (1991) 81–128). aS has been shown to have affinity for unsaturated fatty acids and membranes enriched in polyunsaturated fatty acids, which are especially sensitive to oxidation under conditions of oxidative stress . One of the most important products of lipid oxidation is 4-hydroxy-2-nonenal (HNE), which has been implicated in the pathogenesis of Parkinson disease. Incubation of aS with HNE resulted in covalent modification of the protein. HNE modification of alpha-synuclein led to inhibition of fibrillation, due to the formation of stable oligomers toxic to cells.

Oligomers formed after reactions with 4-hydroxy-2-nonenal and 4-oxo-2-nonenal could have different structures and morphologies. (Nasstrom *et al.,* 2003; Qin *et al.,* 2007; Nasstrom *et al.,* 2011). Overall, lysine modification of α-synuclein tends to promote the formation of oligomers at the expense of fibrils. This is likely due to the ability of more flexible structures of oligomers to accommodate these modifications. Similar behavior has been observed for other amyloidogenic peptides and proteins (Bieschke *et al.,* 2006).

Lipid induced modification of aS and relative pathological implications will be further described in section 3.3.

Oxidative stress

Parkinson's disease (PD) is related to excess production of reactive oxygen species (ROS) or inadequate and impaired detoxification by endogenous antioxidants, alterations in catecholamine metabolism, alterations in mitochondrial electron transfer function, and enhanced iron deposition in the substantia nigra (Reale *et al.,* 2012). The formation of reactive oxygen and nitrogen species damages also other cellular component such as lipids, DNA and proteins. Oxidized proteins may not be adequately ubiquitinate or recognized by the proteosome and may accumulate (Jenner, 2003). The concept that oxidative stress is an important mechanism underlying the degeneration of dopaminergic neurons is reinforced by data documenting that high levels of lipid peroxidation, increased oxidation of proteins and DNA and depletion of glutathione are observed in postmortem studies of brain tissues of PD patients (Reale *et al.,* 2012). Lipid peroxidation leads to the production of toxic species, such as 4-hydroxynonenal (HNE), detected by immunocytochemistry in SN and cerebrospinal fluid of PD patients (Yoritaka *et al.,* 1996). HNE may act by covalently modifying proteins and impairing their function, disrupting neuronal calcium homeostasis and perturbing mitochondrial function, through caspase activation. Activated caspases, in turn, induce activation of JNK, resulting in stimulation of AP-1 DNA-binding protein production. This transcriptional pathway induced by HNE may modulate the cell death process. Moreover HNE has NF-kB inhibitor action that cause the reduction of glutathione levels and the inhibition of complexes I and II of the mitochondrial respiratory chain (Camandola *et al.,* 2000; 2000b). Actually, plenty of evidences underline the prominent role of oxidative stress as cellular damage mechanism in PD. Synucleinopathies are usually associated with inflammation and elevated levels of

oxidative stress in affected brain areas, that could modify aS, especially when it binds to biological membranes. The important aspect is that oxidative modifications can affect aS aggregation. aS is such sensitive to oxidative stress because it could act physiologically as a catalytically regenerated scavenger of oxidants in healthy cells (*et al.,* 2013) with Cu, Zn-SOD and H2O2, then the amount of oligomerization increased, especially for A53T mutant form. This process was inhibited by radical scavenger and antioxidant molecules (Kang *et al.,* 2003). Another reported consequence of oxidative stress in dopaminergic neuron is that of oxidation of Dopamine. It has been demonstrated that oxidation leads to the formation of dopamine-derived orthoquinone (DAQ) that could react and bind to aS. This modification seems to be inhibitory of the fibril formation process, causing accumulation of aS protofibrils. Adduct formation provides an explanation for the dopaminergic selectivity of α-synuclein–associated neurotoxicity in PD. Interestingly, these effects are eliminated by antioxidants. Thus, three established risk factors—oxidative stress, DA, and aS—may, in combination, stabilize protofibrillar aS and promote the pathogenesis of PD (Conway *et al.,* 2001). As a prerequisite, aS levels must exceed the critical concentration for oligomerization. In rare familial forms of PD, that threshold may be lowered by aS point mutations (Conway *et al.,* 2000). Once the critical concentration of aS has been exceeded, the cytoplasmic concentration of DAQ may be one of several factors that determine the amount and lifetime of potentially pathogenic aS protofibrils (Conway *et al.,* 2001). DAQ results from a combination of oxidative stress and elevated cytoplasmic DA concentration, both of which are independently associated with PD (Dunnett *et al.,* 1999).

1.2 α-SYNUCLEIN

aS is a small (140 amino acids) cytoplasmic protein, expressed in all the central nervous system, especially in the neocortex, hippocampus, striatum, thalamus, and cerebellum (Iwai *et al.,* 1995). It represents 0.5–1% of the total cytosolic protein in brain (Kruger, 2000). It is highly expressed at the presynaptic level (Kahle *et al.,* 2004), and locally it is estimated to reach the concentration of 70-140 μM (van Raaij *et al.,* 2008).

aS family is composed of four proteins: aS, β-synuclein (bS), μ-synuclein (mS) and synoretin (synr) (Fig. 1.1). aS and bS have similar level of cellular expression and distribution, while mS and synr are prevalently expressed in peripheral terminals. The proteins in the family show a high degree of homology, however only aS is found in LB. bS is not included in amyloidogenic fibrils because it does not contain aa 71-82 of aS, believed to drive fibrillogenesis (Giasson *et al.,* 2001). The function of these proteins is still unknown. The location and some experimental data suggest an association with presynaptic vesicles (Murphy *et al.,* 2000). aS is proposed to regulate dopamine neurotransmission by modulation of vesicular dopamine storage and catecholamine release from the synaptic vesicles (Lotharius and Brundin, 2002). In particular, the potential function of aS in DA regulation and storage is correlated with its ability to interact with membranes and regulate vesicular trafficking (Lotharius and Brundin, 2002): aS over-expression inhibits a vesicle 'priming' step that occurs after secretory vesicle trafficking to 'docking' sites but before calcium-dependent vesicle membrane fusion (Larsen *et al.,* 2006). In addition, aS seems to be involved in synaptic plasticity and learning (Clayton & George, 1998), indeed it is upregulated in songbirds, during the periods of song-learning, this is a function related with synaptic plasticity (George *et al.,* 1995). Interestingly, knockout mice for aS are quite normal, showing only an increase of dopamine release in response to electrical stimuli (Abeliovich *et al.,* 2000). Genome wide screening in yeast showed that nearly one-third of genes that enhance the toxicity of aS are functionally related to lipid metabolism and vesicle trafficking (Willingham *et al.,* 2003). An analysis of a yeast PD model with dosage sensitivity for aS expression (Outeiro & Lindquist, 2003) revealed that the earliest defects following aS expression were an inhibition of the endoplasmic reticulum to Golgi vesicular trafficking and an impairment

of the endoplasmic reticulum associated degradation (Cooper *et al.,* 2006). Finally, it was revealed that aS regulates.

Another possible hypothesis, on the base of its abundance in the cytosol, its unfolded structure, and its prevention of protein aggregation induced by heat shock or chemical treatment, concerns a putative role of aS as chaperone (Souza *et al.,* 2000). Actually, aS can act as a molecular chaperone assisting in the folding and refolding of synaptic proteins called soluble NSF (N-ethylmaleimide sensitive factor) attachment receptors (Chandra *et al.,* 2005). A recent proteomic study evidenced 587 proteins as aS-binding partners in a neuronal-hybrid cell line (Jin et al, 2007). Even considering the possibility of an overestimation, the chaperone activity could well fit with the huge number of protein-interactions. aS overexpression rescues lethality associated with the lack of CSPα, a co-chaperone (HSP40 kind) associated with synaptic vesicles and implicated in folding of SNARE proteins, confirming that aS may act as an auxiliary chaperone preserving the function and integrity of the synapse (Chandra *et al.,* 2005).

1.2.1 Primary structure

aS is a 140 amino acid protein with four tyrosine residues, four methionine residues and one residue of histidine, deprived of cysteine as well as tryptophan residues. The primary sequence divides the protein in three regions: the *N*-terminal region (amino acid 1–60), the central region (61–95) and the *C*-terminal region (96–140) (Fig. 1.7). The N-terminal region, residues 1–60, includes the sites of three familial PD mutations and contains six imperfect repeats of the motif KTKEGV that is involved in the binding of detergents micelles and liposomes. This region adopts an amphipathic α-helix structure when the protein binds to phospholipids (Davidson *et al.,* 1998), that it is comparable to A2 helix type of apolipoproteins (Clayton &George, 1998). At the interface between the hydrophobic half and the hydrophilic one lysine residues are present to mediate the interaction, as the amine is positively charged and the aliphatic chain can interact with lipids. This is why aS prefers negatively charged vesicle to interact with. The central region, residues 61–95, comprises the highly aggregation-prone NAC sequence (Ueda *et al.,* 1993; Han *et al.,* 1995) and contains the remaining three imperfect repeats. NAC is the acronym of Non β- Amyloid Component, as this part of the molecule is also found in

amyloid plaques of Alzheimer's disease patients brains (Ueda *et al.,* 1993; Weinreb et al. 1996, Goedert, 1997; Jo et al. 2000).

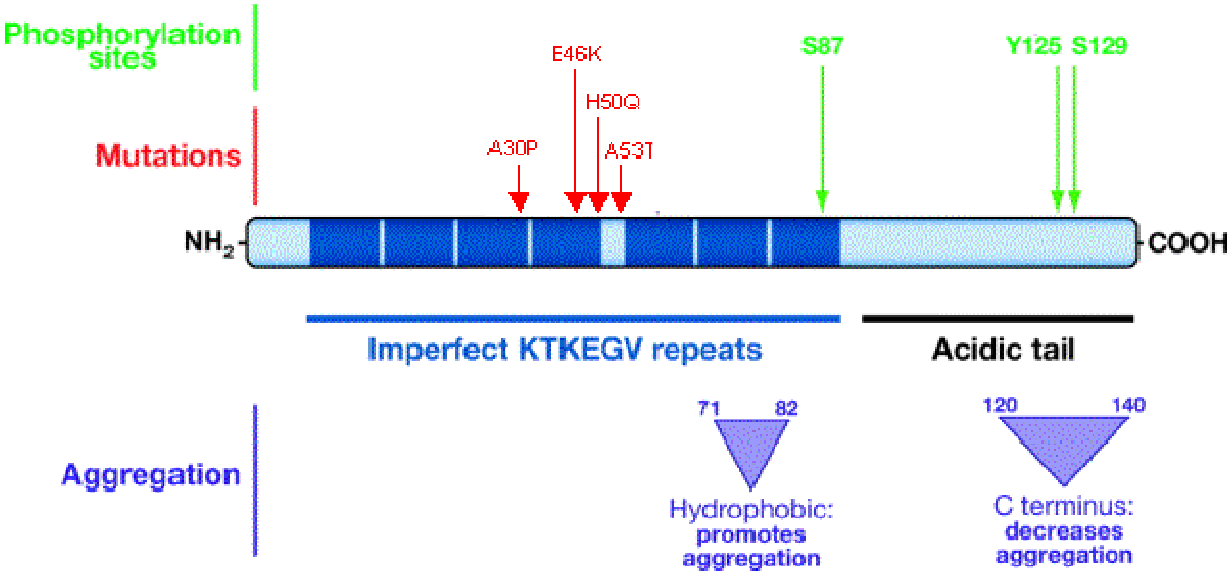

Fig. 1.7. Schematic representation of aS structure. Most important characteristics about aggregation (blue), KTKEGV repeats (light-blue), acidic residues (black), mutations (red) and phosphorilation sites (green) are reported.

This region is highly hydrophobic, and it can acquire β-sheet structure as it is the leader of amyloid fibril formation. In particular, aa 71-82 was described to be the responsible (Giasson *et al.,* 2001) of aS aggregation, as deletion mutants do not form β-sheet structured fibrils, neither do bS, which lacks this region.

The *C*-terminal region is an acidic segment rich in glutamic, aspartic and proline residues. This region determines the acidic isoelectric point of the α-syn (pI = 4.7) (Hoyer *et al.,* 2002). The C-terminal region, residues 96–140, is highly dynamic in most conditions: it does not acquire structure in any condition. A regular repetition of the acidic residues can be observed: The region has a mM affinity for the binding of metals like Ca^{2+}, $Fe^{2+/3+}$, Al^{3+}, Co^{2+} and Mn^{2+} (Uversky *et al.,* 2001). Divalent metal binding has been shown to increase fibril formation rate. Ser129 is site of phosphorylation (Takahashi *et al.,* 2003) and phosphorylated aS forms fibrils slower than wild type protein (Paleologou *et al.,* 2008); phosphorylated aS is also found in PD patients LB (Takahashi *et al.,* 2003). Also C-terminal tail seems to be involved in intermolecular interaction with the N-terminal part of the region, just for electrostatic interactions. Observing the primary sequence, it becomes evident that all the missense mutations diseases-associated, reside in the *N*-terminal region.

1.2.2 Secondary structure of aS

Since the discovery of aS amyloid fibrils as main component of LBs inclusions, the protein has been deeply examined in a massive number of structural studies. aS has been cloned and produced in bacteria for the first time in 1994 (Jakes *et al.,* 1994), and recombinant aS was shown to be able to form amyloid fibrils *in vitro* (Conway *et al.,* 1998). Until recently, aS was valued as a heat-stable protein, with a monomeric natively unfolded structure (Weinreb *et al.,* 1996). *In vitro* studies on recombinant aS show that the aS monomer lacks of ordered secondary structure under physiological conditions, detectable by far-UV circular dichroism (CD), Fourier transform IR (FT-IR) and NMR spectroscopy. For this reason, aS is considered a typical intrinsically disordered (or natively unfolded) protein, which possesses little or no ordered structure under physiological conditions in vitro (Uversky *et al.,* 2001). Intrinsically disordered proteins have been recognized as a protein class, which are gaining considerable attention due to their capability to perform numerous biological functions despite the lack of unique structure (Wright and Dyson 1999; Uversky et al. 2000, 2005, 2007). These proteins exist as dynamic and highly flexible ensembles that undergo a number of distinct interconversions on different time scales. In general, one of the main physical characteristic of this set of protein is the combination of low overall hydrophobicity and large net charge. However, aS does not fit this general trend. In its case, N- and C-terminal regions possess charge of opposite sign and are separated by an extended hydrophobic region (Uversky *et al.,* 2000). Indeed, this monomer could assume different conformational structures that hinder the amyloidogenic region. There are long-range interactions between both the *N*- and *C*-terminal with the non-amyloid component region (NAC). In particular, a long-range intramolecular interaction between the C-terminal region (residues 120–140) and the central part of aS (residues 30–100) was noted (Bertoncini, *et al.,* 2005; Dedmon *et al.,* 2005). These interactions avoid NAC–NAC contact between different monomers, which is the basis for the oligomerization and aggregation of α-syn. This is an intrinsic autoinhibitory mechanism that should be disrupted in order to favor aS oligomers and fibrils formation (Bertoncini, *et al.,* 2005; Bernardo *et al.,* 2005). Small angle X-ray scattering analysis showed that the radius of gyration, *R*g, which is used to describe the dimensions of polypeptide chain, is ~ 40 Å of native aS, which is much larger than that predicted for a folded globular protein of 140 residues (15 Å), but

significantly smaller than that for a fully unfolded random coil (52 Å). Paramagnetic relaxation enhancement (PRE) NMR spectroscopy (Dedmon *et al.,* 2005; Bertoncini *et al.,* 2005) and fluorescence based studies (Lee *et al.,* 2004; 2005) gave a molecular characterization of this partial condensation suggested the presence of the numerous long-range interactions, forming a hydrophobic cluster that comprised the C-terminal part of the highly hydrophobic NAC region (residues 85–95) and the C terminus (residues 110–130), probably mediated by M116, V118, Y125, and M127. Region 110-130 in the negatively charged C-terminal tail can contact residues 85-95 in the centre of the protein. Within the C-terminal region, residues 120-130 can contact residues 105-115, and the region about residues 120 also can interact with the N-terminus about residues 20 (Bertoncini *et al.,* 2005). The forces involved singnificantly decrease in high salt concentration (Hoyer *et al.,* 2004). These long-range interactions was suggested to inhibit the spontaneous aS oligomerization and aggregation. The autoinhibitory conformations fluctuate in the range of nanoseconds to micro-seconds, corresponding to the time scale of secondary structure formation during folding. This highly dynamic tertiary structure could explain the influece of such conditions that favour aS aggregation, as for example temperaure increase (Bertonici *et al.,* 2005). Indeed, this kind of interaction are important for the shielding of NAC region, which has been proposed to lead protein aggregation. So, all the conditions that favour the shielding action of the C-terminal tail result in a faster protein aggregation. The conformational behavior of aS under a variety of conditions was extensively analyzed (Uversky, 2003). The structure of aS is extremely sensitive to its environment and can be easily modulated by a change in conditions. Beside an extended state, aS can acquire a pre-molten globule state in several conditions such as low pH, high temperature, in the presence of various metal ions and as a result of spontaneous oligomerization both *in vitro* and *in vivo* (Uversky, *et al.,* 2001; Uversky, 2007). Moreover, *in vitro* studies demonstrate that recombinant aS can assume various □-helical structures interacting with lipid vesicles (Davidson *et al.,* 1998). Eliezer et al. (2001) documented the tendency of the first 100 residues of aS towards α-helical torsion angles, and the following paper of the same group quantified this trend to exists for the about the 10% of the time (Bussell & Eliezer, 2001). Kim et al. (2007) found that region comprehending aa 39–98 of aS polypeptide chain is able to populate β-sheet conformations in solution at supercooling temperatures. This finding is relevant for the understanding of the first steps

leading to amyloid fibril formation by aS. In addition, other works confirmed that aS is present in solution as an ensemble of conformers able to interchange each other in the microsecond timescale (Maiti *et al.,* 2004; Lee *et al.,* 2004; 2005). aS can also move from a fibrillation prone partially folded conformation to β-sheet species both in monomeric and oligomeric states. Its aggregates can be morphologically different, including spheres or ring oligomers, insoluble amorphous aggregates and amyloid fibrils (Uversky, 2003; Uversky, 2007). Based on this conformational behaviour, Uversky proposed the concept of chameleon protein, which holds that the structure of aS is modulated by its environment to a dramatic degree. That is, the choice among all the above mentioned conformations is determined by the peculiarities of protein surroundings (Uversky, 2003; Uversky *et al.,* 2007). Because of its plasticity, aS chameleon protein could be able to perform multiple functions. Indeed, Wright and Dyson proposed a reassessing of the structure-function paradigm due to the peculiarities of natively unfolded proteins (Wright and Dyson, 1999).

Data summarized so far refers to structural *in vitro* studies on recombinant aS. Some drawbacks of using recombinant are forcing non-physiological conditions, depriving the protein of the physiological modification it could be affected and of physiological binding partners and local ion environment. The native-unfolded paradigm was disputed by the work of Selkoe's laboratory, which showed that aS in its native state is a folded tetramer, rich in α-helix, with greater lipid-binding affinity than the monomer and resistant to fibril formation. In addition this tetrameric aS is *N*-acetylated *in vivo*, at least in human erythrocytes where most of the characterization was done (Bartels, J.G. Choi, D.J. Selkoe, Nature 477 (2011) 107–110]. Tetrameric state was hypothesized on the base of native gels results (about 48 kDa) and scanning transmission electron microscopy (STEM) measurements (55 kDa average). STEM imaging yielded a homogenous distribution of roughly spherical particles measuring about 3-3.5 nm in diameter, and CD measurement demonstrate that this particles have α-helical structure. Purified tetramers show higher affinity for negatively charged lipids than recombinant aS, and, most of all, less ability to aggregate. Soon, this work was challenged and laboratories from different places concluded that aS is a native monomeric and unstructured protein in erythrocytes and in the nervous system (Fauvet *et al.,* 2012). These findings are in disagreement with most of published results obtained studying recombinant aS, and, if confirmed, would

lead to several functional implications on aS physiological role. Authors explain the divergence with the use of denaturing agents, including sample heating, during the standard purification of recombinant aS from bacteria (Bartels *et al.,* 2011). A second study published by Wang and colleagues sustains the thesis of α-helical folded tetramer as native state of aS, that can be present in physiological conditions, while the unfolded structure can be a precursor of the aggregation-prone conformation.

1.2.3 Mutations on aS gene

The first missense mutation found in aS was A53T, followed by two additional disease-causing missense mutations: A30P mutation in a German family (Kruger *et al.,* 1998), and an E46K mutation in a Spanish family (Zarranz *et al.,* 2004). In vitro, aS can readily form fibrils similar to those seen in LBs (Conway *et al.,* 1998, Giasson *et al.,* 1999 and Wood *et al.,* 1999) and the mutations can influence the kinetics of aS fibrillation: E46K and A53T can both increase rate of fibril formation, while A30P decreases it (Conway *et al.,* 1998 and 2000, Giasson *et al.,* 1999 and Greenbaum *et al.,* 2005). Focusing on oligomeric species, A30P and A53T show a higher accumulation of pre-fibrillar species, while E46K reduces them (Conway *et al.,* 2000; Fredenburg *et al.,* 2007). Interestingly, A53T and A30P mutants are able to form prefibrillar intermediates with pore-like activity, providing explanation for their toxicity (Conway *et al.,* 2001; Volles & Lansbury, 2002). AS mutants were analyzed for their secondary structure futures, resulting different from aS WT. Specifically, the analysis of A30P reveals that it has a minor helical propensity compared to that found in the N-terminal region of wt aS, whereas the A53T mutation induce a more subtle and local preference for extended β-sheet like conformations around the site of mutation (Bussell & Eliezer, 2001). These two variants show increased backbone flexibility, while E46K do not. The important long-range interactions that prevent aSWT to assume an aggreation-prone confomration, are absent, so In these mutants the number of conformation available are larger and this could lead to a reduced shielding of hydrophobic NAC. The possibility to an easier overcome of the energetic barrier for self-association has been suggested by the authors as the cause for the increased propensity of these proteins to aggregate (Bertoncini *et al.,* 2005b).

Recently, a new missense mutation have been reported: H50Q (Proukakis *et al.,* 2013; Appel-Cresswell *et al.,* 2013). H50Q's characteristics are still under study, but authors assert that their protein modeling provide additional support for pathogenicity as the amino acid perturbs the same amphipathic alpha helical structure as the previously described pathogenic mutations. The mutation of H50Q was found to significantly accelerate the aggregation and amyloid formation of aS in vitro. This mutation, however, did not alter the overall secondary structure as suggested by two-dimensional nuclear magnetic resonance and circular dichroism spectroscopy. The initial oligomerization study by cross-linking and chromatographic techniques suggested that this mutant oligomerizes to an extent similar to that of the wild-type (Ghosh *et al.,* 2013). Link between aS aggregation and PD was further strengthened with the identification of several PD kindreds with triplication (Farrer *et al.,* 2004 and Singleton *et al.,* 2003) or duplication of the aS gene (Chartier-Harlin *et al.,* 2004). In vitro, increased concentrations of aS have been shown to promote the polymerization into fibrils (Wood *et al.,* 1999), and patients with a gene triplication have greater disease severity and younger age of onset than those with gene duplication, suggesting a possible "*SNCA* gene dosage effect" leading to PD (Singleton and Gwinn-Hardy, 2004). Furthermore, these findings indicate that a 50% increase in the expression of aS due to gene duplication is sufficient to cause disease and is consistent with the aggregation of α-synuclein contributing to disease (Jason et al.,2011).

1.2.4 Aggregation process

Some pathologies, as for example Alzheimer disease, PD and Prion diseases are associated with the formation of protein aggregates that form large deposits (Koo *et al.,* 1999; Serpell, 2000). Each amyloid disease involves predominantly the aggregation of a specific protein, although a range of other components including are incorporated into the deposits *in vivo*. The aggregation process of aS was extensively studied as aS amyloid fibrils were observed in LBs (Fig. 1.1).

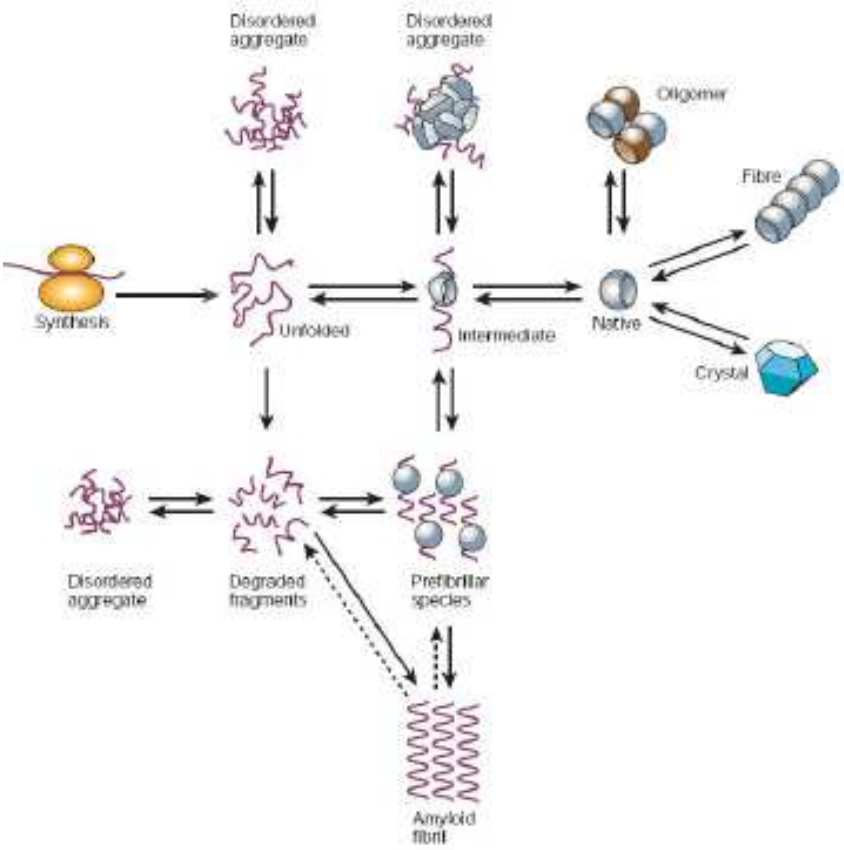

Fig. 1.8. Conformational states of a protein in a cell and subsequent destinies (From Dobson, 2003). The unfolded polypeptide chain can assume 3D structure after translation or it can be degraded or form amorphous aggregates. Intermediates can be assemble into prefibrillar species that lead to amyloid fibril formation.

Those macromolecular structures were reproduced *in vitro*, to be studied in order to identify their 3D structure. The *in vitro* kinetics of aS fibril formation show an initial lag-phase followed by an exponential growth phase and a final plateau, usually attributed to a nucleation-dependent polymerization. aS fibrils obtained *in vitro*, are formed by two or more filaments (Fig. 1.8). They typically vary in length from about 500 nm to 3 µm and, based on AFM analyses, have an average height of 9.8 ±1.2 nm (Fink, 2006; Khurana *et al.,* 2003). The core region of aS, defined by proteolysis studies, encompass the central, highly amyloidogenic NAC region (Miake *et al.,* 2002; Quin et al. 2007). EPR and site-directed spin labelling studies indicate that the fibril core is formed by parallel, in-register arrangement of multiple β-strands that run perpendicular to the fibril axis, where each layer contain a new molecules (Chen *et al.,* 2003). The fibril core is actually supposed to be constituted by five β-strands, as revealed by D/H exchange experiments (Vilar *et al.,* 2008; Karyagina *et al.,* 2011).

Even though the ability to form amyloid fibrils seems to be generic (Dobson, 2001), the propensity to do so under given circumstances can vary markedly between different sequences. The relative aggregation rates for a wide range of peptides and proteins correlates with the physicochemical features of the molecules such as charge, secondary-structure propensities and hydrophobicity (Chiti *et al.,* 2003). As already said, the *in vitro* kinetics of aS fibril formation show an initial lag-phase followed by an exponential growth phase and a final plateau (Fink, 2006). The lag-phase is due to the fact that the process is nucleation-dependent, meaning that the rate limiting step is the formation of a nucleus composed of a critical numbers of monomers (Wood *et al.,* 1999; Murphy, 2007). The constitution of the nucleus is hosted, as monomers has to be in those rare and limited conformations prone to a stable interaction once contact has occurred each other. However, once this passage has been achieved, elongation or enlargement is a thermodynamically favoured process. Uversky and coworkers showed that early stages of fibril formation involve the partial folding of aS into the highly fibrillation-prone pre-molten globule-like conformation, which represents a key intermediate on the fibrillation pathway (Uversky et al. 2001, Fink, 2006). Hence, factors that shift the equilibrium in favor of this partially folded conformation facilitate fibril formation. Thus, an increase in protein concentration is predicted to increase the concentration of the intermediate, and so the rate of fibrillation (Uversky *et al.,* 2001). Since, as previuosly reported, the unstructured monomer presents long-range interactions between the C-terminal and the central NAC regions (Bertoncini *et al.,* 2005), an event that leads to the formation of an unfolded state should be expected prior to the aggregation. Moreover, it has been recently suggested that aS could be folded as an α-helical tetramer (Bartel *et al.,* 2011; Wang *et al.,* 2011). The aggregation-prone conformation may be attained early in the aggregation pathway, through the exposition of the hydrophobic NAC region and facilitating aggregation (Paleček *et al.,* 2008). To favor the aggregation prone conformation, structural perturbations are necessary. They could be caused by different conditions, including for example the presence of positively charged ions able to interact with the C terminus, a decrease in pH that reduce the net charge of the C-terminal region, and the deletion of the C terminus, result in a more rapid aggregation reaction (Hoyer *et al.,* 2004). Even when the partially unfolded states is reached, the probability of interaction of two of pre-molten globule species is low, but it may occur the case in which

stable hydrogen bonds formation is established. Later, dimers can form stable contacts with other units, and oligomers start to grow. Soluble oligomers convert to fibrillation intermediates, designated protofibrils (Harper *et al.,* 1997). Analysis by TEM and AFM has revealed that different final product may arise from the aggregation of aS depending on the experimental conditions: fibrils, oligomers, and insoluble amorphous aggregates (Fink, 2006). Although the central role of aS fibrillation in the pathogenesis of PD is well established, it has been demostrated that aS fibrils may not be the toxic species, but may also have a protective role. On the contrary, soluble oligomers and protofibrils seem to be the toxic species (Volles *et al.,* 2002). The oligomeric species of aS present during the lag-phase of the aggregation process are relatively unstable, transient and present at very low steady-state concentrations (Goldberg *et al.,* 2000). As a result of the unstable and transient nature of these intermediates, the direct detection and characterization of prefibrillar oligomeric species oculd be extremely difficult. Several oligomeric prefibrillar species with various morphologies have been described (Conway et al. 1998, 2000; Ding et al. 2002; Lashuel et al. 2002, Apetri et al. 2006). These species are usually characterized by extensive β-structure and sufficient structural regularity to bind Thioflavin-T (ThT) and Congo Red (CR) (Chiti & Dobson, 2006). However, some types of oligomers are unable to bind Thioflavin T ThT and CR (Apetri *et al.,* 2006). Indeed several oligomeric species have been identified by different techniques: photo-induced cross-linking of aS (Li *et al.,* 2006); electrochemical techniques (Paleček *et al.,* 2007); intrinsic tryptophan fluorescence of Y39W aS (Dusa *et al.,* 2006) and FRET measurements (Kaylor *et al.,* 2005); fluorescence of pyrene-labeled aS (Thirunavukkuarasu *et al.,* 2008). Structured protofibrillar species could form from the reorganization or assembly of small and relatively disorganized oligomers that are formed rapidly after the initiation of aggregation process. In Fig. 1.8 a schematic representation of the hypothetical aggregation pathways of aS is reported. Moreover, also stable oligomers with very slow rates of dissociation, have been decribed. These oligomers could arise as a consequence of different mofications, sucha as oxidation of the four methionine residues to methionine sulfoxide (Hokenson *et al.,* 2004), specific nitration of the tyrosine residues (Uversky *et al.,* 2005) and covalent modification by 4-hydroxynonenal (Qin *et al.,* 2006). Typically these oligomers are formed more rapidly than fibrils and, as a consequence, no significant fibrillation occurs from these modified forms of aS.

1.2.5 Factors that influence aS aggregation process

Even if the comprehension of the aggregation and fibril formation processes is incomplete, several factors have been reported to have an influence on the aggregation pathway and kinetic, with inhibiting or promoting effects. As previously said, aS undergoes a nucleation dependent mechanism of aggregation, so that every factor that can increase the probability of the acquisition of an aggregation-prone conformation, enhance fibrillogenesis. For example, a promoting factor could be the increase in temperature, that is directly correlated with kinetic energy of molecules and also to enhanced reactivity of species. Also a high protein concentration could increases the probability of oligomers formation because conformers able to form the critical nucleus are more concentrated, and this explain the effect of a familiar form of PD due to the triplication of aS, that leads to autosomal dominant PD (Singleton *et al.,* 2004). As a consequence of the partial stability due to the interaction between different regions of aS, proteolytic cleavage of aS, revealed to occur naturally in neuronal cell (Li *et al.,* 2005), increases fibrillogenesis. Specifically, by *in vitro* studies, C-terminal truncation has been reported to enhance fibril formation of aS by exposition of hydrophobic NAC region (Crowther *et al.,* 1998; Hoyer *et al.,* 2004). Also ionic strength enhances fibrillogenesis, since it masks C-terminal negative charges, disrupting tertiary contacts between N-terminal and the C-terminal of the protein, thus leading to exposition of hydrophobic patches (Hoyer *et al.,* 2004). Other mechanisms that involve charge and so the tertiary contacts, is pH. The isoelectric point of aS is 4.6: so more acidic pH leads to disruption of contacts between C-terminal tail and positive charges N-terminal region (Uversky *et al.,* 2001b). Among molecules that enhance aggregation propensity of aS, there are lipids, expecially in the case of polyunsaturated fatty acids like arachidonic acid and docosohexaenoic acid (Perrin *et al.,* 2001). High protein:lipid molar ratio increases fibril formation probabilities (Zhu *et al.,* 2003): lipid membranes could recruite aS molecules and, enhancing local protein concentration, favor protein-protein interaction. Other involved molecules could be proteins that have been identified to stimulate aS in vitro aggregation at substoichometric concentrations, like tau (Norris & Giasson, 2005), histones (Goers *et al.,* 2003), brain specific protein p25α (Lindersson *et al.,* 2005) and tubulin (Alim *et al.,* 2002). Some post-trasductional modifications seem to enhance aS fibril formation propensity. As an example, aS is predominantly present as non-

phosphorylated in normal *in vivo* conditions, but Ser129 phoshorylation forms occur in aS inclusions in post-mortem patients brains (Fujiwara *et al.,* 2002). *In vitro*, Ser129 phoshorylation was found to increase the formation of aS mature fibrils. The demonstration of oxidatively nitrated aS in the syucleinopathic inclusions suggests that oxidative insults may be relevant to the pathogenesis (Duda *et al.,* 2000b; Giasson *et al.,* 2000). Moreover, aS modified by oxidative attachment of a dopamine adduct results in a stabilization and subsequent accumulation of aS oligomers (Conway *et al.,* 2001).

1.3. SYNUCLEIN AND LIPIDS

Although the regognized role of aS in neurodegeneration, its physiological function remains poorly understood (Bendor *et al.,* 2013). Recent studies pointed out that aS interferes with vesicles-trafficking pathways (Lashuel *et al.,* 2013). Scott and colleagues, coupling α-synuclein overexpression and knock-out model-system, reported that aS attenuates the mobility of recycling pool vesicles and maintains the overall size of these vesicles. Specifically, overexpression of aS leds to smaller vesicles and inhibited intersynaptic trafficking, while an absence of aS leads to larger vesicles size and enhanced intersynaptic trafficking. (Scott *et al.,* 2012). aS seems to have a chaperone activity, since it directly binds SNARE-protein synaptobrevin-2/vesicle-associated membrane protein 2 (VAMP2) and promotes SNARE-complex assembly (Burrè *et al.,* 2010). Moreover, in triple-knockout mice, lacking synucleins, the absence of the proteins cause the development of age-dependent neurological impairments, consinsting in decreased SNARE-complex assembly, and premature death (Burrè *et al.,* 2010). On the contrary, also membranes seem to have an effect on aS, especially influencing its aggregation kinetic, with difference depending on the membrane composition (Beyer *et al.,* 2007).

1.3.1 Structural features

A variety of observations suggest that aS, in the cytosol, is normally divided between a helix-rich, membrane-bound and a disordered cytosolic form, a behaviour apparently conferred by structural similarity to the exchangeable apolipoproteins (Perrin *et al.,* 2000). Indeed, aS contains class A2 lipid-binding helices: similarly to this "class A2" helical binding mechanism, lipid association is disrupted by introduction of charged residues along the hydrophobic face of the predicted alpha-helix and also by biotinylation of conserved lysines (which line the interfacial region). aS is able to undergo a large conformational change in the presence of specific phospholipids, ability that is presumed to be related to its functions (Perrin et al.,2000). Structural features of aS allow it to bind to synthetic vesicles containing acidic phospholipids and to cellular membranes with preferences towards acidic detergents like sodium dodecyl sulphate, and phospholipids, like phosphatidylserine (PS), phosphatidylglycerol (PG) and phosphatidyc acid (PA) composed vesicles, or mixture with neutral phospholipids (phosphatidylcholine (PC) and phosphatilylethanolamine (PE)) (Davidson *et al.,* 1998; Zhu & Fink, 2003; Zhu *et al.,* 2003;

Rhoades *et al.,* 2006). In presynaptic termini, monomeric α-synuclein exists in equilibrium between free and membrane- or vesicle-bound states (McLean *et al.,* 2000). This equilibrium is tightly regulated, and it has been estimated that approximately 15% of α-synuclein is membrane-bound within the synaptic termini (Lee *et al.,* 2002). aS binding to the membranes is accompanied by an increase in α-helix content (Perrin *et al.,* 2000; Davidson *et al.,* 1998): different helical structures form upon membrane binding, depending on the composition of the membrane. One well-studied form occured in the presence of SDS micelles that led to the formation of two anti-parallel curved α-helices (Val3-Val37 and Lys45-Thr92) connected by a well-ordered, extended linker, and followed by another short extended region (Gly93-Lys97) (Ulmer *et al.,* 2005). The well ordered conformation of the helix-helix connector indicates a defined interaction with lipidic surfaces. Other α-helix structure have been reported, such as a single curved α-helix encompassing residues 1–90 (Jao *et al.,* 2008; Lokappa and Ulmer, 2011). Also a non-canonical α-helix model has been reported, characterized by a periodicity of 11/3 (Figure 1.9 incollata qui sotto), to better arrange to membrane placing lysine residues on the interface between solvent and membrane surface: in this model lysine's ε-amino groups are responsible of the electrostatic interaction with negative charged headgroups of phospholipids, while the acylic chain suits well in the hydrophobic environment due to lipids tails (Bussell & Eliezer, 2003; Bussell *et al.,* 2005; Jao *et al.,* 2004; 2008).

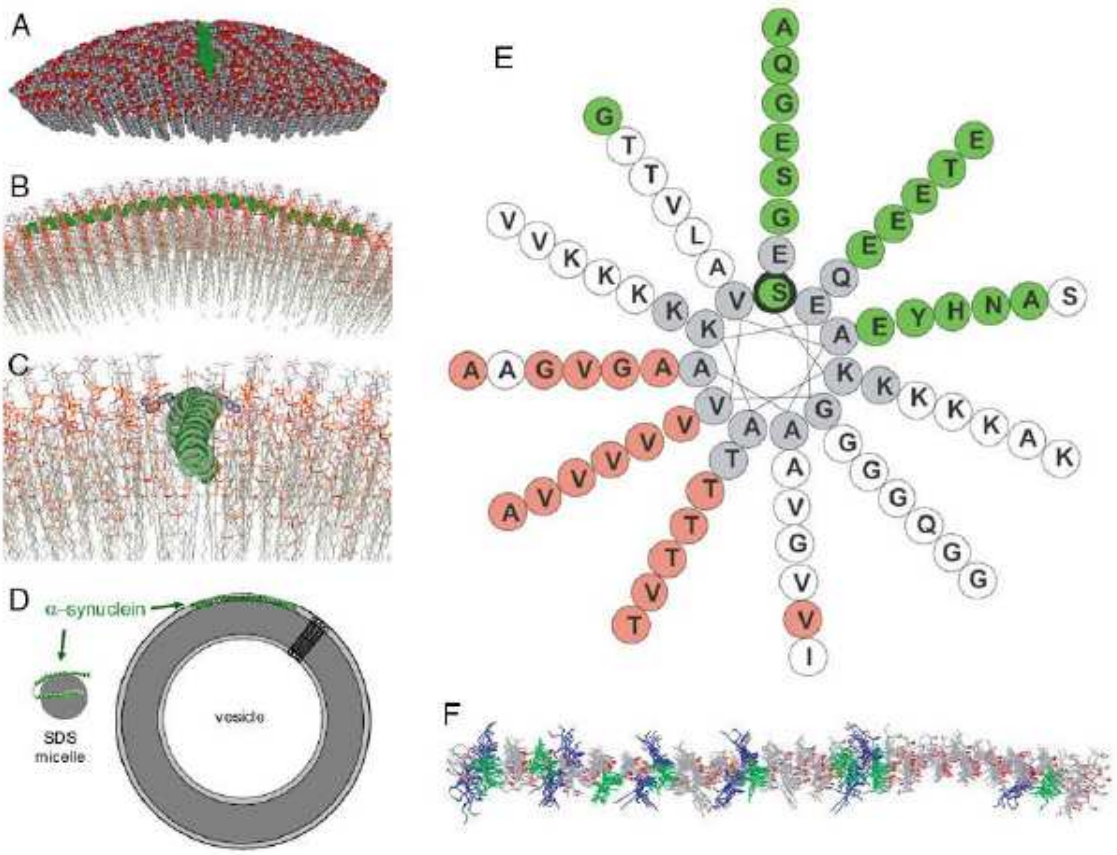

Fig. 1.9. aS binding model to lipid vesicles. **A** and **B** are representations of the interaction of aS with a curved membrane. **C** is a more detailed view of this protein -lipid interaction. **D** schematic representation of aS structure on SUV or on micelles, that differs from large vesicles because highly curved micelles can not accomodate the extended helical structure as in A and B. **E** helical wheel in wich 11 amino acid residues make up three turns. In this way, a lipid-exposed side (red) and solvent-exposed side (green) are formed. **F** view of the overlaid structures from above the lipid surface. In blue, te 11 lysine residues, that are oriented approximately perpendicular to the helical axis (reprinted from Jao *et al.,* 2008).

1.3.2 aS influence on lipid bilayers

aS interaction with membranes strogly influences the lipid bilayer structure (Madine *et al.,* 2006). Using 2H- and 31P-NMR spectroscopy it has been shown that the association of aS with negatively charged membranes can disrupt the integrity of the lipid bilayer, while it has little effect on membranes of zwitterionic phospholipids. (Madine *et al.,* 2006). Two different region of aS show preference for different membrane surface charge: the peptide aS (10−48), a lysine-rich peptide of the N-terminal region, associates with negative lipid, while peptide aS(120−140), a glutamate-rich peptide in the C-terminal region, weakly associates with lipid headgroups but with a slightly higher affinity for membranes with no net surface charge than for negatively charged membrane surfaces. Binding of these peptides to lipid vesicles do not disrupt the lamellar structure of the

membranes, but both peptides induce the lateral segregation of the lipids into clusters of acidic lipid-enriched and acidic lipid-deficient domains. This finding is really important because it could reveal the function of aS: it has been speculated that the N-terminal and C-terminal domains of aS might act in concert to organize membrane and play a role in presynaptic vesicle synthesis, maintenance, and fusion (Madine *et al.,* 2006). Another consequence of aS bound to lipids that could be related to aS function, is the prevention of lipids oxidation (Breydo *et al.,* 2012). The antioxidant function of aS could be attributed to its facile oxidation *via* the formation of methionine sulfoxide. Monitoring the lipid oxidation kinetics in the absence and in the presence of aS, Zhu et colleagues find that monomeric aS prevent unsaturated lipid oxidation while aS fibrils do not (Zhu *et al.,* 2006). The inhibition of lipid oxidation by aS may be a physiological function of the protein (Zhu *et al.,* 2006).

1.3.3 Lipids influence on aS properties

Membranes and aS fibrillogenesis are correlated in two ways: lipids influence aS aggregation and, viceversa, oligomeric species of aS seem to exert their toxic activity on membranes. aS-lipids interaction, causing rearrangement of the structure of aS, influences aS aggregation kinetic. Indeed, it has been reported that the interaction of α-synuclein with the membranes alters the kinetics and pathways of its aggregation *in vitro* (Breydo *et al.,* 2012). Lipids seem to act as anti-chaperones facilitating protein transition into partially folded states more prone to aggregate. The effects of membrane binding varied, from inhibition (Zhu and Fink 2003) to acceleration (Necula *et al.,* 2033) of aS aggregation, (Zhu *et al.,* 2003a; Zhu *et al*., 2003b)and (Jo *et al*., 2000). These opposite effects primarly depend on the protein-lipid molar ratio. Low concentration of fatty acids accelerate aggregation of aS (Necula *et al.,* 2003), probably because membrane-bound α-synuclein can generate nuclei that seed the aggregation of the more abundant cytosolic form (Lee *et al.,* 2002). On the contrary, higher fatty acids concentration induces total aS conversion to the α-helical membrane-bound form, that is unlikely to contribute to aggregation and fibril formation (Zhu *et al.,* 2003b). These observations suggest that the initial phases of aS aggregation may occur on the surfaces of membranes and thus pathological conditions that induce cross-linking of synuclein, such as oxidative stress, may enhance the propensity for aggregation (Cole *et al.,* 2002). Indeed, detection of

oligomeric form of aS formed in the presence of lipids has been reported both *in vivo* and *in vitro* (Sharon *et al.,* 2003; De Franceschi *et al.,* 2011). Specifically, polyunsaturated fatty acid (PUFA), such as arachidonic and docosahexaenoic acids, have been linked to aS oligomerization, also at physiological concentrations (Perrin *et al.,* 2001). However, it has been reported that experimental conditions strongly influenced the structure and heterogenicity of oligomers of aS formed in the presence of lipids (Haque *et al.,* 2010).

1.3.4 Role of fatty acids

Multiple studies have documented interactions of aS with free fatty acids, but the physiological consequences are still not fully understood (Ruipérez *et al.,* 2010). Perrin and coworkers (2001) showed that *in vitro* exposure to vesicles containing certain polyunsaturated fatty (PUFAs) causes the formation of aS oligomers at physiological concentrations. It has been reported that aS interacts with PUFAs in vivo to promote the formation of highly soluble oligomers that precede the insoluble aS aggregates associated with neurodegeneration . Indeed, soluble oligomers of aS were found in the cytosol of mesencephalis neuronal cells derived from murine (normal or aS-transgenic) and human (normal or PD affected) brains. Interestingly, exposure of cells to PUFAs increased aS oligomers levels, while saturated or monounsaturated FAs did not. In addition to the degree of saturation, the length of the carbon chain was important for alpha-synuclein oligomerisation (Sharon *et al.,* 2003). These results have been confirmed *in vitro*: PUFAs, depending on unsaturation and carbon chain length, influence aS aggregationlead to the formation of cytotoxic oligomers (Assayag *et al.,* 2007). Upon interaction with DHA, the normally unstructured α-synuclein rapidly adopts an α-helical conformation. This effect has been observed in the presence of both arachidonic acid or docosahexaenoic acid, but not in the presence of saturated fatty acids (Broersen *et al.,* 2006). The study of DHA is especially important since DHA accounts for 60% of all esterified fatty acids in neuronal plasma membrane (Lukiw *et al.,* 2008). Moreover, the levels of this fatty acid in a non-esterified form appear to be elevated in patients affected by Parkinson's disease (Sharon *et al.,* 2003) and it has also been reported that DHA intake increases expression of aS gene, and in turn aS allows DHA to be present in a soluble rather than micellar form. For these reasons, interest growth on the study of the mode of interaction of aS and DHA: It has been reported that the N-terminal alpha-synuclein fragment of approximately 70–80

amino acids was most resistant to proteolysis in the presence of docosahexaenoic acid, suggesting that PUFAs interact with the N-terminus of the protein (De Franceschi *et al.,* 2009). Recent studies implicated aS specifically in regulation of fatty acid metabolism. Mice lacking the alpha-synuclein gene exhibited reduced incorporation of arachidonic acid (AA) into brain phospholipids, and a simultaneous riseof about 50% in incorporation of docosahexaenoic acid (Golovko *et al.,* 2007). Because AA and DHA are the major polyunsaturated fatty acids in the brain, the increase in DHA incorporation into brain phospholipids is considered to be compensatory for the reduction in rate of AA incorporation into these lipid pools, since both FAs use the same sn-2 position of phospholipids. Further genetic studies in mice have suggested a role for alpha-synuclein in substrate presentation to acyl-CoA synthetase (ACSL), a critical enzyme in the fatty acid re-acylation pathway. The ablation of alpha-synuclein decreased ACSL activity (Golovko, *et al.,* 2006). Importantly, addition of physiologically relevant concentrations (3.15–6.3 nM) of aS WT, but not mutant aS, restores AA-CoA formation in aS KO mice: mutant forms of aS (A30P, E46K, and A53T) fail to modulate acyl-CoA synthetase (Acsl) activities, indicating that expression of these forms may cause a loss of function. Alpha-synuclein was shown to specifically modulate activity of the ACSL6 isoform which is responsible for arachidonic acid incorporation into phospholipids (Golovko *et al.,* 2009). Since aS is a FA binding protein, several studies analyzed consequences on FA incorporation in the absence of aS. Barcelo and colleagues reported that in ethanolamine glycerophospholipids and phosphatidylserine, docosahexaenoic decreases of about 7% (Barcelo-Coblijn *et al.,* 2007). Into astrocytes of WT and aS-KO mice (68), aS deficiency decreased PA and AA incorporation of about 31% and 39%, respectively, while DHA incorporation was unaffected. In the phospholipid fraction, a decreased distribution into this lipid pool of these fatty acids, including DHA, was found (Castagnet *et al.,* 2005). In cells treated with high concentrations of fatty acids, aS WT was found to associate also with lipid droplets, specifically it seems to accumulate on phospholipid monolayers surrounding triglyceride-rich lipid droplets and was able to protect stored triglycerides from hydrolysis (Cole *et al.,* 2002). Treatment of aS-expressing HeLa cells with high levels of oleic acid, determined an increase in the formation of lipid droplets and translocation of aS from the cytosol to the surface of lipid droplets. Interestingly, PD mutant synucleins showed variable distributions on lipid droplets and were less effective in regulating

triglyceride turnover. Also small aS oligomers detected in cells, primarily dimers and trimers, were associated with lipid droplets and cell membranes, suggesting that the initial phases of synuclein aggregation may occur on the surfaces of membranes (Cole *et al.,* 2002). Another important aspect involving FA is the oxidative stress damage. Neurons are particularly susceptible to injury by oxidative stress beacuse of low defence mechanisms and the high rate of oxygen consumption (Ruiperez *et al.,* 2011). Among brain lipids, PUFAs are particularly vulnerable to oxidation due to their unsaturated bonds (Fig. 1.10). Of note, several studies suggest that aS may be neuroprotective toward oxidative stress. Indeed, aS levels increase in neurons exposed to chronic oxidative (Quilty *et al.,* 2006) However, these study do not expalin whether these aS changes are cytotoxic or neuroprotective. It was also proposed that aS could directly prevent oxidation of PUFA, via the formation of methionine sulfoxide, acting as scavengers of ROS (Zhu *et al.,* 2006). These findings suggest that the inhibition of lipid oxidation by α-synuclein may be a physiological function of the protein.

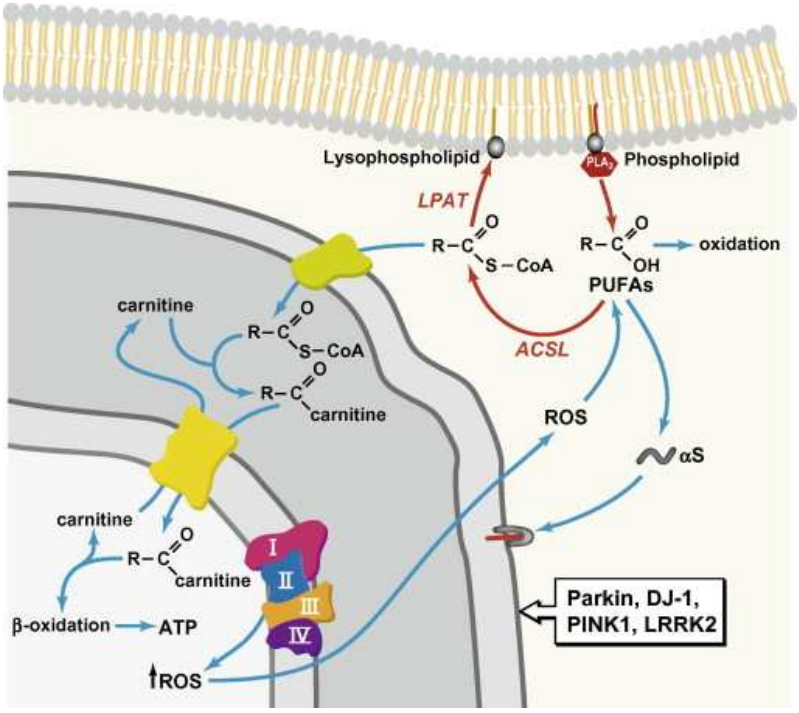

Fig. 1.10. Metabolism of polyunsaturated fatty acids (PUFAs). PUFAs are released from phospholipid membranes through the action of PLA_2. Alpha-synuclein (αS) binds free PUFAs changing its conformation. PUFAs are reincorporated into phospholipids through the action of acyl-CoA synthetases (ACSL) and lysophosphatidyl acyltransferases (LPAT). PUFAs are also transported into mitochondria (bottom left) for degradation generating ATP with a minor production of reactive oxygen species (ROS). PUFAs can be oxidized into eicosanoids through enzymatic actions and also converted into oxidized species in uncontrolled ROS reactions. The interaction of alpha-synuclein with PUFAs (oxidized or not) could lead to mitochondrial changes. Proteins Parkin, DJ-1, PINK1 and LRKK2 are implicated in the regulation of mitochondrial functions. Mutations in these proteins lead to inherited Parkinson's disease (reprinted from Ruiperez *et al.,* 2011).

2. Materials and Methods

2.1 Materials

DHA and fluorescein isothiocyanate dextran (FITC-Dextran) of average molecular weight of 10,000 Da were purchased from Sigma Chem. Co. (St. Louis, MO). Trypsin from bovine pancreas, and thioflavin-T (ThT) were purchased from the Sigma Chemical Company (St. Luis, MO), whereas acetonitrile and triluoroacetic acid (TFA) from Fluka (Buchs, Switzerland). All other chemicals were of analytical reagent grade and were obtained from Sigma or Fluka.

The lipids, 1-palmitoyl-2-oleoyl-*sn*-glycero-3-phosphocholine (POPC), 1,2-dioleoyl-*sn*-glycero-3-phospho-(1'-rac-glycerol) (DOPG), 1-palmitoyl-2-oleoyl-*sn*-glycero-3-phospho-L-serine (POPS), 1-palmitoyl-2-oleoyl-*sn*-glycero-3 phosphoethanolamine (POPE) and Brain Total Lipid Extract, were obtained from Avanti Polar Lipids (Alabaster, AL) as chloroform solution and used without further purification.

2.2 Methods

2.2.1 Expression and purification of recombinant aS and aS mutants

Human aS cDNA was amplified by PCR with synthetic oligonucleotides (Sigma-Genosys) containing NcoI and XhoI restriction sites and designed to obtain the entire sequence of the protein (aS/E46K/A30P/A53T/H50Q 1-140). After digestion with restriction enzymes, the two PCR products were subcloned into the NcoI-XhoI-linearized pET28b expression plasmid (Novagen) and introduced into an Escherichia coli BL21(DE3) strain.

Overexpression of proteins was achieved by growing cells in LB medium (1% Bacto tryptone, 0.5% yeast extract, 0.5% NaCl) at 37 °C to an OD600 of 0.6-0.8 followed by induction with 0.5 mM isopropyl β-thiogalactopyranoside for 4 h.

The purification of aS and its mutants was conduced following this procedure. After osmotic rupture of cells, centrifugation was used to separate lipid and contaminants. After boiling of cell proteic content for 15 min, the soluble fraction, containing the protein, was treated with 55% ammonium sulphate. The pellet was then resuspended, dialyzed and loaded into a Resource Q 6-ml column (Amersham Biosciences) and then eluted using 20 mM Tris buffer, pH 8, with a linear gradient 0-500 mM NaCl.

Further purifications were obtained by RP-HPLC. aS was purified in a Jupiter-C4 column (4.6 x 150 mm) (Phenomenex, CA, USA) eluted with a linear gradient of water (0.1 % TFA), versus acetonitrile (0.085 % TFA) from 5% to 38% in 5 min and from 38% to 43% at a flow rate of 0.6 ml/min. All aS mutants were expressed and purified following the same protocol. Finally, the proteins were lyophilized and stored at -20 °C.

2.2.2 Aggregation studies

In order to analyze the aggregation process of aS, lyophilized protein obtained from purification was dissolved in PBS phosphate buffer (8 mM Na2HPO4, 137 mM NaCl, 2 mM KH2PO4, 2.7 mM KCl), pH 7.4, and filtering the protein solution with a 0,22 µm pore-size filter (Millipore, Bedford, MA, USA). Dissolved samples were incubated at 37 °C at a protein concentration of 50 µM (0.723 mg/ml), under shaking at 500 rpm with a thermo-mixer (Compact, Eppendorf, Hamburg, DE). The same experiment has been conduced in parallel for A30P, A53T, E46K and H50Q mutants, with or without DHA.

2.2.3 Circular Dichroism

Protein concentrations were determined by absorption measurements at 280 nm using a double-beam Lambda-20 spectrophotometer from Perkin Elmer (Norwalk, CT). The extinction coefficients at 280 nm were 5960 M^{-1} for aS and mutants, as evaluated from their amino acid composition by the method of Gill and von Hippel (1989).
Circular dichroism spectra were recorded on a Jasco J-710 (Tokyo, Japan) spectropolarimeter. Far-UV CD spectra were recorded using a 1 mm path-length quartz cell and a protein concentration of 5 μM. The mean residue ellipticity [θ] (deg·cm2·dmol–1) was calculated from the formula [θ] = (θobs/10) ·(MRW/lc), where θobs is the observed ellipticity in deg, MRW is the mean residue molecular weight of the protein, l the optical pathlength in cm and c the protein concentration in g/mL. The spectra were recorded in PBS buffer, pH 7.4, both in the presence of different concentration of DHA (ranging from 0-400 μM) and during aggregation studies.

2.2.4 Gel filtration

Gel filtration chromatography (or size exclusion chromatography) was performed with a Superdex 75 10/300GL column (Amersham Biosciences, Uppsala, Sweden), using an ÄKTA FPLC system (Amersham Biosciences, Uppsala, Sweden). The matrix is composed of cross-linked agarose and dextrane with an average particle size of 13 μm and a 3-70 KDa separation range for globular proteins. The hydrodynamic volume of analytes was determined on the base of the the distribution coefficient, Kd, calculated as the following formula: Kd= (Ve-Vo)/(Vt-Vo), where Ve, Vt and Vo are respectively the analyte elution volume, total and void volume. If the analyte is large and completely excluded from the mobile phase within the gel, Kd = 0 whereas, if the analyte is sufficiently small to gain complete access to the inner mobile phase, Kd = 1. Due to variation in pore size between individual gel particles, there is some inner mobile phase that will be available to analytes of intermediate size; hence Kd values vary between 0 and 1. It is this complete variation of Kd between these two limits that makes it possible to separate analytes within a narrow molecular size range on a given gel.
A calibration controls with globular proteins of known MW was performed. 50 μg of each of the following standard calibration proteins were loaded: bovine α-lattalbumine (MW= 14 kDa), carbonic anhidrase (MW= 29 kDa), ovoalbumin (MW= 45 kDa), BSA(MW= 66 kDa), thyroglobulin (MW= 440 kDa) , β-amilase (MW= 200 kDa) and ferritin (MW= 669 kDa). 200 μg of blue dextran and 0.05% dimethyl sulfoxide (DMSO) were loaded to estimate the void and total volume of the column, respectively. The elution was monitored by recording on-line the absorbance at 214 nm. In order to characterize aS and its mutants behaviour in solution, 144 μg of proteins at different time of incubation were loaded.

2.2.5 RP-HPLC

Reversed-phase high-performance liquid chromatography (RP-HPLC) involves the separation of molecules on the basis of hydrophobicity. The separation depends on the hydrophobic binding of the solute molecule from the mobile phase to the immobilized hydrophobic ligands (n-butyl, n-octyl and n-octadecyl) attached to the stationary phase. This one usually consists of an n-alkylsilica-based matrix from which the solutes are eluted with gradients of increasing concentrations of organic solvent such as acetonitrile. A charged ion-pairing reagent (TFA, trifluoroacetic acid) with an opposite charge to that of

the protein is added to the mobile phase to form a noncharged complex. TFA increases the idrophobicity and consequently the retention of the protein, indeed if it is added in a concentration of 0.085% (v/v), the pH is around 2.5. At this pH, the carboxylic groups of protein are protonated and the trifluoroacetic anion binds to the positively charged amino groups of proteins. Elution proceeds by application of a gradient of increasing organic solvent concentration, which competes with the stationary phase for hydrophobic interaction with the analyte.
The HPLC analyses of aggregated samples were conducted using a Jupiter C4 column (4.6 mm × 150 mm; Phenomenex, CA, USA), eluted with a gradient of water/0.1% TFA vs acetonitrile/0.085% TFA from 5% to 38% in 5 min, from 38% to 43% in 15 min. The elution was monitored by recording the absorbance at 226 nm. The identity of the eluted material was assessed by mass spectrometry.

2.2.6 SDS-PAGE

SDS-PAGE was conducted following the method of Laemmli (1970). In SDS polyacrylamide gel electrophoresis (SDS-PAGE), charged proteins migrate in response to an electric field. Their rate of migration depends on the strength of the field and on the net charge, size and shape of the molecules. Since different proteins with similar molecular weights may migrate differently due to their differences in secondary, tertiary or quaternary structure, sodium dodecyl sulphate (SDS), an anionic detergent, is used in SDS-PAGE to reduce proteins to their primary (linearized) structure and coat them with uniform negative charges. Polyacrylamide gels restrain larger molecules from migrating as fast as smaller molecules. Because the charge-to-mass ratio is nearly the same among SDS-denatured polypeptides, the final separation of proteins is dependent almost entirely on the differences in relative molecular mass of polypeptides. Electrophoresis experiments were conducted with the Mini-Protean II electrophoresis system purchased from Biorad using plates of 5 x 8 cm and spacer of 0.75 mm thickness. For the separation of proteins the gel was composed by 13 % T (% total acrylamide and bis-acrylamide). The electrophoretic buffer (Laemmli buffer) composition was: 25 mM Tris-HCl, 0.25 M glycine, 0.1% SDS, pH 8.5. The acrylamide polymerization was obtained by adding TEMED and 10% solution of ammonium persulfate (APS). Samples were dissolved in 50 mM Tris-HCl, pH 6.8, containing 2% SDS, 2% β-mercaptoethanol, 10% glycerol, traces of bromophenol blue and denaturated by heating at 100 °C for 5 minutes. The electrophoresis was performed at room temperature at 25 mA.

2.2.7 Native-PAGE

Native (non-denaturing) polyacrylamide gel electrophoresis was conducted with the Mini-Protean II electrophoresis system purchased from Biorad using plates of 5 x 8 cm and spacer of 0.75 mm thickness. For the separation of proteins the gel was composed by 13 % T (% total acrylamide and bis-acrylamide). The electrophoretic buffer composition was: 25 mM Tris-HCl, 0.25 M glycine, pH 8.5. Samples were dissolved in 50 mM Tris-HCl, pH 6.8, containing 10% glycerol and traces of bromophenol blue. The electrophoresis was performed at room temperature at 25 mA.

2.2.8 Liposomes preparation

To prepare large and small unilamellar vesicles (LUV, SUV), lipids were transferred in glass tubes. Chloroform was dehydrated by gentle helium stream and then warmed at 45°C to remove residual organic solvent. The lipid film was hydrated with PBS pH 7.4 in the absence or presence of calcein (50 mM) or FITC-dextran (1.6 mM) at 40°C for 2 hours with frequent vortexing. Then it was subjected to 5 cycles of freezing and thawing. The suspension vesicles was extruded 11 times through a 400 nm or 30 nm pore size polycarbonate membrane on lipid extruder (Northern Lipids Inc, Vancouver, BC), in order to obtain LUVs or SUVs. Calcein-loaded and FITC-dextran-loaded vesicles were purified by gel filtration chromatography (Sepharose G-25) to remove unencapsulated dye. The final lipid concentration, determined as total phosphorus, was conducted according to Chen et al.2003.

2.2.9 Thioflavin T binding assay (ThT)

The ThT binding assays were performed accordingly to LeVine (1993) using a freshly prepared 25 μM ThT solution in 25 mM sodium phosphate (pH 6.0) that had been passed through 0.45 μm filters. Aliquots (30 μl) of protein samples from the aggregation incubation were taken at specified times and diluted into the ThT buffer (final volume 500 μl). Fluorescence emission measurements were conducted at 25°C using an excitation wavelength of 440 nm and recording the ThT fluorescence emission at 480 nm.

2.2.10 Dynamic Light Scattering (DLS)

DLS measurements were carried out with a Zetasizer Nano-S instrument (Malvern Instrument, UK). This apparatus, which uses the backscattering detection (scattering angle θ=173°) and an avalanche photodiode detector (APD), is equipped with a Helium–Neon laser source (wavelength 633 nm; power 4.0 mW), and a thermostated sample chamber controlled by a thermoelectric Peltier. DLS measurements were performed at 25°C in PBS pH 7.4 in duplicate. During every measurement 12 runs were collected.
DLS was used to check the size distribution and the stability of vesicles. DOPG LUV and SUV size distributions were measured for vesicles alone and after 30 min of incubation with oligomers.

2.2.11 Transmission Electron Microscopy

In order to evaluate the morphology and the size of the species deriving from the self-assembly of DHA and from the aggregation process of aS, aliquots of the samples were examined by transmission electron microscopy (TEM). The samples relative to aggregation of the proteins were diluted 3 times with PBS. A drop of the samples solution was placed on a Butvar-coated copper grid (400-square mesh) (TAAB-Laboratories Equipment Ltd, Berks, UK), dried and negatively stained with a drop of uranyl acetate solution (1%, w/v). TEM pictures were taken on a Tecnai G2 12 Twin instrument (FEI Company, Hillsboro, OR, USA), operating at an excitation voltage of 100 kV.

2.2.12 Mass spectrometry

Mass determinations were obtained with an electrospray ionization (ESI) mass spectrometer with a Q-TOF analyzer (Micro) from Waters Micromass (Manchester, UK). The measurements were conducted at a capillary voltage of 3 kV and a cone voltage of 35

V. The molecular masses of protein samples were estimated using the Mass-Lynx software 4.1 (Micromass).

2.2.13 Proteolysis

Proteolysis experiments were carried out on monomeric aS and aS mutants to analyze interaction with DHA, using proteinase K (Ebeling et al., 1974) at E/S ratio of 1:1000 (by weight). Experiments of proteolysis were conducted also on oligomeric samples of aS/DHA and H50Q/DHA, to identify aminoacidic residues modified by DHA, using Trypsin at a E/S ratio of 1:100 (by weight). All experiments were conduced in PBS, pH 7.4 and the reactions were quenched at specified times by acidification with TFA in water (4%, v/v) or by direct injection in RP-HPLC. All the proteolysis mixtures were analyzed by RP-HPLC. For all the proteins, the RP-HPLC analyses were conducted using a Vydac C18 column (4.6 mm x 250 mm; The Separations Group, Hesperia, CA), eluted with a gradient of water/0.1% TFA vs. acetonitrile/0.085% TFA from 5% to 25% in 5 min, from 25% to 28% in 13 min, from 28% to 39% in 3 min, from 39% to 45% in 21 min at a flow rate of 1 ml/min. Column was provided by a HPLC security guard column SAX (Phenomenex, USA). The sites of cleavage along the polypeptide chains were identified by mass spectrometry analyses of the protein fragments purified by RP-HPLC.

2.2.14 Ion exchange chromatography

Separation in ion exchange chromatography depends upon the reversible adsorption of charged solute molecules to immobilized ion exchange groups of opposite charge. Separation is obtained since different substances have different degrees of interaction with the ion exchanger due to differences in their charges, charge densities and distribution of charge on their surfaces. An ion exchanger consists of an insoluble matrix to which charged groups have been covalently bound. The charged groups are associated with mobile counter ions which can be reversibly exchanged with other ions of the same charge without altering the matrix. After sample injection, solute molecules carrying the appropriate charge displace counter-ions and bind reversibly to the gel, whereas unbound substances are washed out from the exchanger bed using starting buffer. Desorption of solute molecules is achieved by increasing the ionic strength of the eluting buffer.

The analyses of aS and aS/DHA were conducted using a Resource-Q column (Amersham Pharmacia), a strong anion column pre-packed with SourceTM. SourceTM is based on monodisperse, hydrophilized and rigid polystyrene/divinyl benzene beads, produced by substitution of the base matrices with quaternary amino groups (-O-CH2-CHOH-CH2-O-CH2-CHOH-CH2-N+(CH3)3). The eluting buffer used was 20 mM Tris pH 8 with a 30-minutes linear gradient 150-500 mM NaCl.

2.2.15 DNPH assay

2,4-Dinitrophenylhydrazine (DNPH) or Brady's reagent is a substituted hydrazine used to detect, in lateral chain of aminoacids, carbonyl groups such as aldehydes and ketones. aS monomers and aS/DHA oligomers purified by RP-HPLC were dried and resuspended in 2M HCl + 10mM DNPH, and then incubated for 1h at room temperature in the dark. To stop reaction, proteic material was precipitated with 15% trichloroacetic acid. After centrifugation, pellets were washed 3 times with a solution of ethanol:ethyl-acetate 1:1 and then dried. For RP-HPLC analysis, samples were re-hydrated in 0.1% TFA

and chromatograms were recorded both at 226 nm (to detect the proteic material) and 366 nm (to detect DNPH). Eluted fractions were analyzed by mass-spectrometry. For UV-Vis analysis, samples were resuspended in 6M Guanidinium chloride overnight and spectra were recorded from 380to 240 nm.

2.2.16 Atomic Force Microscopy

aS/DHA oligomers were diluted 500 times using Milli-Q water and 10 µl aliquots were deposited on freshly cleaved mica and dried under mild vacuum. Tapping mode AFM images were acquired in air using a Multimode scanning probe microscope equipped with an "E" scanning head (maximum scan size 10 µm) and driven by a Nanoscope IV controller (Digital Instruments, Bruker, Germany). Single beam uncoated silicon cantilevers (type Olympus OMCL-AC160TS, Olympus, Tokyo, Japan) were employed. The tip of the probe was of 7 nm.The drive frequency was between 280 and 300 kHz, and the scan rate was between 0.5 and 1.0 Hz. TEM pictures were taken on a Tecnai G^2 12 Twin instrument (FEI Company, Hillsboro, OR, USA), operating at an excitation voltage of 100 kV. Samples for TEM were diluted 2 times and a drop of the solution was placed on a Butvar-coated copper grid (400-square mesh) (TAAB-Laboratories Equipment Ltd, Berks, UK), followed by a drop of uranyl acetate solution (1% w/v).

2.2.17 Release Assays

For calcein release assay, SUV or LUV were diluted to 50 µM of lipids. After 30 minutes of incubation in the presence of different protein species (monomers, oligomers, fibrils), fluorescence emission at 515 nm was recorded after excitation at 490 nm. Maximum fluorescence emission was obtained by the addition of 0.1% Triton X-100 to disrupt vesicles. The average values of experiments, performed in triplicate, were expressed as a percentage of the maximum effect due to total vesicles disruption. FITC-dextran-loaded SUVs or LUVs were incubated for 30 minutes in the presence of the protein species at a final lipid concentration of 100 M. Released dye was detected by fluorescence measurement with excitation at 490 nm and emission at 515 nm, after purification of the incubated solution through Microcon (cutoff 50000) to allow FITC-Dextran elution. The minimum and maximum effect was obtained by measurement of a liposome solution respectively with or without 0.1% Triton X-100. The average values of experiments, performed in triplicate, were expressed as a percentage of the maximum effect calculated as total vesicles disruption obtained with Triton X-100.

2.2.18 Cell Permeabilization Assay

To examine whether aS/DHA oligomers can permeabilize cell membranes, we exploited the ability of propidium iodide (PI; MW 668.4 Da) to bind DNA as indirect reporter of membrane damage. Dopaminergic SH-SY5Y cells were cultured in 24-well plates (seeding density ~50000 cells/well) and twenty-four hours after seeding treated with 0.5 µM of aS monomer or aS/DHA oligomers. Impermeant dye PI (2 µg/ml) and counterstain dye Hoechst 33242 (2 µg/ml) were added to cells simultaneously to the treatment. After a 30 min-incubation at 37°C, PI-positive cells were counted in three replicate cultures, acquiring an average of 5 fields per culture (250-350 cells/field). The experiment has been repeated 3 times independently. Saponin (50 µg/ml) was used as positive control of membrane permeabilization.

2.2.19 Planar Lipid Membrane

Solvent-free Planar Lipid Membrane (PLM) was composed of equimolar mixture of 1,2-dioleyl-phosphatidyl-glycerol (DOPG) and 1,2-dioleyl-phosphatidyl-ethanolamine (DOPE) and formed on an aperture in a 25 μm thick Teflon septum separating two chambers, as described in Dalla Serra et al. [26]. Ionic currents were recorded by a patch clamp amplifier (VA-10X npi, Tamm, Germany), filtered at 100 Hz, digitalized and acquired at 2 kHz by the computer using DigiData 1322 A/D converter and pClamp software (Axon Instruments, Sunnyvale, CA).

3. aS/DHA OLIGOMERS CHARACTERIZATION

Multiple studies have documented interactions of aS with phospholipid membranes and free fatty acids even if the physiological consequences are not still understood. *In vivo*, almost the 15% of aS is supposed to be bound to lipid membranes (Lee *et al*., 2002). This binding leads the protein to acquire α-helix structure and can have consequences on its aggregation kinetic, inducing protein oligomerization or preventing amyloid formation (Breydo *et al.,* 2012). As previously reported (Sharon *et al.,* 2003; De Franceschi *et al.,* 2011), aS is able to bind brain fatty acid, such as DHA. We and others have shown that in the presence of DHA aS acquires α-helix structure and undergoes aggregation that rapidly leads to the formation of stable oligomers, that are toxic to cells (De Franceschi *et al*., 2011). A study on the kinetic of aggregation and on the properties of the species formed in the presence of DHA has been conducted by our group in a previous work, but some aspects remained unclear. Considering that the main objective of the present research was to define the activity of the oligomers formed in presence of DHA, a further characterization has been conducted. In particular, a new method for the isolation of the oligomers based on ion exchange chromatography have been proposed as alternative to the gel filtration. Other relevant aspects of this study regard the chemico-psysical characterization of the oligomers by using microscopy and spectroscopic techniques. Finally a large part of the research is dedicated to the analysis of the activity of oligomers on model membranes and cells to the aim to propose a possible mechanism of toxicity.

3.1 Aggregation process of aS in the presence of DHA and isolation of oligomers

aS aggregation is conducted in the presence of DHA, using a molar ratio protein:fatty acid of 1:50. Previously it was found that it was possible to monitoring the aggregation and to isolate oligomeric aS from monomeric one using gel filtration chromatography. In Fig. 3.1 the main points of the purification and chemical characterization are reported. The mixture of aS and DHA corresponding to 48 hours of incubation was used for the studies conducted here. The monomeric species elutes at 24 min, (Fig. 3.1 A). The oligomeric species (Fig. 3.1 A, dashed line), that elutes at 20 min,

increases on time. This fraction was analyzed by RP-HPLC for its identification and to provide further information about the chemical properties of oligomers (Fig. 3.1 B).

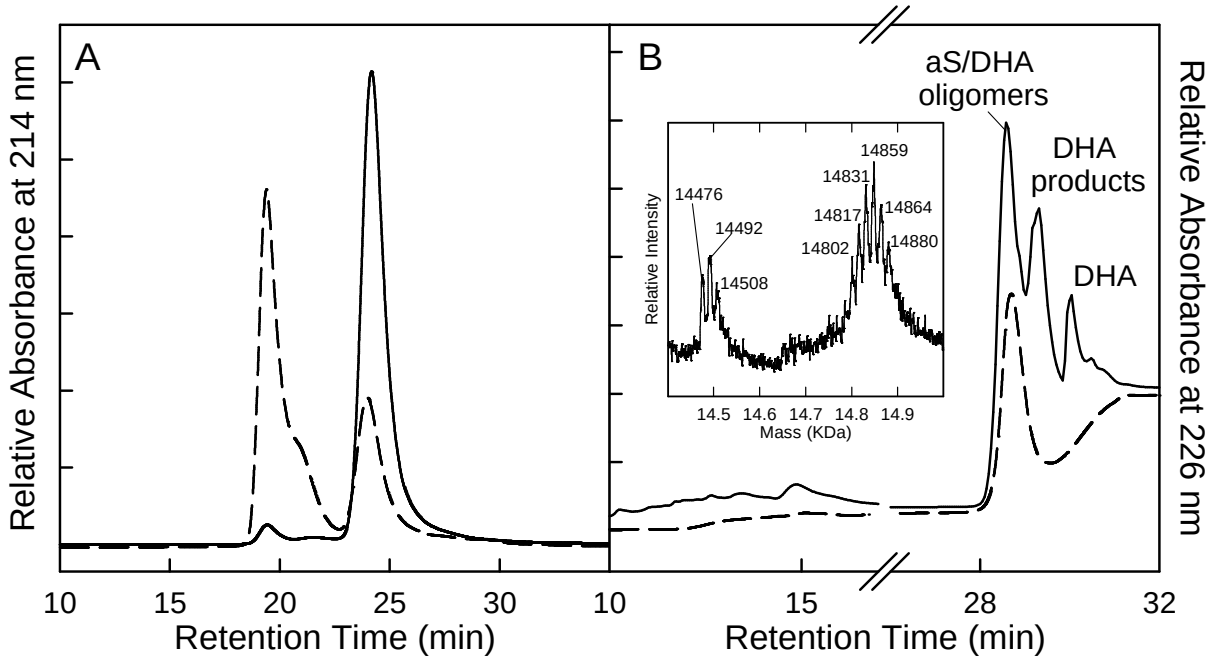

Fig. 3.1. Gel filtration (A) and RP-HPLC (B) chromatograms of aS/DHA mixture. (A) Gel filtration of aS in the absence (solid line) and in the presence (dashed line) of DHA in a molar ratio protein:lipid of 1:50. (B) RP-HPLC analyses were conducted using a Jupiter C4 column (4.6 x 150 mm; Phenomenex, CA, USA), eluted with a gradient of acetonitrile/0.085% TFA *vs* water/0.1% TFA from 5% to 38% in 5 min, from 38% to 43% in 15 min, recording the absorbance at 226 nm. The identity of the eluted material was assessed by mass spectrometry and the spectrum of oligomers (RT 29.5) is reported (inset).

RP-HPLC chromatograms of aS/DHA mixture after 48 hours of incubation shows the presence of the peak relative to oligomer eluting at 29.5 min and two peaks at higher retention time corresponding to DHA and DHA by-products. Oligomeric fraction eluted by gel filtration, shows the same species at 29.5 min but the other two peaks are absent, indicating that the GF step removes the free fatty acid. Mass spectrometry analysis of species eluted at 29.5 min (Fig. 3.1 B, inset) shows that aS contains methionine oxidations and a covalent bound DHA molecule as indicated by the mass increase of 326 Da on the expected mass (14460 Da). The modification is not present in all molecules but from electrospray mass spectrometry data a modification of about 3% can be hypothesized.

Gel filtration is resulted highly suitable for the purification of aS oligomers since that it is possible to remove aS in monomeric form and the excess of DHA. Moreover the native elution conditions, phosphate buffer at pH 7.5, seems to not induce chemical stress of the protein species. The main drawback of this type of method is the dilution of

the sample in the purified fraction. This could affect the dynamic equilibrium between the monomeric and aggregated form of aS. Due to the too low protein concentration in the purified sample, further analyses, such as structural characterizations and functional tests, are sometimes difficult to perform. So we tried another method of isolation based on ion exchange chromatography (IEX). The benefits of IEX are that it has a high throughput, the column has a long lifespan and it has a high resolving power allowing the separation of proteins having isoelectric points differing about 0.5 units of pH. So in this case we can have also information about change in the charge properties of the oligomers. In general separations can be fast, recoveries are high, buffer components are non-denaturing and frequently compatible with further downstream chromatographic separation or assay systems. Moreover this technique provides information on the possible charge modifications on the polypeptide chain of aS. Finally, it can be used as a concentration step, to recover proteins from a dilute solution.

aS/DHA mixture were loaded in an anion-exchanger column and to compare elution pattern also the monomeric aS was analyzed as reference (Fig. 3.2). aS elutes at 12 min and after 48 hours of incubation there is no further peak in the chromatogram (Fig. 3.2 A). The analysis of the mixture aS/DHA just after its preparation shows the same peak at 12 min, but after incubation, there are two main peaks at 12 and 20 min corresponding to 44% of NaCl in the chromatogram (Fig. 3.2 B). In order to identify the material under the peaks, these two main fractions were analyzed by RP-HPLC (Fig. 3.2 C) and they correspond respectively to monomeric and oligomeric aS. The late elution of the oligomers can be explained as higher affinity of these species for DEAE resin than the monomer. The resin is positively charged, so the affinity of aS presumably derives from the negatively charged C-terminal tail. The oligomers are formed by several monomer aS molecules, whose negatively charged C-terminal tails are not expected to be involved in the oligomer structure (De Franceschi *et al.,* 2009), but they are free to interact with the anion exchanger. Moreover, also the presence of bound DHA could provide additional negative charge. The peak corresponding to oligomer seems narrow suggesting that the purified population of oligomers might be almost homogenous in terms of net charge. Unfortunately technical problems hampered the extensive use of this chromatography. Indeed it is resulted partially non-reproducible especially in terms of yield. For this reason we decided to continue to purify oligomers by gel filtration.

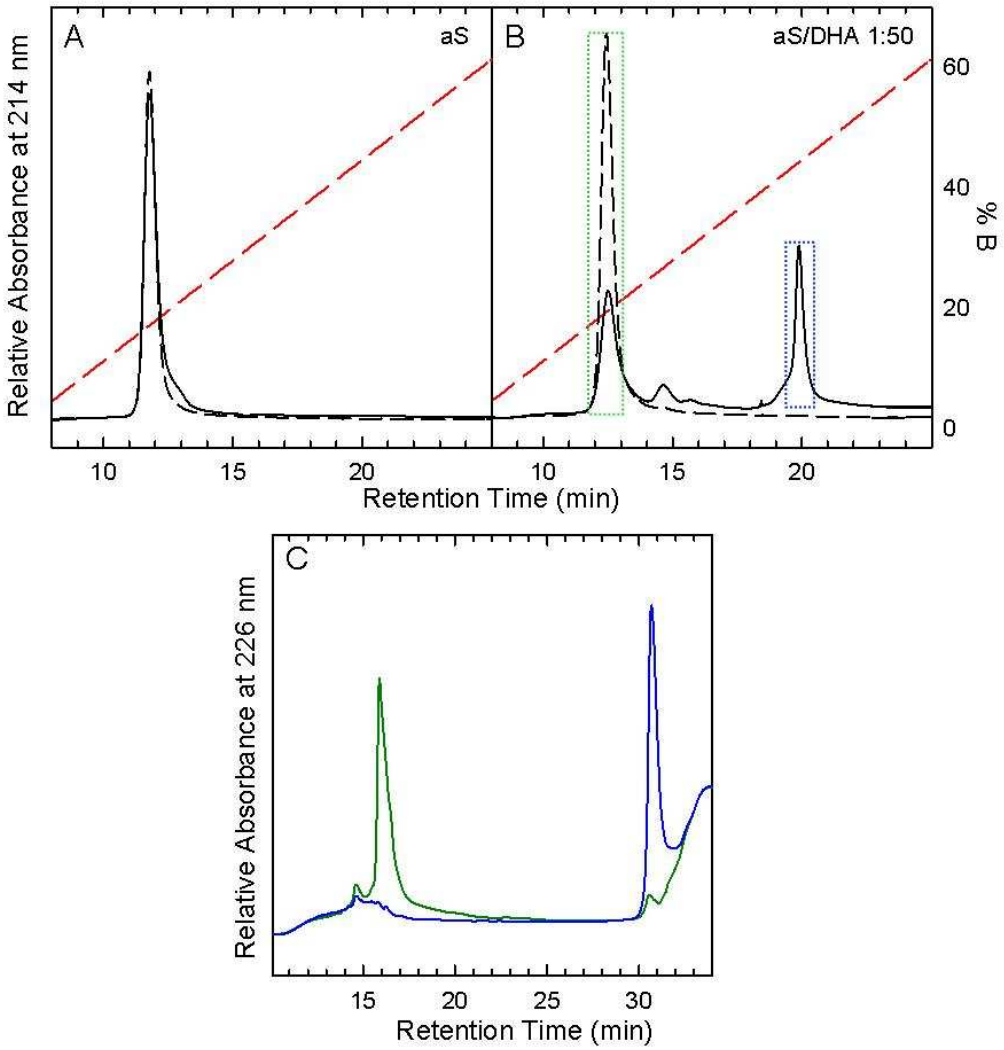

Fig. 3.2. IEX chromatography of aS (A) and aS/DHA 1:50 (B). The IEX chromatograms were obtained from samples just prepared (*dashed line)*) and after 48 hours of incubation (solid line). IEX analyses were conducted using a DEAE column, eluted with a gradient of NaCl from 0 to 1M in 30 minutes, recording the absorbance at 214 nm. (C) RP-HPLC chromatogram of fractions eluted at 12 min (dashed line) and 20 min (solid line) in IEX of aS/DHA after 48 hours. (C) RP-HPLC analyses were conducted using a Jupiter C4 column (4.6 x 150 mm; Phenomenex, CA, USA), eluted with a gradient of acetonitrile/0.085% TFA vs water/0.1% TFA from 5% to 38% in 5 min, from 38% to 43% in 15 min, recording the absorbance at 226 nm.

3.2 Chemico-physical characterization of aS/DHA oligomers

aS/DHA oligomers were characterized by far-UV CD. The mixture corresponding to different times of incubation was analyzed. aS acquires α-helix structure in the presence of DHA and this type of secondary structure is maintained during oligomerization process (Fig. 3.3 A). Upon incubation, a small decrease of signal is detectable, as a consequence of aggregation and probable precipitation of the protein material.

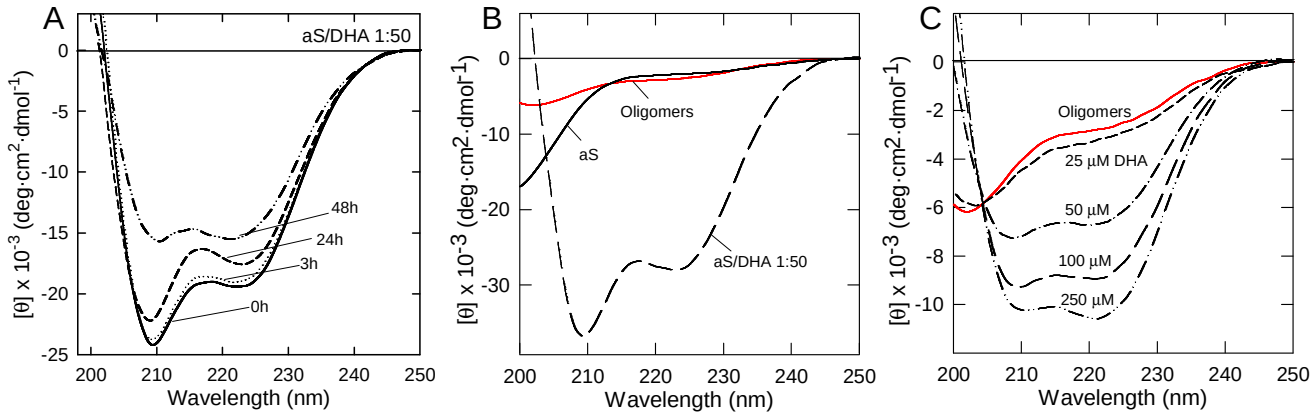

Fig. 3.3. Far-UV CD spectra. (A) aS/DHA mixture during the aggregation process. The spectra were recorded at a protein concentration of 5 mM in PBS pH 7.4, immediately after addition of DHA, and after 3, 24 and 48 hours. (B) Far UV CD of oligomers after purification by gel filtration (red line). The spectra of monomeric aS and aS in the presence of DHA (protein/DHA 1:50) are also reported as reference. (C) Titration experiment by far UV CD of oligomers in the presence of increasing amount of DHA. The numbers close to the spectra indicate the amount (µM) of DHA.

The secondary structure of oligomers was checked also after the purification step by gel filtration. Oligomers show a CD spectrum typical of a protein in a partly folded state with a moderate content of α-helix structure (Fig. 3.3 B, red line). The spectrum of oligomers is shown in comparison with CD spectra of monomeric aS (Fig. 3.3 B, continuous line) and of the mixture of aS/DHA before gel filtration (Fig. 3.3 B, dashed line, from De Franceschi *et al*., JBC 2011). The loss of α-helix structure can derive from the fact that part of DHA was removed by gel filtration step. Interestingly, further addition of DHA to oligomers, isolated by gel filtration, induces again an increase of their α-helical structure (Fig. 3.3 C), as observed for monomeric aS. The transition between partly folded state and α-helix follows a two-state model, for the presence of an isodichroic point at 203 nm in the titration experiment. Since in monomeric aS is the N-terminal region the responsible for membrane recognition and for cooperative formation of helical domains (Bartels *et al.,* 2010), it is reasonable to assume that in the partly folded state, the N-

terminal region or part of it is still free to drive the association of oligomers with membranes and lipids.

Oligomers were then observed by transmission electron microscopy (TEM), atomic force microscopy (AFM) and DLS (Fig. 3.4). These analyses provide information about an average size distribution of the oligomers. As previously reported by De Franceschi et al. (2011), TEM analysis shows that the chromatographic fraction corresponding to oligomers has a spherical morphology, with diameters ranging from 12 to 35 nm. In Fig. 3.4 B the number size distribution from aS/DHA oligomers obtained by DLS analysis is shown, indicating a mean size of 22 ± 8 nm. AFM measurement based on height differences, shows the presence of two main populations, one is smaller (1.1 ± 0.1 nm) and the other is larger (4.1 ± 0.1 nm). To better compare AFM and DLS results, the profile peaks of two section containing oligomers of different size are also reported. The diameter of smaller oligomers (Fig. 3.4 D and E, black arrows) is about 20 nm, in agreement with the average value calculated by DLS measurements. Bigger oligomers (Fig. 3.4 D and E, red arrows) have diameter of about 50-60 nm, values still included in the size distribution curve obtained from DLS.

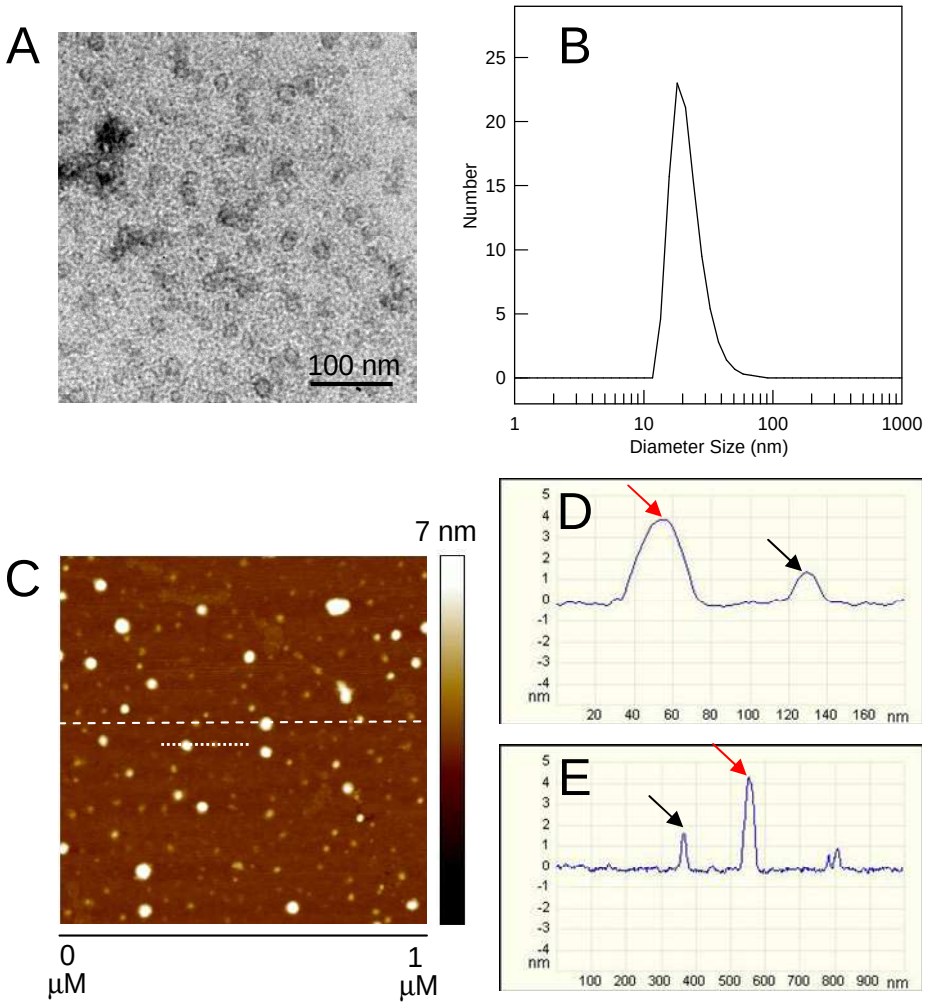

Fig. 3.4. Structural characterization of aS/DHA oligomers after their isolation by gel filtration. (A) Transmission electron microscopy and (B) DLS for particle size estimation of aS/DHA oligomers. (C) Tapping mode AFM image of oligomers and relative XZ profile of sections indicated by dotted line (D) and dashed line (E).

4. INTERACTION WITH MEMBRANES

4.1 Morphological analyses of liposomes

Liposomes were used to obtain membrane-mimetic systems to study oligomers interaction with membrane. Different phospholipid composition vesicles were prepared: DOPG, DOPG-POPE, POPS-POPC, POPC, POPE, TBE, as small unilamellar (SUV) and large unilamellar (LUV) vesicles. Different phospholipids were tested to check aS/DHA oligomers binding preference. Indeed, it is generally recognized that aS has a strong preference for binding to anionic membranes (Davidson et al., 1998; Zhu & Fink, 2003), but this information is lacking for aS/DHA oligomers. Thus, liposomes with -1, -0.5 and 0 net charge were used. Immediately after preparation, dynamic light scattering (DLS) and electron transmission microscopy (TEM) were used to confirm the formation of liposomes of the desired size. Liposomes were tested for their stability on time measuring the average diameter by DLS immediately and after one week of storage at 4°C. The mean diameter for LUV and SUV, measured immediately after extrusion, is different for all the different phospholipid composition, as reported in Table 4.1: the smaller values were obtained with 1POPC:1POPS and the larger with POPE. After one week of storage at 4°C, there are no relevant differences in the average diameter, except for POPE vesicles. Immediately after extrusion with a polycarbonate membrane with pore of 30 nm, POPE SUV appear large as LUV. Moreover, after one week storage, the average diameter of POPE LUV increases of about +1096.8 nm (Table 4.1). This instability is due the tendency of phosphatidylethanolamine to self-aggregate after re-hydration and to form aggregates and floccules. Since other phospholipidic compositions allow to obtain more stable liposomes, POPE was not used for experiments. However, vesicles were always used within few days after preparation. In Fig. 4.1 the three main composition, corresponding to 100% and 50% negatively-charged phospholipids and total brain extract (with less than 40% negative charged lipids) are reported. These three conditions were used also for the experiments as they provide, on the base of far-UV CD measurements, conditions for high (DOPG), middle (1POPC:1POPS) and low (TBE) interaction with aS/DHA oligomers (data reported in §4.2). Also POPC and POPE correspond to 100% zwitterionic or neutral lipids, but the use of an extract (TBE) was preferred, compared to single-phospholipid compositions. DLS and TEM (Fig. 4.1, inset) show comparable diameter size (average

values reported in Table 4.1). From TEM is possible also to control the morphology of liposomes: DOPG and 1POPC:1POPS have more regular distribution, and present the typical aspect of liposomes on mica, due to the drying of the samples. TBE liposomes, that show a larger size distribution with DLS, have also a different morphology on TEM picture, probably due to the unknown components of the extract.

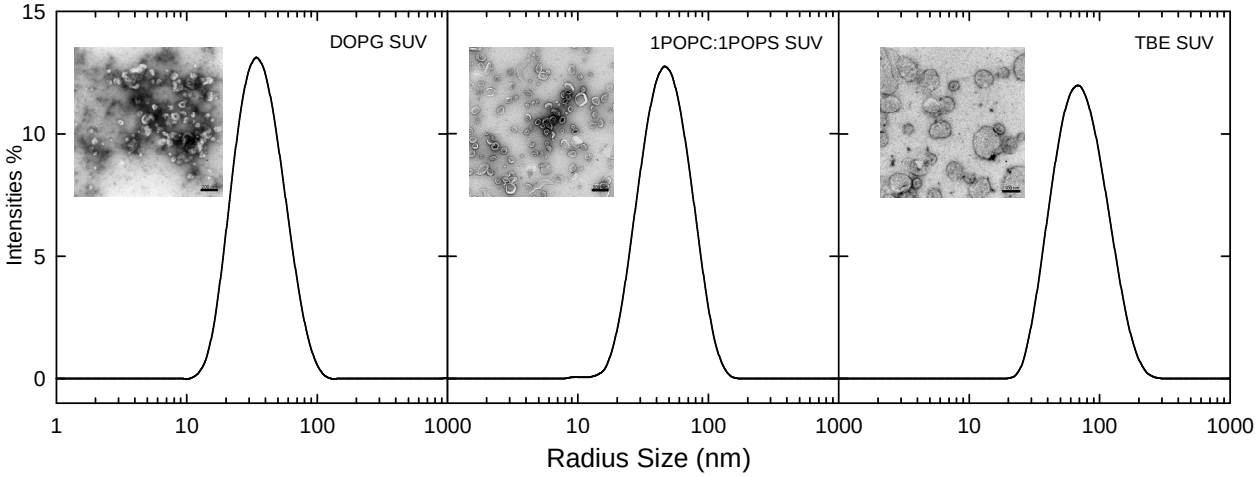

Fig. 4.1 DLS and TEM of SUV of different composition DOPG, 1POPC:1POPS AND TBE liposomes were diluted to a final lipid concentration of 0.5 mM and observed immediately after preparation.

4.2 aS/DHA oligomers interact with membranes

Spectroscopic analyses by CD were conducted in order to study the interaction of oligomers with vesicles. It has been reported in literature that aS adopts an α-helical conformation induced by interactions with membranes, particularly those containing acidic phospholipids, and also with detergent micelles. The N-terminal and NAC regions include the imperfect repeats, xKTK(E/Q)GVxxxx, highly conserved in orthologous genes that can adopt an amphiphilic helical structure, a classical motif for membrane-interacting proteins. So we use this criteria to verify if oligomers are able to interact with membranes. aS/DHA oligomers were diluted to a final concentration of 5 μM, and analyzed by far-UV CD in the absence and in the presence of vesicles with different size and composition. Oligomers, as previously reported, after gel filtration, have a partly α -helix folded state (Fig. 4.4 A, red line). The CD spectra are reported in Fig. 4.2 and show that vesicles containing negative charged phospholipids induce a structural transition of aS/DHA oligomers in a dose dependent manner. DOPG vesicles strongly induce α-helix structure acquisition of aS/DHA oligomers, while vesicles containing 50% of negative

charged lipids such as 1POPS:1POPC and 1DOPG:1POPE have less effect. POPE, POPC (zwitterionic phospholipids) and TBE (mixture with less than 40% negative charged phospholipids) do not induce structural transition. No significant difference was observed using LUV and SUV with the same composition, lacking information about a membrane curvature preference of aS/DHA oligomers.

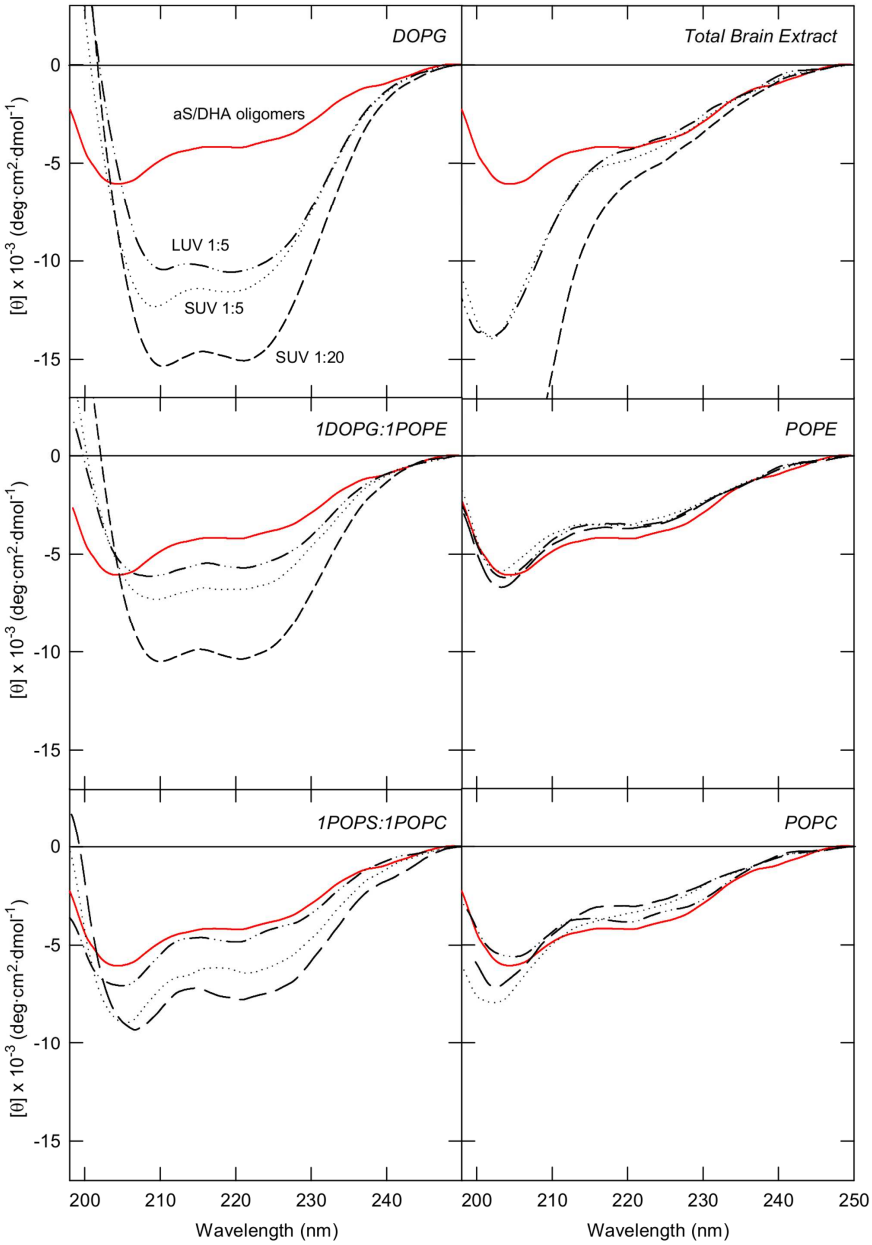

Fig. 4.2. Far-UV CD of aS/DHA oligomers in the absence (red line) and in the presence (black lines) of vesicles. Vesicles of different composition were used, as reported in figure. Both LUV (dashed-dotted lines) and SUV (dotted and dashed lines) were tested.

4.3 Aggregation in the presence of lipids and membranes

Membrane-induced or lipid-accelerated fibril formation of amyloidogenic proteins was frequently observed. Zhu and colleagues (2003) demonstrated that the fibrillation of aS is very significantly affected by acidic phospholipids vesicles in a concentration-dependent fashion. By CD spectra it was demonstrated that, at high lipid/protein ratios, PA/PC and PG/PC vesicles induce α-helical structure in aS, whereas lower ratios of about 5:1 mass ratio of protein to lipid induce a partially folded α-synuclein intermediate (Zhu *et al*., 2003). The presence of this intermediate has been previously correlated with enhancement of formation of aS fibrils (Uversky *et al.,* 2001). More recently, also Reynolds and colleagues reported that aS aggregates when applied on lipid bilayer surface at nanomolar concentrations, causing the extraction of lipid molecules and subsequent membrane thinning, as represented in Fig. 4.3 (Reynolds *et al*., 2011). aS and A53T fibrils formation detected in the presence of synaptosomal lipid vesicles appeared to be associated with vesicles suggesting a partial insertion of aS into the bilayer, which could act as an anchor for site-directed fibril assembly (Jo *et al*., 2004).

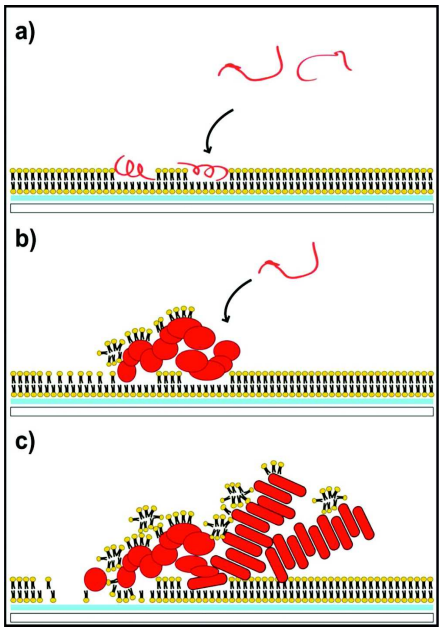

Fig. 4.3. Schematic drawing showing the proposed mechanism of membrane damage caused by aggregation of aS on membrane. (a) Monomeric aS adsorbed to the membrane. (b) Aggregation of aS monomers initiates membrane thinning and lipid extraction around the growing aggregates. (c) A 24 h period of incubation results in the presence of mature aS fibrils. Subsequently, membrane integrity is lost (from Reynolds et al., 2011).

To analyze the effect of membranes on the aggregation properties of aS/DHA oligomers, aS and aS oligomers were incubated in the absence and in the presence of vesicles (molar ratio protein/lipid of 1:20 and 1:50). The aggregation was conducted in the presence of DOPG SUV, since oligomers preferentially interact with negatively charged membranes and DHA (molar ratio protein/fatty acid 1:50), as control. The effect of the lipids on protein aggregation was monitored by ThT fluorescence assay (Fig. 4.4). The aggregation process of aS results sped up in the presence of DOPG SUV (1:20) (Fig.

4.4 A, empty circles), while in the presence of DOPG SUV (1:50) is inhibited (Fig. 4.4 A, empty triangles). TEM analysis shows that in the mixture corresponding to aS incubation for 9 days in the presence of SUV DOPG (1:20) there are aS amyloid-like fibrils associated to the surface of SUV (Fig. 4.4 A, inset). The size and morphology of these fibrils are similar to those of aS fibrils formed in the absence of SUV. In both cases, aS forms straight, unbranched fibrils with a width of 10–15 nm. An additional feature is that the shape of vesicles in contact with fibrils is not changed. In the presence of DHA, as previously observed, there is not formation of aS aggregates that bind ThT dye (Fig. 4.4 A, inverted black triangles). In the case of aS/DHA oligomers, their incubation in the presence or the absence of SUV or DHA does not result in any increase of the fluorescence of ThT dye (Fig. 4.4 B), confirming their nature of off-pathway intermediates (De Franceschi *et al.,* 2011). The aggregation process was further monitored by CD spectroscopy, confirming the presence of β-sheet structure only for ThT-positive fibrils (Fig. 4.5).

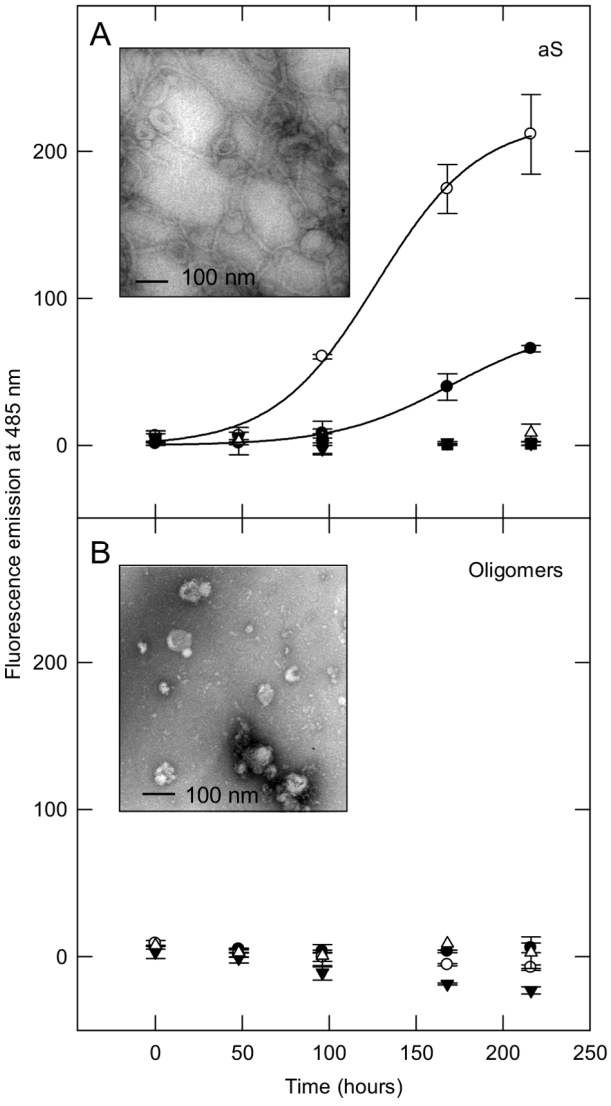

Fig. 4.4. Aggregation studies monitored by ThT assay. aS (A) and aS/DHA oligomers (B) aggregation processes were conducted at 37°C in the presence of lipids and followed by ThT binding assay. aS or aS oligomers were dissolved in 20 mM Tris, 150 mM NaCl pH 7.4 at a 50 μM concentration in order to induce aggregation, in the absence (black circles) and in the presence of DOPG SUV, at molar ratio 1:20 (empty circles), 1:50 (empty triangles) and in the presence of DHA (molar ratio 1:50, inverted black triangles). The excitation wavelength was fixed at 440 nm, and the fluorescence emission was collected at 485 nm. To better visualize the aggregation trend of aS and aS in the presence of DOPG (molar ratio 1:20), the data points are fitted with a sigmoidal equation (SigmaPlot software). Inset: TEM images of protein material relative to aS and aS/DHA oligomers samples after 9 days of incubation in the presence of DOPG SUV (molar ratio 1:20).

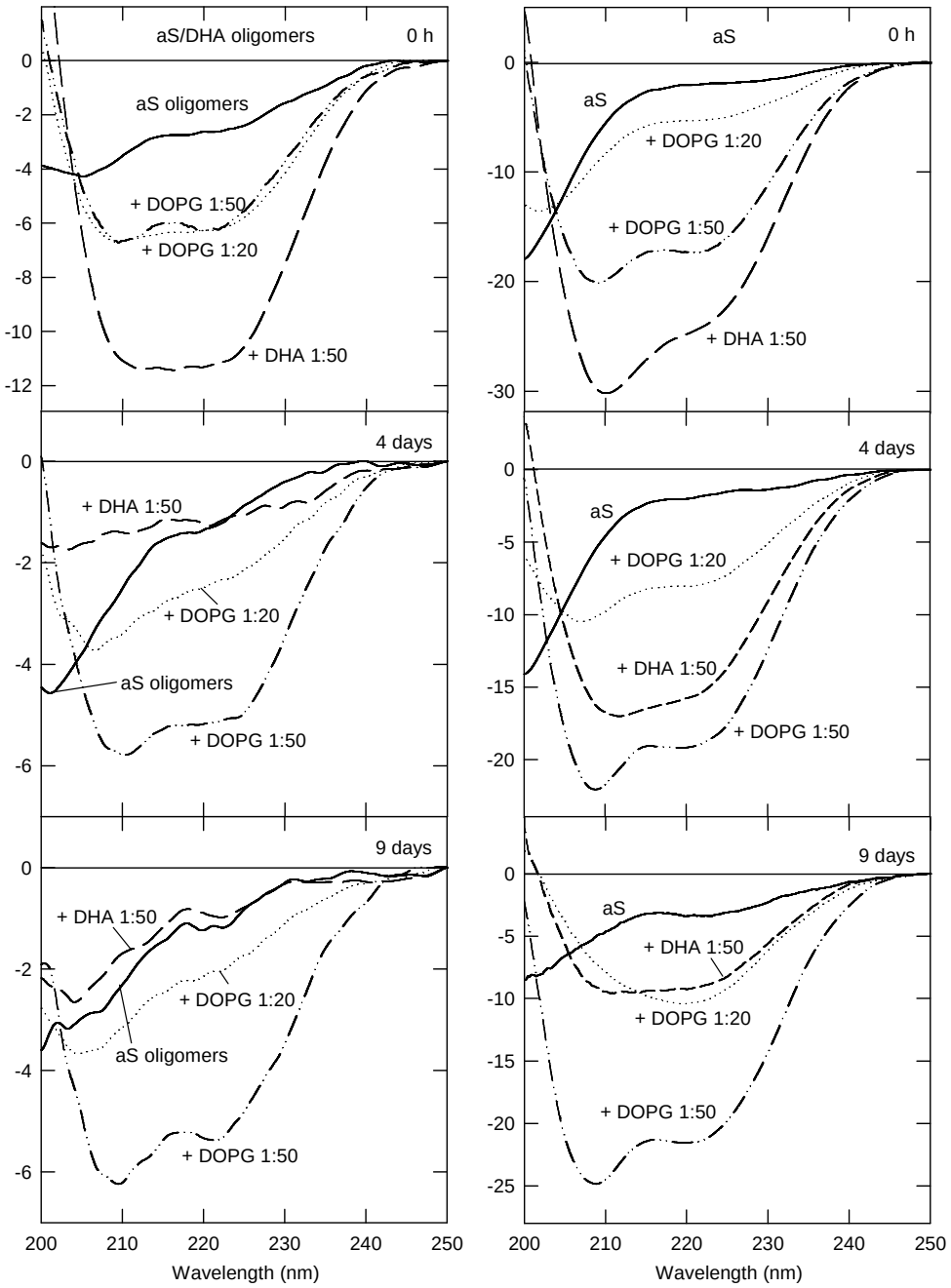

Fig. 4.5. Aggregation studies monitored by far-UV CD. aS or aS oligomers were dissolved in 20 mM Tris, 150 mM NaCl pH 7.4 at a 50 µM concentration in order to induce aggregation, in the absence (solid lines) and in the presence of DOPG SUV, at molar ratio 1:20 (dotted lines), 1:50 (dashed-dotted lines) and in the presence of DHA (molar ratio 1:50, dashed lines).

4.4 aS/DHA oligomers induce permeabilization of synthetic membranes

Since aS/DHA oligomers are able to interact with negative charged phospholipids, the effect of this interaction on liposomes was investigated. A standard test to evaluate the lipid disruption properties of oligomers is the calcein-leakage test. Fluorescence emission of liposomes loaded with calcein is measured before and after oligomers addition. Because of the self-quenching effect due to the high concentration of calcein in the liposomes, the initial fluorescence emission depends only by traces of external dye. After addition of oligomers, if the dye leaks as a consequence of altered permeabilization of membranes, the fluorescence emission of calcein results enhanced because of the dilution in the external environment. aS/DHA oligomers effects were measured 30 min after their addition to different vesicles (Fig. 4.6 A) and we have tested vesicles composed by DOPG, 1POPC:1POPS and TBE. These compositions differ for the percentage of negative charged phospholipids: DOPG and 1POPC:1POPS, composed by 100% and 50% negative-charged phospholipids respectively, and TBE with less than 40% negative charged phospholipids, but the detailed composition is not available. We observed that only DOPG liposomes were permeabilized by oligomers, while the other two tested composition do not show significant difference between aS oligomers, monomers and fibrils. So phospholipids that do not induced structural transition on aS oligomers are not even destabilized by oligomers. Also in the case of 1POPC:1POPS, that induces a minor effect on the oligomer structure (Fig. 4.2), there is no release of calcein from vesicles. Thus, binding of oligomers to membranes not necessarily lead to membrane permeabilization.

aS/DHA oligomers effect on DOPG liposomes were measured at different concentration of protein species, in comparison with aS monomers, fibrils and also DHA alone (Fig. 4.6 B). Oligomer effect is significantly different from those of other species, since they are able to permeabilize vesicles in a dose dependent manner, while aS and fibrils do not, even at that concentration (2.5 μM) that allows aS/DHA oligomers to cause the maximum effect.

Since aS/DHA oligomers are able to destabilize membrane, it is important to characterize the mechanism of action. A critical parameter to understand the type of this destabilization is to verify the presence and eventually the dimension of a pore or membrane aperture. Indeed calcein used for the previous study is a really small molecule

(622.5 Da), that gives no information about the kind of destabilization: pore formation, transient destabilization due to oligomers insertion or even detergent effect on membranes would be not discernible with this test. To deeper characterize oligomers effect on membranes, first step was a supplemental leakage test performed with fluorescein-isothyocianate-dextran loaded vesicles. Dextran, that has an average molecular weight of 10,000 Da, could leak only if a pore/aperture of almost 4 nm occurs. aS/DHA oligomers or aS monomers were added to DOPG SUV and LUV (Fig. 4.5 C): both species show no difference in inducing leakage of Dextran, indicating a size selection of molecule that could leak in the presence of aS/DHA oligomers, and defining an aperture size between 1 and 4 nm (Mazzucca et al., 2010).

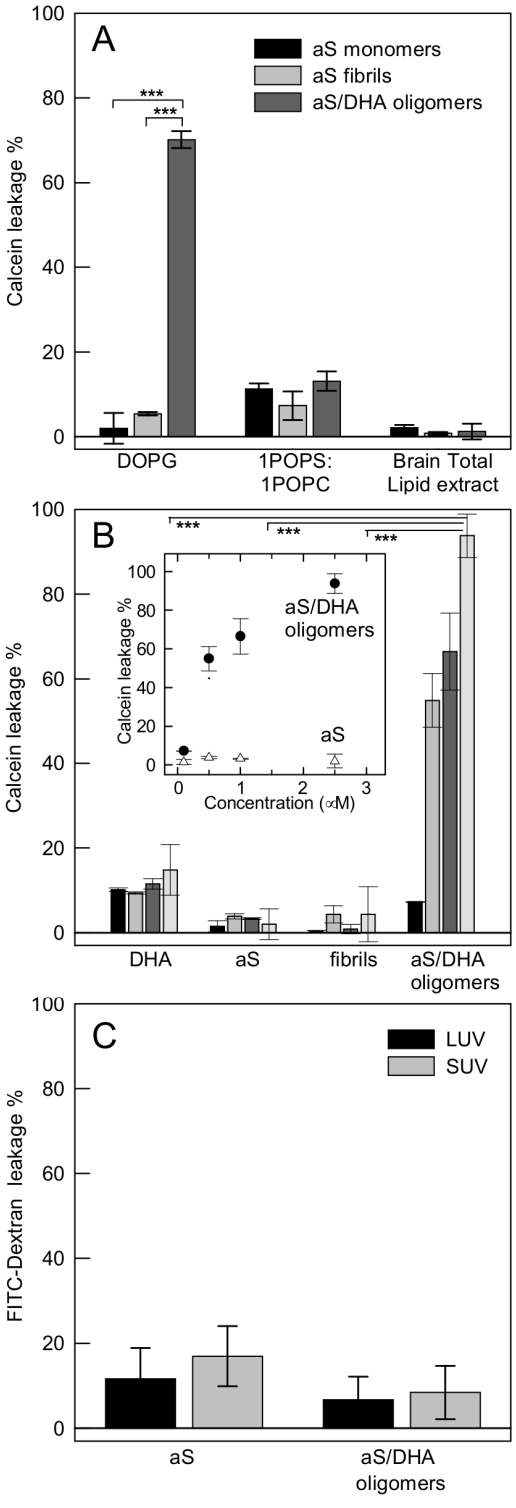

Fig. 4.6. Calcein-leakage test on liposomes. (A) Fluorescence measurement of calcein-loaded LUV of different composition after 30 min incubation with monomeric aS, aS fibrils and aS/DHA oligomers at a final concentration of 1 μM. (B) Fluorescence measurement of calcein-loaded SUV after 30 min incubation with increasing concentration of DHA alone, monomeric aS, aS fibrils and aS/DHA oligomers. Final protein concentration was 0.1, 0.5, 1 and 2.5 μM. (C) Fluorescence measurement of FITC-dextran loaded SUV and LUV after 30 min incubation with aS/DHA oligomers and monomeric aS at a final concentration of 2.5 μM.

4.5 aS/DHA oligomers permeabilize cellular membranes

Previously, it was reported that aS/DHA oligomers are toxic to dopaminergic cells (De Franceschi *et al*., 2011). To correlate this assumption with leakage test, oligomers permeabilization activity was studied also on cells. Standard methods to analyze cells viability or permeabilization consist in a previous phase of exposure to potential toxic species, and then detection of effect with fluorescent dye. This approach would limit the detectable permeabilizing effect only to a stable pore formation that will still be active after the incubation phase. Other mechanism such as transient aperture due to oligomers insertion, detergent effect or flip-flop temporary enhancement would not be detectable adding dye after long time incubation. For this reason, a different method was developed: aS/DHA oligomers, propidium iodide (PI) and Hoechst dye were added simultaneously to cells. In this way, every single event that will cause membrane destabilization would allow PI to enter the cells. After 30 minutes of incubation, fluorescence signal of cells permeabilized to PI were merged with Hoechst-evidenced nuclei. aS/DHA oligomers effect was measured in comparison with aS monomers (Fig. 4.7). Oligomers are able to permeabilize cells, even if in a really minor extent than that exerted on liposomes. The lower effect is due to the complexity of cells membrane toward vesicles and to the minor content of negative-charged phospholipids that allows the higher effect on DOPG vesicles. Moreover, aS/DHA oligomers at the same concentration (0.5 μM) are able to induce the apoptotic death of 2.5% of cells after 24h (De Franceschi *et al*., 2011), a percentage consistent with this extent of permeabilization.

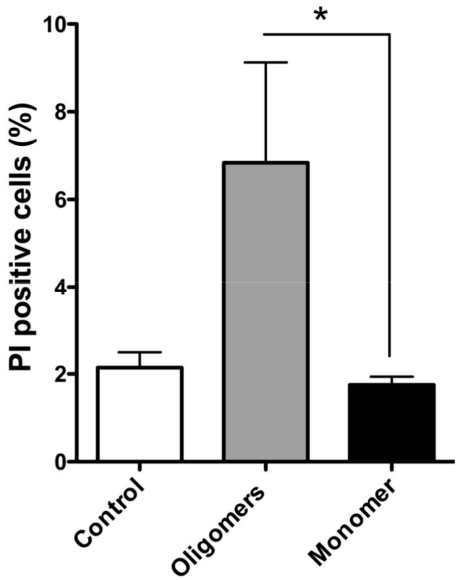

Fig. 4.7. PI influx in dopaminergic cells. SH-SY5Y cells were treated with aS/DHA oligomers and the number of PI-positive cells was calculated as a percentage of the total counterstained cells. Quantization (n = 3 cultures, with 5 fields analyzed per culture, 250-300 cells per field; error bars indicated the S.E.) indicated that aS/DHA oligomers increased the percentage of PI-positive cells. Statistical significance was calculated by one-way ANOVA ($p < 0.05$) compared with mock control or monomeric aS.

4.6 Mechanism of permeabilization of aS/DHA oligomers of membranes

Oligomers can induce permeabilization by several different mechanism (Lashuel and Butterfield, 2013). Indeed, different kind of oligomers could exert different effect on membrane, depending on their chemical properties. The most common mechanisms are pore formation, flip-flop enhancement, detergent effect and transient destabilization subsequent to oligomers insertion in the lipid bilayer or to lipid extraction caused by aggregation on membranes. Thus, it is necessary to investigate how aS/DHA oligomers destabilize membranes. Since several different kind of aS oligomers have been produced, there are standard method reported in literature, used to confirm or exclude a possible mechanism of action. In order to define the mechanism of aS/DHA oligomers, different analysis were performed for aS/DHA oligomers and will be discussed below.

4.6.1 Detergent activity

Detergent-like effect has been reported as mechanism of toxicity on membrane for mellitin, a lytic peptide of bee venom (Chaari et al., 2013), and for aggregated species of IAPP that form small micelle-like protein-lipid aggregates (Sciacca et al., 2012). To analyze this possibility for aS/DHA oligomers, TEM and DLS measurement of vesicles before and after addition of aS/DHA oligomers were conducted, to provide information about the morphology and average size of vesicles after treatment with oligomers (Fig. 4.8 and 4.9). Number relative size distributions of LUV and SUV change upon interaction with oligomers, resulting in a smaller average diameter size (Fig. 4.8 A and B). Comparison with Triton X-100 effect revealed that it was not a detergent effect, also in the concentration of oligomers able to induce 100% of calcein release. On the contrary, intensity relative size distributions revealed even an increment of average diameter size of vesicles (Fig. 4.8 C and D). DLS size distribution of vesicles was measured also after addition of monomeric aS for comparison. Moreover, also 1POPC:1POPS and TBE vesicles were used. Data are reported in Tables 4.2, 4.2, 4.4 and 4.5. Table 4.5 summarized data from Fig. 4.8, obtained using a final molar ratio aS/lipids of 1:20, providing information also for vesicles of different composition. Tables 4.2, 4.3 and 4.4 relate to experiment conducted with aS monomers and aS/DHA oligomers in a molar ratio aS/lipids 1:50. In every case the effect induced by Triton X-100 is remarkably different from that induced

by the protein species. For vesicles composed of TBE or 1POPC:1POPS, the effects induced by aS or aS/DHA oligomers are similar.

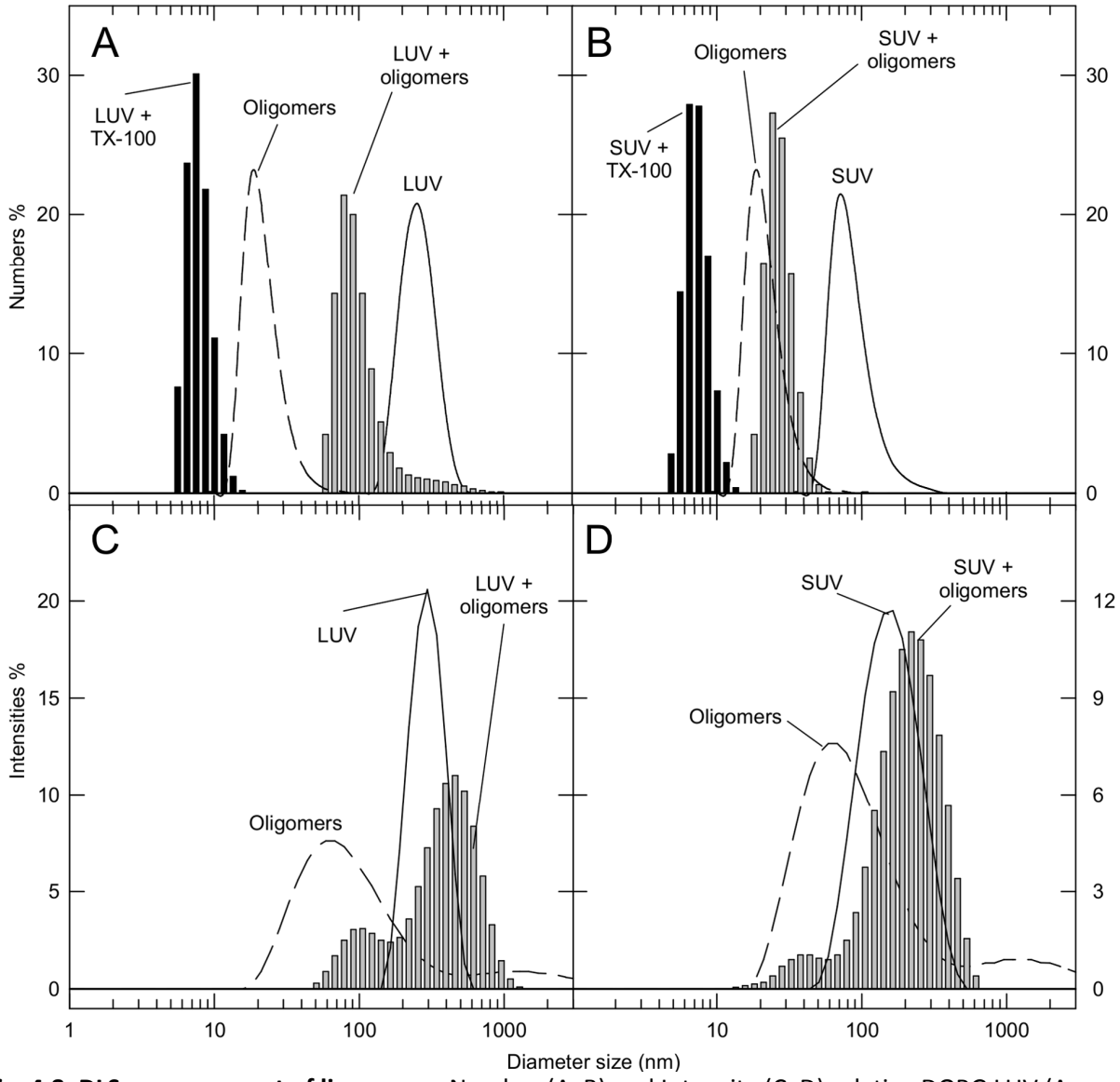

Fig. 4.8. DLS measurement of liposomes. Number (A, B) and Intensity (C, D) relative DOPG LUV (A, C) and SUV (B, D) in the absence (solid line) and in the presence of aS/DHA oligomers (grey bars) and Triton X-100 (black bars). aS/DHA oligomers (dotted line) size distribution is reported for comparison.

In addition to measurement of size distribution of vesicles, also morphology changes were studied, observing sample of vesicles in the absence and in the presence of aS/DHA oligomers by TEM. The images do not show significant difference between liposomes morphology with or without aS/DHA oligomers (Fig. 4.9), allowing to exclude a detergent effect.

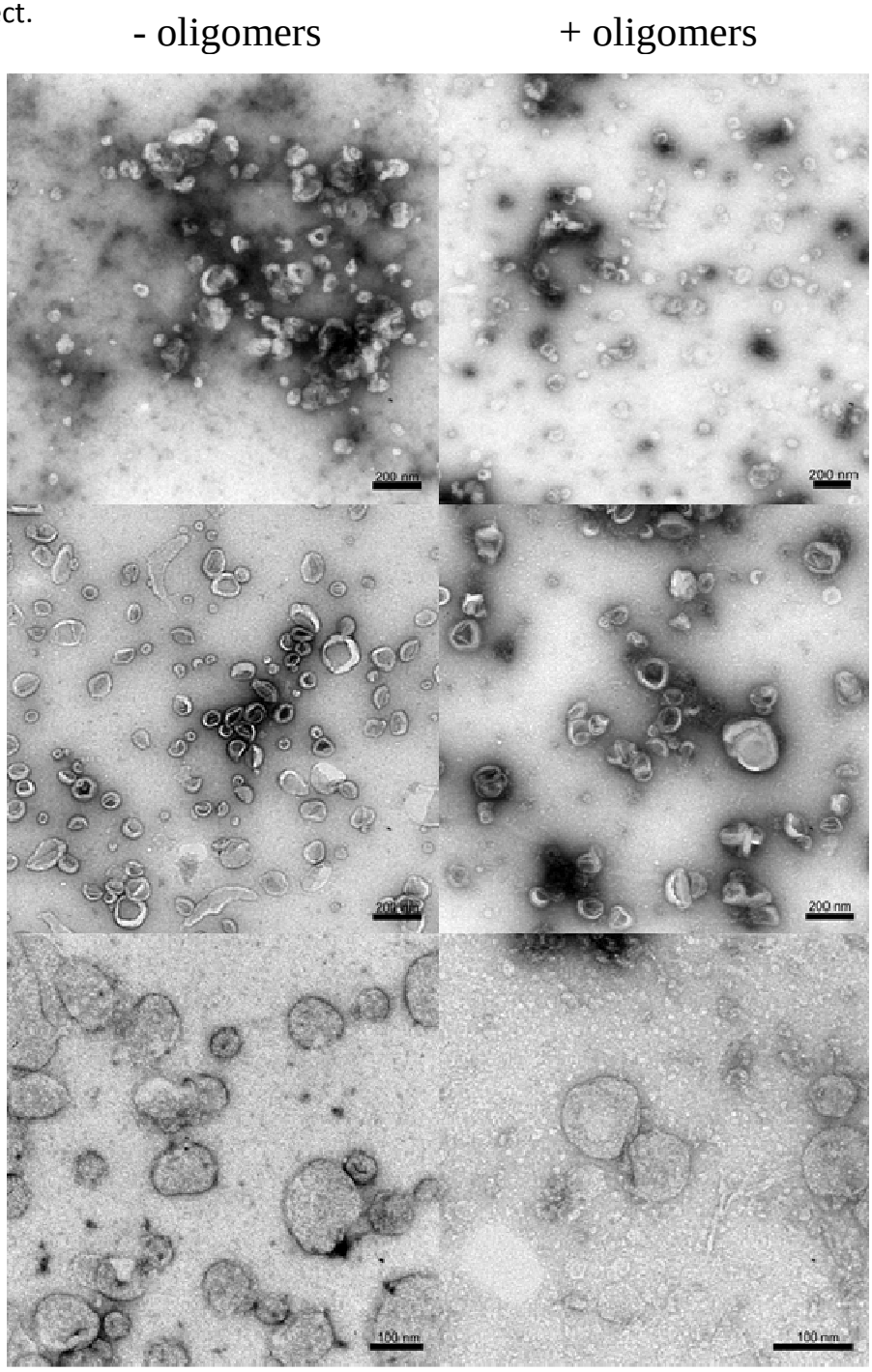

Fig. 4.9. TEM of SUV (0.5 mM) in the absence (left column) and in the presence (right column) of aS/DHA oligomers. Vesicles with different composition were observed, from the top: DOPG, POPS-POPC, TBE.

4.6.2 Pore formation

aS/DHA oligomers activity was tested also on planar lipid membrane (PLM). Lipid bilayer was formed by drying a lipid solution of 1DOPG:1DOPE in pentane. Two 2-ml chambers, separated by a 1DOPG:1DOPE bilayer as represented in Fig. 4.10, were filled with 100 mM KCl, 5 mM HEPES pH 7.00 buffer. After application of current, aS/DHA oligomers were added to the buffer and current alterations were measured on real time. Results show that oligomers induce alteration in the permeability of membrane bilayer to ions, but preferentially in a unstructured manner (Fig. 4.11). About 50% of the cases give weak activity (about 10 pA). Remaining experiments show in the same frequency a stronger (hundreds of pA) or absence of activity. In 25% of the experiments formation of a stable channel was observed, from few seconds to minutes. Relative conductance was not ohmic, as major conductance was recorded with application of negative tension. Rarely, other behaviours were observed, as flickering of single channel or opening of several consecutive channels. As a control, also monomeric aS and DHA alone were tested. The fatty acid addition does not induces any membrane perturbation, while aS causes formation of structured channel, as reported in literature (Tosatto *et al*., 2012).

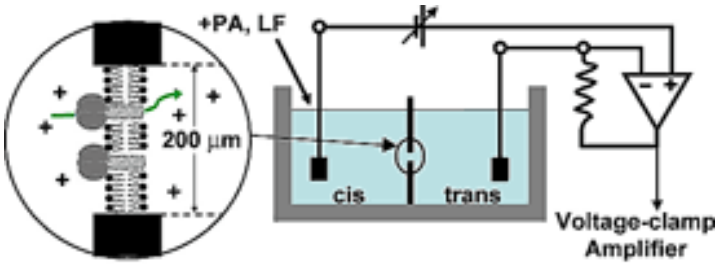

Fig. 4.10. Schematic representation of PLM chambers. Cis and Trans 2-ml chambers are separated by a 25-µm-thick Teflon septum containing a 180-µm hole, where the lipid bilayer is formed.

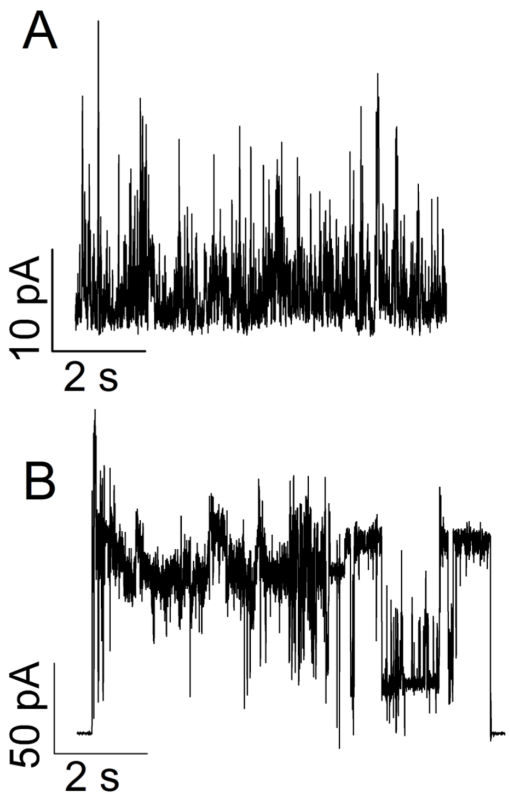

Fig. 4.11. PLM experiments. Electrophysiological activity of aS/DHA oligomers on 1DOPG:1DOPE lipid membranes. Buffer composition was KCl 100 mM, Hepes 5 mM, pH 7.0. Protein concentration was 68 nM. Applied potential +80 mV (A) or +100 mV (B).

Table 4.1. LUV and SUV stability on time.

LUV composition	Diameter (nm)[a]	$Diameter_{1w}$ (nm)[b]	$\Delta_{diameter}$ (nm)[c]
DOPG	370.1	417.6	+47.5
DOPG-POPE	372.3	367.7	-4.6
POPC	135.5	150.5	+15.5
POPS-POPC	289.8	303.3	+13.5
POPE	578.7	1684.5	+1096.8
TBE	381.5	376.3	-5.4

SUV composition	Diameter (nm)[a]	$Diameter_{1w}$ (nm)[b]	$\Delta_{diameter}$ (nm)[c]
DOPG	108.2	118.7	+10.7
DOPG-POPE	112.9	156.9	+44
POPC	108.1	99.4	-8.7
POPS-POPC	99.6	102.1	+2.5
POPE	526.2	506.6	-19.4
TBE	170.4	162.2	-8.2

[a] Average diameters obtained from two DLS measurements of freshly prepared vesicles solutions.

[b] Average diameters obtained from two DLS measurements of vesicles solutions stored for one week at +4°C.

[c] Difference between mean diameters of freshly prepared and stored vesicles.

[d] Net charge of relative phospholipids.

Table 4.2. Diameter size (nm) of DOPG LUV and SUV in the absence and in the presence of monomeric aS and aS/DHA oligomers in a molar ratio protein/phospholipids of 1:50 and in the presence of Triton X-100 (0.1%) Measured were performed immediately after aS addition and after 30 minutes and 1 hour. Values are the mean average of two different measures.

Composition	Intensity[a]	Volume[b]	Number[c]
LUV DOPG	355.3 ± 22.1	441.3 ± 55.6	195.9 ± 76.5
oligomers	94.72 510.2 ± 77.6	87.10 567.6 ± 94.6	77.29 426.65 ± 50.4
oligomers, 30 min	435.2 ± 107.8	450.4 ± 116.1	416.1 ± 97.2
oligomers, 1 h	397.4 ± 36.3	413.9 ± 38.2	375.8 ± 34.1
aS	81.82 357.2 ± 12.9	75.14 431.7 ± 31.2	97.33 ± 43.09 306.6
aS, 30 min	336.3 ± 10.2	369.25 ± 6.0	294.9 ± 16.3
aS, 1h	339.9 ± 37.5	448.2 ± 81.8	88.2 ± 72.5
Triton X-100	11.4 ± 1 68.0 ± 7.9	9.1 ± 0.5	7.6 ± 0.3
SUV DOPG	118.7 ± 8.6	96.2 ± 1.5	69.1 ± 12.4
oligomers	218.6 ± 21.5	58.6 ± 0.6 295.1 ± 51.4	45.04 ± 2.3
oligomers, 30 min	33.7 204.0 ± 12.6	36.3 ± 5.7 268.5 ± 21.8	29.26 ± 2.3
oligomers, 1h	31.8 205.3 ± 11.0	27.8 218.2 ± 15.9	24.6 126.3 ± 15.7
+aS	101.9 ± 1.7	65.1 ± 1.3	41.7 ± 1.7
aS, 30 min	95.5 ± 1.2	17.9 67.5 ± 3.1	17.4 47.4 ± 2.6
aS, 1h	77.9 ± 1.6	59.5 ± 3.3	47.2 ± 4.7
Triton X-100	16.0 ± 0.1 272.3 ± 85.1	11.2 ± 0.01	8.9 ± 0.05

[a] Relative number of particles, multiplied for their light scattering intensity
[b] Relative number of particles, multiplied for their volume.
[c] Relative number of particles of defined size.

Table 4.3. Diameter size (nm) of 1POPS:1POPC LUV and SUV in the absence and in the presence of monomeric aS and aS/DHA oligomers in a molar ratio protein/phospholipids of 1:50 and in the presence of Triton X-100 (0.1%). Measured were performed immediately after aS addition and after 30 minutes and 1 hour. Values are the mean average of two different measures.

Composition	Intensity[a]	Volume[b]	Number[c]
LUV POPS-POPC	352.6 ±3.7	373.5 ±3.2	326.4 ±3.1
oligomers	56.6 ±7.7 398.4 ±21.7	51.05 ±5.8 460.9 ±34.8	45.8 ±3.9 314.5 ±1.5
oligomers, 30 min	308.7 ±10.2	322.7 ±10.0	293.2 ±9.6
oligomers, 1h	376.0 ±7.3	419.3 ±7.2	319.25 ±7.4
aS	329.8 ±31.4	360.8 ±38.9	290.15 ±19.9
aS, 30 min	304.4 ±5.2	312.8 ±5.3	296.5 ± 4.7
aS, 1h	86.6 ±12.4 428.7 ±5.9	80.40 ±13.6 481.25 ±9.7	72.26 ±12.6 355.1 ±10.0
Triton X-100	11.7 ±0.8 201.5 ±43.5	9.8 ±1.1	8.5 ±1.2
SUV POPS-POPC	33.9 163.5 ±5.4	31.6 120.3 ±43.2	40.8 ±16.6
oligomers	131.3 ±6.5	33.0 94.2 ±16.0	32.7 ±4.3
oligomers, 30 min	116.6 ±6.0	86.1 ±5.8	56.0 ± 1.9
oligomers, 1h	118.4 ±2.2	96.2 ±2.8	68.7 ±6.8
aS	156.1 ±6.9	138.4 ±8.4	78.07 ±0.3
aS, 30 min	110.4 ±8.7	75.7 ±4.9	49.19 ±0.5
aS, 1h	94.2 ±1.6	73.2 ±2.4	55.91 ±4.5
Triton X-100	9.1 ±1.40	8.0 ±0.9	7.22 ±0.6

[a,b,c] see reference table 4.2.

Table 4.4. Diameter size (nm) of TBE LUV and SUV in the absence and in the presence of monomeric aS and aS/DHA oligomers in a molar ratio protein/phospholipids of 1:50 and in the presence of Triton X-100 (0.1%) Measured were performed immediately after aS addition and after 30 minutes and 1 hour. Values are the mean average of two different measures.

Composition	Intensity[a]	Volume[b]	Number[c]
LUV TBE	418.8 ±34.1	432.8 ±35.8	401.9 ±33.4
oligomers	423.3 ±44.5	506.2 ±81.3	314.8 ±0.5
oligomers, 30 min	77.2 456.2 ±1.62	70.8 549.8 ±9.1	63.4 326.9 ±2.1
oligomers, 1h	397.3 ±14.1	438.1 ±15.3	343.5 ±11.6
aS	444.7 ±10.5	478 ±17.2	398.7 ±0.6
aS, 30 min	410.6 ±3.1	454.95 12.1	351.75 ±8.1
aS, 1h	426.25 ±34.0	439.2 ± 37.3	411.1 ±30.7
Triton X-100	5.0 224.7 ±7.4	4.8 239.2	4.7 220
SUV TBE	220.4 16.6	74.9 262.5 ±58.2	114.9 ±75.4
oligomers	49.9 209.1 ±16.6	52.4 ±9.8 243.4 ±52.7	45.1 ±5.3
oligomers, 30 min	193.8 ± 14.9	92.3 ± 27.6 299.4 ±0.8	70.2 ±22.4
oligomers, 1h	32.5 151.7 ±3.2	29.7 134.05 ±0.9	27.6 83.5 ±7.4
aS	213.3 ±21.1	88.9 286.3 ±110.0	103.6 ±55.5
aS, 30 min	55.0 196.9 ±9.7	50.7 ±3.1 206.3 ±13.1	50.5 ±2.7
aS, 1h	36.8 197.3 ±7.3	42.1 ±12.6 203.4 ±7.3	43.0 ±17.8 104.6
Triton X-100	6.8 ±0.5 92.2 ±10.7	6.0	5.8 ±0.3

[a, b, c] see reference table 4.2.

Table 4.5. Diameter size (nm) of different composition LUV and SUV in the absence and in the presence of monomeric aS and aS/DHA oligomers in a molar ratio protein/phospholipids of 1:20 and in the presence of Triton X-100 (0.1%). Measurements were performed after 30 minutes.

Composition	Intensity[a]	Volume[b]	Number[c]
LUV DOPG	301.1 ±16.6	326.5 ±21.2	269.0 ±9.8
oligomers	42.9 ±1.0	40.9 ±1.3	38.9 ±1.4
oligomers, 30 min	109.65 ±36.7	98.355 ±33.7	89.61 ±35.3
Triton X-100	10.5 ±0.6	9.1 ±0.4	8.13 ±0.3
SUV DOPG	170.5 ±3.1	51.0 ±0.5	82.9 ±7.9
oligomers	203.5 ±6.6	214.9 ± 10.2	160.2 ± 4.4
oligomers, 30 min	27.2 ±11.4	24.95 ±8.6	22.06 ±7.7
Triton X-100	8.9 ±0.3	8.1 ±0.1	7.47 ±0.1
LUV POPS-POPC	92.9	86.2 ±0.8	78.21 ±7.8
oligomers	68.2 ±19.4	58.9 ±16.2	50.7 ±12.9
oligomers, 30 min	43.2 ±5.3	41.3 ±4.8	39.3 ±4.2
Triton X-100	9.0 ±0.3	8.29 ±0.03	7.6 ±0.2
SUV POPS-POPC	95.7 ±5.3	69.08 ±0.02	50.1 ±2.9
oligomers	138.6 ±4.0	107.5 ±16.9	44.6 ±42.5
oligomers, 30 min	144.0 ±10.5	63.9 ±6.2	31.7 ±1.1
Triton X-100	11.4 ±1.0	8.8 ±0.4	7.3 ±0.1
LUV TBE	356.3 ±4.9	375.25 ±4.0	331.6 ± 5.8
oligomers	345.5 ±41.3	366.85 ±47.4	318.4 ±31.5
oligomers, 30 min	348.9 ±43.1	418.8 ±42.9	238.8 ±63.1
Triton X-100	8.5 ±0.4	8.1 ±0.3	7.6 ±0.2
SUV TBE	219.8 ±3.4	84.95 ±3.9	55.7 ±8.6
oligomers	137 ±2.1	104.3 ±5.1	43.9 ±23.9
oligomers, 30 min	168.8 ± 22.6	104.5 ±31.5	60.1 ±7.9
Triton X-100	9.4 ±1.1	8.1 ±0.4	7.2 ±0.01

[a,b,c] see reference Table 4.2.

5. CHEMICAL MODIFICATIONS ON aS/DHA OLIGOMERS

5.1 *DHA induces oxidative modifications on aS*

In aS aggregates formed in the presence of DHA several oxidative modifications were found, in terms of oxidation of Met residues, covalent addition of allylic radical (+326 Da) and hydroperoxide radical (+358 Da) of DHA (De Franceschi *et al.,* 2011) and the presence of carbonyl groups that should result from the reaction of Lys, Pro or Thr with reactive oxygen species (ROS) or from the reaction of Lys and His with lipid peroxidation products (Thakur and Nehru, 2013). An important goal would be to obtain a complete chemical characterization of the oxidative modifications in aS aggregates by both the identification of modified residue(s) and the evaluation of the extent and the randomness of these several modifications. This study would be of utmost importance to understand the role of lipid peroxidation in oligomers formation in synucleinopathies.

The first type of modification is due to the presence of four Met residues, in position 1, 5, 116 and 127 in the aS sequence. Met residues are easily oxidized to methionine sulfoxide by ROS, but generally these residues are particularly susceptible to undergo oxidation even under acid conditions in the presence of oxygen. Mass spectrometry analysis shows aS containing from 1 (+16 Da), 2 (+32 Da), 3 (+48 Da) to 4 (+64 Da) oxidations. Both monomer and oligomer contain this pattern of Met oxidation and the corresponding RP-HPLC peaks are almost resolved. This type of modification is not easy to control, so it is difficult to say whether it has a role in oligomerization or the activity of the oligomers.

The presence of other chemical modifications was investigated. To this aim the derivatization of modified aS with dinitrophenylhidrazine (DNPH) coupled with MS analysis was tried. DNPH reacts with carbonyls groups that form in the lateral side chain of specific amino acidic residues (lysine, proline, arginine, and threonine) in oxidative conditions as represented in Fig. 5.1 (Linares *et al.,* 2011).

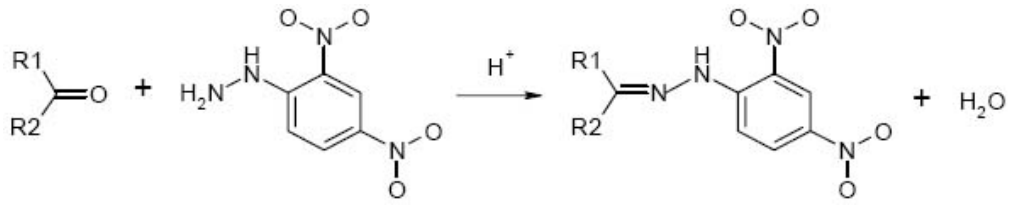

Fig. 5.1. Schematic representation of reaction of DNPH on carbonyls of lateral chain of aminoacidic residues.

The idea is to distinguish carbonyl contributions derived from reactions of Lys, Pro, Thr with ROS (Δmass from 0/-1 to +180) and from addition of allylic or hydroperoxide radicals of DHA. To this aim aS/DHA mixture corresponding to 24-hr of incubation was purified by RP-HPLC and the fraction relative to oligomers (RT of 29.5 min, Fig. 1.1) was collected and dried. This species was incubated in the presence of DNPH, to allow the reaction with carbonyls. Exceeding DNPH was washed with ethanol-ethylacetate extraction and UV absorbance was measured. The same reaction was conducted on monomeric form of aS. In Fig. 5.2 the UV-vis spectra of aS and aS/DHA oligomers reacted with DNPH were shown in comparison with spectra of the same species not reacted. All species absorbe at 280 nm, but only oligomers show a specific UV signal at wavelength 366 nm. This wavelength corresponds to the maximum DNPH absorbance, indicating the presence of an increased amount of carbonyl in oligomers. DNPH labelled-proteins were analyzed by RP-HPLC, monitoring the chromatogram at 226 nm and 366 nm. It was possible to detect the presence of protein and the protein reacted with the fluorescent dye. The chromatogram relative to the analysis of aS does not show any peaks at 366 nm (Fig. 5.3 B), while for aS/DHA oligomers a peak co-eluting with oligomers at 29.5 min is detectable (Fig. 5.3 D). This result shows that carbonyls are present in the oligomeric form of aggregated aS, but non in the monomeric protein. The peak at 366 nm is visible just upon 1 hr incubation (data not shown). This provides an important conclusion: the carbonylation is an early event, being within 1 hr of incubation of aS with DHA. We can speculate that the presence of DHA enhances the oxidative stress on aS as a consequence of its suggested physiological function, as inhibitor of lipid oxidation (Zhu et al., 2006).

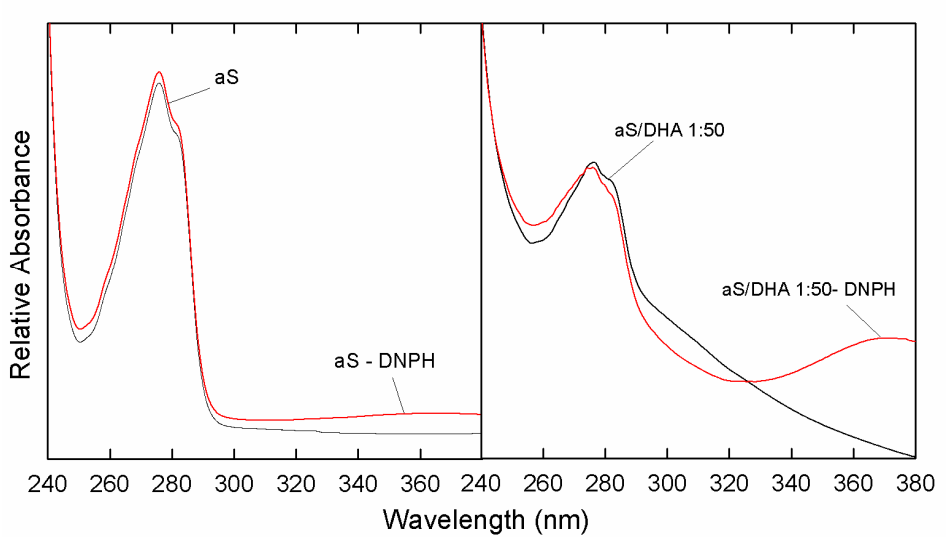

Fig. 5.2. UV-Vis spectra. (A) aS and (B) aS/DHA oligomers spectra of protein before (black lines) and after (red lines) reactions with DNPH. Spectra were recorded in PBS pH 7.4.

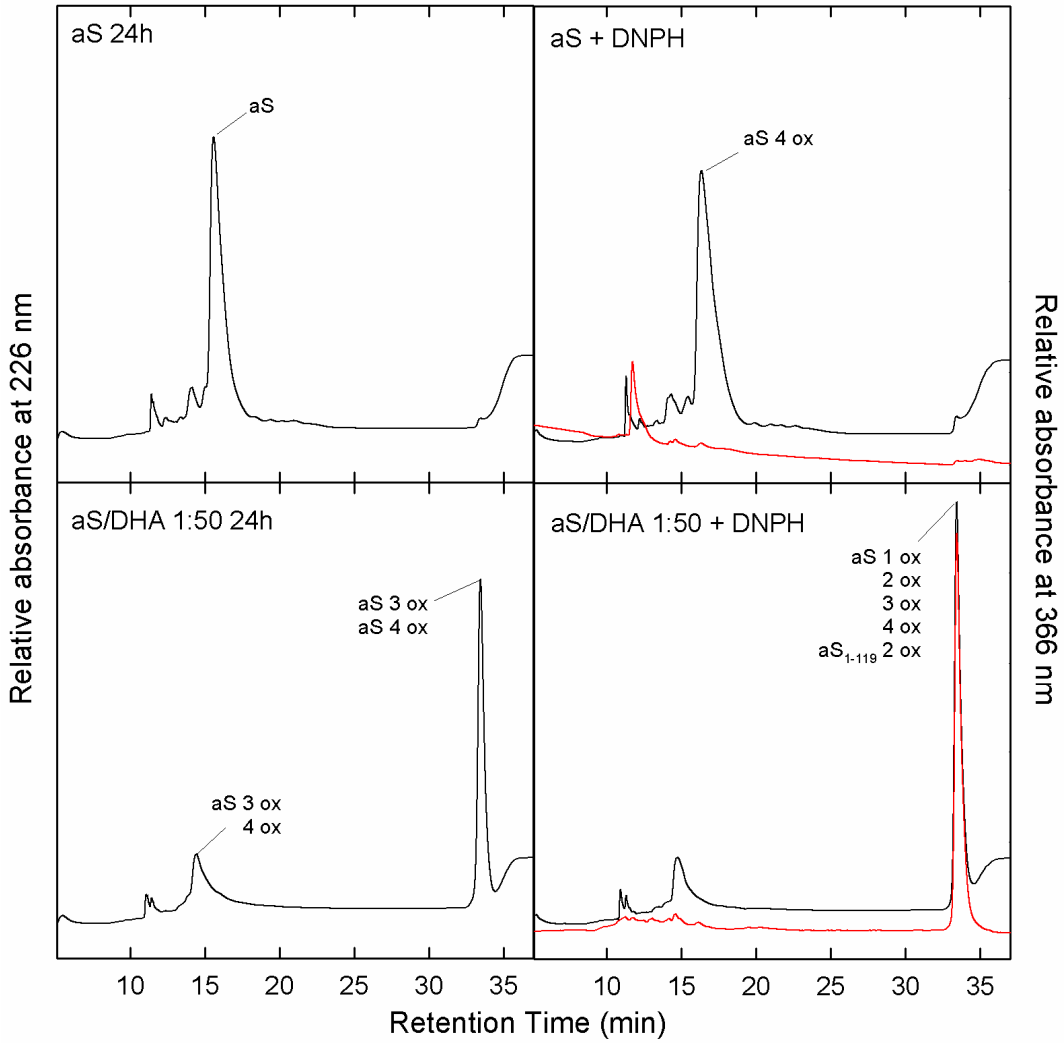

Fig. 5.3. RP-HPLC analyses. aS in the absence (A,B) and in the presence (C,D) of DHA was analysed by RP-HPLC before (A,C) and after (B,D) reaction with DNPH. Samples were eluted with a gradient of acetonitrile and 0.085% TFA and elution was followed at 226 nm (black line) and 366 nm (red line) to detect protein reacted with DNPH.

We made a tentative to identify the amino acid residue(s) modified by carbonylation. We used a standard approach consisting in subjecting the protein samples to proteolysis by trypsin and derivatizing the peptides with DNPH (Fig. 5.4). Unfortunately by this procedure only a fragment containing the Δ mass of 180 Da was found and it corresponds to the sequence 24-32. This peptide contains a Lys residue in position 32 and this could be a possible target of carbonylation. However the presence of a single modification does not justify the signals obtained in UV and RP-HPLC analyses. It could be happen that some peptides can be lost in the extraction step of DNPH being too small and hydrophobic. Moreover the oligomeric species is quite resistant to proteolysis and the yield in peptide is very low. Finally it is reasonable that residues in the protein are randomly modified and so it is difficult to detect them.

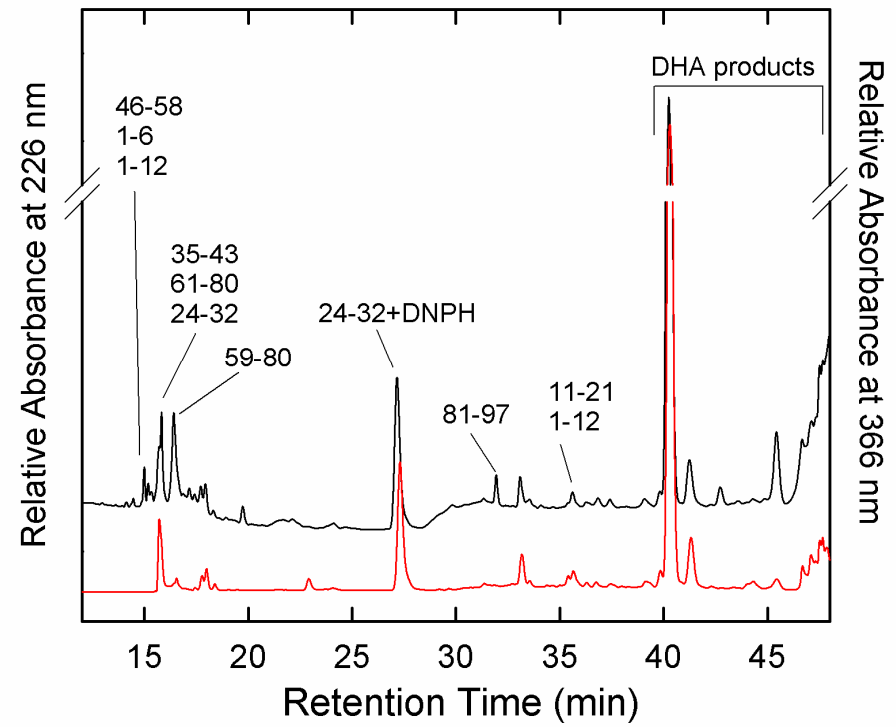

Fig. 5.4. RP-HPLC analyses of proteolysis. aS/DHA oligomers proteolyzed with Tripsin and derivatized with DNPH was analyzed by RP-HPLC. Samples were eluted with a gradient of acetonitrile and 0.085% TFA and elution was followed at 226 nm (black line) and 366 nm (red line) to detect fragments containing DNPH.

5.2 Detection of DHA covalent adduct on aS

Mass spectrometry analysis has revealed the presence of a covalent adduct on aS oligomers formed in the presence of DHA (De Franceschi et al., 2011). A series of signals with a mass increase of 326 and 358 Da was observed. These mass differences are consistent with the covalent modification of the protein for the addition of allylic radical of DHA (326 Da) and hydroperoxide radical (358 Da), the earlier products of DHA autoxidation. In order to identify the site(s) of modification on aS, a proteolysis followed by mass spectrometry analysis was performed. aS/DHA oligomers were purified by RP-HPLC (cfr. Fig. 1.1 B) after 3 hours of aS incubation in the presence of DHA (P/DHA 1:50). HPLC fractions at 29.5 min of retention time containing oligomers were collected then digested with trypsin for 3 hr, using an enzyme to substrate ratio of 1:100. Proteolytic fragments were analyzed in RP-HPLC (Fig. 5.5). Mass spectrometry identification were performed for all eluted peaks, to find DHA-adduct containing fragments (Table 5.1). In the chromatogram several peaks are detectable. Found fragments span all aS sequence. Met-containing peptides are present also in oxidized form (+16 Da) as previously observed. Fragments corresponding to sequence 1-80, 1-60, 35-80, 46-80 and 46-58 were found with a mass increase of 326 Da (Fig. 5.5). The residue that reasonably is modified is His in position 50. Another possible site of modification would be Lys58, but we can exclude it since if Lys58 were modified, it wouldn't be recognized by trypsin. The peptides containing the Δ mass of 326 Da are 1-60 (6475.2 Da), 35-80 (4923.2 Da), 46-80 (3760.9 Da) and 46-58 (1621.5 Da). There are two aspects of particular interest to evidence in this analysis. One is the degree of modification. In fact, the modified peptide constitutes about 2-3% of the unmodified one, making very challenging its identification. Moreover ms-ms analysis on double-charged ions relative to modified peptides causes the removal of the covalent adduct, also using very low collision energy. Ms-ms analysis of double charged ion at m/z 811 relative to peptide 46-58 +326 Da forms again the peptide 46-58 without the modification, while the analysis of the double charged ion at m/z 648 give rise to a ms-ms spectrum of peptide 46-58 (Fig. 5.6). The same behaviour was observed for other DHA-modified peptides. In the light of these considerations and overlapping the sequences (Fig. 5.7) of the indentified peptides we concluded that the modification is located on His50.

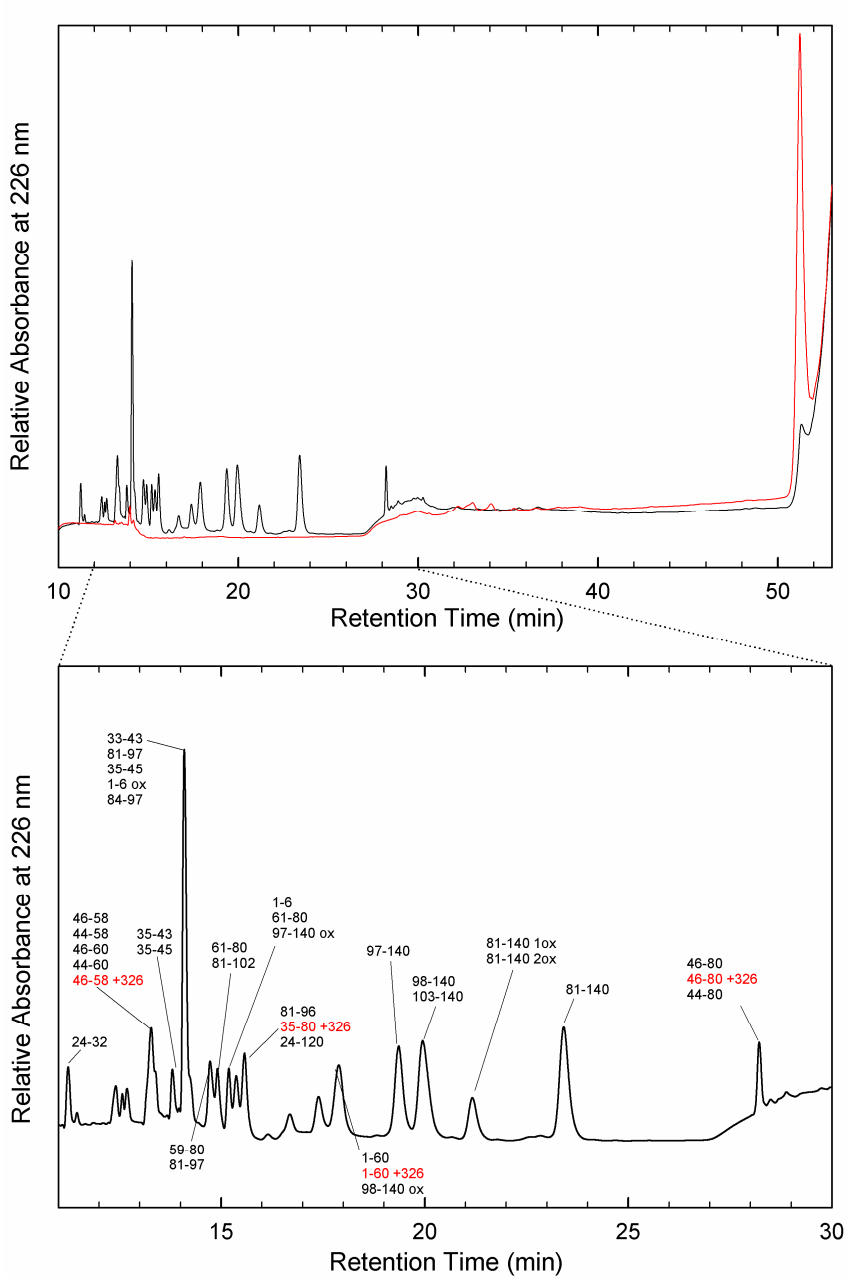

Fig. 5.5. RP-HPLC analysis. A. Chromatogram of the proteolysis mixture of aS/DHA oligomers with trypsin before (black lines) and after (red lines) reaction. Proteolysis was conduced in PBS pH 7.4 buffer with a E:S ratio 1:100 (by weight). B. Detail of the chromatogram from 10 to 30 min to better see the identified fractions Numbers close the peak indicate the fragments identified by mass spectrometry. Peaks relative to species containing DHA adduct are labelled in red.

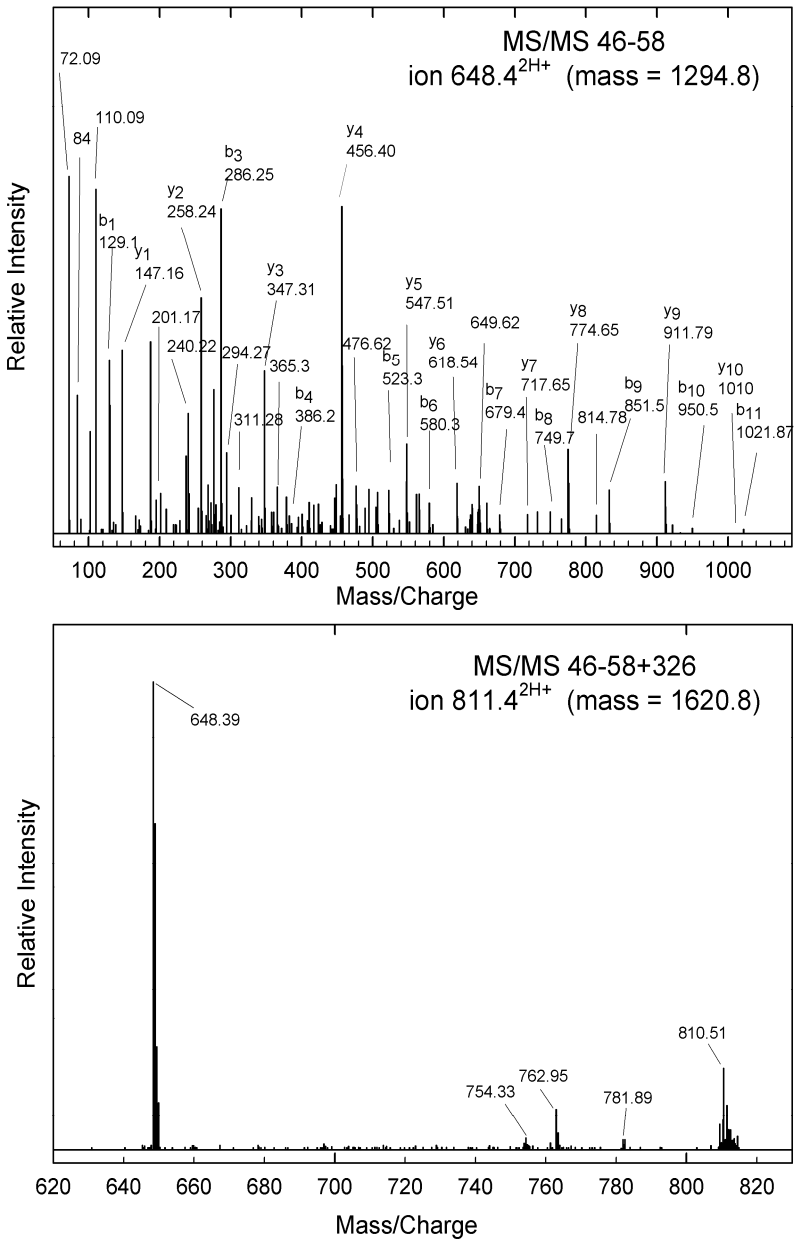

Fig. 5.6. MS-MS of peptide 46-58. MS-MS analysis of peptide 46-58 of aS, eluted from RP-HPLC results in the whole fragmentation of the fragment (top). MS-MS analysis of peptide 46-58 modified by DHA (bottom) was performed in order to detct the precise residue modified by DHA. Spectrum reveals that the adduct dissociate and formation of unmodified 46-58 fragment occurs.

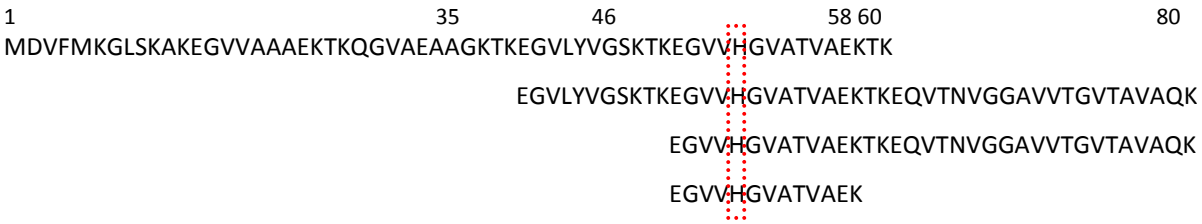

Fig. 5.7. Sequences of peptides characterized by a Δ mass of 326 Da. The hypothesised His 50 as site of modification is highlighted.

5.3 Role of His50 in oligomerization

Histidine and lysine are nucleophilic amino acids and therefore vulnerable to modification by lipid peroxidation derived electrophiles, such as 2-alkenals, 4-hydroxy-2-alkenals, and ketoaldehydes, derived from lipid peroxidation. Histidine shows also a specific reactivity toward 2-alkenals and 4-hydroxy-2-alkenals, whereas lysine is a ubiquitous target of aldehydes, generating various types of adducts (Uchida, 2003). Covalent binding of reactive aldehydes to histidine and lysine is associated with the appearance of carbonyls and antigenecity of proteins. In our case His50 is resulted the most frequent site of formation of an adduct with DHA. It is of great interest after that to investigate the importance of the position of the DHA adduct for aS oligomerization. To this aim we have studied a mutant of aS containing in position 50 a glutamine residue (H50Q). Moreover this species is naturally occurring mutant, found in familiar form of PD (Proukakis *et al.,* 2013). The protein was obtained by recombinant technique and it was characterized by mass spectrometry, after purification by RP-HPLC (Fig 5.8).

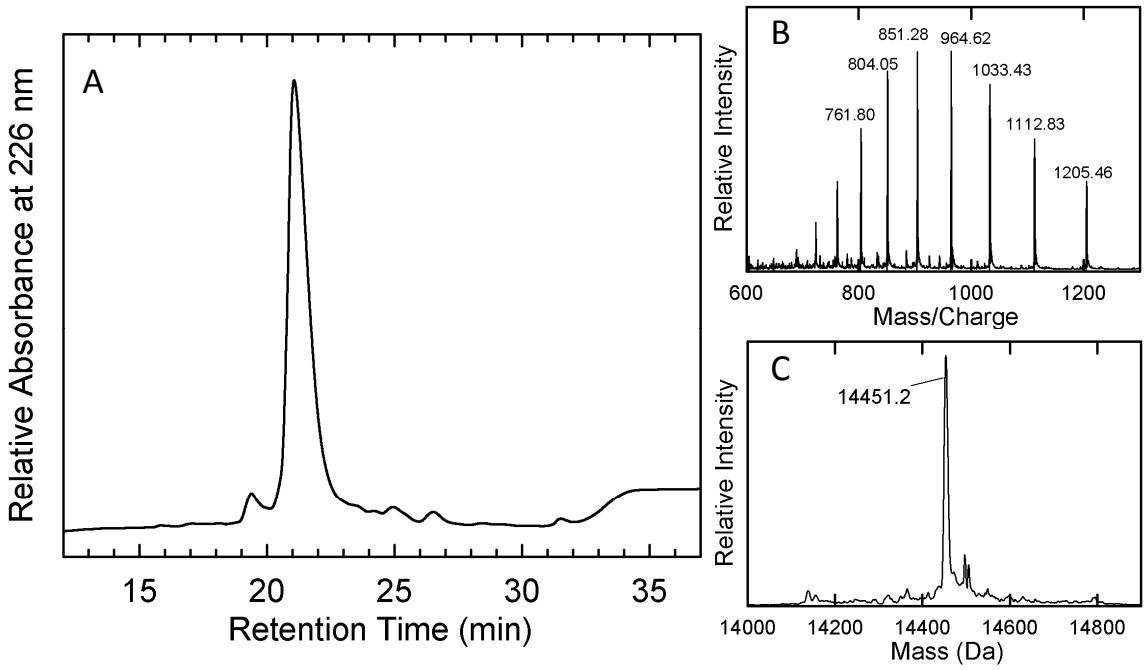

Fig. 5.8. (A) RP-HPLC of H50Q after purification by ion exchange and (B, C) MS spectra of the major fraction. Further details are described in Methods section.

To investigate the influence of H50Q variant on the interaction with DHA, far-UV CD measurement were performed (Fig. 5.9), in the presence of increasing amount of DHA. In comparison with aS, H50Q shows a similar extent of acquisition of a-helical

structure. To further investigate the possible occuring differences, aS and H50Q were proteolyzed with pK in the presence of saturating amount of the FA. After 5 min of reaction, the first fragments were detectable. RP-HPLC and mass spectrometry analysis (Fig. 5.10) (Table 5.2) of obtained species reveal that the same cleavage sites were present in the two protein, suggesting a really similar interaction mode of aS and H50Q.

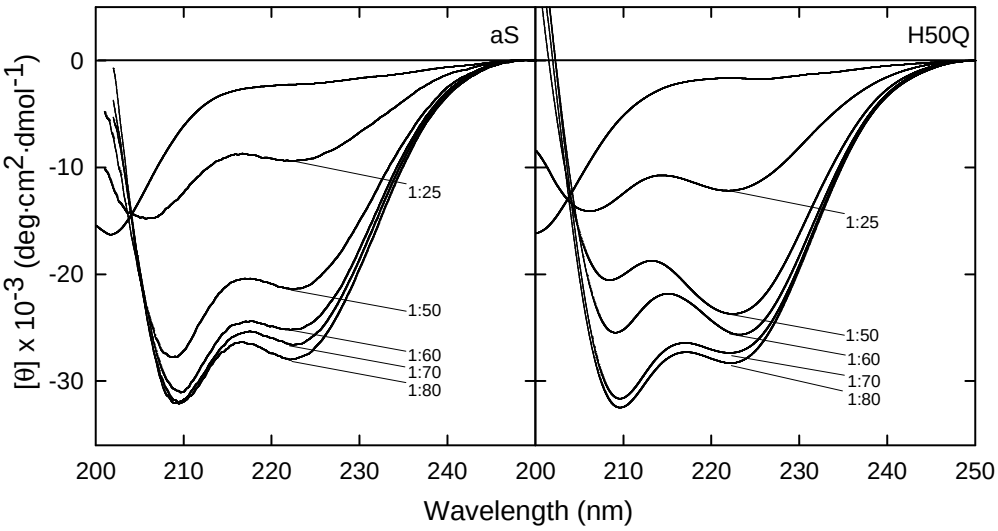

Fig. 5.9. CD measurements. Far-UV CD spectra of aS and H50Q in the absence and in the presence of DHA at different molar ratio. Spectra were recorded in PBS pH 7.4, at a protein concentration of 5 μM, and in the absence or in the presence of DHA in a final molar ratio protein:lipid of 1:25, 1:50, 1:60, 1:70 and 1:80.

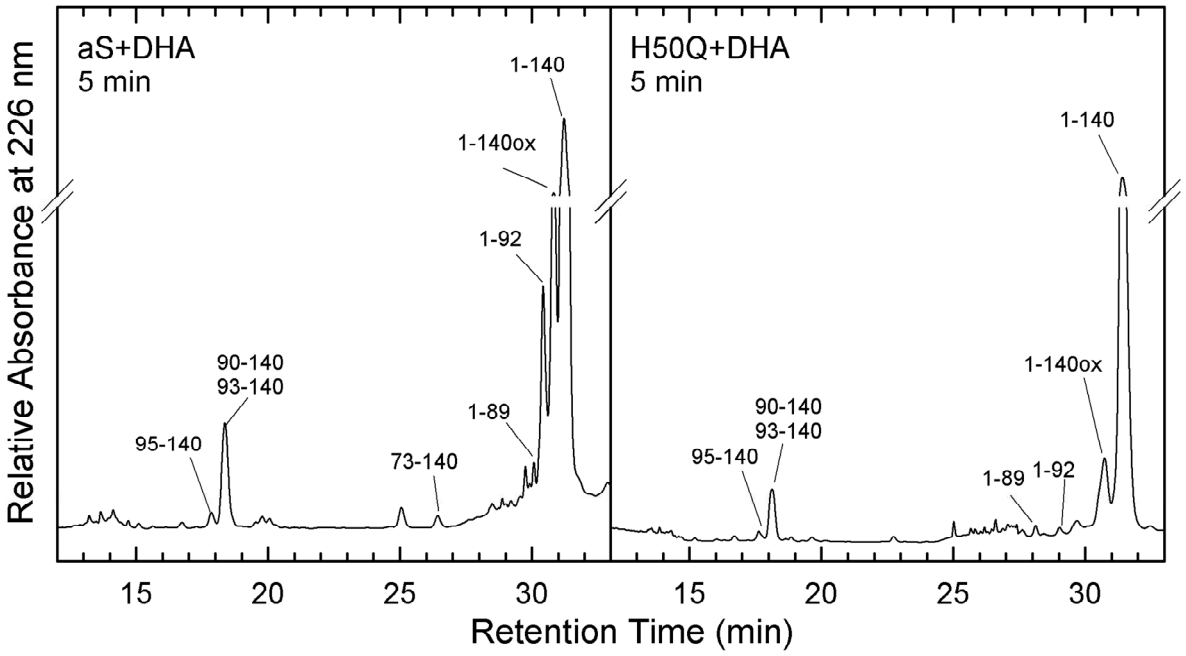

Fig. 5.10. RP-HPLC chromatograms of the proteolytic mixture of aS and H50Q with pK in the presence of DHA with a molar ration protein:lipid 1:70, after 5 min of incubation. Proteolysis were conducted with proteinase K in a E:S ratio of 1:1000. The fractions are collected and analyzed by mass spectrometry to identify the peaks.

H50Q was incubated with DHA under the same conditions used to obtain aS/DHA oligomers and its aggregation process was monitored by GF (Fig. 5.11) and RP-HPLC (Fig. 5.12). The aggregation process of H50Q in the presence of DHA shows a comparable extent of oligomerization. The retention volume of oligomers is the same for the two species, meaning that they have the same hydrodynamic volume.

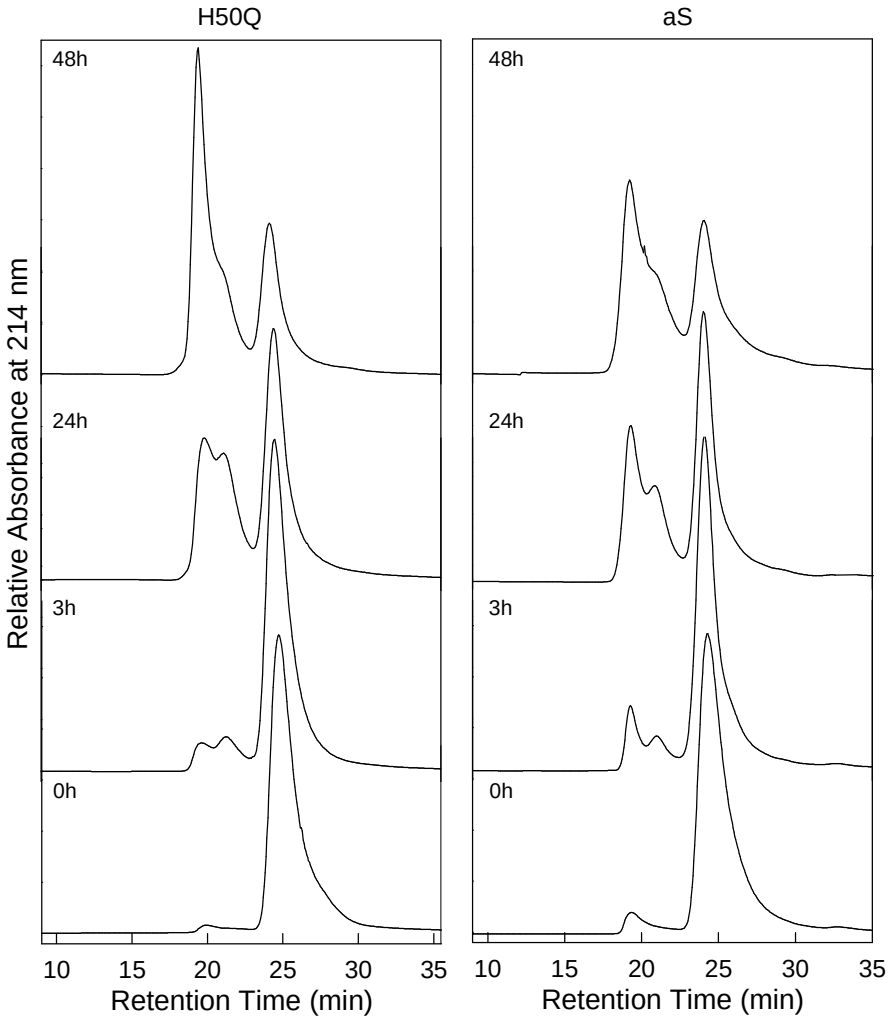

Fig. 5.11. Gel filtration analysis. Chromatograms of the mixtures of H50Q (left) and aS (right) with DHA in a molar ratio 1:50 during aggregation. The number on the left refers to the time of incubation.

The mixture of H50Q in the presence of DHA was also analyzed by RP-HPLC (Fig. 5.10 and Table 5.3) and the behaviour of oligomers compared to aS. The patterns are quite similar and just after 3 hours H50Q oligomers form with similar RT of 29.5 min, indicative of very hydrophobic species. Moreover after 48 hours most of the monomeric protein is converted in oligomer.

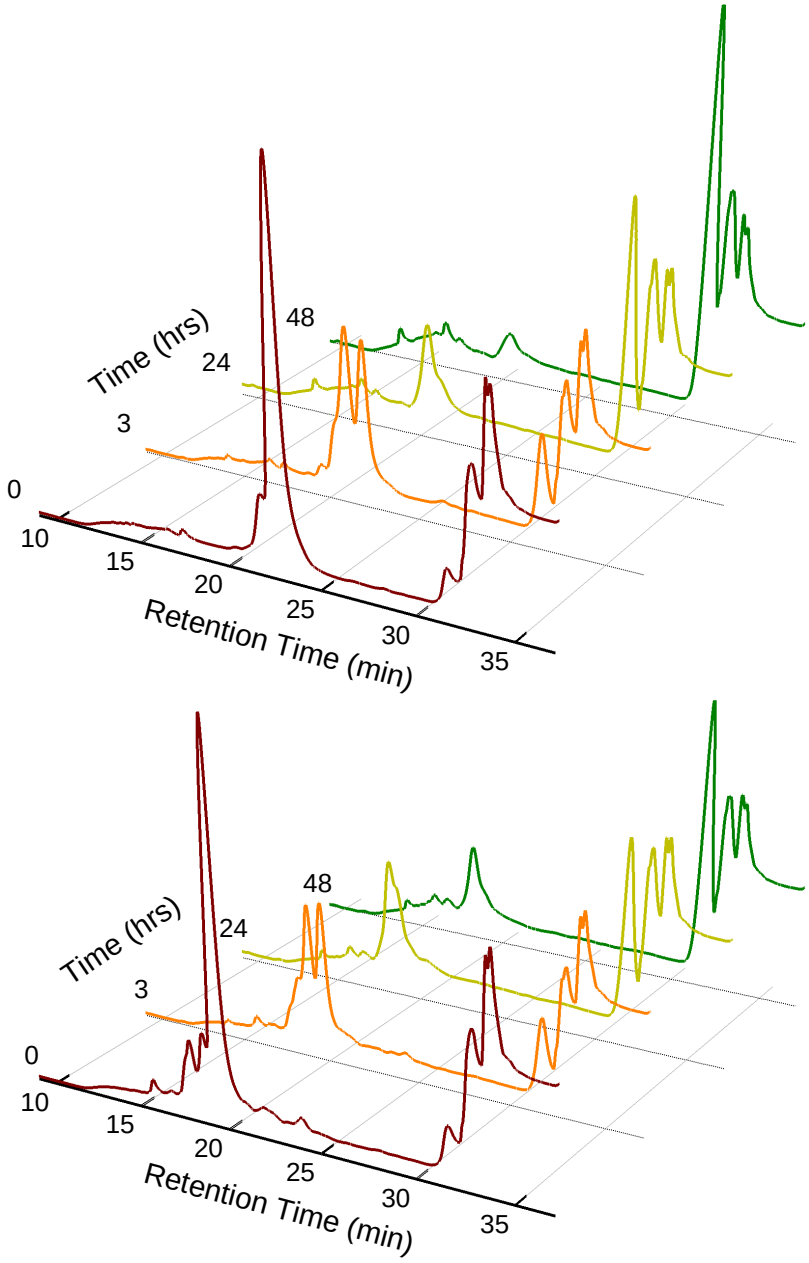

Fig. 5.12. RP-HPLC analysis. Chromatograms of H50Q (A) or aS WT (B) in the presence of DHA in a molar ratio 1:50 during aggregation. The colour indicate the time of incubation: 0 (red), 3- (orange), 24- (yellow) and 48- (green) hours.

The most important feature of H50Q oligomers to compare to aS ones is the presence, and eventually the position, of DHA adducts. For this reason, H50Q/DHA oligomers were purified by RP-HPLC and analyzed by mass spectrometry (Fig. 5.13). Analysis showed that DHA still binds to the protein and moreover more than one DHA adduct was present on single protein molecules. As done for aS, proteolysis experiments were conducted in order to identify possible favourite sites of modification.

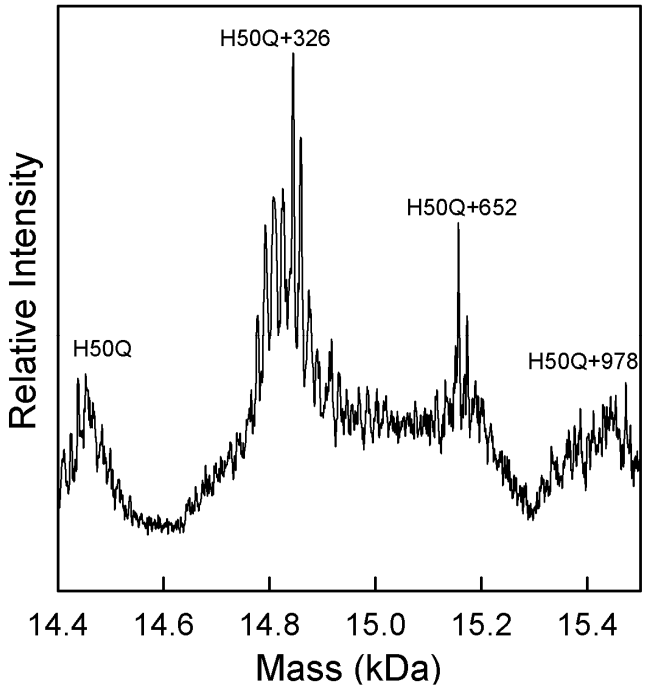

Fig. 5.13. Mass spectrometry analysis. Mass spectrum of H50Q/DHA oligomers purified by RP-HPLC after 3 hours incubation.

Proteolysis was conducted using trypsin, in a E:S ratio 1:100 by weight. Proteolytic solutions were analyzed in RP-HPLC after 30 min (Fig. 5.14). Mass spectrometry identification were performed for all eluted peaks, to find DHA-adduct containing fragments (Table 5.4). We identify the same peptides as aS, and those containing Q50 show the correct mass decrease of 9 Da due to substitution of His with Gln (table 5.4). Since His50 had been removed, different modified fragments were sought. We were not able to find modified peptides. This means that probably a favoured site for modification is absent and this leads to spread DHA between the several lysine present on the protein. As a consequence, a single specific lysine is rarely modified, thus it is not detectable with this kind of analysis.

To further characterize H50Q/DHA oligomers, their ability to affect synthetic membranes was tested. As already done for aS (§ 3.6), calcein test was used. DOPG LUV loaded with calcein were treated with 1 µM solution of H50Q oligomers (Fig. 5.15). Oligomers show to be able to destabilize vesicles at the same extent of aS oligomers.

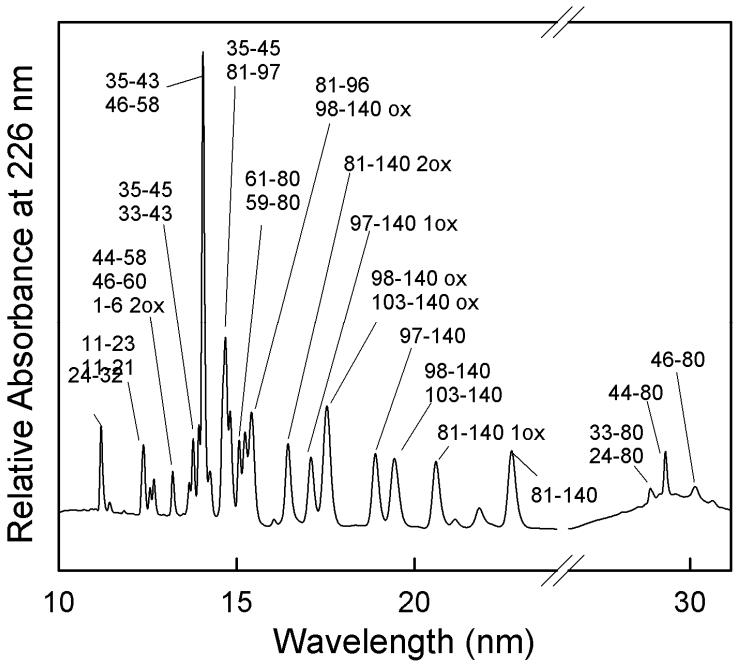

Fig. 5.14. RP-HPLC analysis. Chromatogram of H50Q/DHA oligomers after 30 minutes of proteolysis with trypsin. Proteolysis was conducted in PBS pH 7.4 buffer at 37°C with a E:S ratio 1:100 (by weight).

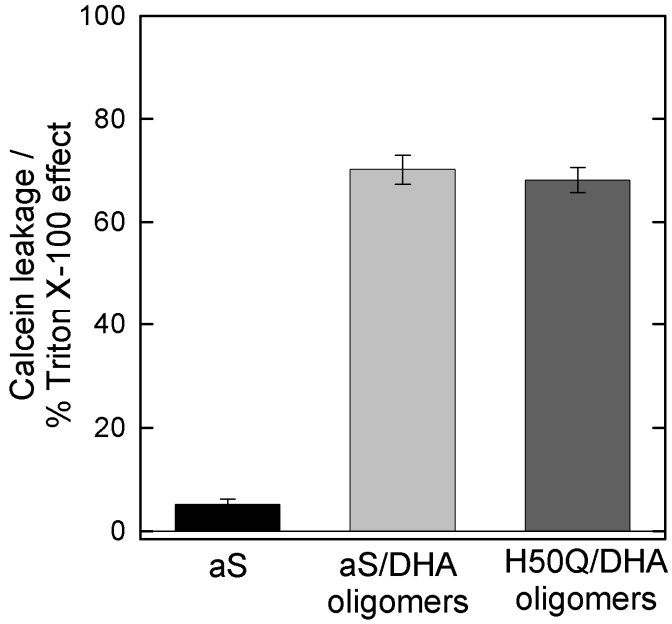

Fig. 5.15. Calcein-leakage test for H50Q/DHA oligomers. Fluorescence measurement of calcein-loaded DOPG LUV after 30 min incubation with oligomers of H50Q or aS formed in the presence of DHA 1:50.

This result allows us to deduce that the specific position of the modification in aS sequence by DHA is not essential for oligomers formation and activity. Considering that we never obtained unmodified oligomers, we can not exclude a role of this adduct considering that it not possible to obtain oligomers without modification.

Table 5.1. Chemical characterization of fragments corresponding to mayor peaks of the chromatogram relative to the fragmentation of aS/DHA oligomers with trypsin after 3 hr of incubation.

RT[a] (min)	Molecular Mass (Da) Found[b]	Calculated[c]	Peptide species[d]
11.2	830.43	829.91	24-32
13.2	1524.16±0.01	1523.74	44-58
	1294.99±0.05	1294.68	46-58
	1294.8±0.1	1621.46	46-58+326
	1754.37±0.02	1754.02	44-60
13.8	1406.9±0.1	1409.65	33-45
	1179.93±0.05	1180.37	35-45
14.1	950.7±0.01	951.09	35-43
14.7	2157.17±0.04	2157.45	59-80
14.9	1607.16±0.01	1606.84	81-97
15.1	2148.14±0.11	2148.44	81-102
15.4	1928.41±0.05	1928.17	61-80
15.6	1478.05±0.04	1478.66	81-96
	4923.6±0.13	4923.25	35-80 +326
17.9	4847.06±0.38	4846.03	98-140+1ox
	6472.55±0.75	6475.19	1-60+326
19.3	4958.66±0.01	4958.20	97-140
19.9	4288.74±0.34	4288.43	103-140
	4830.5±0.1	4830.03	98-140
21.2	6434.93±0.04	6434.86	81-140+1ox
	6451.22±0.46	6450.86	81-140+2ox
23.4	6418.65±0.13	6418.86	81-140
28.2	3434.52±0.05	3434.89	46-80
	3760.8±0.05	3760.89	46-80+326
	3664.32±0.01	3664.18	44-80

[a] Peptides or proteins were purified by RP-HPLC and listed in order of retention times (RT).
[b] Experimental molecular masses determined by ESI-MS.
[c] Molecular masses calculated from the amino acid sequence of aS.
[d] Species containing Met residues are present also as oxidized form.

Table 5.2. Chemical characterization of peptide material corresponding to mayor peaks of the chromatograms relative to the fragmentation of aS and H50Q bound to DHA with proteinase K after 5 min of incubation.

	RT[a] (min)	Molecular Mass (Da) Found[b]	Molecular Mass (Da) Theoretical[c]	Species[d]
aS	18.4	5633.10±0.11	5633.0	90-140
		5390.01±0.11	5389.7	93-140
	29.7	7174.57±0.06	7173.7	73-140
	30.1	8846.32±0.74	8845.2	1-89
	30.4	9088.98±0.59	9088.5	1-92
H50Q	30.8	14477.41±0.4	14476	1-140+1ox
	31.5	14460.05±0.27	14460	1-140
	18.4	5633.14±0.12	5633.0	90-140
		5389.77±0.48	5389.7	93-140
	29.6	8837.24±0.36	8836.2	1-89
	29.9	9079.42±0.42	9079.45	1-92
	30.4	14452.58±0.40	14451.2	1-140

[a ,b, c, d] see reference Table 5.1

Table 5.3. Chemical characterization of protein material corresponding to mayor peaks of the chromatogram relative to the aggregation of aS and H50Q in the presence of DHA.

	RT[a] (min)	Molecular Mass (Da) Found[b]	Molecular Mass (Da) Theoretical[c]	Species[d]
aS	19.5	14508.13 ±0.05	14508.1	aS 3ox
		14491.8 ±0.5	14492.1	aS 2ox
	21	14459.92 ±0.01	14460.1	aS
	31.5	14817.1 ±0.7	14818.1	aS 2ox 326
		14831.3 ±0.9	14834.1	aS 3ox 326
H50Q	17.8	14522.4±1.1	14522.2	H50Q 2ox
		14554.6 ±0.2	14554.2	H50Q 4ox
	18.5	14506.3 ±0.6	14506.2	H50Q 1ox
	18.9	14490.5 ±0.3	14490.2	H50Q
	31.5	14824.0±1.13	14825.2	H50Q 3ox 326
	[e]32	326.28 ±0.08	326.24	DHA (-2H)
	33	328.29 ±0.16	328.24	DHA

[a ,b, c, d] see reference Table 5.1

[e] Peaks eluted at 32 and 33 min correspond to DHA for all analyzed protein.

Table 5.4. Chemical characterization of peptide material corresponding to mayor peaks of the chromatograms relative to the fragmentation of H50Q/DHA oligomers with trypsin after 30 min of incubation.

RT[a] (min)	Molecular Mass (Da) Found[b]	Calculated[c]	Species[d]
11.3	829.42	829.43	24-32
	1058.59	1058.57	22-32/24-34
12.5	1071.6	1071.59	11-21
	872.47	872.46	13-21
	1300.78	1300.74	11-23
12.7	1101.63	1101.60	13-23
13.2	801.37	801.35	1-6 2ox
13.7	1179.74	1179.65	35-45/33-43
	1285.66	1285.69	46-58
13.9	1744.10	1743.97	44-60
14.1	950.56	950.51	35-43
	785.39	769.35	1-6 1ox
14.3	1514.97	1514.83	46-60
	1170.68	1170.58	1-10 1ox
	950.5	950.51	35-43
	1688.82	1685.97	7-23
	1285.78	1285.69	46-58
14.7	1605.98	1605.87	81-97
15.1	1910.64±0.46	1927.04	61-80
	2157.36	2156.18	59-80
15.5	4862.2	4862.03	98-140 2ox
	1477.3	1478.7	81-96
17.1	4972.99±1.57	4974.20	97-140 1ox
18.9	4958.46±0.03	4958.20	97-140
19.4	4288.07±0.39	4288.43	103-140
	4829.38±0.75	4830.03	98-140
22.8	6418.11±0.51	6418.86	81-140
29.1	3655.36±0.07	3655.17	44-80
	4819.30±0.19	4817.52	33-80
	5629.74	5629.41	24-80
29.4	3425.1	3423.80	46-80

[a,b,c,d] see reference Table 5.1

6. aS FAMILIAR VARIANTS AND DHA

Genetic studies of the aS gene in familial cases of PD have demonstrated that overexpression of normal aS is associated with this disease. However also pathogenic missense mutations, A53T (Polymeropoulos et al., 1997), A30P (Kruger et al., 1998), and E46K (Zarranz et al., 2004) and multiplication (Chartier-Harlin et al., 2004; Farrer et al., 2004; Fuchs et al., 2007; Singleton et al., 2003) of the aS gene have been identified in kindreds of autosomal dominantly inherited familial PD and DLB (Fig. 6.1). Recently other missense mutations have been found, such as H50Q (Proukakis *et al.,* 2013) and G51D (Kiely et al, 2013).

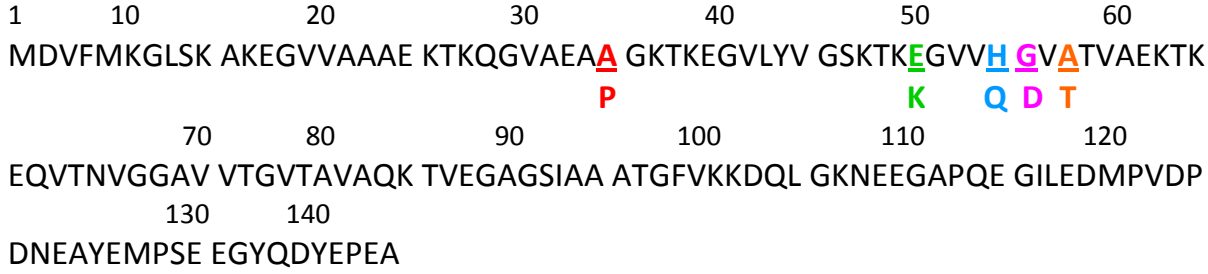

Fig. 6.1. Schematic representation of the localization of main aS mutations.

It is not yet fully clear how these mutations affect the pathogenesis of PD. It is seems that E46K mutation produces aS peptides displaying an increased propensity to form relatively large oligomers, whereas the A30P mutation produces aS peptides displaying decelerated secondary structure transitions and a decreased propensity to form oligomers (Ono et al., 2011). Another aspect concerns the ability of aS mutants to bind phospholipids and fatty acids. The mutant A30P is defective in binding to phospholipid vesicles, while the A53T substitution displays a normal membrane-binding activity, comparable to wild-type aS (Jo et al., 2002). Bodner and coll. (2010) have reported the phospholipid binding properties of the variants, viewed by solution NMR. They show overall decreased lipid affinity for the A30P mutation, comparable affinity for A53T, and an increased level of binding of E46K, relative to wild-type aS.

We investigated the ability of a group of aS mutants to bind DHA by circular dichroism and proteolysis experiments. Further we have evaluated the propensity of these protein species to oligomerize in the presence of DHA. This study could help to get more

information about the interaction between aS and fatty acids and the role of this interaction in the pathogenesis of PD.

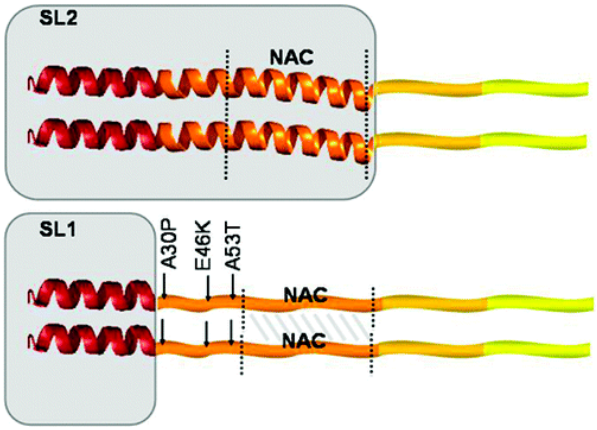

Fig. 6.2. Scheme depicting the increased vulnerability of aS to self-association when engaged in the SL1 binding mode vs SL1. SL1 and SL2 refer to two different bound state to phospholipids: SL1 comprise a short bound α-helix followed by dynamic disordered residues ~25-140; SL2 engages the full N-terminal domain, up to residue ~100, in the α-helical conformation, while the 40 residues of the C-terminal tail remain flexible in solution. All variants increase the relative population of SL1, for which a long unstructured stretch of N-terminal residues is exposed (reprinted from Bodner et al., 2010).

6.1. Conformational analysis.

The secondary structure of A30P, A53T and E46K in the presence of DHA was analyzed by far UV circular dichroism (CD). All mutants are unfolded in solution while increasing the amount of DHA, the appearance of the two typical minima at 2008 and 222 nm is observed, indicating the acquisition of α-helical secondary structure (Fig. 6.3).

The overall behaviour of the proteins is similar and they show a similar susceptibility to acquire α-helix conformation upon addition of the fatty acid. The presence of an isodichroic point at 203 nm in the titration experiments suggest a two state transition from random coil to α-helix. To further analyze the interaction the ellipticity was shown as a function of the molar ratio between the proteins and DHA. Especially the ellipticity at 208 nm or the ratio between the ellipticity at 208 in the presence of DHA and at 208 nm in the absence of the fatty acid as a function of protein/DHA ratio was reported (Fig. 6.4).

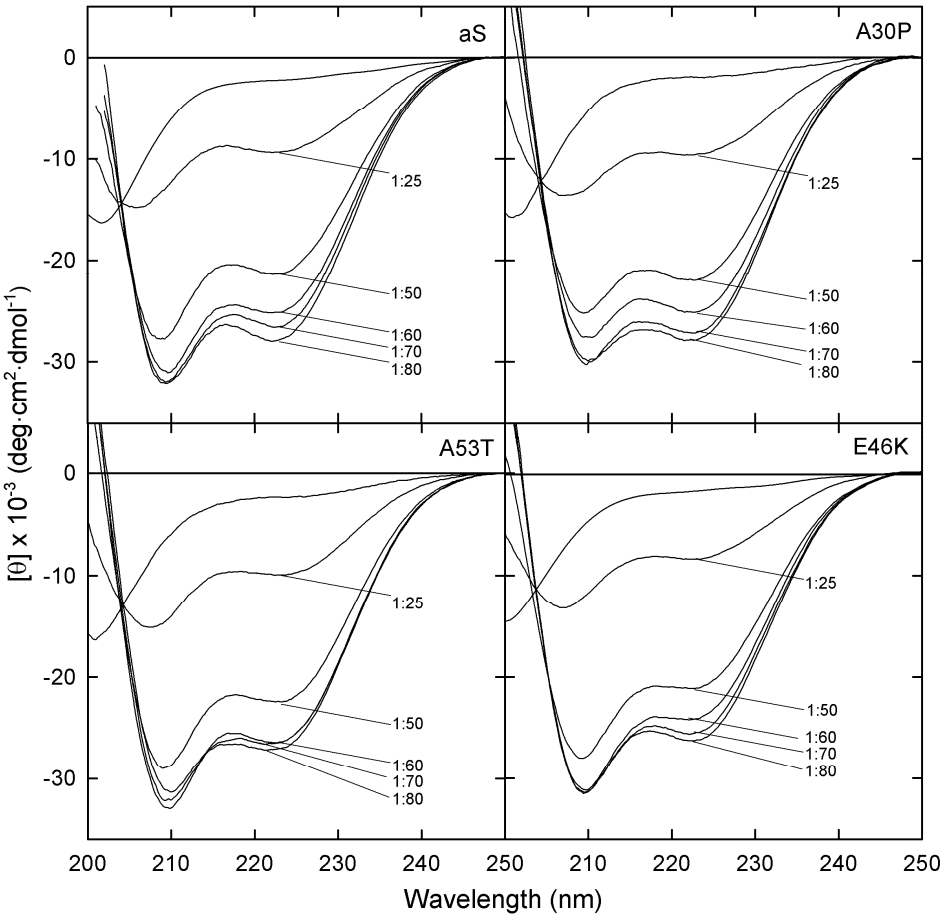

Fig. 6.3. CD measurements. Far-UV CD spectra of aS, A53T, E46K, A30P in the absence and in the presence of DHA at different molar ratio. Spectra were recorded in PBS pH 7.4, at a protein concentration of 5 μM, and in the absence or in the presence of DHA in a final molar ratio protein:lipid of 1:25, 1:50, 1:60, 1:70 and 1:80 for all proteins.

A30P shows a slight reduced ellipticity and requires more DHA to complete its conformational transition. Indeed, while aS, E46K and A53T CD signals at 208 and 222 nm do not increase further at a molar ratio of 1:50, A30P requires more that 350 μM of DHA (protein/DHA 1:70) to reach the saturation. So accordingly to previous results (Bodner et al., 2010), it seems that A30P does not have the same affinity for DHA as the other mutants and aS.

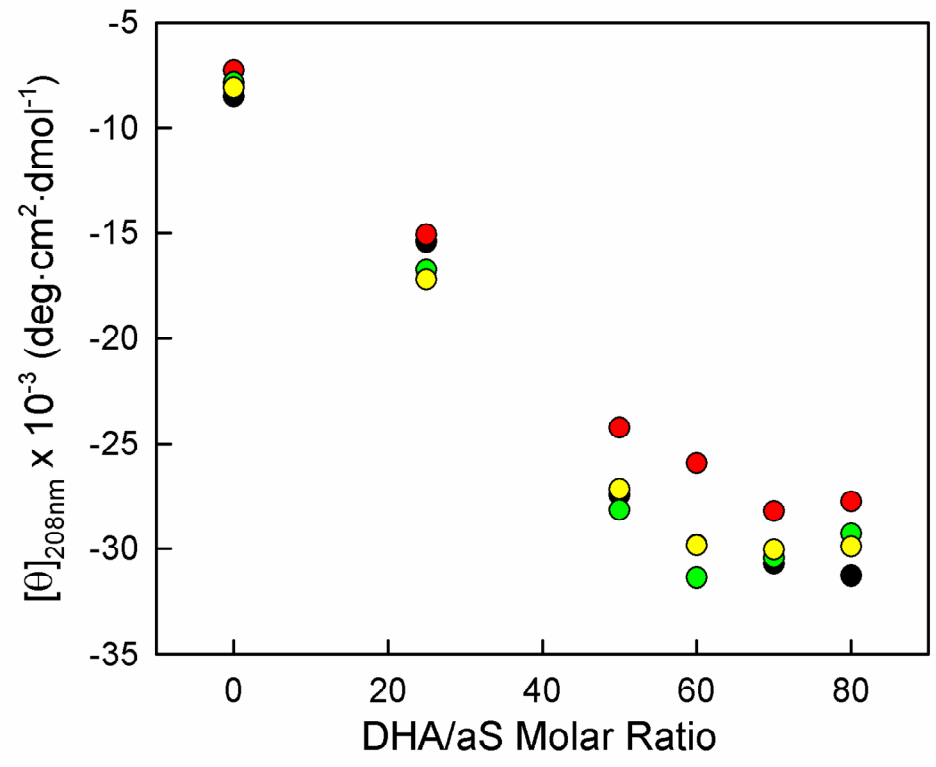

Fig. 6.4. Ellipticity at 208 nm as a function of DHA/protein ratio. Black circles refer to aS, red circles to A30P, green circles to A53T and yellow circles to E46K.

6.2 Proteolytic mapping of the complex protein/DHA

To define the region(s) of interaction of aS variants with DHA, an approach based on proteolytic digestion and mass spectrometry was used as previously done for aS (De Franceschi et al., 2009). This strategy relies on the consideration that regions of the protein normally available to proteases exhibit limited accessibility when involved in interaction with lipids (Fontana et al., 2004; Polverino de Laureto et al., 2006). We used proteinase K (pK) (Ebeling et al., 1974), a particularly voracious protease, which displays broad substrate specificity to correlate the site of enzyme fission with enhanced backbone flexibility or local unfolding of the substrates. Moreover this protease retains proteolytic activity in the presence of DHA (De Franceschi et al., 2009). Proteolysis experiments were conducted in the absence and in the presence of DHA using a ratio with the protein of 1:70 to be sure that the equilibrium between the free and bound molecule were shifted towards the bound one. From previous studies, we know that aS displays the same pattern of proteolysis in the presence of DHA in ratio 50:1 -70:1 on the protein.

In the absence of DHA the protein variants are readily fragmented, as already observed for aS (De Franceschi et al., 2009), according to the fact that these proteins are unfolded in solution and prone to protease attack. A remarkable fact concerns the behaviour of A30P. Intact A30P is, indeed, found in the proteolytic mixture after 1 hour of incubation with the protease, and after 3 hours of incubation is completely cleaved by pK. At variance all other proteins are completely degraded by the protease just after few minutes of reaction. The chromatograms RP-HPLC of the proteolytic mixture of A30P and E46K with pK in the absence of DHA after 1 hour of incubation are reported in Fig. 6.5 to evidence this aspect.

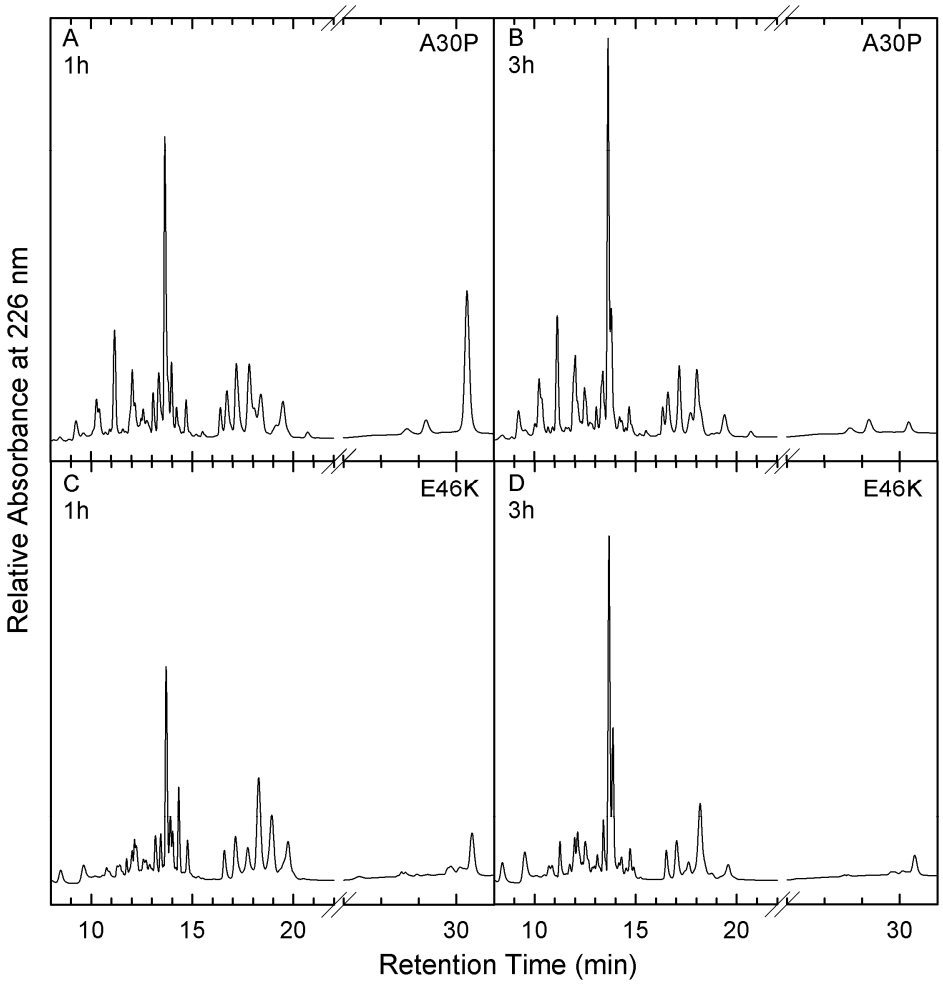

Fig. 6.5. RP-HPLC chromatograms of the proteolytic mixture of A30P and E46K with pK in the absence of DHA after 1 and 3-hr of incubation. The fractions are collected and analyzed by mass spectrometry to identify the peaks.

The proteolysis of the variants with pK in the presence of DHA is stopped after 5 min (Fig. 6.6) and 1 hour of incubation (Fig. 6.7), to see the initial and the late sites of

fragmentation. In all species the initial sites of proteolysis are located in the protein segment 89-92. Indeed, the intact protein is the main species after 5-min of incubation and only few peaks of low intensity are visible in the chromatogram. The fractions were analyzed by mass spectrometry (Table 6.1).

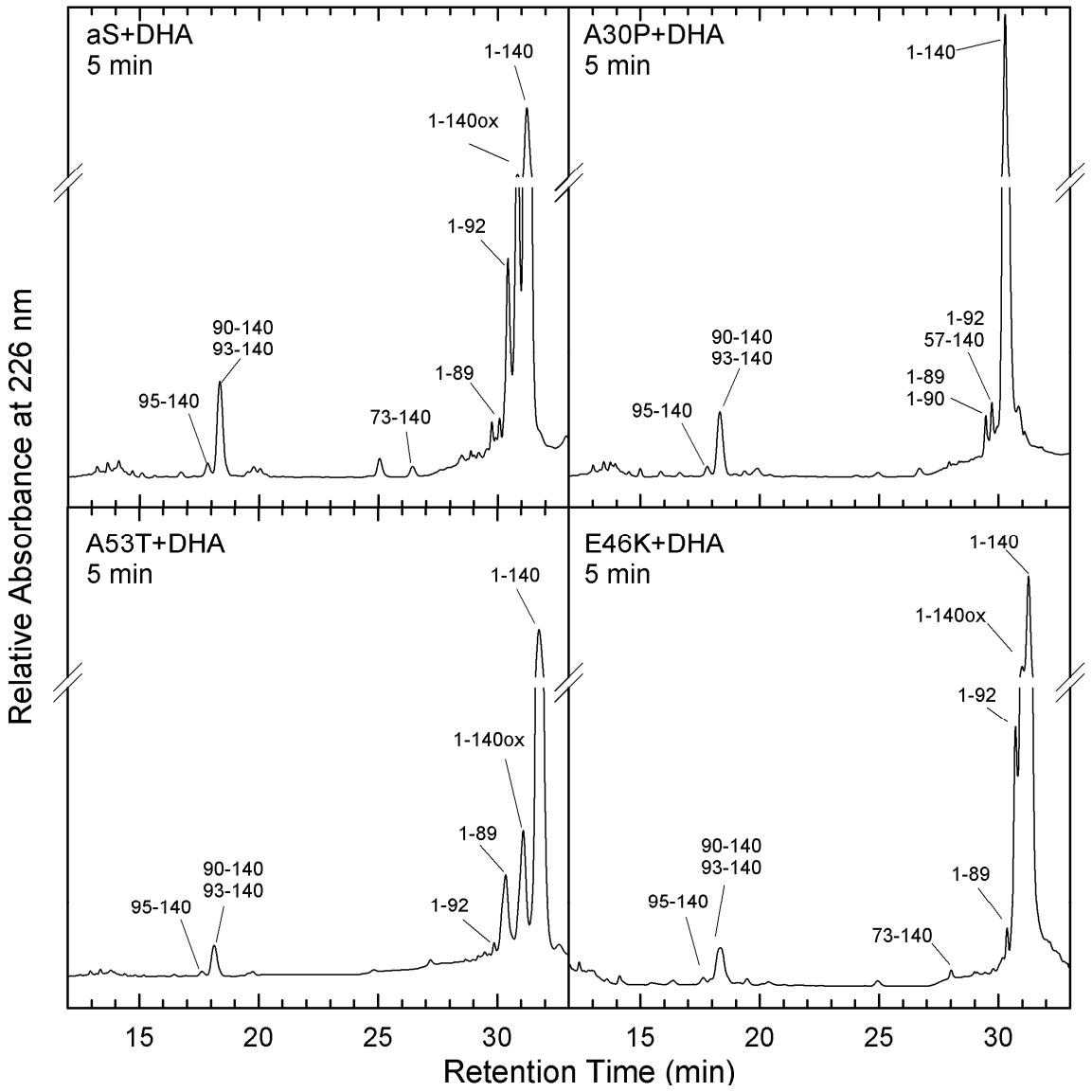

Fig. 6.6. RP-HPLC chromatograms of the proteolytic mixture of aS, A30P, A53T and E46K with pK in the presence of DHA with a molar ration protein:lipid 1:70, after 5 min of incubation. Proteolysis were conducted with proteinase K in a E:S ratio of 1:1000. The fractions are collected and analyzed by mass spectrometry to identify the peaks.

The main species found in the proteolytic mixture correspond to full length protein, and in very low amounts to fragments 1-89 and 1-92 and the complementary fragments 90-140 and 93-140, indicating that the proteins are initially cleaved at the peptide bonds Ala89-Ala90 and Thr92-Gly93. After 1-hr of proteolysis the predominant

product observed for aS is the peptide 1-72 (MM 7299.9 Da) (De Franceschi et al., 2009). The fragment 1-89 (MM 8839.7 Da) does not accumulate and it is further cleaved forming fragment 1-72. This species remains in the proteolysis mixture also after prolonged (3-hr) incubation with the protease (De Franceschi et al., 2009). Fragment 90-140 seems to be quite resistant to proteolysis and fragments 93-140, 95-140 and 126-140 are produced in minor extent. In the case of E46K after 1-hr of proteolysis the main species are fragments 1-50 and 1-72 (Fig. 6.7 and Table 6.2), showing a remarkable difference with aS. For A30P an unexpected resistance to proteolysis is shown, considering that in the presence of DHA there is still intact protein in the mixture after even after 3-hr of reaction with pK. Unfortunately we don't have data regarding the prolonged proteolysis of A53T.

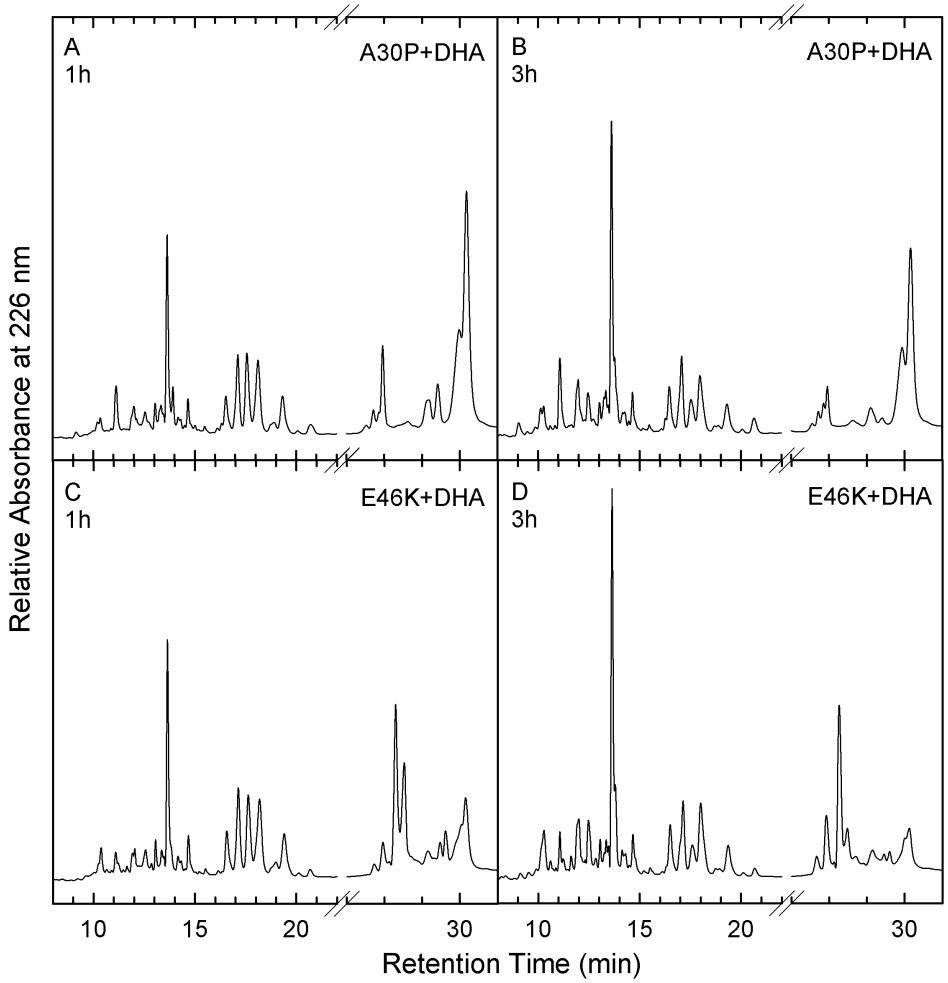

Fig. 6.7. RP-HPLC chromatograms of the proteolytic mixture of A30P and E46K with pK in the presence of DHA with a molar ration protein:lipid 1:70, after 1 and 3-hr min of incubation. The fractions are collected and analyzed by mass spectrometry to identify the peaks.

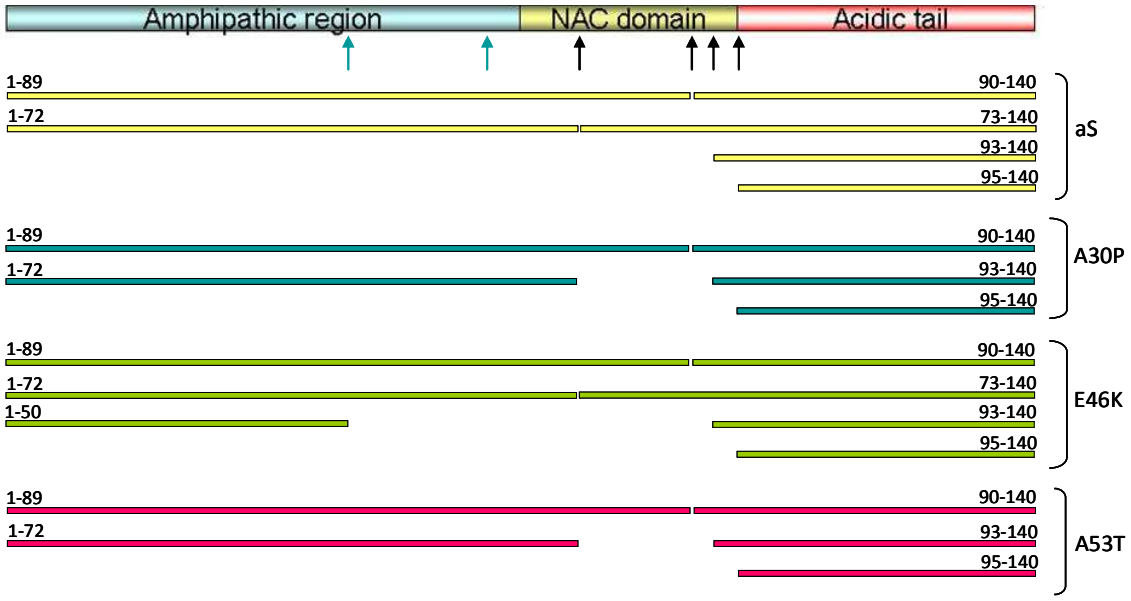

Fig. 6.8. Scheme of proteolysis. The main cleavage sites for aS, E46K, A30P and A53T with PK are reported.

6.3 Aggregation of as variants in the presence of DHA.

A general consensus is that these aS variants form insoluble fibrillar aggregates with antiparallel β-sheet structure upon incubation at physiological temperature and are able to accelerate fibril formation. However their precise effects at early stages of the aS aggregation process remain unknown. In respect to the tendency to oligomerize, it seems that E46K produces an oligomer distribution in which the highest observed oligomer order is bigger than that of aS, while A30P produces an oligomer distribution with a lower oligomer order than aS (Ono et al., 2011). We have studied the behaviour of the variants upon incubation in the presence of DHA. Aggregation process was followed by gel filtration (GF), TEM, circular dichroism (CD) and RP-HPLC. The results were compared to those obtained for wild type aS.

The mixtures of proteins and DHA (molar ratio P/DHA 1:50) were analyzed by GF chromatography with the purpose of correlating the physical properties of the samples with their chemical composition. Aliquots corresponding to different times of incubation (from 0 to 48 hr) of the mixture composed of protein and DHA were loaded onto a Superdex 75 column. The GF profile shows a major species eluting at 24 min (Fig. 6.9) and a minor species (1%) with lower retention time (RT 20 min) for all variants. After 3 h of incubation, the fraction of the low RT species increases, and after 48 h this species is the main component of the mixture (Fig. 6.9). Comparing the four different proteins, it is

evident that a difference resides in the yield of oligomers. A53T has a behaviour quite similar to aS. Conversely the peak of oligomers in E46K is quite low and elutes split in three forms with different RT. In the case of A30P the yield in oligomers appears higher than the others.

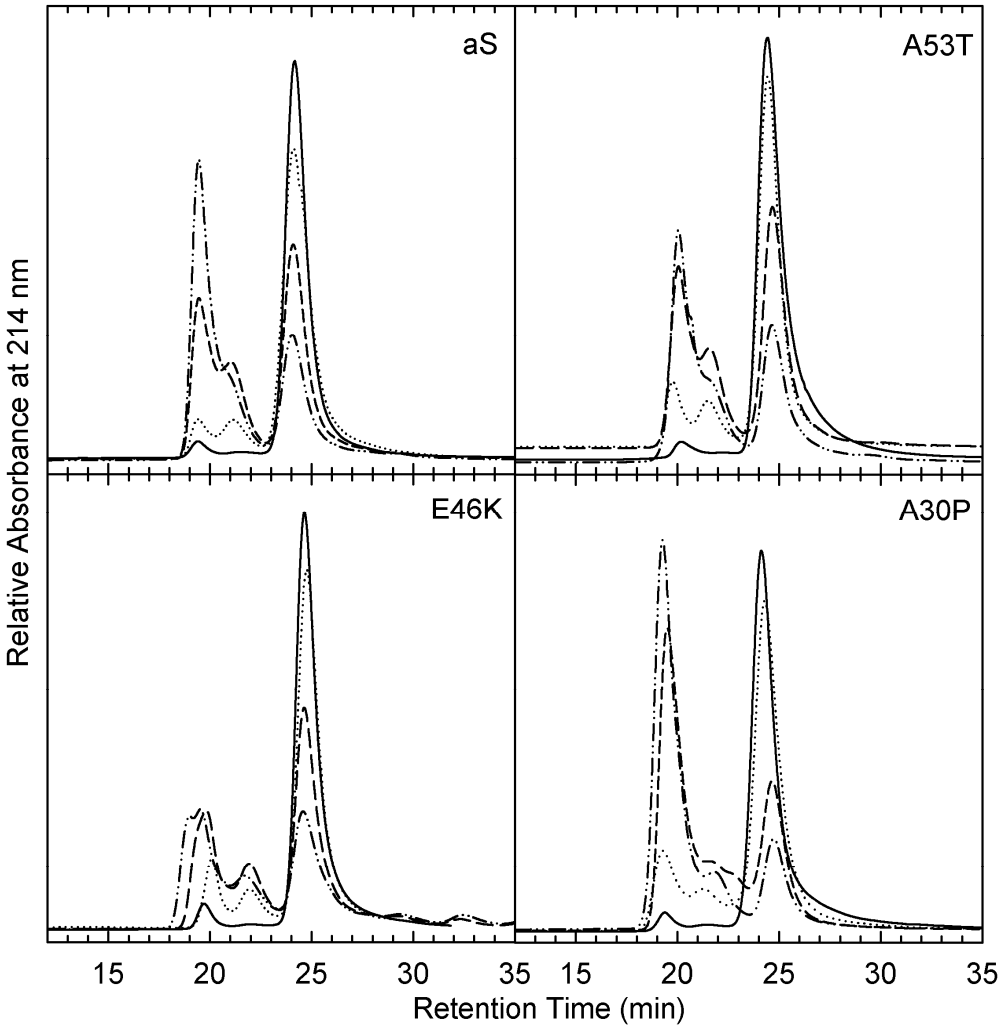

Fig. 6.9. Gel filtration analysis. GF chromatograms of the mixture of aS, A53T, E46K and A30P with DHA. Aliquots were taken from the mixtures at 3, 24 and 48-hr of incubation. The chromatogram relative to mixture just after preparation is also reported.

The fractions relative to oligomers were collected and analyzed by TEM, shown in Fig. 6.10. TEM analysis showed that the chromatographic fraction corresponding to oligomers of A30P and A53T contains heterogeneous population of aggregates in which a part has a spherical morphology, with diameters ranging from 15 to 35 nm. For E46K we were not able to obtain better images, so we don't have definitive results. In the figure,

the TEM images of fibrils produced by the variants under the same experimental conditions in the absence of DHA are shown on the right. All mutants are able to form long and unbranched fibrils in the absence of the fatty acid.

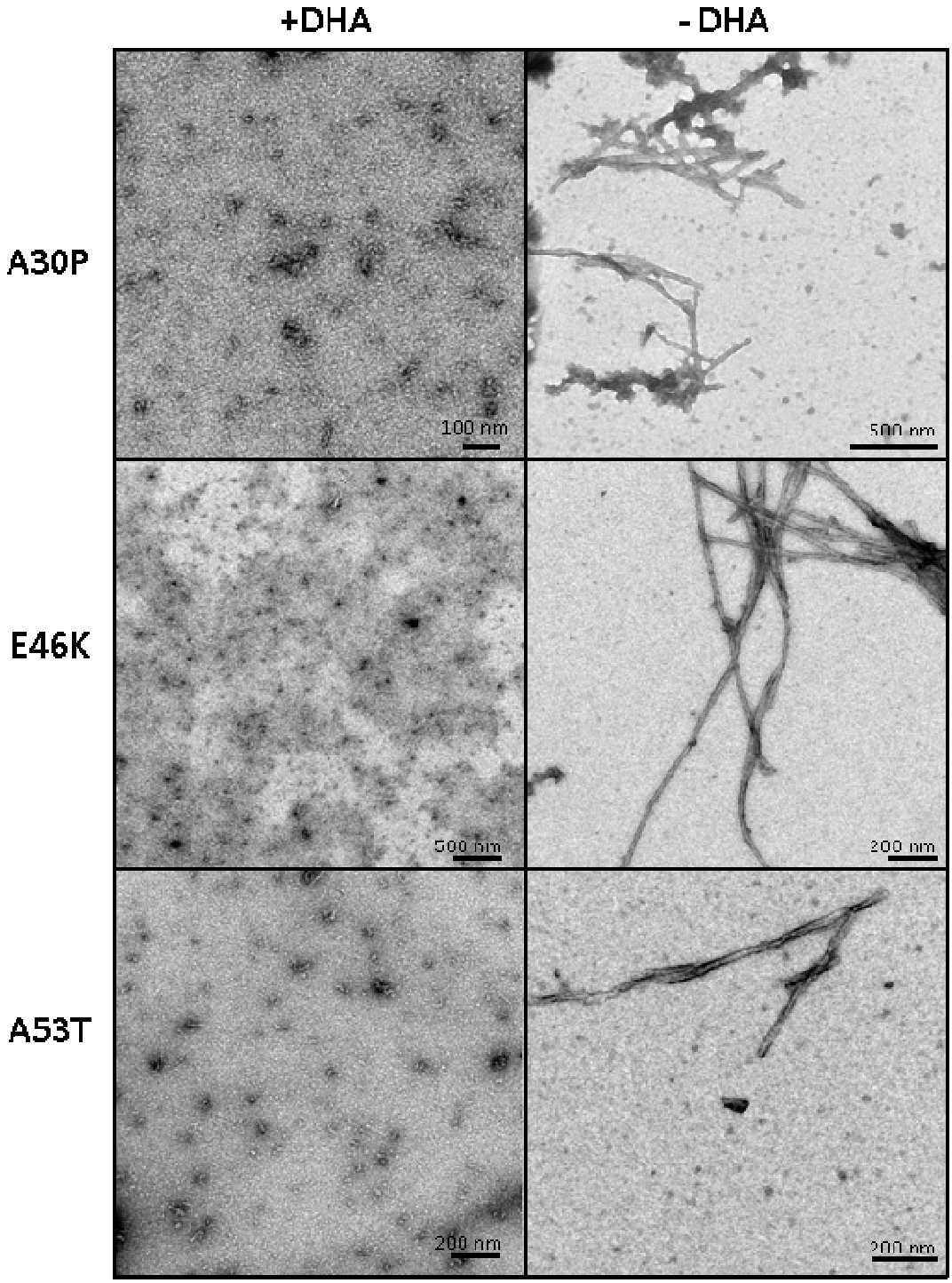

Fig. 6.10. **TEM pictures.** The aggregation of aS variants in the presence of DHA were analyzed by TEM. Pictures are relative to the oligomeric fractions of A30P, E46K and A53T eluted from GF.

The aggregation process was also followed by CD (Fig. 6.11) and no conformational change was observed, only a partial reduction of the intensity of the CD signals as observed for aS, although the spectrum shape does not change over time.

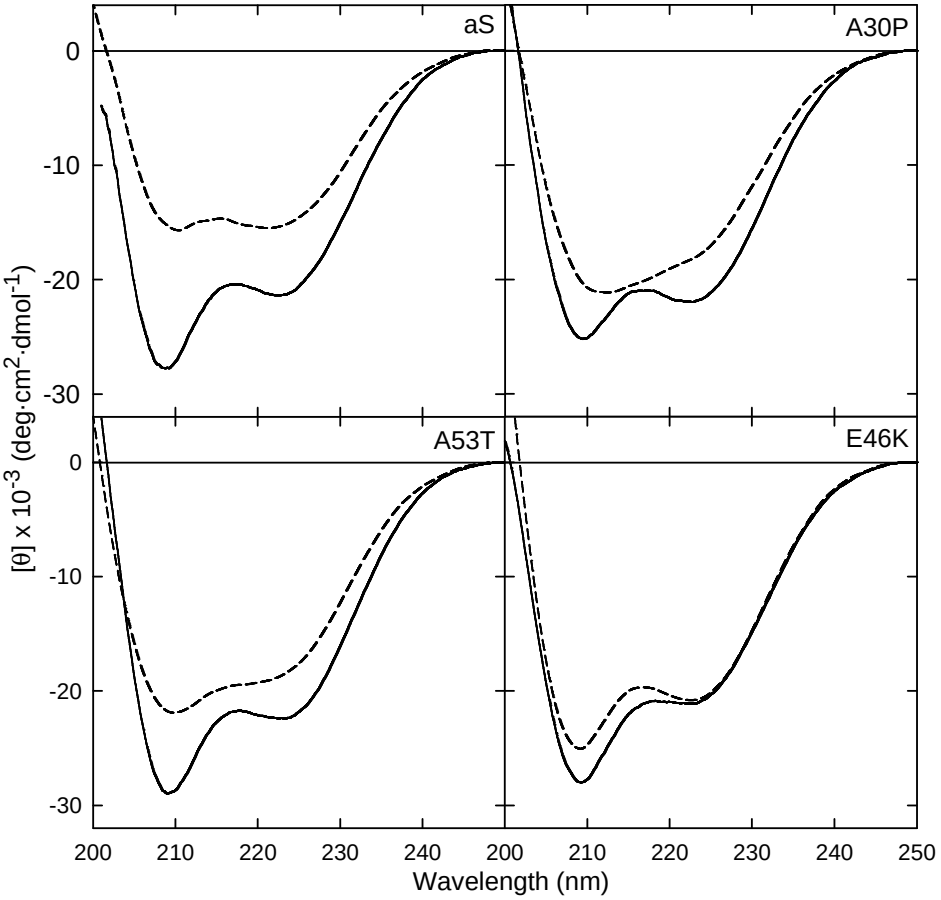

Fig. 6.11. CD measurements. Far-UV CD spectra of aS, A53T, E46K, A30P in the presence of DHA during aggregation. Spectra were recorded in PBS pH 7.4, at a protein concentration of 5 μM. The spectra relative to 0 (solid lines) and 48 (dashed lines) hr of incubation are reported.

The mixtures of proteins and DHA were injected in RP-HPLC. The chromatogram corresponding to the starting condition (Fig. 6.12 and Table 6.3) shows two main peaks. The first peak is around 18 min and corresponds to the monomeric species, and the other peak is centred at 32 min and includes three peaks (RT of 30.5, 32, and 33 min). As incubation proceeds, the peak with a RT of 30.5 min corresponding to the oligomeric species increases. Of note again the RP-HPLC patterns of the three variants are similar to that obtained from aS (Fig. 6.12), but the intensity of the peak relative to the oligomers formed by A30P and E46K is lower than the other species. In the case of A30P a reasonable explanation is based on the possibility that the oligomers were less stable to

the conditions used for RP-HPLC analysis. Further analysis will be done in order to deepen these aspects.

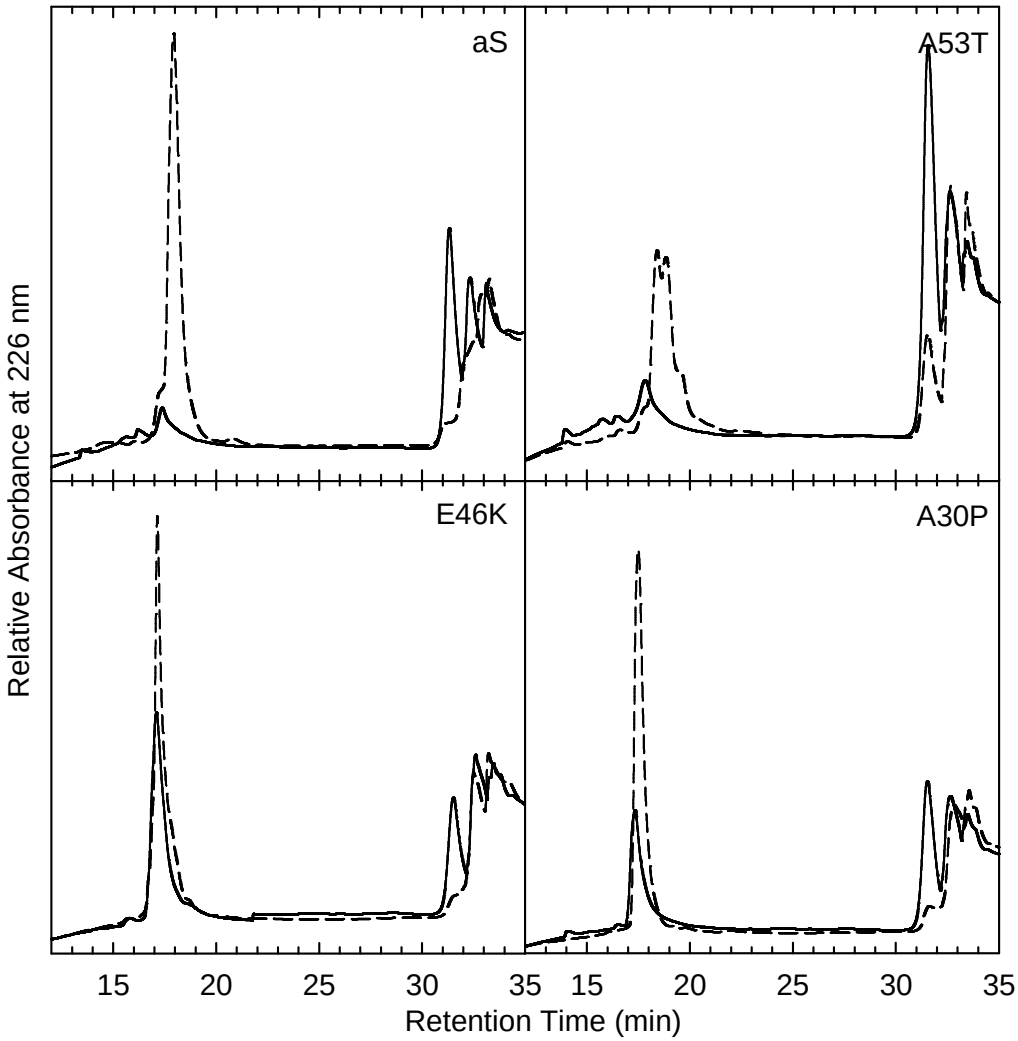

Fig. 6.12. RP-HPLC analysis. Chromatograms of aS, A53T, E46K and A30P during aggregation in the presence of DHA, after 0 (dashed lines) and 48- (solid lines) hours.

Table 6.1. Chemical characterization of peptide material corresponding to mayor peaks of the chromatograms relative to the fragmentation of aS and its mutants in the presence of DHA with pK after 5 min of incubation.

	RT[a] (min)	Molecular Mass (Da) Found[b]	Theoretical[c]	Species[d]
aS	18.4	5633.10±0.11	5633.0	90-140
		5390.01±0.11	5389.7	93-140
	29.7	7174.57±0.06	7173.7	73-140
	30.1	8846.32±0.74	8845.2	1-89
	30.4	9088.98±0.59	9088.5	1-92
	30.8	14477.41±0.4	14476	1-140+1ox
	31.5	14460.05±0.27	14460	1-140
A30P	18.4	5633.59±0.20	5633.0	90-140
		5390.16±0.11	5389.7	93-140
	29.6	8871.96±0.02	8871.2	1-89
		8942.10±0.13	8942.3	1-90
	29.9	9115.96±0.26	9114.5	1-92
		8816.91±0.57	8815.6	57-140
	30.4	14486.34±0.20	14486.2	1-140
A53T	18.7	5632.83±0.10	5633.0	90-140
		5389.76±0.05	5389.7	93-140
	30.0	9115.56±0.16	9118.5	1-92
	30.4	8876.64±0.09	8875.2	1-89
	30.8	14490.76±0.77	14490.2	1-140
	31.6	14509.58±0.35	14506.2	1-140+1ox
	32.3	14490.76±0.77	14490.2	1-140
E46K	18.5	5185.58±0.02	5185.1	95-140
	19.0	5632.83±0.10	5633.0	90-140
		5389.76±0.05	5389.7	93-140
	27.8	7171.30±0.90	7172.7	73-140
	29.8	8845.12±0.26	8844.2	1-89
		9088.55±0.28	9087.5	1-92
	30.2	14490.98±0.68	14491.2	1-140+2ox
	30.5	14475.95±0.33	14475.2	1-140+ox
	30.8	14459.75±1.27	14459.2	1-140

[a] Peptides or proteins were purified by RP-HPLC and listed in order of retention times (RT).
[b] Experimental molecular masses determined by ESI-MS.
[c] Molecular masses calculated from the amino acid sequence of aS.
[d] Species containing Met residues are present also as oxidized form.

Table 6.2. Mass-spectrometry identification of peptide material corresponding to major peaks of the chromatograms in Fig. 30 relative to the fragmentation of A30P and E46K in the presence of DHA with pK after 1- and 3-hr of reaction.

	RT[a] (min)	Molecular Mass (Da) Found[b]	Theoretical[c]	Species[d]
A30P	27.8	7347.29±0.28	7346.49	1-72 ox
		7030.93±0.14	7031.12	1-69
	27.9	7331.25±0.10	7330.49	1-72
	29.4	8872.86±0.15	8871.23	1-89
	30	14520.51±0.36	14518.22	1-140
		14537.35±0.98	14534.22	2ox
	30.3	14488.86±0.28	14486.22	1-140
		14504.60±0.29	14502.22	1-140 ox
E46K	28.4	5162.84±0.02	5163.1	1-50
		7319.19±0.09	7319.52	1-72 ox
		5661.68±0.57	5661.68	1-56
		5318.98±0.10	5319.28	1-52
	29.2	7303.89±0.63	7303.52	1-72
		8845.47±1.9	8844.26	1-89
		9087.92±0.04	9087.52	1-92
	30.1	14460.360.04	14459.24	1-140

[a, b, c, d] see reference Table 6.1.

Table 6.3. Chemical characterization of protein material corresponding to mayor peaks of the chromatogram relative to the aggregation of aS and its mutants in the presence of DHA.

	RT[a] (min)	Molecular Mass (Da) Found[b]	Theoretical[c]	Species[d]
aS	19.5	14508.13 (±0.05)	14508.1	aS 3ox
		14491.8 (±0.5)	14492.1	aS 2ox
		14476.1 (±0.3)	14476.1	aS 1ox
	21	14459.92 (±0.01)	14460.1	aS
	31	14801.9 (±0.05)	14802.1	aS 1ox 326
		14817.1 (±0.7)	14818.1	aS 2ox 326
		14831.3 (±0.9)	14834.1	aS 3ox 326
A53T	17.8	14522.4(±1.1)	14522.2	A53T 2ox
		14554.6 (±0.2)	14554.2	A53T 4ox
	18.5	14506.3 (±0.6)	14506.2	A53T 1ox
	18.9	14490.5 (±0.3)	14490.2	A53T
	31.5	14864.6 (±1.7)	14864.2	A53T 3ox 326
E46K	17	14464.8 (±0.6)	14459.2	E46K
		14479.1 (±0.6)	14475.2	E46K 1ox
		14496.6 (±0.6)	14491.2	E46K 2ox
	31	14791.6 (±1)	14785.2	E46K 326
A30P	17.4	14486.9 (±0.2)	14486.2	A30P
		14502.6 (±0.6)	14502.2	A30P 1ox
		14518.6 (±0.3)	14518.2	A30P 2ox
		14534.0 (±1.2)	14534.2	A30P 3ox
	17.8	14486.9 (±0.2)	14486.2	A30P
	31.5	14859.8 (±3.2)	14860.2	A30P 3ox 326
	[e]32	326.28 (±0.08)	326.24	DHA (-2H)
	33	328.29 (±0.16)	328.24	DHA

[a, b, c, d] see reference Table 6.1.

[e] Peaks eluted at 32 and 33 min correspond to DHA for all analyzed protein.

7. DISCUSSION AND CONCLUSION

There is growing interest in finding a possible link between aS toxicity in synucleinopathies and aS-lipid interaction. The precise biological function of aS is still under investigation, but it is implicated in a range of interactions with phospholipid membranes and free fatty acids. A current hypothesis about its pathological behaviour is that the association of aS with oxidized lipid metabolites can lead to mitochondrial dysfunction in turn leading to dopaminergic neuron death and thus to Parkinson's disease (Ruipérez et al., 2010). aS toxicity might also be related to abnormal membrane interactions and alterations in vesicles trafficking (Auluck et al., 2010). Many studies link toxicity to the existence of various intermediate structures, such as oligomers originating in early stages of aS fibrillation, and their specific interaction with membranes. Such intermediates are yet not fully characterized and there are several different possible mechanisms of toxicity (Fig. 7.1).

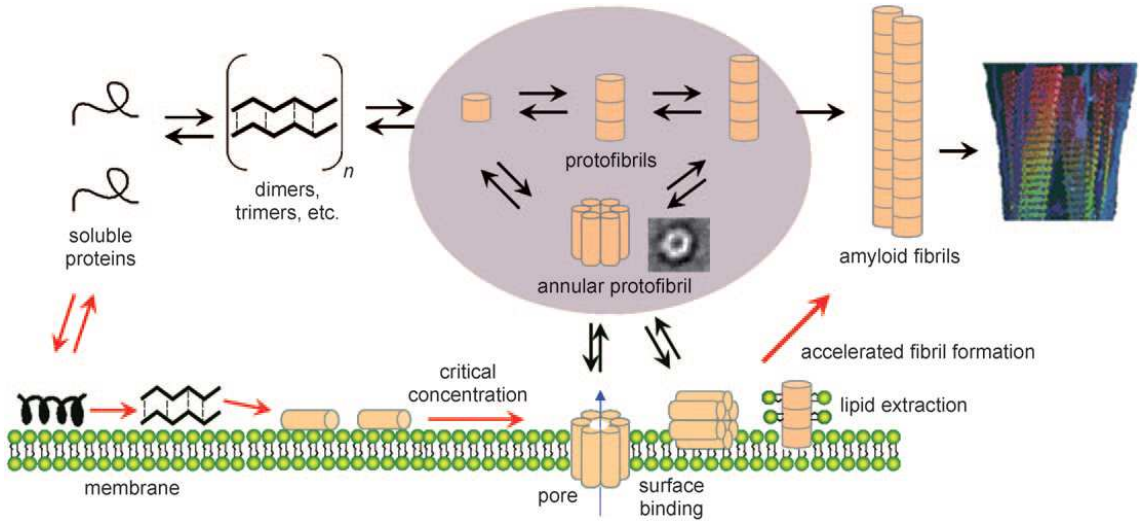

Fig. 7.1. Schematic representation of interconnectivity between amyloid formation and membrane disruption. Top: The process of amyloid-fibril formation. Amyloid formation involves the misfolding of soluble proteins into β-sheet oligomers, which further aggregate into protofibrils, including ringlike annular protofibrils, and then into amyloid fibrils. Bottom: The role of membranes in amyloid formation and toxicity. Soluble proteins bind to membrane surfaces with a shift to α-helix structure. The accumulation of proteins on the surface of the membrane induces their aggregation. When a critical threshold concentration is reached, a trans-membrane pore (annular protofibril) develops in the membrane and enables the leakage of membrane contents. As other possible or coexistent mechanisms, annular protofibrils formed in solution may insert into the membrane, undefined prefibrillar aggregates may bind to the membrane surface and induce membrane thinning, and lipids may be extracted from the membrane and incorporated into the developing fibril in a detergent-like process (from Lashuel and Butterfield, 2010).

Many evidences are in favour of oligomers able to form membrane pores (Kostka et al., 2008; Zakharov et al., 2007). A new model of amyloid interaction with membranes by a "raft-like" mode of insertion could explain important destabilization of membranes and thus amyloid toxicity (Berthelot et al., 2013). Many reports suggest that PUFAs are strictly connected to neurological disorders, including Parkinson's disease (Marszalek & Lodish, 2005). Specifically, alterations in PUFAs levels have been found related to aggregation of aS (Necula et al., 2003; Perrin et al. 2001; Sharon et al., 2003; Assayag et al., 2007). It has been proposed that aS could interact with free FAs (Sharon et al., 2001; Broersen et al., 2006), or, alternatively, with FAs in a micellar or bilayer state (Necula et al. 2003; Lücke et al., 2006). Interestingly, It has been shown that elevated brain DHA levels accelerate aS accumulation and oligomerization: treating dopaminergic cells expressing aS with polyunsaturated fatty acids (PUFAs) induced the formation of stable oligomers whereas saturated fatty acids did not. These oligomers were associated with cyto-toxicity, whereas the development of Lewy-like inclusions appeared to be protective (Assayag et al., 2007). A recent study demonstrated that dietary changes in brain DHA levels affect aS cytopathology in mice transgenic for the PD-causing A53T mutation in human aS. A diet enriched in DHA increased the accumulation of soluble and insoluble neuronal aS, neuritic injury and astrocytosis (Yakunin et al., 2012).

We previuosly produced *in vitro* oligomeric species of aS in the presence of DHA, which resulted toxic in cultured dopaminergic cells (De Franceschi et al., 2009; 2011). The aim of this thesis is to characterize the main biophysical properties of this type of oligomers, in order to explain their possible mechanism of toxicity. Moreover, studies about their chemical modification have been conducted, considering also differences that may occur between aS and its variants A30P, E46K, H50Q and A53T.

7.1 aS/DHA oligomers characterization

In the presence of DHA, it is induced the formation of relatively stable oligomers that are off-pathway in aS aggregation process (De Franceschi et al., 2011). The first aim of this study was to better characterize oligomers structure and shape, in order to correlate them with their activity. We have used a number of biophysical techniques such as TEM, AFM and DLS. These measurements show that aS/DHA oligomers are a heterogeneous

population of species, with diameters ranging from 12-30 nm. Different types of oligomers have been described in literature, depending on the conditions of preparation. Indeed, different conditions such as the presence of metals or lipids can affect the shape and the dimension of oligomers (Paik et al., 2002; Lee et al., 2002). Moreover, studies of the kinetics of fibril formation have given important insights into the overall mechanism of amyloid assembly, but little is known in any detail about the oligomeric structure (Lashuel et al., 2002; Luheshi et al., 2007; Winner et al., 2011). A variety of distinct morphologies of aS oligomers have been observed using imaging techniques, such as atomic force microscopy or transmission electron microscopy (Conway et al., 2000; Ding et al., 2002; Lashuel et al., 2002; Hoyer et al., 2004). Structural studies on aS oligomers have also been carried out using FTIR, Raman, CD, and fluorescence spectroscopy (Apetri et al., 2006; Goldberg and Lansbury, 2000; Hong et al., 2008; Nath et al., 2010; Thirunavukkuarasu et al., 2008), which have revealed the formation of various oligomeric structures during aS aggregation, consistent with a progressive increase in β sheet structure occurring concomitantly with the formation of more ordered aggregates. Oligomers formed in the presence of DHA show a similar size and morphological features with those previously described, but they acquire α-helical conformation (De Franceschi et al., 2009; 2011). This structure is almost partially lost after a gel filtration purification step. We presume that exchangeable DHA, not the covalently bound one, is removed and with it the effect on oligomers structure. Consequently the oligomers acquire a partly folded state, significantly different from the natively unfolded structure of monomeric aS. These partly folded oligomers are able to acquire again α-helical structure upon addition of DHA. This behaviour lead us to speculate about a possible structure model of these oligomers, sectioning the structure of oligomers into two parts, the N-terminal and the NAC region, and evaluating separately their contribute. In monomeric aS, the N-terminal region is essential for membrane recognition and for cooperative formation of helical domains. By CD and isothermal titration calorimetry, Bartels and colleagues (2010) tested different fragments and domains of aS for their binding affinity, concluding that N-terminus results necessary for the membrane-induced helical folding and the interaction of the first 25 residues with lipids is driven by electrostatic attraction. Transferring this to oligomers, since they in their partly folded

state can undergo conformational transition in the presence of lipids and membranes, it is reasonable to assume that the N-terminal region, or part of it, is free.

Another property of aS/DHA oligomers is that they are off-pathway and do not proceeds in the aggregation process, even in the presence of membranes. In aS, experiments on fragments of NAC have enabled this region as responsible for aggregation, in particular fragment 8-18 of NAC is the smallest fragment that aggregates and forms fibrils (El-Agnaf et al., 2002). Furthermore, membranes work as a catalyst of aggregation (Berthelot et al., 2013) since membrane-bound aS can generate nuclei that seed the aggregation also *in vivo* (Lee et al., 2002). So it seems that the NAC region (residues 61-95) in aS/DHA oligomers is not available or is hidden in their interior. In conclusion aS/DHA oligomers have two main structural features: the conformational sensitivity to environment for the ability to interact with lipids and to undergo structural transition, and secondly the stability under conditions that favours aggregation. The overall structure of the oligomers could be stabilized by hydrophobic interactions deriving from the association of NAC regions.

7.2 aS/DHA oligomers activity on membranes

Here we have studied aS/DHA oligomers activity on membranes in an attempt to understand their mechanism of toxicity, because the latter, as yet said, is object of debate in the literature for the difficulty to define a unifying picture of the toxic activity. The controversy springs from both the transient nature of aS oligomers and from the many different types of oligomers that have been described. Volles and colleagues (2001), demonstrated that protofibrillar aS, in contrast to the monomeric and the fibrillar forms, binds synthetic vesicles very tightly via a β-sheet-rich structure and transiently permeabilizes these vesicles. An interesting property of aS/DHA oligomers is their ability to permeabilize membranes, as verified using a leakage assay from unilamellar phospholipid vesicles. By calcein leakage test we demonstrated that aS/DHA oligomers destabilize both LUV and SUV composed of negative charged phospholipids. Interestingly, vesicles composed of only 50% negative-charged phospholipids show really low extent of calcein release after incubation with aS oligomers, even if this kind of vesicles is able to induce acquisition of α-helix structure on aS/DHA oligomers, even if with a minor extent than that induced by 100% acidic phospholipids. This result is in line

with a previously reported behaviour of aS oligomers (Van Rooijen et al., 2008), that bind negative charged membranes acquiring α-helix structure. In a similar way, these oligomers are not able to induce calcein leakage in vesicles of 50% zwitterionic lipids, allowing to conclude that membrane binding of aS does not necessarily lead to vesicle permeabilization.

We tested also the activity of aS/DHA oligomers on dopaminergic cells. Treatment with oligomers significantly increases the number of cells internalizing the membrane-impermeant dye propidium iodide. These results suggest that membranes can be a possible target of aS oligomers activity. This can be particularly harmful for neuronal cells, where electrical activity and action potential firing are finely regulated by transient, voltage-gated channel-mediated variation of membrane potential and intracellular calcium concentration. Indeed, increased membrane permeability could result in a variety of intracellular processes and leads to cytotoxicity, as well as dissipation of sodium and potassium gradients with deleterious impact on electrical neuronal activity.

Several mechanisms have been proposed to explain oligomers activity on membranes. One possible mechanism is that of the pore-like mechanism (Zakharov et al., 2007; Kostka et al., 2008; Lashuel and Butterfield 2010). Protofibrils with β-sheet-rich structure transiently permeabilizes vesicles and the activity is comparable for aS WT and its A53T and A30P mutants (Volles et al., 2001). A thinning effect due to lipid extraction from the bilayer has been also reported. aS WT, A53T and the designed A57T mutant were found to follow the same mechanism of polymerization and membrane damage, involving the extraction of lipids from the bilayer and their clustering around growing α-synuclein aggregates (Reynolds et al., 2011). Leakage could be due also to a complete disruption of the membrane, reported for mellitin (Bechinger and Lohner, 2006), or a transient membrane destabilization, possibly related to the intrinsic instability of the bilayer. Indeed, vesicles composed of negatively charged lipids, which are generally used for measuring aS-lipid interactions, are unstable to protein adsorption in general (van Rooijen et al., 2010). The pore-like hypothesis is especially accepted for those proteins forming oligomers or protofibrils with annular or ring-like structure (Butterfield and Lashuel 2010). In our case the leakage activity tested on synthetic liposomes shows selectivity of markers size, evidencing that the average dimension of the aperture should be between 1 and 4 nm (Mazzuca et al., 2010). The enhanced membrane-

permeabilization activity of amyloid oligomers relative to that of soluble monomers and mature fibrils and the reported size dependence with respect to dye leakage from model vesicle membranes are considered consistent with the pore-like mechanism (Butterfield and Lashuel 2010). Other characteristic are required to assume the formation of pores, such as the induction of single-ion-channel currents characteristic of ion-channel or pore-forming proteins. The activity of aS/DHA oligomers on a planar lipid membrane system seems due to a non-specific membrane permeabilization rather than to the formation of structured membrane apertures like those previously demonstrated also for monomeric aS (Tosatto et al., 2012).

The complete disruption effect could be excluded by DLS and microscopy measurements of aS/DHA oligomers in the presence of phospholipids vesicles. Indeed DLS measurements of both LUV and SUV in the presence of aS/DHA oligomers show that the vesicles size distribution is modified, but TEM shows no changes to the overall vesicles morphology. The reported effect of Triton X-100 on vesicles measured by DLS clearly exclude a similar effect by oligomers. In conclusion, aS/DHA oligomers interacting with negatively charged membranes induce a perturbation of the phospholipid bilayer with the release of encapsulated small molecules. Oligomeric molecules remain entrapped on the vesicles, as peripheral membrane proteins, acquiring α-helical structure. Damaging of membrane structural integrity seems to be an essential step in the cytotoxic activity of aS oligomers formed in the presence of DHA.

This part of the thesis is object of a publication (Fecchio C., De Franceschi G., Relini A., Greggio E., Dalla Serra M., Bubacco L., Polverino de Laureto P (2013) α-Synuclein Oligomers Induced by Docosahexaenoic Acid Affect Membrane Integrity. *PlosOne 8:*e82732.

7.3. Chemical modification of aS in the presence of DHA

The chemical protein modifications, that form under oxidative stress conditions, occur on specific amino acid residues. The direct oxidation of proteins by ROS involves Lys, Arg, Pro and Thr residues. The secondary reactions with reactive derivatives (ketoamines, ketoaldehydes, deoxyosones) produced by sugars oxidation product occur especially on Lys, while the formation of adducts of oxidized lipids derived from the metal-catalysed oxidation of PUFA involves Lys, Cys and His residues (Esterbauer et al.,

1991; Uchida and Stadtman, 1992; Refsgaard et al., 2000; Dalle Donne et al., 2006). In the case of aS, the modifications on Lys residues can affect the charge distribution of the basic KXKE repeats of the N-terminal region, and so influence the interaction with membranes that is primarily mediated by a charge effect (Davidson et al., 1998; van Rooijen et al., 2010). One of the main features of aS/DHA oligomers is the chemical heterogeneity that derive from the presence of covalently bound DHA and of oxidative additional modifications (De Franceschi et al., 2011). In previous studies we detect the presence of modification, but we didn't identify which amino acids are involved, so another aim of the present work was to define the modified residues in aS/DHA oligomers and eventually the role of these modifications in their activity.

A first attempt was done to detect the increase of carbonylation (Dalle Donne et al., 2006) of aS in the presence of DHA. A reaction with by DNPH was used that have demonstrated an increased presence of carbonyls, but unfortunately it was not possible to assess which residues were mainly modified. Only a fragment containing the Δ mass of 180 Da was found and it corresponds to the sequence 24-32. This peptide contains Lys32 as possible target of carbonylation. However the presence of a single modification does not justify the signals obtained in UV and RP-HPLC analyses. It is reasonable that residues in the protein are randomly modified and so it is difficult to detect them.

DHA-adduct is the most evident modification, among the several possible ones, so we focused on its characterization. Trypsin digestion of the aS/DHA oligomers followed by peptide 'finger-printing' revealed that DHA binds the peptide $_{46}$EGVVHGVATVAEK$_{58,}$ providing an indirect evidence that His50 is modified. This could be predictable since the reactivity of lipid peroxidation products, such as allylic radicals, is known and involves Cysteine, Histidine and Lysine residues (Uchida et al., 1997). Moreover, 4-hydroxy-2(E)-

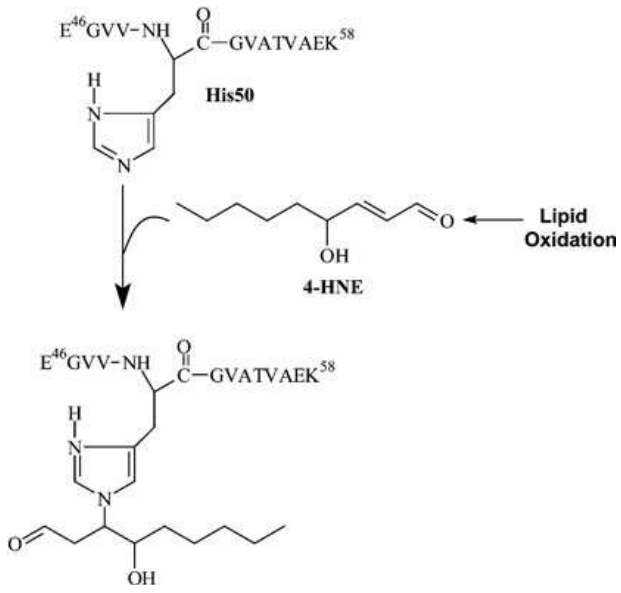

Fig. 2. Schematic representation of Michael addition of 4-HNE on His50, contained in the fragment E46-K58.

nonenal, a product of peroxidation of lipids, preferentially binds to His50 on aS (Fig. 2, from Trostchansky et al., 2006), or more rarely to Lys60 and Lys69 (Bae et al., 2013; Xiang et al., 2013,). His50 results a suitable target for the formation of an adduct with DHA. In view of the fact that His50 is preferentially modified by DHA, in comparison with the several lysine residues present in the polypeptide chain, we investigated the importance of this residue by using a mutant containing a Gln in spite of His in position 50. Interestingly this specific variant has been recently found in a familiar form of PD. H50Q behaviour in the presence of DHA is very similar to that of aS. H50Q acquires α-helix structure and by limited proteolysis a similar interaction with DHA was evidenced. Moreover, also the aggregation process results similar to that of aS and oligomers form. Surprisingly, a mass increase of 326 Da is still detectable on the protein, and sometimes more than one FA adduct was found, meaning that other residues were modified. This result suggests that the position of the modification on aS is not essential for the formation of oligomers. The preference for His50 could be due to chemical reasons, since the reaction toward His is favoured. Indeed, His50 is surely in excess on reactive DHA, that is its radical form, which constitutes about 0.3% of the initial content of FA.

After His, the binding of DHA can occur at the level of Lysine residues, that are 14 in the whole protein. It was not possible to detect any modified lysine by finger printing analysis of H50Q oligomers. We can explain it considering that it was possible to find modified His50 because it was the preferred site of modification. On the contrary, without His all the 14 lysines are possible target of DHA binding, leading to the formation of a heterogeneous population of H50Q, modified in different lysine residues. As a consequence, the extent of modification on a specific lysine is too low to be detectable with this kind of analysis.

Finally the fact that the oligomers obtained from aS and H50Q have the same extent of activity on synthetic membrane, allowing to conclude that the position of the modification is not essential even for oligomers activity.

7.4 aS variants in the presence of DHA

To complete the study, also the other three known mutants found in familiar forms of PD (A30P, A53T and E46K) were investigated. In the presence of DHA, all mutants acquire α-helix structure in a similar way, but A30P in minor extent. Upon

incubation at a molar ratio protein/lipid 1:50, all the proteins form stable oligomers but, interestingly, the oligomers formation rate was different, resulting in a minor oligomeric content for E46K and A30P. To define the region of aS more directly interacting with DHA, proteolysis experiments coupled with mass spectrometry have been performed. aS, as a natively unfolded protein, is largely sensitive to proteases because it lacks secondary and tertiary structure (Uversky, 2002). As a matter of fact, there are no regions with such persistent structure as to hinder protease's attack. Upon binding to DHA, aS appears to be quite resistant to proteolysis, as expected from the fact that the polypeptide has adopted an α-helix conformation which strictly involves the first 70 amino acid residues. A considerable accessibility of aS polypeptide chain to proteinase K is confined only at the level of region 70-90, providing evidence that this segment is the most flexible and sufficiently protruded to be protease-sensitive (Hubbard et al., 1994; Fontana et al.,2004). Comparing proteolytic patterns of aS and its variants in the presence of DHA, it became evident that first cleavage sites are identical for all the proteins, suggesting that the overall interaction with membrane is mediated by the same region encompassing the first ~100 amino acids (De Franceschi et al., 2009). Prolonging the proteolysis to 1 and 3 hr for A30P and E46K, it is shown that fragments that accumulate in the proteolytic mixture are 1-72 for A30P, and 1-50 for E46K. To explain these differences, we can consider the data reported by Bodner et al. (2010). The mutation of E in K raises the net charge of the first 100 residues from +4 to +6, resulting in higher affinity for negative charged lipid. By NMR it was observed that this fact determines a slower dissociation from lipid. As a consequence E46K increase the bound fraction in a SL1 binding mode, in which the first 10 or 24 N-terminal residues adopt a stable α-helical conformation upon lipid binding, while the lasting ~25-140 residues are dynamically disordered (Fig. 25). A second binding state, SL2, populated by aS, engages the whole N-terminal domain until to the residue ~100. E46K in SL1 state allows the protease to cleave peptide bond H50-G51 located in the dynamically disordered region 25-100.

A30P doesn't form a canonical α-helix upon binding to lipids, for the presence of proline residue. This determines a reduced association rate to lipids and a shift of the equilibrium between SL1 and SL2 binding mode towards the SL1 one. Intriguingly the A30P is not fragmented at the level of peptide bond H50-G51, since intact A30P is found also upon prolonged incubation with the protease. This doesn't imply necessary presence

of regular secondary structure but can be due to a backbone rigidity imposed by proline (Polverino de Laureto et al., 2006). In conclusion, in the presence of DHA, the variant E46K appears to be highly susceptible to proteases hydrolysis in correspondence of the region 50-89, included in the NAC region, while aS in the region 73-89. A30P shows an unusual rigidity. However the initial sites of proteolysis clearly indicate that in the presence of saturating concentration of DHA, considerable accessibility of the polypeptide chains to proteinase K is located to residues 70-90, providing evidence that this segment for all variants, by limited proteolysis criteria, is the most flexible and protruded to be protease-sensitive.

8. REFERENCES

- Aebersold R., Goodlett DR. (2001) Mass spectrometry in proteomics. *Chem. Rev.* 101:269–295.
- Alim M.A., Hossain M.S., Arima K., Takeda K., Izumiyama Y., Nakamura M., Kaji H., Shinoda T., Hisanaga S., Ueda K. (2002) Tubulin seeds alpha–synuclein fibril formation. *J Biol Chem*. 277:2112–7.
- Andersen JK. (2009) Arvid Carlsson: an early pioneer in translational medicine. *Sci Transl Med.* 14:2–3.
- Apetri M.M., Maiti N.C., Zagorski M.G., Carey P.R., Anderson V.E. (2006) Secondary structure of alpha–synuclein oligomers: characterization by raman and atomic force microscopy. *J Mol Biol.* 355:63–71.
- Appel–Cresswell S., Vilarino–Guell C., Encarnacion M., Sherman H., Yu I., Shah B., Weir D., Thompson C., Szu–Tu C., Trinh J., Aasly JO., Rajput A., Rajput AH., Jon Stoessl A., Farrer M.J. (2013) Alpha–synuclein p.H50Q, a novel pathogenic mutation for Parkinson's disease. *Mov Disord.* 28:811–3.
- Assayag, E. Yakunin, V. Loeb, D.J. Selkoe, R. Sharon (2007) Polyunsaturated fatty acids induce alpha–synuclein–related pathogenic changes in neuronal cells. *Am J Pathol.* 171:2000–2011.
- Barcelo–Coblijn G., Golovko M.Y., Weinhofer I., Berger J., Murphy E.J. (2007) Brain neutral lipids mass is increased in alpha–synuclein gene–ablated mice. *J Neurochem.* 101:132–141.
- Bartels T., Choi J.G., Selkoe D.J. (2011) α-Synuclein occurs physiologically as a helically folded tetramer that resists aggregation. Nature 477:107–110.
- Bendor JT., Logan TR., Edwards RH. (2013) The function of α–synuclein. *Neuron* 79:1044–1066.
- Bertoncini C. W., Jung Y. S., Fernandez C. O., Hoyer W., Griesinger C., Jovin T. M. & Zweckstetter M. (2005) Release of long–range tertiary interactions potentiates aggregation of natively unstructured alpha–synuclein. *Proc Nat Acad Sci USA* 102:1430–1435.
- Beyer K., (2006) alpha–Synuclein structure, posttranslational modification and alternative splicing as aggregation enhancers, Acta Neuropathol. 112:237–251.
- Beyer K. (2007) Mechanistic aspects of Parkinson's disease: alpha–synuclein and the biomembrane. *Cell Biochem Biophys.* 47:285–99.
- Bieschke J., Q. Zhang, D.A. Bosco, R.A. Lerner, E.T. Powers, P. Wentworth Jr., J.W. Kelly, (2006) Small molecule oxidation products trigger disease–associated protein misfolding. *Acc. Chem. Res.* 39:611–619.
- Bisaglia M., Tosatto L., Munari F., Tessari I., de Laureto P.P., Mammi S., Bubacco L., (2010) Dopamine quinones interact with alpha–synuclein to form unstructured adducts. *Biochem. Biophys. Res. Commun*. 394:424–428.
- Biskup S., West A.B. (2009) Zeroing in on LRRK2–linked pathogenic mechanisms in Parkinson's disease. *Biochim Biophys Acta* 1792:625–33.
- Bodner C.R., Maltsev A.S., Dobson C.M., Bax A. (2010) Differential phospholipid binding of alpha-synuclein variants implicated in Parkinson's disease revealed by solution NMR spectroscopy. *Biochemistry* 49:862-71.

- Braak H., Del Tredici K., Rüb U., de Vos R. A., Jansen Steur E. N., Braak E. (2003) Staging of brain pathology related to sporadic Parkinson's disease. *Neurobiol Aging* 24:197−211.
- Breydo L., Jessica W. Wu, Vladimir N. Uversky (2012) α–Synuclein misfolding and Parkinson's disease*. Biochimica et Biophysica Acta (BBA) – Molecular Basis of Disease* 1822:261–285.
- Broersen K., van den Brink D., Fraser G., Goedert M., Davletov B. (2006) Alpha–synuclein adopts an alpha–helical conformation in the presence of polyunsaturated fatty acids to hinder micelle formation. *Biochemistry* 45:15610–16.
- Burrè J, Sharma M, Tsetsenis T, Buchman V, Etherton MR, Südhof TC (2010) α–Synuclein promotes SNARE–complex assembly in vivo and in vitro. *Science* 329:1663–1667.
- Bussell R. Jr & Eliezer D. (2001) Residual structure and dynamics in Parkinson's disease–associated mutants of alpha–synuclein. *J Biol Chem.* 276:45996–46003.
- Bussell R. Jr, Ramlall T.F., Eliezer D. (2005) Helix periodicity, topology, and dynamics of membrane–associated alpha–synuclein. *Protein Sci* 14:862–872.
- Camandola S., Poli G., Mattson M. P. (2000) The lipid peroxidation product 4–hydroxy–2,3–nonenal increases AP–1–binding activity through caspase activation in neurons*. J. Neurochem.* 74:159–168.
- Castagnet P.I., Golovko M.Y., Barcelo–Coblijn G.C., Nussbaum R.L., Murphy E.J. (2005) Fatty acid incorporation is decreased in astrocytes cultured from alpha–synuclein gene–ablated mice. *J Neurochem* 94:839–849.
- Chaari A., Horchani H., Frikha F., Verger R., Gargouri Y., Ladjimi M. (2013) Surface behavior of α-Synuclein and its interaction with phospholipids using the Langmuir monolayer technique: a comparison between monomeric and fibrillar α-Synuclein. *Int J Biol Macromol*. 58:190-8.
- Chartier–Harlin M. C., Kachergus B.S., Roumier C., Mouroux V., Lincoln S., Levecque C., Larvor L., Andrieux J., Hulihan M., Waucquier N., Defebvre L., Amouyel P., Farrer M., Destee A. (2004). α–Synuclein locus duplication as a cause of familiar Parkinson's disease. *The Lancet* 364:1167–1169.
- Chavarría C., José M. (2013) Souza Oxidation and nitration of α-synuclein and their implications in neurodegenerative diseases. *Archives of Biochemistry and Biophysics* 533:25–32.
- Chen X., Liu Y.T., Li J.R., Chen L., Xu Y.M., Pan Y.H., Meng X.H., Xing S.H., (2003) Study on exons 3 and 4 of alpha–synuclein gene in Chinese familial Parkinson disease patients. *Zhonghua Yi Xue Yi Chuan Xue Za Zhi.* 20:536–8.
- Childknecht S., Gerding HR, Karreman C, Drescher M, Lashuel HA, Outeiro TF, Di Monte DA, Leist M (2013) Oxidative and nitrative alpha–synuclein modifications and proteostatic stress: implications for disease mechanisms and interventions in synucleinopathies. *J. Neurochem.* 125:491–511.
- Chiti F., Stefani M., Taddei N., Ramponi G., Dobson C.M. (2003) Rationalization of the effects of mutations on peptides and protein aggregation rates. *Nature* 424:805–808.
- Choi W., Zibaee S., Jakes R., Serpell L.C., Davletov B., Crowther R. A. & Goedert M. (2004) Mutation E46K increase phosholipid binding and assembly into filaments of human alpha–synuclein. *FEBS Lett* 576:363–368.

- Cole N.B., Murphy D.D., Grider T., Rueter S., Brasaemle D., Nussbaum R.L. (2002) Lipid droplet binding and oligomerization properties of the Parkinson's disease protein alpha–synuclein. *J Biol Chem.* 277:6344–6352.
- Conway K.A., Harper J.D. & Lansbury P.T. Jr (1998) Accelerated in vitro fibril formation by a mutant alpha–synuclein linked to early onset Parkinson's disease. *Nature Med* 4:1318–1320.
- Conway K.A., Lee S.J. Rochet J.C., Ding T.T., Williamson R. E. & Lansburt P.T. Jr (2000) Acceleration of oligomerization, not fibrillation, is a shared property of both alpha–synuclein mutations linked to early–onset Parkinson's disease: implications for pathogenesis and therapy. *Proc Nat Acad Sci USA* 97:571–576.
- Conway K.A., Rochet J.C., Bieganski R.M. & Lansbury P.T. Jr. (2001) Kinetic stabilization of the alpha–synuclein protofibril by a dopamine–alpha–synuclein adduct. *Science* 294:1346–1349.
- Cookson M. R. (2005) The biochemistry of Parkinson's disease. *Annu Rev Biochem* 74:29– 52.
- Covy J.P., Giasson B.I. (2011) α–Synuclein, leucine–rich repeat kinase–2, and manganese in the pathogenesis of parkinson disease. *NeuroToxicology* 32:622–629.
- Crowther R. A., Jakes R., Spillantini M. G. & Goedert M. (1998) Synthetic filaments assembled from C–terminally truncated alpha–synuclein. *FEBS Lett* 436:309–312.
- Dachsel J.C., Wider C., Vilariño–Güell C., Aasly J.O., Rajput A., Rajput A.H., Lynch T., Craig D., Krygowska–Wajs A., Jasinska–Myga B., Opala G., Barcikowska M., Czyzewski ., Wu R.M., Heckman M.G., Uitti R.J., Wszolek Z.K., Farrer M.J., Ross O.A. (2011) Death–associated protein kinase 1 variation and Parkinson's disease. *Eur J Neurol.* 18:1090–3.
- Danielson S.R., Held J.M., Schilling B., Gibson B.W., Andersen J.K., (2009) Preferentially increased nitration of alpha–synuclein at tyrosine–39 in a cellular oxidative model of Parkinson's disease. *Anal. Chem.* 81 :7823–7828.
- Dauer, W., Przedborski, S. (2003) Parkinson's disease: mechanisms and models. *Neuron.* 39:889−909.
- Davidson W. S., Jonas A., Clayton D. F., George J. M. (1998) Stabilization of alpha–synuclein secondary structure upon binding to synthetic membranes. *J Biol Chem*. 273:9443– 9449.
- De Franceschi G., Frare E., Bubacco L., Mammi S., Fontana A., de Laureto P.P. (2009) Molecular insights into the interaction between alpha–synuclein and docosahexaenoic acid. *J Mol Bio.* 394:94–107.
- De Franceschi G., Frare E., Pivato M., Relini A., Penco A., Greggio E., Bubacco L., Fontana A., de Laureto P.P. (2011) Structural and morphological characterization of aggregated species of α–synuclein induced by docosahexaenoic acid. *J Biol Chem.* 286:22262–74.
- de Laureto P.P., Tosatto L., Frare E., Marin O., Uversky V.N., Fontana A. (2006) Conformational properties of the SDS-bound state of alpha-synuclein probed by limited proteolysis: unexpected rigidity of the acidic C-terminal tail. *Biochemistry* 45:11523–31.
- de Rijk M. C., Launer L. J., Berger K., Breteler M. M., Dartigues J. F., Baldereschi M., Fratiglioni L., Lobo A., Martinez–Lage J., Trenkwalder C., Hofman A. (2000). Prevalence of Parkinson's disease in Europe: A collaborative study of population–based cohorts Neurologic Diseases in the Elderly Research Group. *Neurology* 54S21−S23.

- Dev K. Hofele S. Barbieri V.L. Buchman H. van der Putten (2003) Part II: alphasynuclein and its molecular pathophysiological role in neurodegenerative disease. *Neuropharmacology* 45:14–44.
- Di Fonzo A., Rohe C. F., Ferreira J., Chien H. F., Vacca L., Stocchi F., Guedes L., Fabrizio E., Manfredi M., Vanacore N., Goldwurm S.,Breedveld G., Sampaio C., Meco G., Barbosa E., Oostra B. A. & Bonifati V. (2005) A frequent LRRK2 gene mutation associated with autosomal dominant Parkinson's disease. *Lancet* 365, 412–415.
- Ding T.T., Lee S.J., Rochet J.C., Lansbury P.T. Jr. (2002) Annular alpha–synuclein protofibrils are produced when spherical protofibrils are incubated in solution or bound to brain–derived membranes. *Biochemistry* 41:10209–10217.
- Dobson C.M. (2001) The structural basis of protein folding and its links with human disease. *Phil Trans R Soc Lond B* 356:133–145.
- Duda J.E., Giasson B.I., Gur T.L., Montine T.J., Robertson D., Biaggioni I., Hurtig H. I., Stern M.B., Gollomp S.M., Grossman M., Lee V.M.Y., Trojanowski J.Q. (2000) Immunohistochemical and biochemical studies demonstrate a distinc profile of alpha–synclein permutations in multiple system atrophy. *J Neuropathol Exp Neurol* 59:830–841.
- Dunnett SB, Björklund A. (1999) Prospects for new restorative and neuroprotective treatments in Parkinson's disease. Nature 399:A32–9.
- Ebeling W., Hennrich N., Klockow M., Metz H., Orth H.D., Lang H. (1974) Proteinase K from Tritirachium album Limber. *Eur J Biochem.* 47):91-7.
- Esterbauer H., Schaur R.J., Zollner H., (1991) Chemistry and biochemistry of 4–hydroxynonenal, malonaldehyde and related aldehydes. *Free Radic. Biol. Med.* 11:81–128.
- Farooqui A.A., Horrocks L.A. (2006) Phospholipase A2-generated lipid mediators in the brain: the good, the bad, and the ugly. *Neuroscientist* 12:245–260.
- Farrer M., Kachergus J., Forno L., Lincoln S., Wang D. S., Hulihan M., Maraganore D., Gwinn–Hardy K., Wszolek Z., Dickson D., Langston J. W. (2004) Comparison of kindreds with parkinsonism and alpha–synuclein genomic multiplications. *Ann. Neurol,* 55:174−179.
- Fauvet B., Mbefo M.K., Fares M.B., Desobry C., Michael S., Ardah M.T., Tsika E., Coune P., Prudent M., Lion N., Eliezer D., Moore D.J., Schneider B., Aebischer P., El-Agnaf O.M., Masliah E., Lashuel H.A., (2012) α-Synuclein in central nervous system and from erythrocytes, mammalian cells, and Escherichia coli exists predominantly as disordered monomer. *J. Biol. Chem*. 287:15345–64.
- Fink A.L. (2006) The aggregation and fibrillation of alpha–synuclein. *Acc. Chem. Res.* 39:628–634.
- Fontana A., de Laureto P.P., Spolaore B., Frare E., Picotti P., Zambonin M. (2004) Probing protein structure by limited proteolysis. Acta Biochim Pol. 51:299–321.
- Fredenburg R. A., Rospigliosi C., Meray R. K., Kessler J. C., Lashuel H. A., Eliezer D. & Lansbury P. T. Jr (2007) The impact of the E46K mutation on the properties of alpha–synuclein in its monomeric and oligomeric states. Biochemistry 46, 7107–7118.
- Fuchs J., Nilsson C., Kachergus J., Munz M., Larsson E.M., Schüle B., Langston J.W., Middleton F.A., Ross O.A., Hulihan M., Gasser T., Farrer M.J. (2007) Phenotypic variation in a large Swedish pedigree due to SNCA duplication and triplication. *Neurology* 68:916-22.

- Fujiwara H., Hasegawa M., Dohmae N., Kawashima A., Masliah E., Goldberg M.S., Shen J., Takio K., Iwatsubo T., (2002) alpha–Synuclein is phosphorylated in synucleinopathy lesions. Nat. Cell Biol. 4:160–164
- Galter D., Westerlund M., Carmine A., Lindqvist E., Sydow O., Olson (2006) LRRK2 expression linked to dopamine–innervated areas. Ann Neurol. 59714–9.
- Giasson B.I., Van Deerlin V.M. (2008) Mutations in LRRK2 as a cause of Parkinson's disease. Neurosignals. 1699–105.
- Giasson B.I., Covy J.P., Bonini N.M., Hurtig H.I., Farrer M.J., Trojanowski J.Q., Van Deerlin V.M. (2006) Biochemical and pathological characterization of Lrrk2. Ann Neurol. Feb;59(2):315–22.
- Ghosh D., Mondal M., Mohite GM., Singh PK., Ranjan P., Anoop A., Ghosh S., Jha NN., Kumar A., Maji SK. (2013) the Parkinson's Disease–Associated H50Q Mutation Accelerates α–Synuclein Aggregation in Vitro. Biochemistry 52:6925–7.
- Goers J., Manning–Bog A.B., McCormack A.L., Millett I.S., Doniach S., Di Monte D.A., Uversky V.N. & Fink A.L. (2003) Nuclear localization of alpha–synuclein and its interaction with histones. Biochemistry 42:8465–8471.
- Golovko M.Y., Rosenberger T.A., Faergeman N.J., Feddersen S., Cole N.B., Pribill I., Berger J., Nussbaum R.L., Murphy E.J., (2006) Acyl–CoA synthetase activity links wild–type but not mutant alpha–synuclein to brain arachidonate metabolism. Biochemistry, 45:6956–6966.
- Golovko M.Y., Rosenberger T.A., Feddersen S., Faergeman N.J., Murphy E.J. (2007) Alpha–synuclein gene ablation increases docosahexaenoic acid incorporation and turnover in brain phospholipids. J Neurochem 101:201–211.
- Golovko M.Y., Barcelo–Coblijn G., Castagnet P.I., Austin S., Combs C.K., Murphy E.J. (2009) The role of alpha–synuclein in brain lipid metabolism: a downstream impact on brain inflammatory response. Mol Cell Biochem, 326:55–66.
- Greenbaum E. A., Graves C. L., Mishizen–Eberz A. J., Lupoli M. A., Lynar D. R., Englander S. W., Axelsen P. H. & Giasson G. I. (2005) The E46K mutantion in alpha–synuclein increases amyloid fibril formation. *J Biol Chem.* 280:7800–7807.
- Greggio E., Lewis P.A., van der Brug M.P., Ahmad R., Kaganovich A., Ding J., Beilina A., Baker A.K. & Cookson M.R. (2007) Mutations in LRRK2/dardarin associated with Parkinson disease are more toxic than equivalent mutations in the homologous kinase LRRK1. *J Neurochem* 102:93–102.
- Gloeckner C.J., Kinkl N., Schumacher A., Braun R.J., O'Neill E., Meitinger T., Kolch W., Prokisch H., Ueffing M. (2006) The Parkinson disease causing LRRK2 mutation I2020T is associated with increased kinase activity. *Hum Mol Genet*. 15:223–32.
- Haque F., Pandey AP, Cambrea LR, Rochet JC, Hovis JS. (2010) Adsorption of alpha–synuclein on lipid bilayers: modulating the structure and stability of protein assemblies. *J Phys Chem B*. 114:4070–81.
- Harper J.D., Wong S.S., Lieber C.M., Lansbury P.T. (1997) Observation of metastable Abeta amyloid protofibrils by atomic force microscopy. *Chem Biol.* 4:119–125.
- Hamilton B. A. (2004) α–Synuclein A53T substitution associated with Parkinson disease also marks the divergence of old word and new world primates. Genomics 83:739–742.
- Hardy J. (2010) Genetic analysis of pathways to Parkinson disease. *Neuron.* 68:201–206.
- Hasegawa K, Kowa H. (1997) Autosomal dominant familial Parkinson disease: older onset of age, and good response to levodopa therapy. *Eur Neurol.* 38:39–43.

- Herrera F.E., Chesi A., Paleologou K.E., Schmid A., Munoz A., Vendruscolo M., Gustincich S., Lashuel H.A., Carloni P., (2008) Inhibition of alpha–synuclein fibrillization by dopamine is mediated by interactions with five C–terminal residues and with E83 in the NAC region. *PLoS One* 3:e3394.
- Higashi S., Iseki E., Yamamoto R., Minegishi M., Hino H., Fujisawa K., Togo T., Katsuse O., Uchikado H., Furukawa Y., Kosaka K., Arai H. (2007) Concurrence of TDP–43, tau and alpha–synuclein pathology in brains of Alzheimer's disease and dementia with Lewy bodies. *Brain Res.* 1184:284–94.
- Higashi S., Biskup S., West A.B., Trinkaus D., Dawson V.L., Faull R.L., Waldvogel H.J., Arai H., Dawson T.M., Moore D.J., Emson P.C. (2007) Localization of Parkinson's disease–associated LRRK2 in normal and pathological human brain. *Brain Res*. 2007 Jun 25;1155:208–19.
- Hokenson M.J., Uversky V.N., Goers J., Yamin G., Munishkina L.A., Fink A.L., (2004) Role of individual methionines in the fibrillation of methionine–oxidized alphasynuclein. *Biochemistry* 43:4621–4633.
- Hoyer W., Cherny D., Subramaniam V., Jovin T.M. (2004) Impact of the acidic C–terminal region comprising amino acids 109–140 on alpha–synuclein aggregation in vitro. *Biochemistry* 43:16233–42.
- Hoyer W., Cherny D., Subramaniam V., Jovin T.M. (2004) Rapid self–assembly of alpha–synuclein observed by in situ atomic force microscopy. *J Mol Biol*. 340:127–39.
- Hornykiewicz O. (2002) L–DOPA: from a biologically inactive amino acid to a successful therapeutic agent. *Amino Acids*. 23:65−70.
- Irvine G. B., El–Agnaf O. M., Shankar G. M., Walsh D. M. (2008) Protein aggregation in the brain: the molecular basis for Alzheimer's and Parkinson's diseases. *Mol. Med.* 14:451−464.
- Jao, B.G. Hegde, J. Chen, I.S. Haworth, R. Langen (2008) Structure of membrane–bound alpha–synuclein from site–directed spin labeling and computational refinement. *Proc. Natl. Acad. Sci. U. S. A.* 105:19666–19671
- Jenner P. (1989) Clues to the mechanism underlying dopamine cell death in Parkinson's disease. *J Neurol Neurosurg Psychiatry* Suppl:22–8.
- Jenner P. (2003).Oxidative stress in Parkinson's disease. Ann. Neurol. 53:S26–S38.
- Jensen P. H., Nielsen M. S., Jakes R., Dotti C. G. & Goedert M. (1998) Binding of alpha–synuclein to brain vesicles is abolished by familial Parkinson's disease mutation. *J Biol Chem.* 273:26292–4.
- Jo E., McLaurin J., Yip C. M., St George–Hyslop P. & Fraser P. E. (2000) alpha–Synuclein membrane interaction and lipid specificity. *J Biol Chem.* 275:34328–34334.
- Kachergus J., Mata IF., Hulihan M., Taylor J.P., Lincoln S., Aasly J., Gibson J.M., Ross O.A., Lynch T., Wiley J., Payami H., Nutt J., Maraganore D.M., Czyzewski K, Styczynska M., Wszolek Z.K., Farrer M.J., Toft M. (2005) Identification of a novel LRRK2 mutation linked to autosomal dominant parkinsonism: evidence of a common founder across European populations. *Am J Hum Genet.* 76:672–80.
- Kang J.H., Kim K.S. (2003) Enhanced oligomerization of the alpha–synuclein mutant by the Cu,Zn–superoxide dismutase and hydrogen peroxide system. *Mol Cells.* 15:87–93.
- Karyagina I, Becker S, Giller K, Riedel D, Jovin TM, Griesinger C, Bennati M. (2011) Electron paramagnetic resonance spectroscopy measures the distance between the external β–strands of folded α–synuclein in amyloid fibrils. *Biophys J.* 101:L1–3.

- Kiely AP, Asi YT, Kara E, Limousin P, Ling H, Lewis P, Proukakis C, Quinn N, Lees AJ, Hardy J, Revesz T, Houlden H, Holton JL. (2013) α-Synucleinopathy associated with G51D SNCA mutation: a link between Parkinson's disease and multiple system atrophy? *Acta Neuropathol.* 125:753–69.
- Klivenyi, P., Siwek, D., Gardian, G., Yang, L., Starkov, A., Cleren, C., Ferrante, R. J., Kowall, N. W., Abeliovich, A., Beal, M. F. (2006) Mice lacking alpha–synuclein are resistant to mitochondrial toxins. *Neurobiol. Dis.* 21:541−548.
- Koo H.C., Park Y.H., Lee B.C., Chae C., O'Rourke K.I., Baszler T.V. (2001) Immunohistochemical detection of Prion protein (PrP-Sc) and epidemiological study of BSE in Korea*. J Vet Sci.* 2:25–31.
- Kösel S., Przuntek H., Epplen J.T., Schöls L., Riess O. (1998) Ala30Pro mutation in the gene encoding alpha–synuclein in Parkinson's disease. *Nat Genet.* 18:106–8.
- Kruger R., Kuhn W., Müller T., Woitalla D., Graeber M., Kösel S., Przuntek H., Epplen J.T., Schöls L., Riess O. (1998)*et al.* Ala30Pro mutation in the gene encoding α-synuclein in Parkinson's disease. *Nature Genet.* 18:106−108.
- Kumar K.R., Lohmann K., Klein C. (2012) Genetics of Parkinson disease and other movement disorders. *Curr. Opin. Neurol.* 25:466–474.
- Khurana R., Ionescu–Zanetti C., Pope M., Li J., Nielson L., Ramírez–Alvarado M., Regan L., Fink A.L., Carter S.A. (2003) A general model for amyloid fibril assembly based on morphological studies using atomic force microscopy. *Biophys J.* 85:1135–44.
- Lai H.J., Lin C.H., Wu R.M. (2012) Early–onset autosomal–recessive parkinsonian–pyramidal syndrome. *Acta Neurol Taiwan.* 21:99–107.
- Langston JW, Ballard P, Tetrud JW, Irwin I. (1983) Chronic Parkinsonism in humans due to a product of meperidine–analog synthesis. *Science* 219:979–80.
- Langston J.W. (1985) MPTP neurotoxicity: an overview and characterization of phases of toxicity. *Life Sci.* 36:201−206.
- Lashuel H.A., Petre B.M., Wall J., Simon M., Nowak R.J., Walz T., Lansbury P.T. Jr. (2002) Alpha–synuclein, especially the Parkinson's disease–associated mutants, forms pore–like annular and tubular protofibrils. *J Mol Biol.* 322:1089–102.
- Lashuel H.A., Hartley D., Petre B.M., Walz T., Lansbury P.T. Jr. (2002) Neurodegenerative disease: amyloid pores from pathogenic mutations. *Nature* 418:291.
- Lashuel H.A., Overk C.R., Oueslati A., Masliah E. (2013) The many faces of α–synuclein: from structure and toxicity to therapeutic target. *Nat Rev Neurosci* 14:38–48.
- Lee C., Choi C., Lee S.J., (2002) Membrane–bound alpha–synuclein has a high aggregation propensity and the ability to seed the aggregation of the cytosolic form. *J. Biol. Chem.* 277:671–678.
- Lees, A. J. (2009). The Parkinson chimera. *Neurology* 72:S2–S11.
- Lees, A. J., Hardy, J., Revesz, T. (2009). Parkinson's disease. *Lancet* 373:2055–2066.
- Lewy, F. H. (1923). Die Lehre vom Tonus und der Bewegung: zugleich systematische Untersuchungen zur Klinik, Physiologie, Pathologie und Pathogenese der Paralysis agitans. *Julius Springer Verlag*.
- Lesage S, Brice A. (2009) Parkinson's disease: from monogenic forms to genetic susceptibility factors. *Hum Mol Genet.* 18:48–59.
- Lewitt P.A. (2008) Levodopa for the treatment of Parkinson's disease. *N. Engl. J. Med*. 359:2468−2476.

- Li X., Tan Y.C., Poulose S., Olanow C.W., Huang X.Y., Yue Z. (2007) Leucine–rich repeat kinase 2 (LRRK2)/PARK8 possesses GTPase activity that is altered in familial Parkinson's disease R1441C/G mutants. *J Neurochem.* 103:238–47.
- Lim S.Y., Lang A.E. (2010) The nonmotor symptoms of Parkinson's disease—an overview. *Mov Disord.* 25:S123–30.
- Lokappa S.B., Ulmer T.S., (2011) α–Synuclein populates both elongated and brokenhelix states on small unilamellar vesicle. *J. Biol. Chem.* 286:21450–2145.
- Lukiw W.J., Bazan N.G. (2008) Docosahexaenoic acid and the aging brain. *J Nutr.* 138:2510–2514.
- Madine, Doig A.J., Middleton D.A., (2006) A study of the regional effects of alpha–synuclein on the organization and stability of phospholipid bilayers. *Biochemistry* 45:5783–5792.
- Maekawa T., Kubo M., Yokoyama I., Ohta E., Obata F. (2010) Age–dependent and cell–population–restricted LRRK2 expression in normal mouse spleen*. Biochem Biophys Res Commun.* 392:431–5.
- Mazzuca C., Orioni B., Coletta M., Formaggio F., Toniolo C., Maulucci G., De Spirito M., Pispisa B., Venanzi M., Stella L. (2010) Fluctuations and the rate-limiting step of peptide-induced membrane leakage. *Biophys J.* 99:1791–800.
- McLaurin J., Yip C.M., StGeorge–Hyslop P., Fraser P.E., (2000) alpha–Synuclein membrane interactions and lipid specificity. *J. Biol. Chem.* 275:34328–34334.
- Murphy RM. (2007) Kinetics of amyloid formation and membrane interaction with amyloidogenic proteins. *Biochim Biophys Acta* 1768:1923–34.
- Mata I.F., Wedemeyer W.J., Farree M.J., Taylor J.P., Gallo K.A. (2006). LRRK2 in Parkinsoni's disease: protein domains and functional insights. *TRENDS in Neuroscience* 29:286–293.
- McLean P.J., Kawamata H., Ribich S., Hyman B.T., (2000) Membrane association and protein conformation of alpha–synuclein in intact neurons. Effect of Parkinson'sdisease–linked mutations, *J. Biol. Chem.* 275:8812–8816.
- Melrose H.L., Lincoln S.J., Tyndall G., Dickson D., Farrer M. (2006) Anatomical localization of leucine–rich repeat kinase 2 in mouse brain. *Neuroscience* 139:791–4.
- Melrose H.L., Kent C.B., Taylor J..P, Dachsel J..C, Hinkle K.M., Lincoln S.J., Mok S.S., Culvenor J.G., Masters C.L., Tyndall G.M., Bass D.I., Ahmed Z., Andorfer C.A., Ross O.A., Wszolek Z.K., Delldonne A., Dickson D.W., Farrer M.J. (2007) A comparative analysis of leucine–rich repeat kinase 2 (Lrrk2) expression in mouse brain and Lewy body disease. *Neuroscience* 147:1047–58.
- Miake H., Mizusawa H., Iwatsubo T., Hasegawa M. (2002) Biochemical characterization of the core structure of alpha–synuclein filaments. *J Biol Chem.* 277:19213–9.
- Nasstrom T., Wahlberg T., Karlsson M., Nikolajeff F., Lannfelt L., Ingelsson M., Bergstrom J., (2009) The lipid peroxidation metabolite 4–oxo–2–nonenal cross–links alpha–synuclein causing rapid formation of stable oligomers. *Biochem. Biophys. Res. Commun.* 378:872–876.
- Nasstrom T., Fagerqvist T., Barbu M., Karlsson M., Nikolajeff F., Kasrayan A., Ekberg M., Lannfelt L., Ingelsson M., Bergstrom J. (2011) The lipid peroxidation products 4–oxo–2–nonenal and 4–hydroxy–2–nonenal promote the formation of alphasynuclein oligomers with distinct biochemical, morphological, and functional properties. *Free Radic. Biol. Med.* 50:428–437.

- Lee H.J., Choi C., Lee S.J. (2002) Membrane–bound alpha–synuclein has a high aggregation propensity and the ability to seed the aggregation of the cytosolic form. *J Biol Chem.* 277:671–8.
- Necula M., Chirita C.N., Kuret J., (2003) Rapid anionic micelle–mediated alpha–synuclein fibrillization in vitro. *J. Biol. Chem.* 278:46674–46680.
- Nonaka T., Iwatsubo T., Hasegawa M., (2005) Ubiquitination of alpha–synuclein. *Biochemistry* 44:361–368.
- Norris E.H., Giasson B.I., Ischiropoulos H., Lee V.M., (2003) Effects of oxidative and nitrative challenges on alpha–synuclein fibrillogenesis involve distinct mechanisms of protein modifications. *J. Biol. Chem.* 278:27230–27240.
- Okochi M., Walter J., Koyama A., Nakajo S., Baba M., Iwatsubo T., Meijer L., Kahle P.J., Haass C., (2000) Constitutive phosphorylation of the Parkinson's disease associated alpha–synuclein. *J. Biol. Chem.* 275:390–397.
- Ozansoy M, Başak AN. (2013) The central theme of Parkinson's disease: α–synuclein. *Mol Neurobiol*. 47:460–5.
- Paleček E., Ostatná V., Masarík M., Bertoncini C.W., Jovin T.M. (2008) Changes in interfacial properties of alpha–synuclein preceding its aggregation. *Analyst.* 133:76–84.
- Paleologou K.E., Oueslati A., Shakked G., Rospigliosi C.C., Kim H.Y., Lamberto G.R., Fernandez C.O., Schmid A., Chegini F., Gai W.P., Chiappe D., Moniatte M., Schneider B.L., Aebischer P., Eliezer D., Zweckstetter M., Masliah E., Lashuel H.A. (2010) Phosphorylation at S87 is enhanced in synucleinopathies, inhibits alphasynuclein oligomerization, and influences synuclein–membrane interactions. *J. Neurosci.* 30:3184–3198.
- Papapetropoulos, S., Paschalis, C., Athanassiadou, A., Papadimitriou, A., Ellul, J., Polymeropoulos, M., Papapetropoulos, T. (2001) Clinical phenotype in patients with α–synuclein Parkinson's disease living in Greece in comparison with patients with sporadic Parkinson's disease. *J. Neurol. Neurosurg. Psychiatry* 70:662–665.
- Paisan–Ruiz C., Jain S., Evans E. W., Gilks W. P., Simon J., van der Brug M., Lopez de Munain A., Aparicio S., Gil A. M., Khan N., Johnson J., Martinez J. R., Nicholl D., Carrera I. M., Pena A. S., de Silva R., Lees A., Marti–Masso J. F., Perez–Tur J., Wood N. W. & Singleton A. B. (2004) Cloning of the gene containing mutations that cause PARK8–linked Parkinson's disease. *Neuron* 44:595–600.
- Perrin R.J., Woods W.S., Clayton D.F. & George J.M. (2000) Interaction of human alpha–synuclein and Parkinson's disease variants with phospholipids. Structural analysis using site– directed mutagenesis. *J Biol Chem.* 275:34393–34398.
- Perrin R.J., Woods W.S., Clayton D.F., George J.M., (2001) Exposure to long chain polyunsaturated fatty acids triggers rapid multimerization of synucleins. *J. Biol. Chem.* 276:41958–41962.
- Polymeropoulos M. H., Lavedan C., Leroy E., Ide S. E., Dehejia A., Dutra A., Pike B., Root H., Rubenstein J., Boyer R., Stenroos E. S., Chandrasekharappa S., Athanassiadou A., Papapetropoulos T., Johnson W. G., Lazzarini A. M., Duvoisin R. C., Di Iorio G., Golbe L. I., Nussbaum R. L. (1997) Mutation in the alpha–synuclein gene identified in families with Parkinson's disease. *Science* 276:2045–2047.
- Proukakis C., Dudzik C.G., Brier T., MacKay D.S., Cooper J.M., Millhauser G.L., Houlden H., Schapira A.H. (2013) A novel aS missense mutation in Parkinson disease. *Neurology* 801062–4.

- Przedborski S., Vila M. (2001) The last decade in Parkinson's disease research. Basic sciences. *Adv Neurol* 86:177–86.
- Qin Z., Hu D., Han S., Reaney S.H., Di Monte D.A., Fink A.L., (2007) Effect of 4–hydroxy–2– nonenal modification on alpha–synuclein aggregation. *J. Biol. Chem.* 282:5862–5870.
- Quilty M.C., King A.E., Gai W.P., Pountney D.L., West A.K., Vickers J.C. (2006), Alpha-synuclein is upregulated in neurones in response to chronic oxidative stress and is associated with neuroprotection*. Exp Neurol*, 199 pp. 249–256.
- Quin Z., Hu D., Han S., Hong D. P., Fink A. L. (2007) Role of different regions of α–synuclein in assembly of fibrils. *Biochemistry* 46:13322–30.
- Ramsay R.R., Salach J.I., Dadgar J., Singer T.P. (1986) Inhibition of mitochondrial NADH dehydrogenase by pyridine derivatives and its possible relation to experimental and idiopathic parkinsonism. *Biochem. Biophys. Res. Commun.* 135:269–75.
- Ramakrishnan M., Jensen P.H., Marsh D. (2003) Alpha–synuclein association with phosphatidylglycerol probed by lipid spin labels. *Biochemistry* 42:12919−12926.
- Reale M., Pesce M., Priyadarshini M., Kamal M.A., Patruno A. (2012) Mitochondria as an easy target to oxidative stress events in Parkinson's disease. *CNS Neurol Disord Drug Targets* 11430–8.
- Rhoades E., Ramlall T.F., Webb W.W., Eliezer D. (2006) Quantification of alpha–synuclein binding to lipid vesicles using fluorescence correlation spectroscopy. *Biophys J.* 90:4692–4770.
- Rott E., Szargel R., Haskin J., Shani V., Shainskaya A., Manov I., Liani E., Avraham E., Engelender S. (2008) Monoubiquitylation of alpha–synuclein by seven in absentia homolog (SIAH) promotes its aggregation in dopaminergic cells, *J. Biol. Chem.* 283:3316–3328.
- Ruipérez V, Darios F, Davletov B. (2010) Alpha–synuclein, lipids and Parkinson's disease. *Prog Lipid Res.* 49:420–8.
- Sampathu D.M., Giasson B.I., Pawlyk A.C., Trojanowski J.Q., Lee V.M. (2003) Ubiquitination of alpha–synuclein is not required for formation of pathological inclusions in alpha–synucleinopathies. *Am. J. Pathol*. 163:91–100
- Sandal M., Valle F., Tessari I., Mammi S., Bergantino E., Musiani F., Brucale M., Bubacco L., Samorì B (2008) Conformational equilibria in monomeric alpha–synuclein at the single– molecule level. *PLoS Biol.* 6:e6.
- Sciacca M.F., Brender J.R., Lee D.K., Ramamoorthy A. (2012) Phosphatidylethanolamine enhances amyloid fiber-dependent membrane fragmentation. *Biochemistry* 51:7676-84.
- Scott D., Roy S. (2012) α–Synuclein inhibits intersynaptic vesicle mobility and maintains recycling–pool homeostasis. *J Neurosci.* 32:10129–10135.
- Serpell L.C. (2000) Alzheimer's amyloid fibrils: structure and assembly. *Biochim Biophys Acta* 1502:16–30.
- Sharon R., Bar–Joseph I., Frosch M.P., Walsh D.M., Hamilton J.A., Selkoe D.J. (2003) The formation of highly soluble oligomers of alpha–synuclein is regulated by fatty acids and enhanced in Parkinson's disease. *Neuron* 37:583–595.
- Sharon R., Bar–Joseph I., Frosch M.P., Walsh D.M., Hamilton J.A., Selkoe D.J., (2003) The formation of highly soluble oligomers of alpha–synuclein is regulated by fatty acids and enhanced in Parkinson's disease. *Neuron* 37:583–595.
- Shults C. W. (2006) Lewy bodies. *Proc. Natl. Acad. Sci. U S A* 103:1661−1668.

- Singleton A. B., Farrer M., Johnson J., Singleton A., Hague S., Kachergus J., Hulihan M., Peuralinna T., Dutra A., Nussbaum R., Lincoln S., Crawley A., Hanson M., Maraganore D., Adler C., Cookson M. R., Muenter M., Baptista M., Miller D., Blancato J., Hardy J., Gwinn–Hardy K. (2003) alpha–Synuclein locus triplication causes Parkinson's disease. *Science* 302:841.
- Singleton A., Gwinn–Hardy K., Sharabi Y., Li S.T., Holmes C., Dendi R., Hardy J., Singleton A., Crawley A., Goldstein D. S. (2004) Association between cardiac denervation and parkinsonism caused by alpha–synuclein gene triplication. *Brain* 127:768–772.
- Singleton A.B., Farrer M.J., Bonifati V. (2013) The genetics of Parkinson's disease: progress and therapeutic implications*. Mov Disord.* 28:14–23.
- Smith W.W., Margolis R.L., Li X., Troncoso J.C., Lee M.K., Dawson V.L., Dawson T.M., Iwatsubo T., Ross C.A., (2005) Alpha–synuclein phosphorylation enhances eosinophilic cytoplasmic inclusion formation in SH–SY5Y cells. *J. Neurosci.* 25:5544–5552.
- Spillantini M. G., Crowther R. A., Jakes R., Hasegawa M. ,Goedert M. (1998) alpha–Synuclein in filamentous inclusions of Lewy bodies from Parkinson's disease and dementia with Lewy bodies. *Proc. Natl. Acad. Sci. U S A*, 95:6469–6473.
- Taymans J.M., Van den Haute C., Baekelandt V. (2006) Distribution of PINK1 and LRRK2 in rat and mouse brain. *J Neurochem.* 98:951–61.
- Thakur P., Nehru B. (2013) Long-term heat shock proteins (HSPs) induction by carbenoxolone improves hallmark features of Parkinson's disease in a rotenone-based model. *Neuropharmacology.* 79:190–200.
- Thomas B., and Beal M.F. (2007) Parkinson's disease. Hum. Mol. Genet. 16:183–193.
- Tolleson C.M., Fang J.Y. (2013) Advances in the mechanisms of Parkinson's disease. *Discov Med.* 15:61–6.
- Tosatto L., Andrighetti A.O., Plotegher N., Antonini V., Tessari I., Ricci L., Bubacco L., Dalla Serra M. (2012) Alpha-synuclein pore forming activity upon membrane association. *Biochim Biophys Acta* 1818:2876–2883.
- Turnbull S., Tabner B.J., El–Agnaf O.M., Moore S., Davies Y., Allsop D. (2001) alpha–Synuclein implicated in Parkinson's disease catalyses the formation of hydrogen peroxide in vitro. *Free Radic. Biol. Med*. 30:1163–70.
- Uchida K. (2003) Histidine and lysine as targets of oxidative modification. *Amino Acids.* 25:249–57.
- Ulmer T.S. & Bax A. (2005) Comparison of structure and dynamics of micelle–bound human alpha–synuclein and Parkinson disease variants. *J Biol Chem.* 280:43179–43187.
- Uversky V.N., Li J., Fink A.L. (2001) Metal–triggered structural transformations, aggregation, and fibrillation of human α–synuclein. *J Biol Chem*. 276:44284–96.
- Uversky V.N., Li J., Fink A.L. (2001b) Evidence for a partially folded intermediate in α–synuclein fibril formation. *J Biol Chem.* 276:10737–44.
- Uversky V.N., Yamin G., Munishkina L.A., Karymov M.A., Millett I.S., Doniach S., Lyubchenko Y.L., Fink A.L. (2005). Effects of nitration on the structure and aggregation of alpha–synuclein. *Brain Res. Mol. Brain Res.* 134:84−102.
- Van Den Eeden S.K., Tanner C.M., Bernstein A.L., Fross R.D., Leimpeter A., Bloch D.A., Nelson L.M. (2003) Incidence of Parkinson's disease: variation by age, gender, and race/ethnicity. *Am J Epidemiol.* 157:1015–22.
- Venda L.L., Cragg S.J., Buchman V.L., Wade–Martins R. (2010) α–Synuclein and dopamine at the crossroads of Parkinson's disease. *Trends Neurosci*. 33:559–68.

- Vilar M., Chou H.T., Luehrs T., Maji S. K., Riek–Loher D., Vere R., Manning G., Stahlberg H., Riek R. (2008). The fold of α–synuclein fibrils. *Proc. Natl. Acad. Sci. USA* 105:8637–42.
- Vilarino–Guell C., Wider C., Ross O.A., (2011) VPS35 mutations in Parkinson disease. *Am J Hum Genet.* 89:162–7.
- Volles M. J. & Lansbury P. T. Jr (2002) Vesicle permeabilization by protofibrillar alpha–synuclein is sensitive to Parkinson's disease–linked mutations and occurs by a pore–like mechanism. *Biochemistry* 41:4595–4602.
- Yoritaka A., Hattori N., Uchida K., Tanaka M., Stadtman E. R., Mizuno Y. (1996) Immunohistochemical detection of 4–hydroxynonenal protein adducts in Parkinson disease. *Proc. Natl. Acad. Sci. USA* 93:2696–2701.
- Wakabayashi K., Engelender S., Yoshimoto M., Tsuji S., Ross C. A. & Takahashi H. (2000) Synphilin–1 is present in Lewy bodies in Parkinson's disease. Ann Neurol 47:521–523.
- Wang A., Costello S., Cockburn M., Zhang X., Bronstein J., Ritz B (2011) Parkinson's disease risk from ambient exposure to pesticides. *European Journal of Epidemiology* 26:547–555.
- West A.B., Moore D.J., Biskup S., Bugayenko A., Smith W.W., Ross C.A., Dawson V.L., Dawson T.M. (2005) Parkinson's disease–associated mutations in leucine–rich repeat kinase 2 augment kinase activity. *Proc. Natl. Acad. Sci. U S A* 102:16842–16847.
- Westerlund M, Hoffer B, Olson L. (2010) Parkinson's disease: Exit toxins, enter genetics. *Prog Neurobiol.* 90:146–56.
- Wood S.J., Wypych J., Steavenson S., Louis J.C., Citron M., Biere A.L. (1999) α–Synuclein fibrillogenesis is nucleation dependent. *J Biol Chem.* 278:19509–19512.
- Wood–Kaczmar A., Gandhi S., Wood N. W. (2006) Understanding the molecular causes of Parkinson's disease. *Trends Mol Med*. 12:521–528.
- Zakharov S.D., Hulleman J.D., Dutseva E.A., Antonenko Y.N., Rochet J.C. & Cramer W.A. (2007) Helical alpha–synuclein forms highly conductive ion channels. *Biochemistry* 46:14369–14379.
- Zarranz J. J., Alegre J., Gómez–Esteban J. C., Lezcano E., Ros R., Ampuero I., Vidal L., Hoenicka J., Rodriguez O., Atarés B., Llorens V., Gomez Tortosa E., del Ser T., Muñoz D. G., de Yebenes J.G. (2004). The new mutation, E46K, of alpha–synuclein causes Parkinson and Lewy body dementia. *Ann. Neurol.* 55:164–173.
- Zhu, Li J., Fink A.L., (2003) The association of alpha–synuclein with membranes affects bilayer structure, stability, and fibril formation. *J. Biol. Chem.* 278:40186–40197
- Zhu, Fink A.L., (2003) Lipid binding inhibits alpha–synuclein fibril formation. *J. Biol.Chem.* 278:16873–16877.
- Zhu M., Qin Z.J., Hu D., Munishkina L.A., Fink A.L., (2006) Alpha–synuclein can function as an antioxidant preventing oxidation of unsaturated lipid in vesicles. *Biochemistry* 45:8135–8142.
- Zimprich A., Biskup S., Leitner P., Lichtner P., Farrer M., Lincoln S., Kachergus J., Hulihan M., Uitti R. J., Calne D. B., Stoessl A. J., Pfeiffer R. F., Patenge N., Carbajal I. C., Vieregge P., Asmus F., Muller–Myhsok B., Dickson D. W., Meitinger T., Strom T. M., Wszolek Z. K. & Gasser T. (2004) Mutations in LRRK2 cause autosomal–dominant parkinsonism with pleomorphic pathology. *Neuron* 44:601–607.
- Zimprich A., Benet–Pagès A., Struhal W., Graf E., Eck S.H., Offman M.N., Haubenberger D., Spielberger S., Schulte E.C., Lichtner P., Rossle S.C., Klopp N., Wolf E., Seppi K.,Pirker W., Presslauer S., Mollenhauer B., Katzenschlager R., Foki T., Hotzy C., Reinthaler E.,

Harutyunyan A., Kralovics R., Peters A., Zimprich F., Brücke T., Poewe W., Auff E., Trenkwalder C., Rost B., Ransmayr G., Winkelmann J., Meitinger T., Strom T.M. (2011) A mutation in VPS35, encoding a subunit of the retromer complex, causes late–onset Parkinson disease. *Am J Hum Genet*. 89:168–175.

OPEN ACCESS Freely available online

PLOS ONE

α-Synuclein Oligomers Induced by Docosahexaenoic Acid Affect Membrane Integrity

Chiara Fecchio[1], Giorgia De Franceschi[1], Annalisa Relini[2], Elisa Greggio[3], Mauro Dalla Serra[4], Luigi Bubacco[3], Patrizia Polverino de Laureto[1*]

1 CRIBI, Biotechnology Centre, Department of Pharmaceutical Sciences, University of Padova, Padova, Italy, **2** Department of Physics, University of Genova, Genova, Italy, **3** Department of Biology, University of Padova, Padova, Italy, **4** Institute of Biophysics, National Research Council of Italy and Bruno Kessler Foundation, Trento, Italy

Abstract

A key feature of Parkinson disease is the aggregation of α-synuclein and its intracellular deposition in fibrillar form. Increasing evidence suggests that the pathogenicity of α-synuclein is correlated with the activity of oligomers formed in the early stages of its aggregation process. Oligomers toxicity seems to be associated with both their ability to bind and affect the integrity of lipid membranes. Previously, we demonstrated that α-synuclein forms oligomeric species in the presence of docosahexaenoic acid and that these species are toxic to cells. Here we studied how interaction of these oligomers with membranes results in cell toxicity, using cellular membrane-mimetic and cell model systems. We found that α-synuclein oligomers are able to interact with large and small unilamellar negatively charged vesicles acquiring an increased amount of α-helical structure, which induces small molecules release. We explored the possibility that oligomers effects on membranes could be due to pore formation, to a detergent-like effect or to fibril growth on the membrane. Our biophysical and cellular findings are consistent with a model where α-synuclein oligomers are embedded into the lipid bilayer causing transient alteration of membrane permeability.

Citation: Fecchio C, De Franceschi G, Relini A, Greggio E, Dalla Serra M, et al. (2013) α-Synuclein Oligomers Induced by Docosahexaenoic Acid Affect Membrane Integrity. PLoS ONE 8(11): e82732. doi:10.1371/journal.pone.0082732

Editor: David Holowka, Cornell University, United States of America

Received September 17, 2013; **Accepted** November 4, 2013; **Published** November 29, 2013

Funding: This work was supported by a Research Project of University of Padova (CPDA125928, 2012), by University of Genova (Fondi di Ateneo) and by the Rientro dei Cervelli Program (Incentivazione alla mobilita` di studiosi stranieri e italiani residenti all'estero) from the Italian Ministry of Education, University and Research (EG). The funders had no role in study design, data collection and analysis, decision to publish, or preparation of the manuscript.

Competing interests: The authors confirm that co-author Dr. Elisa Greggio is a PLOS ONE Editorial Board member and that this does not alter their adherence to all the PLOS ONE policies on sharing data and materials.

* E-mail: patrizia.polverinodelaureto@unipd.it

Introduction

Parkinson disease (PD) is the most common movement disorder, currently affecting approximately 2% of the population older than age 60 years. Hallmarks of PD are the loss of dopaminergic neurons in the substantia nigra (SN) region of the brain and the presence of cytoplasmatic inclusions of α-synuclein (aS) in fibrillar form, known as Lewy bodies and Lewy neurites [1]. aS is a 14 kDa protein that predominantly exists as unfolded monomer under native conditions. Its sequence is characterized by an amphipathic lysine-rich amino terminus, which governs binding to lipids and interactions with membranes [2]; by a hydrophobic central region (NAC, non-amyloid-beta component), responsible for protein aggregation and β-sheet formation [3,4] and a highly acidic C-terminal, rich in Pro and acidic residues. How the fibrillar aggregation of aS is related to PD and neurodegeneration is still an unsolved question. *In vivo* and *in vitro* studies support the hypothesis that oligomers and species formed in the early stage of aggregation of aS, rather than the monomeric or fibrillar protein, represent the toxic species involved in PD [5-7]. Diverse types of oligomers have been described, in terms of structure and toxic activity. It should be mentioned that the methods used for the preparation of oligomers *in vitro* strongly affect their properties, so up to date a robust *in vitro* model of the mechanism by which oligomers exert their toxic activity is not available.

Although the physiological function of aS is still poorly understood [8], it appears to be involved in modulating synaptic vesicle dynamics [9-11] and may contribute to the activity of controlling synaptic homeostasis-associated proteins [12-14]. Several studies have recently shown a strong link between aS and fatty acids (FAs), in particular brain FAs, such as arachidonic and docosahexaenoic acid (DHA). aS expression affects FAs uptake and metabolism [15,16] and aS interactions with polyunsaturated fatty acids (PUFAs) can rapidly and dynamically affect its oligomerization and further aggregation [17-19]. The appearance of aS toxic oligomers *in vivo* has been

linked to the presence of long PUFAs in the brain [20]. Yakunin and colleagues [21] demonstrated that a DHA enriched diet increases the concentration of insoluble aS species in mouse brain. Many evidences suggest a critical role of lipids in both PD and Alzheimer disease, such as changes in activity of phospholipase A_2 (an enzyme that hydrolyses membrane phospholipids and causes release of FAs) that have been correlated with brain injury, apoptosis and phospholipid metabolism alteration, ultimately leading to neurodegeneration. As a consequence, the interaction between aS and FAs has been proposed to be a key factor in the onset of neurodegeneration and PD [16].

In previous studies, we analyzed the aggregation process of aS in the presence of DHA using different protein to DHA molar ratios [19,22]. We demonstrated that DHA exerts an important role in the aggregation of aS, recruiting protein molecules on the droplets surface and being itself part of the aggregates structure. The presence of DHA to the aggregating aS (50:1 mol/mol) leads to the formation of stable oligomers, that are DMSO- and SDS-resistant, do not bind ThT and lack seeding properties, demonstrating that they are off-pathway in the aggregation process of aS. Structurally they contain α-helical and random structure. Furthermore, these oligomers are toxic to cells, compared to aS, suggesting that they are potentially relevant in the pathogenesis of PD.

In the present work we conducted experiments to test the hypothesis that aS oligomers exert their toxic effect by undermining the integrity of lipid membranes. The interaction between aS/DHA oligomers with lipid bilayer was studied by circular dichroism (CD), transmission electron microscopy (TEM) and dynamic light scattering (DLS). We show that aS/DHA oligomers bind to negatively charged membranes and acquire an increased amount of α-helical structure. Upon binding to negatively charged vesicles, oligomers induce leakage of small molecules such as calcein (mw 0.6 kDa) but not of FITC-dextran (mw 10 kDa). Treatment of dopaminergic SH-SY5Y cells with aS/DHA oligomers results in increased permeability to propidium iodide.

Materials and Methods

DHA and fluorescein isothiocyanate dextran (FITC-Dextran) of average molecular weight of 10,000 Da were purchased from Sigma Chem. Co. (St. Louis, MO). All other chemicals (analytical reagent grade) were obtained from Sigma or Fluka (Buchs, Switzerland). The lipids, 1-palmitoyl-2-oleoyl-sn-glycero-3-phosphocholine (POPC), 1,2-dioleoyl-*sn*-glycero-3-phospho-(1'-rac-glycerol) (DOPG), 1-palmitoyl-2-oleoyl-sn-glycero-3-phospho-L-serine (POPS), 1-palmitoyl-2-oleoyl-*sn*-glycero-3 phosphoethanolamine (POPE) and Brain Total Lipid Extract, were obtained from Avanti Polar Lipids (Alabaster, AL) as chloroform solution and used without further purification.

aS cloning and expression

The pET28b (Novagen) plasmid was used for the expression of recombinant human aS in *E. coli* BL21 (DE3). The expression and purification of the protein were conducted using the procedure previously described [22]. Protein concentrations were determined by absorption measurements at 280 nm using a double-beam Lambda-20 spectrophotometer (Perkin Elmer, Norwalk, CT). The extinction coefficient of aS at 280 nm is 5960 cm^{-1} M^{-1}, as evaluated from its amino acid composition by the method of Gill and von Hippel [23].

Preparation of oligomers

To prepare oligomeric species, aS was incubated at 37 °C for up to 48 hours at a protein concentration of 50 μM, in PBS (8 mM Na_2HPO_4, 137 mM NaCl, 2 mM KH_2PO_4, 2.7 mM KCl, pH 7.4) in the presence of DHA (2.5 mM) to obtain a protein/fatty acid molar ratio of 1:50, under shaking at 500 rpm with a thermo-mixer (Compact, Eppendorf, Hamburg, DE). Aliquots of the samples were examined by thioflavin T (ThT) binding assay, CD, TEM, gel filtration (GF) chromatography and RP-HPLC, as previously described [19] to verify the identity and structure of the oligomers and to assure experimental reproducibility. The identity of the eluted material was assessed by mass spectrometry carried out with an electrospray ionization (ESI) mass spectrometer with a Q-Tof analyzer (Micro) (Waters, Manchester, UK). Oligomers were used after purification by GF and concentrated by Amicon Ultra ultrafiltration (10K membrane cutoff) (Millipore, Billerica, MA, USA).

Circular dichroism

CD spectra were recorded on a J-710 spectropolarimeter (Jasco, Tokyo, Japan). Far-UV CD spectra were recorded using a 1 mm path-length quartz cell and a protein concentration of 5-7 μM. The mean residue ellipticity [θ] (deg cm^2 $dmol^{-1}$) was calculated from the equation [θ] = (*θobs*/10) (MRW//*c*), where θ_{obs} is the observed ellipticity in deg, MRW is the mean residue molecular weight of the protein, *l* the optical pathlength in cm and *c* the protein concentration in g/mL. The spectra were recorded in PBS buffer, pH 7.4.

Atomic force and electron transmission microscopy

aS/DHA oligomers were diluted 500 times using Milli-Q water and 10 μl aliquots were deposited on freshly cleaved mica and dried under mild vacuum. Tapping mode AFM images were acquired in air using a Multimode scanning probe microscope equipped with an “E” scanning head (maximum scan size 10 μm) and driven by a Nanoscope IV controller (Digital Instruments, Bruker, Germany). Single beam uncoated silicon cantilevers (type Olympus OMCL-AC160TS, Olympus, Tokyo, Japan) were employed. The tip of the probe was of 7 nm. The drive frequency was between 280 and 300 kHz, and the scan rate was between 0.5 and 1.0 Hz. TEM pictures were taken on a Tecnai G^2 12 Twin instrument (FEI Company, Hillsboro, OR, USA), operating at an excitation voltage of 100 kV. Samples for TEM were diluted 2 times and a drop of the solution was placed on a Butvar-coated copper grid (400-square mesh) (TAAB-Laboratories Equipment Ltd, Berks, UK), followed by a drop of uranyl acetate solution (1% w/v).

Vesicles preparation

To prepare large and small unilamellar vesicles (LUV, SUV), lipids were transferred in glass tubes. Chloroform was dehydrated by gentle helium stream and then warmed at 45°C to remove residual organic solvent. The lipid film was hydrated with PBS pH 7.4 in the absence or presence of calcein (50 mM) or FITC-dextran (1.6 mM) at 40°C for 2 hours with frequent vortexing. Then it was subjected to 5 cycles of freezing and thawing. The suspension of vesicles was extruded 11 times through a 400 nm or 30 nm pore size polycarbonate membrane on lipid extruder (Northern Lipids Inc, Vancouver, BC), in order to obtain LUVs or SUVs. Calcein-loaded and FITC-dextran-loaded vesicles were purified by gel filtration chromatography (Sepharose G-25) to remove unencapsulated dye. The final lipid concentration, determined as total phosphorus, was conducted according to Chen et al., [24].

Dynamic light scattering

The size distribution and the stability of vesicles were checked by DLS experiments, performed on a Zetasizer Nano-ZS instrument (Malvern Instrument, UK). DLS measurements were performed at 25 °C in PBS pH 7.4 in duplicate. During every measurement 12 runs were collected. DOPG LUV and SUV size distributions were measured for vesicles alone and after 30 min of incubation with oligomers.

Release assays

For calcein release assay, SUV or LUV were diluted to 50 μM of lipids. After 30 minutes of incubation in the presence of different protein species (monomers, oligomers, fibrils), fluorescence emission at 515 nm was recorded after excitation at 490 nm. Maximum fluorescence emission was obtained by the addition of 0.1% Triton X-100 to disrupt vesicles. The average values of experiments, performed in triplicate, were expressed as a percentage of the maximum effect due to total vesicles disruption. FITC-dextran-loaded SUVs or LUVs were incubated for 30 minutes in the presence of the protein species at a final lipid concentration of 100 μM. Released dye was detected by fluorescence measurement with excitation at 490 nm and emission at 515 nm, after purification of the incubated solution through Microcon (cutoff 50000) to allow FITC-Dextran elution. The minimum and maximum effect was obtained by measurement of a liposome solution respectively with or without 0.1% Triton X-100. The average values of experiments, performed in triplicate, were expressed as a percentage of the maximum effect calculated as total vesicles disruption obtained with Triton X-100.

Cell permeabilization assay

To examine whether aS/DHA oligomers can permeabilize cell membranes, we exploited the ability of propidium iodide (PI; MW 668.4 Da) to bind DNA as indirect reporter of membrane damage. Dopaminergic SH-SY5Y cells were cultured in 24-well plates (seeding density ~50000 cells/well) and twenty-four hours after seeding treated with 0.5 μM of aS monomer or aS/DHA oligomers. Impermeant dye PI (2 μg/ml) and counterstain dye Hoechst 33242 (2 μg/ml) were added to cells simultaneously to the treatment. After a 30 min-incubation at 37°C, PI-positive cells were counted in three replicate cultures, acquiring an average of 5 fields per culture (250-350 cells/field). The experiment has been repeated 3 times independently. Saponin (50 μg/ml) was used as positive control of membrane permeabilization.

Aggregation study

In order to induce aggregation, a 50 μM solution of aS/DHA oligomers (calculated as monomer concentration) was incubated in 20 mM Tris·HCl, 150 mM NaCl pH 7.4 in the absence or in the presence of DHA (2.5 mM, molar ratio 1:50) or DOPG SUVs (1 mM or 2.5 mM, molar ratio protein/lipid 1:20 and 1:50) at 37°C, under shaking at 500 rpm with a thermo-mixer (Compact, Eppendorf, Hamburg, DE). Aliquots of the samples were examined by ThT binding assay, CD and TEM. The ThT binding assays were performed accordingly to LeVine [25] using a 25 μM ThT solution in 25 mM sodium phosphate (pH 6.0). Aliquots (30 μl) of protein samples containing aggregates were taken at specified times and diluted into the ThT buffer. Fluorescence emission measurements were conducted at 25°C using an excitation wavelength of 440 nm and recording the ThT fluorescence emission at 484 nm.

Planar Lipid Membrane experiments

Solvent-free Planar Lipid Membrane (PLM) was composed of equimolar mixture of 1,2-dioleyl-phosphatidyl-glycerol (DOPG) and 1,2-dioleyl-phosphatidyl-ethanolamine (DOPE) and formed on an aperture in a 25 μm thick Teflon septum separating two chambers, as described in Dalla Serra et al. [26]. Ionic currents were recorded by a patch clamp amplifier (VA-10X npi, Tamm, Germany), filtered at 100 Hz, digitalized and acquired at 2 kHz by the computer using DigiData 1322 A/D converter and pClamp software (Axon Instruments, Sunnyvale, CA).

Results

Biophysical properties of oligomers

aS oligomers, induced by DHA, were obtained as previously described [19,22] and were purified by gel filtration from monomeric aS, after 48 h incubation [19]. The fraction corresponding to oligomers was analyzed by RP-HPLC (Figure 1A, red line) and compared with RP-HPLC profile of the same sample before its purification by gel filtration. The peak (RT 29.6 min) corresponding to DHA is lacking, indicating that exchangeable DHA is removed. Mass spectrometry (Figure 1A, inset) shows that aS molecules in the oligomers are chemically modified for the presence of covalently bound DHA, as previously determined [19]. Previously, TEM analysis showed that the chromatographic fraction corresponding to oligomers had a spherical morphology, with diameters ranging from 12 to 35 nm [19]. In Figure 1B the number size distribution from aS/DHA oligomers obtained by DLS analysis is shown, indicating a mean size of 22±8 nm. AFM measurement (inset), based on height differences, shows the presence of smaller (1.1±0.1 nm) and larger (4.1±0.1 nm) oligomers.

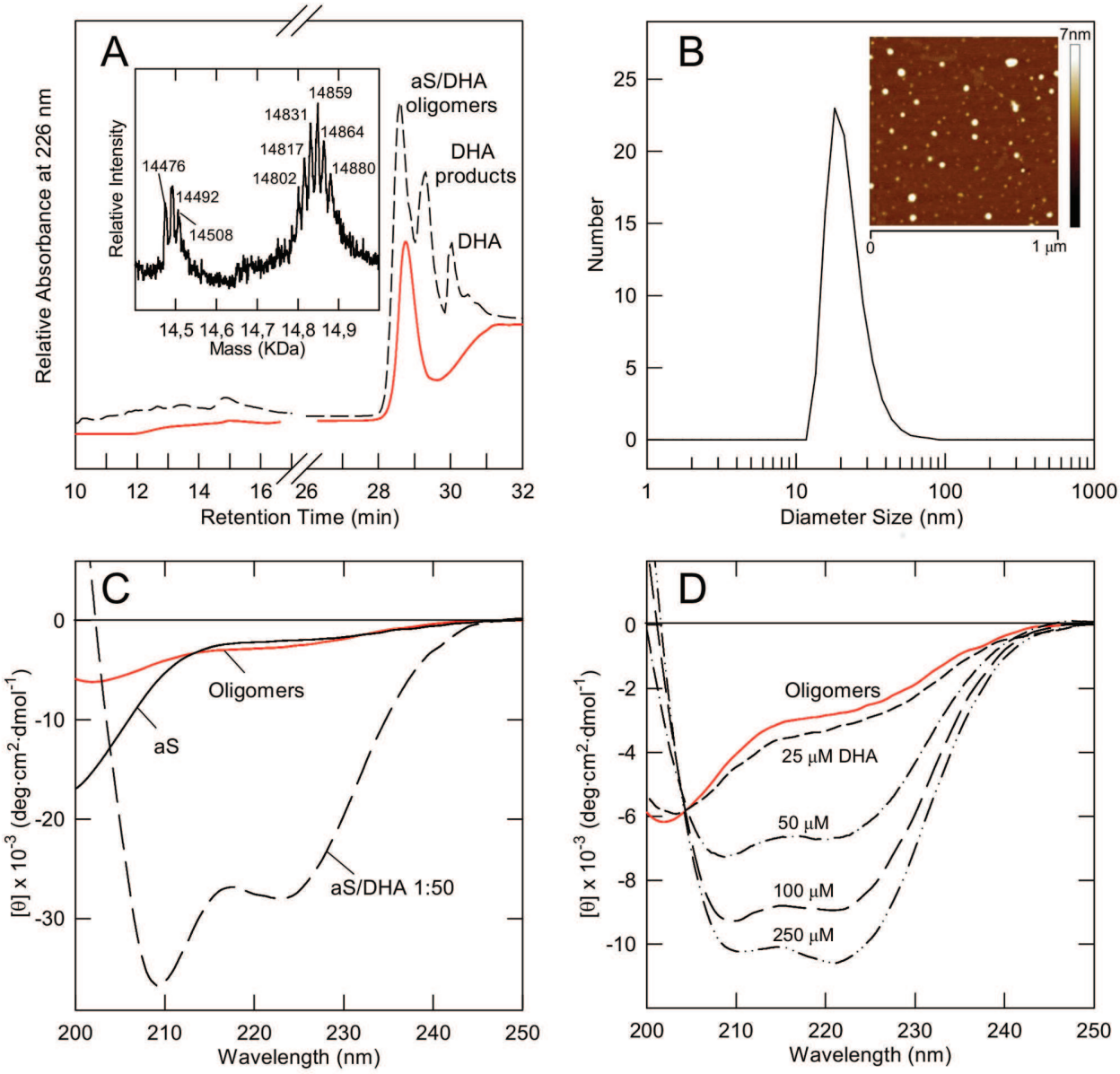

Figure 1. Chemico-physical characterization of aS/DHA oligomers after their isolation by gel filtration. (A) RP-HPLC of aS/DHA oligomers after their isolation by gel filtration (red line) and before (dashed line). HPLC analyses were conducted using a Jupiter C4 column (4.6 x 150 mm; Phenomenex, CA, USA), eluted with a gradient of acetonitrile/0.085% TFA vs water/0.1% TFA from 5% to 38% in 5 min, from 38% to 43% in 15 min, recording the absorbance at 226 nm. The identity of the eluted material was assessed by mass spectrometry and the spectrum of oligomers is reported (inset). (B) DLS for particle size estimation of aS/DHA oligomers. (Inset) Tapping mode AFM image of oligomers. Scan size was 1.0 μm; Z range was 7 nm. (C) Far UV CD of oligomers after purification by gel filtration (red line). The spectra of monomeric aS and aS in the presence of DHA (protein/DHA 1:50) are also reported as reference. (D) Titration experiment by far UV CD of oligomers in the presence of increasing amount of DHA. The numbers close to the spectra indicate the amount (μM) of DHA.

doi: 10.1371/journal.pone.0082732.g001

Spectroscopic analysis by far UV CD of oligomers after purification by gel filtration is reported (Figure 1C). The spectrum of oligomers (red line) is shown in comparison with CD spectra of monomeric aS (continuous line) and of the mixture of aS/DHA before gel filtration (dashed line, see ref. 19). This analysis indicates that oligomers acquire a partly folded conformational state with a moderate content of α-helical structure. Further addition of DHA to oligomers, isolated by gel

filtration, induces an increase of their α-helical structure (Figure 1D), as observed for monomeric aS [22]. The transition between partly folded state and α-helix follows a two-state model, for the presence of an isodichroic point at ~203 nm in the titration experiment.

Oligomers interact with negatively charged membranes

In order to elucidate the mechanism by which DHA/aS oligomers exert their toxic activity, the interaction with model membranes has been studied. CD spectroscopy was used to determine the effects of lipid binding on the secondary structure of aS/DHA oligomers and various combinations of charged and uncharged lipids have been used. In Figure 2 the CD spectra of aS/DHA oligomers recorded in the presence of SUV or LUV are reported. aS/DHA oligomers interact with synthetic membranes containing negatively charged DOPG, or a mixture of negative and neutral phospholipids as 1DOPG: 1POPE and 1POPS:1POPC (Figure 2), as more pronounced minima at 208 and 222 nm are observed in the spectra upon binding to these membranes, indicating an increase of α-helical conformation. SUV or LUV containing neutral phospholipids (POPC or POPE) do not induce any conformational change in aS oligomers, as well as vesicles constituted by a mixture of lipid extracted from brain (Figure 2). SUV and LUV with the same composition exert similar effect on oligomers secondary structure suggesting that curvature is not a discriminating factor.

Oligomers do not aggregate in the presence of lipids and membranes

Membrane-induced or lipid-accelerated fibril formation of amyloidogenic proteins was frequently observed [27-29]. To analyze the effect of membranes on the aggregation properties of aS/DHA oligomers, aS and aS oligomers were incubated in the absence and in the presence of vesicles (molar ratio protein/lipid of 1:20 and 1:50). The aggregation was conducted in the presence of DOPG SUV, since oligomers preferentially interact with negatively charged membranes and DHA (molar ratio protein/fatty acid 1:50), as control. The effect of the lipids on protein aggregation was monitored by ThT fluorescence assay (Figure 3). The aggregation process of aS results sped up in the presence of DOPG SUV (1:20) (Figure 3A, empty circles), while in the presence of DOPG SUV (1:50) is inhibited (Figure 3A, empty triangles). TEM analysis show that in the mixture corresponding to aS incubation for 9 days in the presence of SUV DOPG (1:20) there are individual aS amyloid-like fibrils associated to the surface of SUV (Figure 3A, inset). The size and morphology of these fibrils are similar to those of aS fibrils formed in the absence of SUV. In both cases, aS forms straight, unbranched fibrils with a width of 10–15 nm. An additional feature is that the shape of vesicles in contact with fibrils is not changed. In the presence of DHA, as previously observed, there is not formation of aS aggregates that bind ThT dye (Figure 3A, inverted black triangles). In the case of aS/DHA oligomers, their incubation in the presence or the absence of SUV or DHA does not result in any increase of the fluorescence of ThT dye, confirming their nature of off-pathway intermediates (Figure 3B). The aggregation process was further monitored by CD spectroscopy, confirming the presence of β-sheet structure only for ThT-positive fibrils (data not shown).

Oligomers induce permeabilization of artificial membranes

The calcein leakage test was performed to detect changes in membrane permeabilization as result of oligomers binding. The amount of calcein release from LUV or SUV was determined after 30 min of incubation with the oligomers. In Figure 4A the leakage of calcein from LUV was shown in comparison with the effect induced by monomeric and fibrillar aS. We used LUV containing phospholipids which interact (DOPG), partially interact (1POPC:1POPS) or do not interact (TBE) with oligomers, as shown by CD measurements. It is evident that oligomers are able to induce a significant dye release, in comparison to monomeric aS and fibrils. The effect is selective for negatively charged membranes. This effect was also analyzed on DOPG SUV using different protein/lipid molar ratio (Figure 4B). The leakage occurs in a dose-dependent manner and reaches about 50% at 0.5 μM protein concentration (Figure 4B, inset). The permeabilizing activity of aS/DHA oligomers shows selectivity as a function of molecular dimension of the dye, indeed calcein passes through the membrane in the presence of oligomers, while larger molecules such as FITC-dextran with a Stoke's radius 1.9-2.3 nm do not (Figure 4C). By the way, this value roughly defines an upper limit to the pore radius.

Oligomers increase permeability of dopaminergic cells

Although we clearly see that aS/DHA oligomers are capable of permeabilizing artificial membranes, we next asked whether this activity is also observed in a more complex system such as the cell membrane. We used PI, a cell-impermeant DNA dye, to evaluate the effect of oligomers to modify membrane permeability of dopaminergic SH-SY5Y cells. SH-SY5Y cells treated with both aS oligomeric aggregates purified by gel filtration and monomeric aS were observed within 1 hour. We observed a modest but significant increase of PI-positive cells upon treatment with aS/DHA oligomers compared to monomer or vehicle control as quantified by one way ANOVA with Tukey's post hoc test (*, $P<0.05$; Figure 5).

Oligomers do not exert detergent-like effect

To test the possibility that aS/DHA oligomers were able to compromise the integrity of the membrane by a detergent-like mechanism, large and small unilamellar vesicles were analyzed by dynamic light scattering (DLS) after incubation with oligomers for 30 minutes, using a molar ratio protein:lipid of 1:20. In Figure 6 the numbers and intensities size distributions of DOPG LUV (A,C) and SUV (B,D) before and after addition of aS oligomers are shown. The peak relative to vesicles alone (solid lines) is centered at 270±10 nm for LUV (A) and at 83±8 nm for SUV (B). The mean size of oligomers alone (dashed line) is 22±8 nm. The addition of oligomers to vesicles induces a change in the size distribution of vesicles (grey bars) different from that induced by Triton X-100 (A-B, black bars). Since the addition of Triton results in

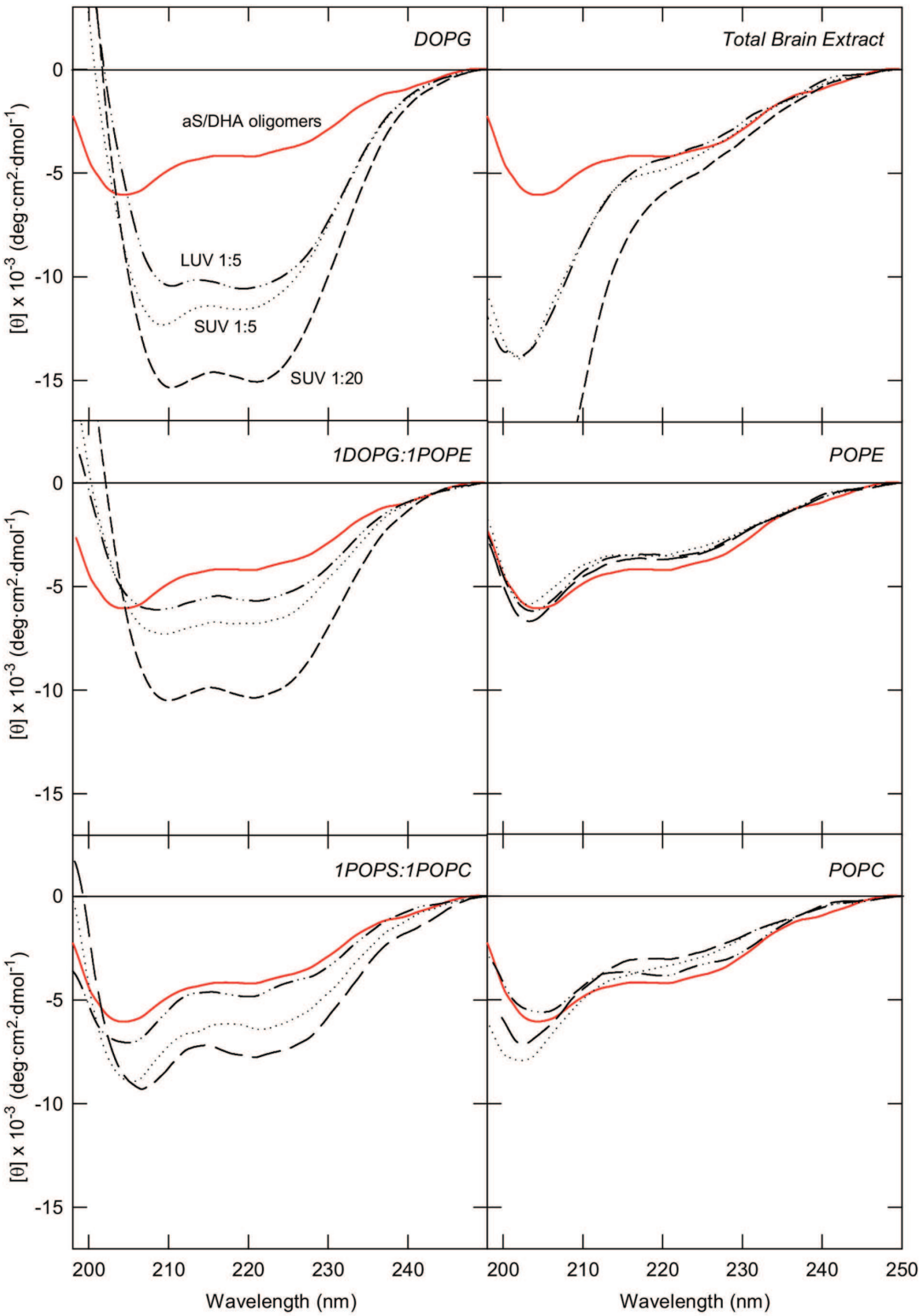

Figure 2. Interaction of aS/DHA oligomers with lipid vesicles with different composition monitored by far UV CD. The spectra relative to aS/DHA oligomers alone (red continuous line), aS/DHA oligomers in the presence of SUV at molar ratio 1:5 (dotted line) and 1:20 (dashed line) and in the presence of LUV at molar ratio 1:5 (dotted-dashed line) are reported.

doi: 10.1371/journal.pone.0082732.g002

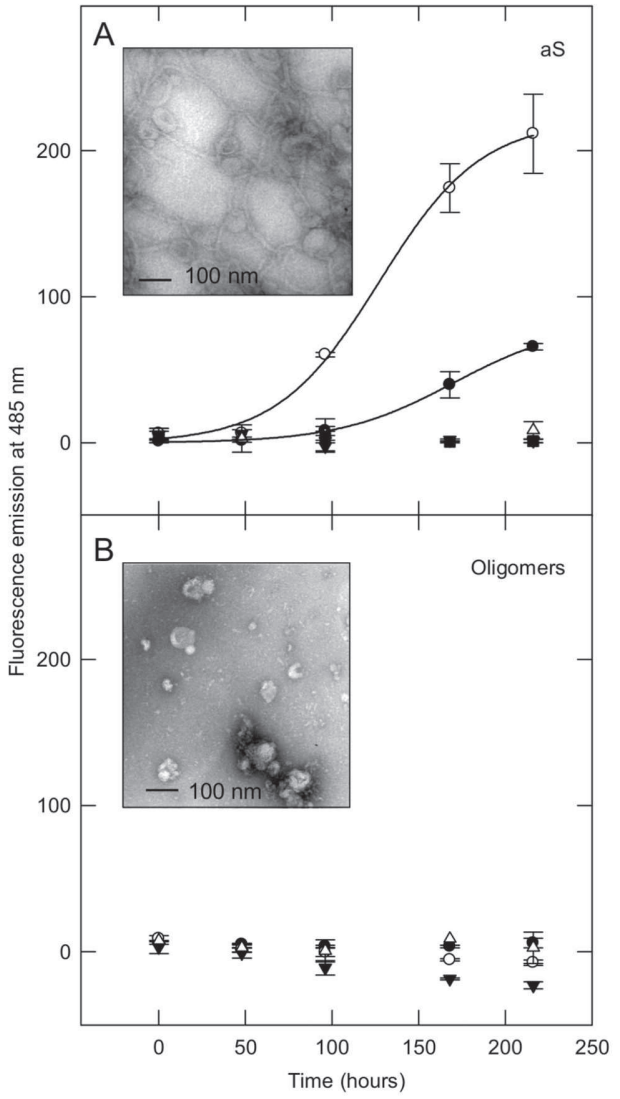

Figure 3. Aggregation studies. aS (A) and aS/DHA oligomers (B) aggregation process at 37°C in the presence of lipids, followed by ThT binding assay. aS or aS oligomers were dissolved in 20 mM Tris, 150 mM NaCl pH 7.4 at a 50 μM concentration in order to induce aggregation, in the absence (black circles) and in the presence of DOPG SUV, at molar ratio 1:20 (empty circles), 1:50 (empty triangles) and in the presence of DHA (molar ratio 1:50, inverted black triangles). The excitation wavelength was fixed at 440 nm, and the fluorescence emission was collected at 485 nm. To better visualize the aggregation trend of aS and aS in the presence of DOPG (molar ratio 1:20), the data points are fitted with a sigmoidal equation (SigmaPlot software). Inset: TEM images of protein material relative to aS and aS/DHA oligomers samples after 9 days of incubation in the presence of DOPG SUV (molar ratio 1:20).

doi: 10.1371/journal.pone.0082732.g003

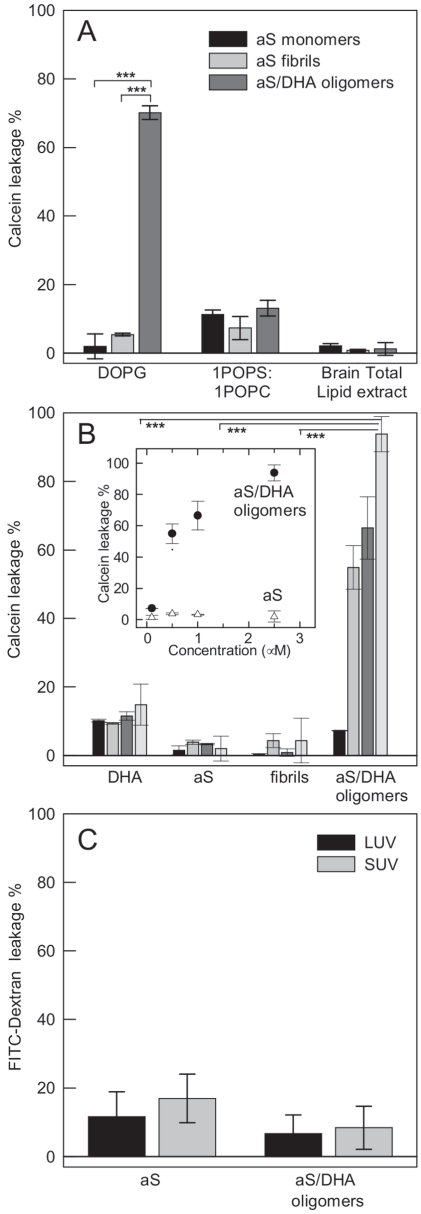

Figure 4. Leakage assays. (A) Calcein efflux from 50 μM LUV of different lipid composition induced after 30 min by monomeric, fibrillar and oligomeric aS at a protein/lipid molar ratio of 1:20. (B) Calcein efflux from 50 μM DOPG SUV upon addition of increasing amount (0.1, black bars; 0.5, grey bars; 1, dark grey bars; 2.5 μM, light grey bars) of protein species. Inset: Dependence of the leakage from 50 μM DOPG SUV on the concentration of protein or oligomers. The effect induced by increasing concentration of monomeric aS is also reported. (C) FITC-dextran leakage from 50 μM DOPG LUV and SUV induced after 30 min of incubation by aS/DHA oligomers and aS. Leakage is expressed as percentage of the maximum possible effect induced by the addition of Triton X-100. Statistical significance was calculated by student's t-test (p<0.001).

doi: 10.1371/journal.pone.0082732.g004

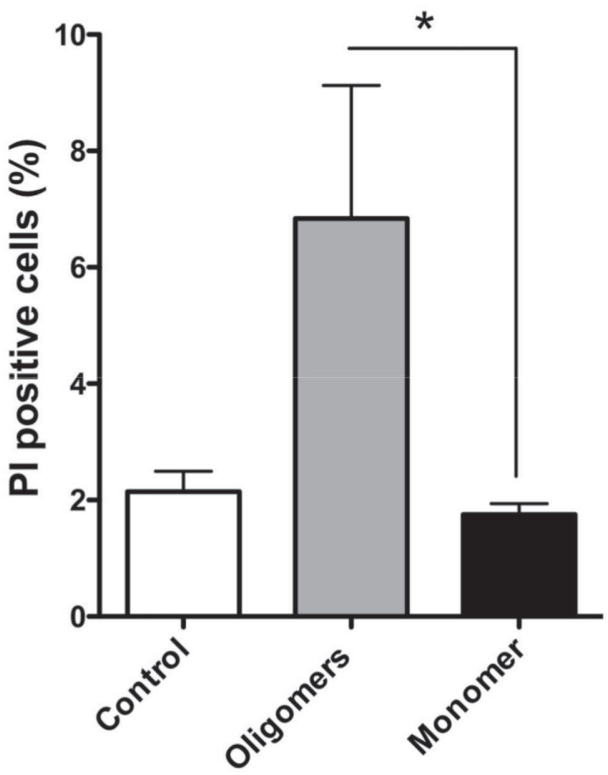

Figure 5. PI influx in dopaminergic cells. SH-SY5Y cells were treated with aS/DHA oligomers and the number of PI-positive cells was calculated as a percentage of the total counterstained cells. Quantitation (n = 3 cultures, with 5 fields analyzed per culture, 250-300 cells per field; error bars indicated the S.E.) indicated that aS/DHA oligomers increased the percentage of PI-positive cells. Statistical significance was calculated by one-way ANOVA ($p < 0.05$) compared with mock control or monomeric aS.

doi: 10.1371/journal.pone.0082732.g005

disaggregation of the vesicles into micelles, we can conclude that the oligomers do not act as detergents. To have a better view of the size distribution of vesicle upon addition of oligomers, the measurements expressed as intensities are also reported (C,D). The peak relative to vesicles splits into two peaks (gray bars) corresponding to two vesicles population with increased (centered at ~470 nm for LUV and at ~235 nm for SUV) and decreased size (centered at ~135 nm for LUV and at ~35 nm for SUV). This resizing can be ascribable to clustering/fusion of the vesicles in the case of the increased size or to remodeling in the case of the smaller species. Of interest, the same experiment was followed by TEM (Figure 6 E,F), that does not evidence substantial difference in vesicles shape after oligomer addition.

Oligomers activity on planar lipid membrane

aS/DHA oligomers at a final concentration of 68 nM are able to increase the conductance of PLM composed of DOPG/DOPE:1/1 upon the application of either positive or negative high potentials (absolute values larger than 100 mV). In 50% of experiments current fluctuations appeared non structured with short living spikes with small ionic currents (roughly 10 pA at +80 mV) as reported in Figure 7A. This permeabilizing activity generally disappeared after few minutes without causing membrane rupture, with protein concentration up to 380 nM. In 25% of experiments a more intense current, up to 100 pA, has been recorded as reported in Figure 7B. Sometimes more stable apertures can also be seen as reported in the right side of Figure 7B. In this case the current-voltage curve has a non-ohmic characteristic with higher current at negative applied voltages. No membrane destabilization has been recorded in the remaining 25% of experiments. Control experiments with DHA alone (up to 38 μM in EtOH) did not show any membrane perturbation (not shown).

Discussion

There is growing interest in understanding a possible link between aS toxicity in synucleinopathies and aS-lipid interaction [16,29,30]. aS toxicity is indeed associated with alteration in vesicle trafficking [31], mitochondrial function [32], and lipids, especially brain FAs biosynthesis and metabolism [33]. Increasing evidence shows that oligomers originating in early stages of aS fibrillation are responsible for toxicity. It has been shown that elevated brain DHA levels accelerate aS accumulation and oligomerization [20] leading to neurotoxicity [21]. We produced *in vitro* oligomeric species of aS in the presence of DHA, which resulted toxic in cultured dopaminergic cells [19]. Here we have studied their activity on membranes in an attempt to understand their mechanism of toxicity. The latter is object of debate in the literature for the difficulty to define a unifying picture of the toxic activity. The controversy springs from both the transient nature of aS oligomers and from the many different types of oligomers that have been described, a consequence of the variety of the method of preparation. In the presence of DHA, it is induced the formation of relatively stable oligomers that are off-pathway in aS aggregation process.

aS oligomers have been described as annular and spherical-shaped and are generally characterized by beta-sheet structure, some of them resulted toxic to cells [6,34-36]. Based on TEM and AFM measurements, aS/DHA oligomers share similar size with diameters ranging from 12-30 nm. A specific difference with oligomers described above resides in the secondary structure. aS in the presence of DHA acquires α-helical structure [22] and oligomers, obtained upon aS/DHA incubation (3-48 hours), maintain α-helical structure. After a gel filtration purification step, exchangeable DHA, not the covalently bound one, is removed and with it the effect on oligomers structure. Consequently, part of the DHA dependent secondary structure is lost, and the oligomers acquire a partly folded state, significantly different from the natively unfolded structure of monomeric aS. These partly folded oligomers are able to acquire again α-helical structure upon addition of DHA or in the presence of SUV or LUV containing negatively charged head groups. A similar behavior was previously observed for aS [2,27,37-40]. In monomeric aS the N-terminal

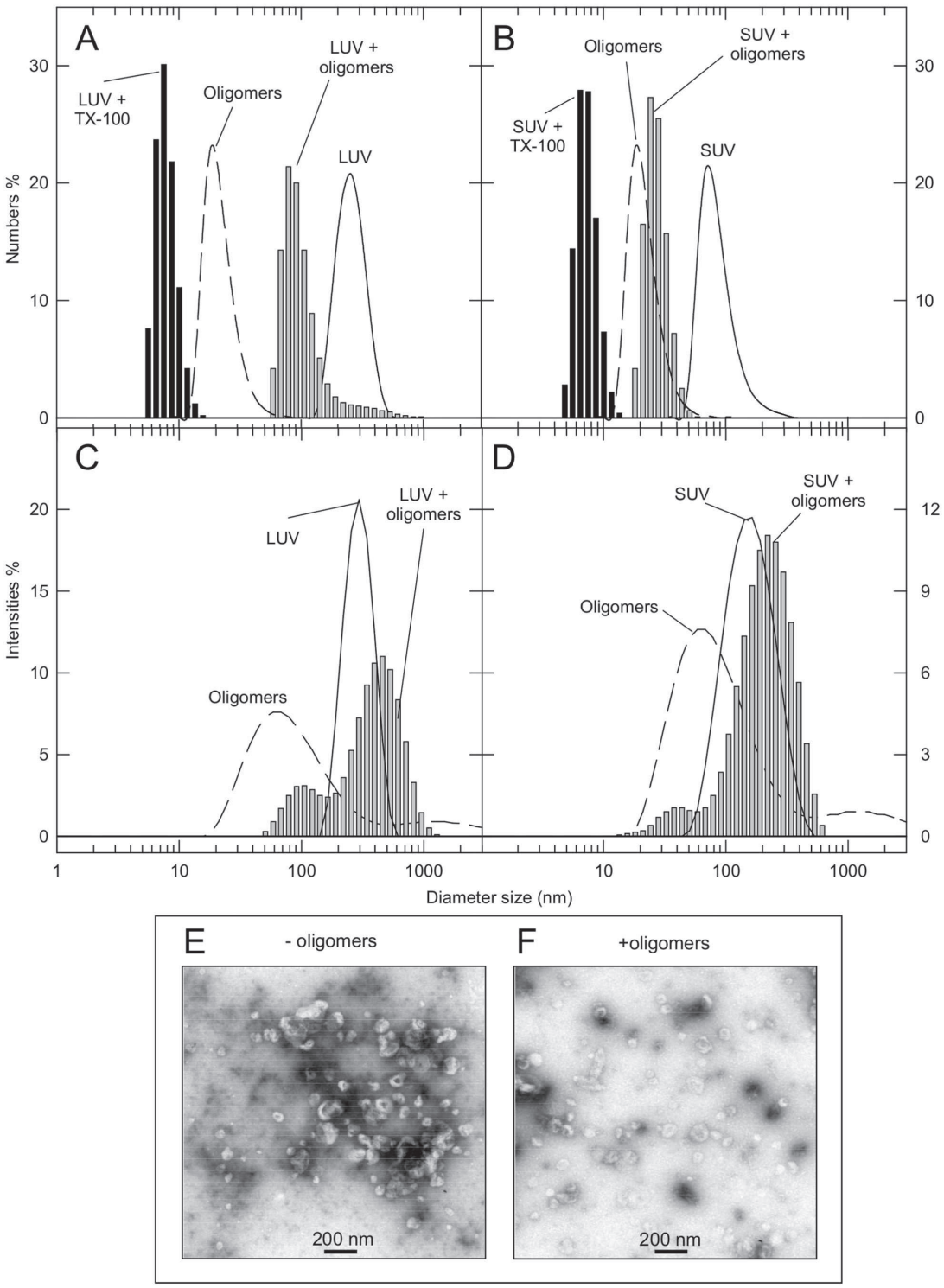

Figure 6. Interaction of aS/DHA oligomers with DOPG vesicles by DLS and TEM. DLS analysis, expressed as numbers (A,B) or as intensities (C,D) and TEM images (E,F) are reported. DLS measurements of DOPG LUV (A,C) and SUV (B,D) are conducted in the absence of oligomers (continuous lines), and upon 30 min-addition of oligomers (molar ratio 1:20, light grey bars). aS/oligomers alone are represented by dashed lines. The effect induced by Triton X-100 on LUV and SUV is reported (A,B, dark grey bars). TEM images of DOPG SUV (E) or in the presence (F) of aS/DHA oligomers were taken after 30 min of incubation.

doi: 10.1371/journal.pone.0082732.g006

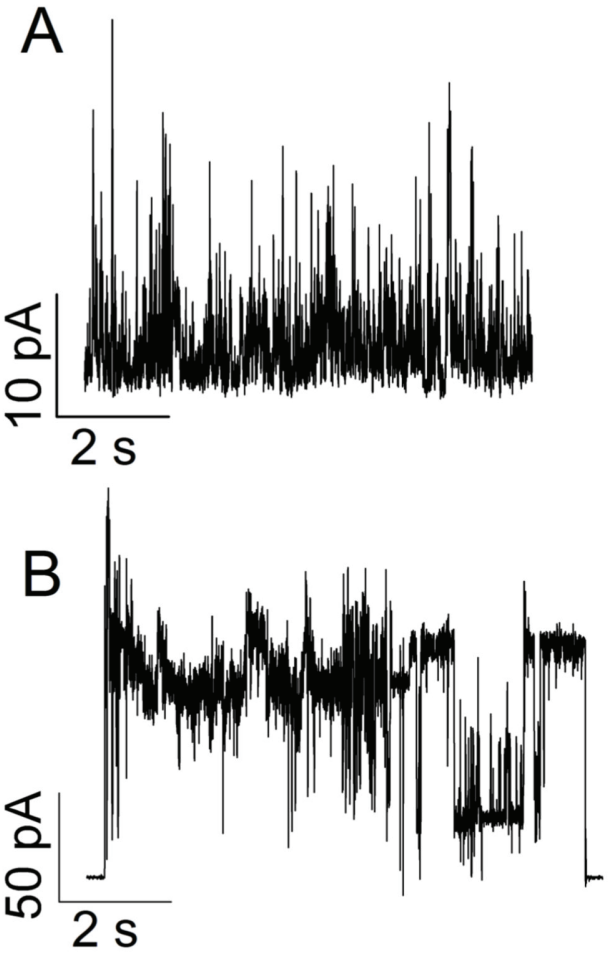

Figure 7. PLM experiments. Electrophysiological activity of aS/DHA oligomers on DOPG/DOPE:1/1 lipid membranes. Buffer composition was KCl 100 mM, Hepes 5 mM, pH 7.0. Protein concentration was 68 nM. Applied potential +80 mV (A) or +100 mV (B).

doi: 10.1371/journal.pone.0082732.g007

region is essential for membrane recognition and for cooperative formation of helical domains [41]. So it is reasonable to assume that in the partly folded state, the N-terminal region or part of it is free to drive the association of oligomers with membranes and lipids. On the other hand, the NAC region (residues 61-95) seems not available or hidden in the interior of the oligomer in view of the fact that these species do not aggregate even in the presence of membranes. Indeed the membranes can affect the fibril formation process of aS and other amyloidogenic proteins [27,28]. Fibrillation can be accelerated or even modulated by lipids and membranes and this strictly depends on the relative protein/lipid ratio [42-44]. In conclusion aS/DHA oligomers have two main structural features: the conformational sensitivity to environment for the ability to interact with lipids and to undergo structural transition, and secondly the stability under conditions that favor aggregation. The overall structure of the oligomers could be stabilized by hydrophobic interactions deriving from the association of NAC regions.

An interesting property of aS/DHA oligomers is their ability to permeabilize membranes, as verified using a leakage assay from unilamellar phospholipid vesicles and ionic current measurements. Also dopaminergic cells membranes are perturbed as treatment with oligomers significantly increases the number of cells internalizing the membrane-impermeant dye propidium iodide. These results suggest that membranes can be a possible target of aS oligomers activity. This can be particularly harmful for neuronal cells, where electrical activity and action potential firing are finely regulated by transient, voltage-gated channel-mediated variation of membrane potential and intracellular calcium concentration. Indeed, increased membrane permeability could result in a variety of intracellular processes and leads to excitotoxicity, as well as dissipation of sodium and potassium gradients with deleterious impact on electrical neuronal activity. Several mechanisms have been proposed to explain oligomers activity on membranes, such as the pore-like mechanism [34], a thinning effect due to lipid extraction from the bilayer [28], a complete disruption of the membrane [45] or a transient membrane destabilization [46]. The pore-like hypothesis is especially accepted for those proteins forming oligomers or protofibrils with annular or ring-like structure [44,47]. In our case the leakage activity tested on synthetic liposomes shows selectivity of markers size, evidencing that the average dimension of the aperture should be between 1 and 4 nm [48]. The permeabilization effect is induced in cells just after 30 min of treatment. These observations would be consistent with the pore-like mechanism [44]. Nevertheless the activity of oligomers on a planar lipid membrane system seems due to a non-specific membrane permeabilization rather than to the formation of structured membrane apertures like those previously demonstrated for monomeric aS [49]. DLS and microscopy measurements allow also to exclude a detergent-like activity of aS/DHA oligomers on phospholipids vesicles. Indeed DLS measurements of both LUVs and SUVs in the presence of aS/DHA oligomers show that the vesicles size distribution is modified, even if without changes to the overall vesicles morphology.

We are analyzing a population of oligomers that contain a source of heterogeneity deriving from the presence of covalently bound DHA and additionally of oxidative modifications [19]. The degree of chemical modification of aS molecules embedded in the oligomers is very likely to affect the affinity for and the permeabilizing activity on membranes. We can reasonably hypothesize that these modifications occur especially at the level of His or Lys residues localized in the N-terminal region of aS [50,51]. Therefore the charge distribution of the basic KXKE repeats of the N-terminal region of aS/DHA oligomers could be altered, affecting the interaction with membrane that is primarily mediated by a charge effect [2,46].

In conclusion, aS/DHA oligomers interacting with negatively charged membranes induce a perturbation of the phospholipid bilayer with the release of encapsulated small molecules. Oligomer molecules remain entrapped on the vesicles, as peripheral membrane proteins, acquiring α-helical structure.

Damaging of membrane structural integrity seems to be an essential step in the cytotoxic activity of aS oligomers formed in the presence of DHA.

Acknowledgements

We thank Dr. Amanda Penco (University of Genova) for help in AFM measurements and Dr. Alberto O. Andrighetti (CNR-IBF Trento) for the technical assistance with PLM experiments.

Author Contributions

Conceived and designed the experiments: PPDL CF GDF. Performed the experiments: CF GDF AR. Analyzed the data: PPDL CF GDF EG LB MDS AR. Contributed reagents/ materials/analysis tools: PPDL EG. Wrote the manuscript: PPDL CF.

References

1. Spillantini MG, Crowther RA, Jakes R, Hasegawa M, Goedert M (1998) Alpha-synuclein in filamentous inclusions of Lewy bodies from Parkinson's disease and dementia with Lewy bodies. Proc Natl Acad Sci U S A 95: 6469–6473. doi:10.1073/pnas.95.11.6469. PubMed: 9600990.
2. Davidson WS, Jonas A, Clayton DF, George JM (1998) Stabilization of alpha-synuclein secondary structure upon binding to synthetic membranes. J Biol Chem 273: 9443–9449. doi:10.1074/jbc.273.16.9443. PubMed: 9545270.
3. Bodles AM, Guthrie DJ, Greer B, Irvine GB (2001) Identification of the region of non-A beta component (NAC) of Alzheimer's disease amyloid responsible for its aggregation and toxicity. J Neurochem 78: 384–395. doi:10.1046/j.1471-4159.2001.00408.x. PubMed: 11461974.
4. Giasson BI, Murray IV, Trojanowski JQ, Lee VM (2001) A hydrophobic stretch of 12 amino acid residues in the middle of alpha-synuclein is essential for filament assembly. J Biol Chem 276: 2380−2386. doi:10.1074/jbc.M008919200. PubMed: 11060312.
5. Conway KA, Lee SJ, Rochet JC, Ding TT, Williamson RE et al. (2000) Acceleration of oligomerization, not fibrillization, is a shared property of both alpha-synuclein mutations linked to early-onset Parkinson's disease: implications for pathogenesis and therapy. Proc Natl Acad Sci U S A 97: 571−576. doi:10.1073/pnas.97.2.571. PubMed: 10639120.
6. Cremades N, Cohen SI, Deas E, Abramov AY, Orte A et al. (2012) Direct observation of the interconversion of normal and toxic forms of alpha-synuclein. Cell 149: 1048–1059. doi:10.1016/j.cell.2012.03.037. PubMed: 22632969.
7. Danzer KM, Haasen D, Karow AR, Moussaud S, Habeck M et al. (2007) Different species of α-synuclein oligomers induce calcium influx and seeding. J Neurosci 27: 9220–9232. doi:10.1523/JNEUROSCI.2617-07.2007. PubMed: 17715357.
8. Bendor JT, Logan TR, Edwards RH (2013) The function of α-synuclein. Neuron 79: 1044–1066. doi:10.1016/j.neuron.2013.09.004. PubMed: 24050397.
9. Larsen KE, Schmitz Y, Troyer MD, Mosharov E, Dietrich P et al. (2006) α-Synuclein overexpression in PC12 and chromaffin cells impairs catecholamine release by interfering with a late step in exocytosis. J Neurosci 26: 11915–11922. doi:10.1523/JNEUROSCI.3821-06.2006. PubMed: 17108165.
10. Nemani VM, Lu W, Berge V, Nakamura K, Onoa B et al. (2010) Increased expression of alpha-synuclein reduces neurotransmitter release by inhibiting synaptic vesicle reclustering after endocytosis. Neuron 65: 66–79. doi:10.1016/j.neuron.2009.12.023. PubMed: 20152114.
11. Scott D, Roy S (2012) α-Synuclein inhibits intersynaptic vesicle mobility and maintains recycling-pool homeostasis. J Neurosci 32: 10129–10135. doi:10.1523/JNEUROSCI.0535-12.2012. PubMed: 22836248.
12. Dalfó E, Ferrer I (2005) α-Synuclein binding to rab3a in multiple system atrophy. Neurosci Lett 380: 170–175. doi:10.1016/j.neulet.2005.01.034. PubMed: 15854772.
13. Burré J, Sharma M, Tsetsenis T, Buchman V, Etherton MR et al. (2010) α-Synuclein promotes SNARE-complex assembly in vivo and in vitro. Science 329: 1663–1667. doi:10.1126/science.1195227. PubMed: 20798282.
14. Lashuel HA, Overk CR, Oueslati A, Masliah E (2013) The many faces of α-synuclein: from structure and toxicity to therapeutic target. Nat Rev Neurosci 14: 38–48. PubMed: 23254192.
15. Castagnet PI, Golovko MY, Barceló-Coblijn GC, Nussbaum RL, Murphy EJ (2005) Fatty acid incorporation is decreased in astrocytes cultured from alpha-synuclein gene-ablated mice. J Neurochem 94: 839–849. doi:10.1111/j.1471-4159.2005.03247.x. PubMed: 16033426.
16. Ruipérez V, Darios F, Davletov B (2010) Alpha-synuclein, lipids and Parkinson's disease. Prog Lipid Res 49: 420–428. doi:10.1016/j.plipres.2010.05.004. PubMed: 20580911.
17. Perrin RJ, Woods WS, Clayton DF, George JM (2001) Interaction of human alpha-synuclein and Parkinson's disease variants with phospholipid. J Biol Chem 275: 34393−34398.
18. Sharon R, Bar-Joseph I, Frosch MP, Walsh DM, Hamilton JA et al. (2003) The formation of highly soluble oligomers of alpha-synuclein is regulated by fatty acids and enhanced in Parkinson's disease. Neuron 37: 583–595. doi:10.1016/S0896-6273(03)00024-2. PubMed: 12597857.
19. De Franceschi G, Frare E, Pivato M, Relini A, Penco A et al. (2011) Structural and morphological characterization of aggregated species of α-synuclein induced by docosahexaenoic acid. J Biol Chem 286: 22262–22274. doi:10.1074/jbc.M110.202937. PubMed: 21527634.
20. Assayag K, Yakunin E, Loeb V, Selkoe DJ, Sharon R (2007) Polyunsaturated fatty acids induce alpha-synuclein-related pathogenic changes in neuronal cells. Am J Pathol 171: 2000–2011. doi:10.2353/ajpath.2007.070373. PubMed: 18055555.
21. Yakunin E, Loeb V, Kisos H, Biala Y, Yehuda S et al. (2012) α-Synuclein neuropathology is controlled by nuclear hormone receptors and enhanced by docosahexaenoic acid in a mouse model for Parkinson's disease. Brain Pathol 22: 280–294. doi:10.1111/j.1750-3639.2011.00530.x. PubMed: 21929559.
22. De Franceschi G, Frare E, Bubacco L, Mammi S, Fontana A et al. (2009) Molecular insights into the interaction between α-synuclein and docosahexaenoic acid. J Mol Biol 394: 94–107. doi:10.1016/j.jmb.2009.09.008. PubMed: 19747490.
23. Gill SG, von Hippel PH (1989) Calculation of protein extinction coefficients from amino acid sequence data. Anal Biochem 182: 319–326. doi:10.1016/0003-2697(89)90602-7. PubMed: 2610349.
24. Chen PS, Toribara TY, Warner H (1956) Microdetermination of phosphorus. Anal Chem 28: 1756–1758. doi:10.1021/ac60119a033.
25. LeVine H 3rd (1993) Thioflavine T interaction with synthetic Alzheimer's disease beta-amyloid peptides: detection of amyloid aggregation in solution. Protein Sci 2: 404−410. PubMed: 8453378.
26. Dalla Serra M, Menestrina G (2000) Characterization of molecular properties of pore-forming toxins with planar lipid bilayers. Methods Mol Biol 145: 171–188. PubMed: 10820722.
27. Jo E, McLaurin J, Yip CM, St George-Hyslop P, Fraser PE (2000) Alpha-synuclein membrane interactions and lipid specificity. J Biol Chem 275: 34328−34334. doi:10.1074/jbc.M004345200. PubMed: 10915790.
28. Reynolds NP, Soragni A, Rabe M, Verdes D, Liverani E et al. (2011) Mechanism of membrane interaction and disruption by α-synuclein. J Am Chem Soc 133: 19366−19375. doi:10.1021/ja2029848. PubMed: 21978222.
29. Berthelot K, Cullin C, Lecomte S (2013) What does make an amyloid toxic: Morphology, structure or interaction with membrane? Biochimie 95: 12–19. doi:10.1016/j.biochi.2012.07.011. PubMed: 22824150.
30. Auluck PK, Caraveo G, Lindquist S (2010) α-Synuclein: Membrane interactions and toxicity in Parkinson's Disease. Annu Rev Cell Dev Biol 26: 211–233. doi:10.1146/annurev.cellbio.042308.113313. PubMed: 20500090.
31. Murphy DD, Rueter SM, Trojanowski JQ, Lee VM (2000) Synucleins are developmentally expressed, and alpha-synuclein regulates the size of the presynaptic vesicular pool in primary hippocampal neurons. J Neurosci 20: 3214−3220. PubMed: 10777786.
32. Henchcliffe C, Beal MF (2008) Mitochondrial biology and oxidative stress in Parkinson disease pathogenesis. Nat Clin Pract Neurol 4: 600–609. doi:10.1038/ncpneuro0924. PubMed: 18978800.
33. Golovko MY, Rosenberger TA, Feddersen S, Faergeman NJ, Murphy EJ (2007) Alpha-synuclein gene ablation increases docosahexaenoic acid incorporation and turnover in brain phospholipids. J Neurochem 101: 201–211. PubMed: 17250657.

34. Volles MJ, Lee SJ, Rochet JC, Shtilerman MD, Ding TT et al. (2001) Vesicle permeabilization by protofibrillar α-synuclein: implications for the pathogenesis and treatment of Parkinson's disease. Biochemistry 40: 7812−7819. doi:10.1021/bi0102398. PubMed: 11425308.
35. Kim HY, Cho MK, Kumar A, Maier E, Siebenhaar C et al. (2009) Structural properties of pore-forming oligomers of alpha-synuclein. J Am Chem Soc 131: 17482−17489. doi:10.1021/ja9077599. PubMed: 19888725.
36. Giehm L, Svergun DI, Otzen DE, Vestergaard B (2011) Low-resolution structure of a vesicle disrupting alpha-synuclein oligomer that accumulates during fibrillation. Proc Natl Acad Sci U S A 108: 3246–3251. doi:10.1073/pnas.1013225108. PubMed: 21300904.
37. Eliezer D, Kutluay E, Bussell R Jr, Browne G (2001) Conformational properties of alpha-synuclein in its free and lipid-associated states. J Mol Biol 307: 1061–1073. doi:10.1006/jmbi.2001.4538. PubMed: 11286556.
38. Nuscher B, Kamp F, Mehnert T, Odoy S, Haass C et al. (2004) Alpha-synuclein has a high affinity for packing defects in a bilayer membrane. A thermodynamics study. J Biol Chem 279: 21966-21975. doi:10.1074/jbc.M401076200. PubMed: 15028717.
39. van Rooijen BD, Claessens MMAE, Subramaniam V (2008) Membrane binding of oligomeric α-synuclein depends on bilayer charge and packing. FEBS Lett 582: 3788–3792. doi:10.1016/j.febslet.2008.10.009. PubMed: 18930058.
40. Uversky VN (2007) Neuropathology, biochemistry, and biophysics of α-synuclein aggregation. J Neurochem 103: 17–37. PubMed: 17623039.
41. Bartels T, Ahlstrom LS, Leftin A, Kamp F, Haass C et al. (2010) The N-terminus of the intrinsically disordered protein α-synuclein triggers membrane binding and helix folding. Biophys J 99: 2116–2124. doi: 10.1016/j.bpj.2010.06.035. PubMed: 20923645.
42. Lee HJ, Choi C, Lee SJ (2002) Membrane-bound alpha-synuclein has a high aggregation propensity and the ability to seed the aggregation of the cytosolic form. J Biol Chem 277: 671−678. PubMed: 11679584.
43. Sparr E, Engel MF, Sakharov DV, Sprong M, Jacobs J et al. (2004) Islet amyloid polypeptide-induced membrane leakage involves uptake of lipids by forming amyloid fibers. FEBS Lett 577: 117−120. doi: 10.1016/j.febslet.2004.09.075. PubMed: 15527771.
44. Butterfield SM, Lashuel HA (2010) Amyloidogenic protein-membrane interactions: mechanistic insight from model systems. Angew Chem Int Ed Engl 49: 5628−5654. doi:10.1002/anie.200906670. PubMed: 20623810.
45. Bechinger B, Lohner K (2006) Detergent-like actions of linear amphipathic cationic antimicrobial peptides. Biochim Biophys Acta 1758: 1529–1539. doi:10.1016/j.bbamem.2006.07.001. PubMed: 16928357.
46. van Rooijen BD, Claessens MMAE, Subramaniam V (2010) Membrane permeabilization by oligomeric α-synuclein: in search of the mechanism. PLOS ONE 5: e14292. doi:10.1371/journal.pone.0014292. PubMed: 21179192.
47. Volles MJ, Lansbury PT Jr (2002) Vesicle permeabilization by protofibrillar alpha-synuclein is sensitive to Parkinson's disease-linked mutations and occurs by a pore-like mechanism. Biochemistry 41: 4595−4602. doi:10.1021/bi0121353. PubMed: 11926821.
48. Mazzuca C, Orioni B, Coletta M, Formaggio F, Toniolo C et al. (2010) Fluctuations and the rate-limiting step of peptide-induced membrane leakage. Biophys J 99: 1791−1800. doi:10.1016/j.bpj.2010.07.010. PubMed: 20858423.
49. Tosatto L, Andrighetti AO, Plotegher N, Antonini V, Tessari I et al. (2012) Alpha-synuclein pore forming activity upon membrane association. Biochim Biophys Acta 1818: 2876–2883. doi:10.1016/j.bbamem.2012.07.007. PubMed: 22820150.
50. Bae EJ, Ho DH, Park E, Jung JW, Cho K et al. (2013) Lipid peroxidation product 4-hydroxy-2-nonenal promotes seeding-capable oligomer formation and cell-to-cell transfer of α-synuclein. Antioxid Redox Signal 18: 770–783. doi:10.1089/ars.2011.4429. PubMed: 22867050.
51. Xiang W, Schlachetzki JC, Helling S, Bussmann JC, Berlinghof M et al. (2013) Oxidative stress-induced posttranslational modifications of alpha-synuclein: specific modification of alpha-synuclein by 4-hydroxy-2-nonenal increases dopaminergic toxicity. Mol Cell Neurosci 54: 71−83. doi:10.1016/j.mcn.2013.01.004. PubMed: 23369945.